NASA CR-151936

WIND TUNNEL TEST ON A 1/4.622 FROUDE SCALE, HINGELESS ROTOR, TILT ROTOR MODEL

VOLUME I

J. P. Magee
H. R. Alexander

September 1976

Prepared under Contract NAS2-9015

for

National Aeronautics and Space Administration
Ames Research Center

by

BOEING VERTOL COMPANY
A DIVISION OF THE BOEING COMPANY
P. O. BOX 16858
PHILADELPHIA, PENNSYLVANIA 19142

D238-10000-1

REV LTR

BOEING VERTOL COMPANY

A DIVISION OF THE BOEING COMPANY
P.O. BOX 16858
PHILADELPHIA, PENNSYLVANIA 19142

CODE IDENT. NO. 77272

NUMBER D238-10000-1

TITLE WIND TUNNEL TESTS ON A 1/4.622 FROUDE SCALE, HINGELESS ROTOR, TILT ROTOR MODEL

ORIGINAL RELEASE DATE ________. FOR THE RELEASE DATE OF SUBSEQUENT REVISIONS, SEE THE REVISION SHEET. FOR LIMITATIONS IMPOSED ON THE DISTRIBUTION AND USE OF INFORMATION CONTAINED IN THIS DOCUMENT, SEE THE LIMITATIONS SHEET.

MODEL ________ CONTRACT NAS2-9015

ISSUE NO. ________ ISSUED TO: ________

PREPARED BY John P. Magee DATE 9/14/76
J. P. Magee

PREPARED BY H R Alexander DATE 9/14/76
H. R. Alexander

APPROVED BY W. C. Boehm DATE 9/14/76
W. C. Boehm

APPROVED BY ________ DATE ________

FORM 46280 (5/73)

LIMITATIONS

This document is controlled by Research & Development - 7040

All revisions to this document shall be approved by the above noted organization prior to release.

ACTIVE SHEET RECORD

SHEET NUMBER	REV LTR	ADDED SHEETS				SHEET NUMBER	REV LTR	ADDED SHEETS			
		SHEET NUMBER	REV LTR	SHEET NUMBER	REV LTR			SHEET NUMBER	REV LTR	SHEET NUMBER	REV LTR
I						XLIX					
III						L					
IV						LI					
V						LII					
VI						LIII					
VII						LIV					
VIII						LV					
IX						LVI					
X						LVII					
XI						LVIII					
XIII						LIX					
XIV						LX					
XV						LXI					
XVII						LXII					
XVIII						LXIII					
XIX						LXIV					
XX						LXV					
XXI						LXVI					
XXII						LXVII					
XXIII						LXVIII					
XXIV						LXIX					
XXV						LXX					
XXVI						LXXI					
XXVII						LXXII					
XXVIII						1					
XXIX						2					
XXX						3					
XXXI						4					
XXXII						5					
XXXIII						6					
XXXIV						7					
XXXV						8					
XXXVI						9					
XXXVII						10					
XXXVIII						11					
XXXIX						12					
XL						13					
XLI						14					
XLII						15					
XLIII						16					
XLIV						17					
XLV						18					
XLVI						19					
XLVII						20					
XLVIII						21					

(7/67)

ACTIVE SHEET RECORD

SHEET NUMBER	REV LTR	ADDED SHEETS SHEET NUMBER	REV LTR	SHEET NUMBER	REV LTR	SHEET NUMBER	REV LTR	ADDED SHEETS SHEET NUMBER	REV LTR	SHEET NUMBER	REV LTR
22						67					
23						68					
24						69					
25						70					
26						71					
27						72					
28						73					
29						74					
30						75					
31						76					
32						77					
33						78					
34						79					
35						80					
36						81					
37						82					
38						83					
39						84					
40						85					
41						86					
43						87					
44						88					
45						89					
46						90					
47						91					
48						92					
49						93					
50						94					
51						95					
52						96					
53						97					
54						98					
55						99					
56						100					
57						101					
58						102					
59						103					
60						104					
61						105					
62						106					
63						107					
64						108					
65						109					
66						110					

ACTIVE SHEET RECORD

SHEET NUMBER	REV LTR	ADDED SHEETS SHEET NUMBER	REV LTR	SHEET NUMBER	REV LTR	SHEET NUMBER	REV LTR	ADDED SHEETS SHEET NUMBER	REV LTR	SHEET NUMBER	REV LTR
111						159					
112						160					
113						161					
114						162					
115						163					
116						164					
117						165					
118						166					
119						167					
120						168					
121						169					
122						170					
123						171					
124						172					
125						173					
126						174					
127						175					
128						176					
129						177					
131						178					
132						179					
133						180					
134						181					
135						182					
136						183					
137						184					
138						185					
139						186					
140						187					
141						188					
143						189					
144						190					
145						191					
147						192					
149						193					
150						194					
151						195					
152						196					
153						197					
154						198					
155						199					
156						200					
157						201					
158						202					

FORM 46283 (7/67)

ACTIVE SHEET RECORD

SHEET NUMBER	REV LTR	ADDED SHEETS SHEET NUMBER	REV LTR	ADDED SHEETS SHEET NUMBER	REV LTR	SHEET NUMBER	REV LTR	ADDED SHEETS SHEET NUMBER	REV LTR	ADDED SHEETS SHEET NUMBER	REV LTR
203						247					
204						248					
205						249					
206						250					
207						251					
208						252					
209						253					
210						254					
211						255					
212						256					
213						257					
214						258					
215						259					
216						260					
217						261					
218						262					
219						263					
220						264					
221						265					
222						266					
223						267					
224						268					
225						269					
226						270					
227						271					
228						272					
229						273					
230						274					
231						275					
232						276					
233						277					
234						278					
235						279					
236						280					
237						281					
238						282					
239						283					
240						284					
241						285					
242						286					
243						287					
244						288					
245						289					
246						290					

FORM 46283 (7/67)

ACTIVE SHEET RECORD

SHEET NUMBER	REV LTR	ADDED SHEETS SHEET NUMBER	REV LTR	ADDED SHEETS SHEET NUMBER	REV LTR	SHEET NUMBER	REV LTR	ADDED SHEETS SHEET NUMBER	REV LTR	ADDED SHEETS SHEET NUMBER	REV LTR
291						335					
292						336					
293						337					
294						338					
295						339					
296						340					
297						341					
298						342					
299						343					
300						344					
301						345					
302						346					
303						347					
304						348					
305						349					
306						350					
307						351					
308						352					
309						353					
310						354					
311						355					
312						356					
313						357					
314						358					
315						359					
316						360					
317						361					
318						362					
319						363					
320						364					
321						365					
322						366					
323						367					
324						368					
325						369					
326						370					
327						371					
328						372					
329						373					
330						374					
331						375					
332						376					
333						377					
334						378					

FORM 46283 (7/67)

ACTIVE SHEET RECORD

SHEET NUMBER	REV LTR	ADDED SHEETS SHEET NUMBER	REV LTR	SHEET NUMBER	REV LTR	SHEET NUMBER	REV LTR	ADDED SHEETS SHEET NUMBER	REV LTR	SHEET NUMBER	REV LTR
379						424					
380						425					
381						426					
382						427					
383						428					
384						429					
385						430					
386						431					
387						432					
388						433					
389						434					
390						435					
391						436					
392						437					
393						438					
394						439					
395						440					
396						441					
397						442					
398						443					
399						444					
400						445					
401						446					
402						447					
403						448					
404						449					
405						450					
406						451					
407						452					
408						453					
409						454					
410						455					
411						456					
412						457					
413						458					
414						459					
415						460					
416						461					
417						462					
418						463					
419						464					
420						465					
421						466					
422						467					
423											

FORM 46283 (7/67)

ACTIVE SHEET RECORD

SHEET NUMBER	REV LTR	ADDED SHEETS SHEET NUMBER	REV LTR	ADDED SHEETS SHEET NUMBER	REV LTR	SHEET NUMBER	REV LTR	ADDED SHEETS SHEET NUMBER	REV LTR	ADDED SHEETS SHEET NUMBER	REV LTR
468						512					
469						513					
470						514					
471						515					
472						516					
473						517					
474						518					
475						519					
476						520					
477						521					
478						522					
479						523					
480						524					
481						525					
482						526					
483						527					
484						528					
485						529					
486						530					
487						531					
488						532					
489						533					
490						534					
491						535					
492						536					
493						537					
494						538					
495						539					
496						540					
497						541					
498						542					
499						543					
500						544					
501						545					
502						546					
503						547					
504						548					
505						549					
506						550					
507						551					
508						552					
509						553					
510						554					
511						555					

FORM 46283 (7/67)

ACTIVE SHEET RECORD

SHEET NUMBER	REV LTR	ADDED SHEETS SHEET NUMBER	REV LTR	ADDED SHEETS SHEET NUMBER	REV LTR	SHEET NUMBER	REV LTR	ADDED SHEETS SHEET NUMBER	REV LTR	ADDED SHEETS SHEET NUMBER	REV LTR
556						601					
557						602					
558						603					
559						604					
560						605					
561						606					
562						607					
563						608					
564						609					
565						610					
566						611					
567						612					
568						613					
569						614					
570						615					
571						616					
572						617					
573						618					
574						619					
575						620					
576						621					
577						622					
578						623					
579						624					
580						625					
581						626					
582						627					
583						628					
584						629					
585						630					
586						631					
587						632					
588						633					
589						634					
590						635					
591						636					
592						637					
593						638					
594						639					
595						640					
596						641					
597						642					
598						643					
599						644					
600						645					

FORM 46283 (7/67)

ACTIVE SHEET RECORD

SHEET NUMBER	REV LTR	ADDED SHEETS SHEET NUMBER	REV LTR	ADDED SHEETS SHEET NUMBER	REV LTR	SHEET NUMBER	REV LTR	ADDED SHEETS SHEET NUMBER	REV LTR	ADDED SHEETS SHEET NUMBER	REV LTR
646						691					
647						692					
648						693					
649						694					
650						695					
651						696					
652						697					
653						698					
654						699					
655						700					
656						701					
657						702					
658						703					
659						704					
660						705					
661						706					
662											
663											
664											
665											
666											
667											
668											
669											
670											
671											
672											
673											
674											
675											
676											
677											
678											
679											
680											
681											
682											
683											
684											
685											
686											
687											
688											
689											
690											

FORM 46283 (7/67)

REVISIONS			
LTR	DESCRIPTION	DATE	APPROVAL

ABSTRACT

This document is Volume I of four volumes which contain the results of a wind tunnel test of a 1/4.622 Froude scale, hingeless rotor tilt rotor model. The test was performed under NASA Contract NAS2-9015. The test program generated parametric rotor data over the range of nacelle incidences and airspeeds for normal tilt rotor operation up to the equivalent of 300 knots full scale speed. In addition, information on blade loads, rotor/airframe and airframe/rotor interactions and control loads was obtained. Data in hover and transition are presented in Volumes I, II and III and cruise flight data is given in Volume IV.

FOREWORD

This report was prepared by the Boeing Vertol Company of Philadelphia, Pennsylvania for the National Aeronautics and Space Administration, Ames Research Center under NASA Contract NAS2-9015.

Mr. M. A. Shovlin and Mr. T. Galloway of Ames Research Center were technical monitors for this work.

The Boeing program manager was Mr. J. P. Magee. The contributions of the Boeing Vertol Wind Tunnel staff are acknowledged.

The experimental data is presented in four volumes:

NASA CR-151936

NASA CR-151937

NASA CR-151938

NASA CR-151939

This document is volume I NASA CR-151936.

TABLE OF CONTENTS

LIST OF ILLUSTRATIONS

Note: Subsequent figures in this report are numbered in accordance with the Appendix No. and data file to which the information belongs.

LIST OF TABLES

LIST OF SYMBOLS

SYMBOL	NOMENCLATURE	UNITS
A_1	Lateral cyclic pitch	Deg
B_1	Longitudinal cyclic pitch	Deg
b	Span	Ft
CTB-L	Left Rotor Thrust Coefficient	$\frac{T_L}{\rho \pi R^2 V_T^2}$
CPB-L	Left Rotor Power Coefficient	$\frac{HP_L \times 550}{\rho \pi R^2 V_T^3}$
CNFB-L	Left Rotor Normal Force Coefficient	$\frac{NF_L}{\rho \pi R^2 V_T^2}$
CSFB-L	Left Rotor Side Force Coefficient	$\frac{SF_L}{\rho \pi R^2 V_T^2}$
CPMB-L	Left Rotor Pitching Moment	$\frac{PM_L}{\rho \pi R^3 V_T^2}$
CYMB-L	Left Rotor Yawing Moment	$\frac{YM_L}{\rho \pi R^3 V_T^2}$
CTB-R	Right Rotor Thrust Coefficient	$\frac{T_R}{\rho \pi R^2 V_T^2}$
CPB-R	Right Rotor Power Coefficient	$\frac{HP_L \times 550}{\rho \pi R^2 V_T^3}$
CNFB-R	Right Rotor Normal Force Coefficient	$\frac{NF_R}{\rho \pi R^2 V_T^2}$
CSFB-R	Right Rotor Side Force Coefficient	$\frac{SF_R}{\rho \pi R^2 V_T^2}$
CPMB-R	Right Rotor Pitching Moment	$\frac{PM_R}{\rho \pi R^3 V_T^2}$

LIST OF SYMBOLS (continued)

SYMBOL	NOMENCLATURE	UNITS
CYMB-R	Right Rotor Yawing Moment	$\frac{YM_R}{\rho \pi R^3 V_T^2}$
CLW-AC	Aircraft Lift Coefficient	$\frac{Lift}{1/2 \rho V^2 S}$
CSFW-AC	Aircraft Side Force Coefficient	$\frac{SF}{1/2 \rho V^2 S}$
CAFN-AC	Aircraft Axial Force Coefficient	$\frac{Axial\ Force}{1/2 \rho V^2 S}$
CPMW-AC	Aircraft Pitching Moment	$\frac{Pitch\ Moment}{1/2 \rho V^2 S \bar{c}}$
CYMW-AC	Aircraft Yawing Moment	$\frac{Yaw\ Moment}{1/2 \rho V^2 Sb}$
CRMW-AC	Aircraft Rolling Moment	$\frac{Roll\ Moment}{1/2 \rho V^2 Sb}$
$\bar{c}$	Wing Chord	FT
D	Diameter	-
D'	Airframe Drag	LB
EI_{FLAP}	Flapwise Bending Stiffness	-
EI_{CHORD}	Chordwise Bending Stiffness	-
FM	Figure of Merit	-
GJ	Torsional Stiffness	-
GW	Gross Weight	LB
HP	Rotor Horsepower	HP
I_{xx}, I_{yy}, I_{zz}	Mass Moment of Inertia about the Three Axes	IN-LB SEC^2
I_N	Nacelle Incidence	Deg
I_p	Acceleration Pitch Inertia	-
H_Z	Hertz	-

LIST OF SYMBOLS (continued)

SYMBOLS	NOMENCLATURE	UNITS
I^*_p	Centrifugal Pitch Inertia	-
I_{PIVOT}	Moment of Inertia - Polar	LB-FT
i_w	Wing Incidence	Deg
L	Lift	LB
NA	Neutral Axis	-
p	Per Rotor Revolution	-
PM	Pitching Moment	FT LB
q	Freestream Dynamic Pressure $1/2\rho V^2$	LB/FT^2
R	Rotor Radius	FT
r	Radial Location to a Blade Station	FT
RM	Rolling Moment	FT LB
S	Wing Area	FT^2
SF	Side Force	LB
T	Rotor Thrust	LB
t	Airfoil Thickness	FT
V	Freestream Velocity	FT/SEC
V_T	Rotor Tip Speed	FT/SEC
X	Aircraft Propulsive Force	LB
X/R or r/R	Non-Dimensional Radius	-
YM	Yawing Moment	FT LB
α	Angle of Attack	-
α_f	Fuselage Pitch Deflection	Deg
α_s	Nacelle Shaft Pitch Deflection	Deg

LIST OF SYMBOLS (continued)

SYMBOLS	NOMENCLATURE	UNITS
β	Side Slip Angle	Deg
δ_A	Aileron Deflection	Deg
δ_F	Flap Deflection	Deg
∂	Partial Derivative Operator	-
Δ	Increment In Coefficient	-
$\Delta\theta$	Incremental Blade Pitch	-
ρ	Density of Air	LB SEC^2/FT^4
σ	Rotor Solidity $\frac{bcR}{\pi R^2}$	-
ψ	Rotor Azimuth Angle	Deg
θ_{75}	Rotor Blade Collective Pitch at the Three Quarter Radius	Deg
μ	Advance Ratio V/V_T	-
ω_α	Wing Torsional Frequency	cps
ω_β	2nd Mode Bending Blade Frequency	-
ω_C	Wing Chordwise Bending Frequency	cps
ω_L	1st Mode Bending Blade Frequency	-
ω_P	Aircraft Pitch Frequency	cps
ω_V	Wing Vertical Bending Frequency	cps
Ω	Rotor Angular Velocity	-
$1\Omega, 2\Omega$	Integer Frequency Ratio	-
$\Omega-\omega\ell$	Lower Blade Lag Rotational Frequency	cps
$\Omega+\omega\beta$	Upper Blade Flap Rotational Frequency	cps
$\Omega-\omega\beta$	Lower Blade Flap Rotational Frequency	cps

LIST OF SYMBOLS (continued)

SYMBOLS	NOMENCLATURE	UNITS
ζ_V	Wing Vertical Bending Damping % Critical	-
ζ_C	Wing Chord Bending Damping % Critical	-
ζ_α	Wing Torsion Damping % Critical	-

SUMMARY

This report and the three appendix volumes present the results of a wind tunnel test of a 1/4.622 Froude scale tilt rotor model. This test was performed by the Boeing Vertol Company for the National Aeronautics and Space Administration Ames Research Center under NASA Contract NAS2-9015.

The test was designed to provide parametric force, moment and blade fatigue loads data over the normal anticipated flight range of the tilt rotor aircraft. This was done by selecting seventeen initial flight conditions ranging from hover through transition and out to 300 knots simulated full scale airspeed and measuring the effects of aircraft attitude, rotor control inputs, wing flap deflection and rotor RPM. The information obtained is contained in seventeen data files, four of which are in this volume and the remainder in volumes II, III and IV. Each file contains the experimental results at one flight condition.

The large volume of data produced makes it difficult to summarize. Instead a synopsis of the data is provided in section 2 of this report which demonstrates the quality and scope of the experimental results by means of specific examples.

Load control in cruise was investigated by means of "cyclic on the stick" (Reference 1) and it was found that a single

control law could provide low alternating loads over the cruise speed range.

The data provided needs further analysis and application to the mathematical model used to describe the rotor system in real time simulation by means of regression analyses. In this manner the large bulk of data can be reduced to manageable proportions and provide an understanding of the influence of the important parameters.

This volume contains details of the model, test program and data system and presents four data files in hover and transition. The rest of the transition data can be found in Volumes II and III and the cruise data in Volume IV.

1.0 INTRODUCTION

This document contains wind tunnel test data obtained on a 1/4.622 scale dynamically similar model of a tilt rotor aircraft which has composite hingeless blades. The test was performed under NASA contract NAS2-9015.

The objective of the test was to generate information on the behavior of rotor and airframe effects over a range of flight parameters representing the complete operating envelope of the tilt rotor vehicle. The information which was required included the magnitude and sensitivity of:

(1) Rotor forces and moments

(2) Blade loads and pitch link loads

(3) Wing rotor interference effects

(4) Airframe forces and moment

for values of such flight parameters as:

(1) Nacelle tilt angle

(2) Forward speed

(3) Aircraft attitude in pitch and yaw

(4) Collective and cyclic pitch control

(5) Wing flap deflection

The selection of test points and true variations for parameters was made in such a way that a comprehensive set of data was obtained for all potential flight conditions through hover, a wide envelope of transitions, and cruise at speeds up to 300 knots.

The purpose of this acquisition of comprehensive rotor and airframe test data is to provide the knowledge and basis for understanding rotor and airframe behavior which is an essential prerequisite to the development of an efficient system of integrated rotor and aircraft controls.

A secondary objective of the test was to determine the feasibility of a control system which minimizes blade loads in cruise. The characteristic feature of this system is the use of cyclic pitch geared by a simple mechanical linkage to the motion of the stick and control surfaces. These must be properly phased and scheduled to achieve good flying qualities in all flight regimes, subject to the overall design requirement of an optimal control system to maintain simplicity and reliability as far as is consistent with the loads, maneuver envelope and flying qualities of the aircraft.

The rotor controls provide a major portion of the control capability from hover through the low transition speed range, although the conventional control surfaces are operative in all regimes of flight including hover. As speed is increased, and the aerodynamic surfaces become effective for trim and control, the rotor controls can be directed at minimizing rotor loads. In cruise the problem reduces to determining the rotor control required to maintain minimum loads. Prior to this test, a limited amount of full scale experimental data existed for transition, and for cruise up to speeds of 192

knots (Reference 2). This test program extends the range of this data in the transition regime, and in cruise flight the range was extended up to the simulated speed of 300 knots.

The data obtained on this test goes a long way toward providing the information which is necessary to tackle the job of designing an optimized and integrated control system for a tilt rotor aircraft using a soft inplane hingeless rotor. Work which remains to be done involves reducing the data obtained in the test, to an analytical format with forces, moments, loads, etc., expressed as functions of the relevant flight parameters. This is necessary for two reasons:

(1) to provide an understanding of the significance and relative importance of the parameters which will permit efficient planning of future full scale tests

(2) to provide a set of simple functions representing the body of test data, from which the rotor effects may be calculated within the context of a real time simulation

This reduction of the test data to analytical functions of the parameters is beyond the scope of the current contract. It is planned that this additional step will be accomplished in the near future under separate funding.

The data obtained during this test is presented in four volumes.

Volume I contains a detailed description of the model, the test installation, test procedures and data reduction: for the convenience of the user, an abbreviated discussion of these is included in Volumes II, III and IV. It was felt that the amount of data generated was too voluminous to be readily presented in a single volume, and Volumes II, III and IV present all the data in a logical sequence.

2.0 SYNOPSIS OF RESULTS

The scope of the test program is sufficiently large that a comprehensive analysis and review of the test data would be a major undertaking. The analysis, correlation and modelling of the experimental information is beyond the scope of the contractual work reported here; however, some examples have been taken and correlation effected to provide some insight as to the range and validity of the information available.

The primary objective of the test was to measure force and moment parametrics over the flight range. The examples discussed in the following paragraphs provide an indication of the range and validity of the experimental data.

The normal force produced by a lateral cyclic (test axes system) control input is shown as a function of rotor shaft angle in hover and transition in figures 1 and 2.

In hover, the derivative is over predicted by the real time mathematical model of the rotor system (Ref. 7). Correlation is good at 45 knots (full scale) and 100 knots (full scale). The 100 knot (full scale) data also shows good agreement with the data point taken from full scale tests in the NASA-Ames 40' x 80' wind tunnel performed in 1972 (Reference 2). Similar correlation is apparent at 140 knots, Figure 2; however, at 180 knots a discrepancy in the curve shape is evident.

In cruise, with almost axial flow conditions, the magnitude of the $\partial CN/\partial A_1$ derivative should be equal to $\partial CSF/\partial B_1$ from considerations of symmetry. Figure 3 shows the measured derivative data as a function of forward speed out to 300 knots (full scale). Three data points taken from full scale tests (Reference 2) are superimposed and show good agreement. The line shown is the $\partial CN/\partial A_1$ derivative as computed from the real time simulation math model and indicates an adequate representation of the experimental data.

The effect of B_1 cyclic on normal force in transition is shown in figures 4 and 5. In hover the derivative is under predicted. Referring back to the A_1 data (figure 1) it is possible to compare the resultant force magnitude due to cyclic from both test and the math model. The test indicates a 9% increase in control power over the math model representation; however, there is a discrepancy in the azimuthal angle at which the control input must be made which needs to be resolved. The $\partial CN/\partial B_1$ derivative is under predicted at both 45 and 100 knots, although the functional variation with angle of attack has clearly the correct form. At 140 knots (figure 5) the correlation of the math model representation is good at the higher values of α. A discrepancy exists between the model data and the full scale data of Reference 2 which needs further examination. The data at 180 knots display a similar trend to the A_1 derivative data of figure 2 and need a modification of the math model to adequately describe the data in this area of the envelope.

The cruise $\partial CN/\partial B_1$ derivatives are of the same magnitude as the $\partial CSF/\partial A_1$ derivatives again from symmetry and are plotted as a function of forward speed in figure 6. The data agree well with both the real time simulation math model and the 40' x 80' tunnel test data (Reference 2).

The behavior of the rotor hub pitching moment derivative with B_1 cyclic pitch in hover and transition is provided in figures 7 and 8. The hub moment data are under predicted by the simple model and the data show an initial rise due to angle of attack not adequately accounted for in the simulation representation. The conditions where full scale data are available from Reference 2 again show good agreement with the model scale data.

The hub pitching moment due to B_1 cyclic are the same magnitude as hub yaw moment due to A_1 cyclic in symmetrical in flow conditions. Figure 9 shows a comparison of the measured data out to 300 knots (full scale).

For an isolated rotor the derivative of rotor normal force with shaft angle of attack would be expected to be of the same magnitude as the side force due to yaw angle from symmetry considerations. This symmetry is disturbed on the airplane by the interference effects of the airframe, primarily due to the wing circulation induced velocities at the rotor. The

derivatives of normal force with angle of attack and side force with yaw angle are plotted as functions of forward speed in figure 10. The amplification of the normal force derivative due to airframe/rotor interference is clearly visible. The simulation math model does an adequate job of predicting the total normal force derivative.

The rotor hub pitching moment derivative with angle of attack data is shown for cruise conditions in figure 11 and clearly indicates a sign reversal at approximately 220 knots. Above this airspeed the rotor hub moment is a stabilizing influence on the aircraft. The model scale data agree well with full scale test results; however, the real time math model does not take advantage of the stabilizing effect. The pitch moment due to yaw is shown in figure 12 and shows good correlation up to 220 knots full scale. The correlation deteriorates beyond this airspeed. Alternating blade bending loads occur on the blade as a result of the one per rev forcing produced by inclination of the rotor shaft to the airstream. Figures 13 and 14 show the increase in sensitivity of alternating blade chord and flap bending loads as airspeed increases. The data agree well with full scale data. The application of cyclic pitch control in cruise also causes one per rev forcing of the blade modes. The bending loads per degree of cyclic in cruise are shown in figure 15 and indicate an approximately constant sensitivity over the cruise flight range.

One of the objectives of the test program was to test the "cyclic on the stick" control as a means of blade load alleviation in cruise flight. This system introduces cyclic pitch as a function of longitudinal stick position in cruise to trim out the one per rev loads in much the same manner as is done on a helicopter in forward flight. It should be noted that this system is not an adaptive feedback controller but a straight forward link between stick position and rotor controls.

Figure 16 shows the resultant alternating blade bending moments measured on angle of attack sweeps plotted as a function of maneuver load factor at 140 knots for three different sets of conditions. The load levels which correspond to 10^8 cycles and 10^7 cycles (mean - 3σ) fatigue life from reference 3 are shown superimposed. For 1g level flight at this speed, the aircraft trims at a nose up attitude and would produce alternating load levels of about 4630 N-m (41,000 in lbs) if no cyclic pitch is used. Tests were performed where cyclic pitch was introduced as a function of angle of attack in an attempt to match the cyclic pitch - angle of attack relationship produced by the cyclic pitch on the stick design of reference 1 . The schedules did not match precisely. This test shows a reduction in rotor blade fatigue loads of about 25% at 1g level flight.

A third test was made to determine the optimum cyclic schedule and the loads resulting from it and this is shown in figure 16

as the minimum loads cyclic schedule line. Similar data is shown in figure 17 for 220 knots full scale. In this case the 1g trim angle of attack is a small nose up angle and the "no cyclic" loads would provide less than 10^8 cycles level up to 1.46g's. The precalculated cyclic schedule would increase the g range within this load level to approximately 1.9g's. If the optimum cyclic pitch schedule were used then the loads can be maintained at 28% of the 10^8 cycles level up to and beyond a 2g maneuver. At 260 knots (full scale) figure 18, the aircraft can pull 1.9g's with less than 10^8 cycles $(m - 3\sigma)$ loads. With the pretest calculated cyclic schedule the loads at 1.9g's reduce to approximately 2598 N-m (23,000 in lbs) or 65% of the 10^8 cycles $(m - 3\sigma)$. At 300 knots full scale (figure 19) the pretest schedule provides loads less than 10^8 cycles $(m - 3\sigma)$ from 1g out to at least 2.3g's.

The cyclic pitch required to minimize the alternating loads at any angle of attack (or load factor) can be deduced from the test data obtained. Figure 20 shows the cyclic pitch levels required for minimum loads as a function of longitudinal stick position which can be related to airplane angle of attack by means of the simulation model. It is clear that no single relationship between cyclic pitch and stick position will provide optimum loads over the entire range; however, judicious selection of a control law can provide loads well

within the fatigue limits. The heavy line drawn through the data is one such law which has been selected so as to pass through the 1g points and is biased towards the low speed conditions. If this cyclic control law were used then the loads would reduce as shown in figures 21, 22 and 23 at 140, 220 and 300 knots (full scale) respectively. For 1g level flight, the loads are never greater than 30% of the 10^8 cycles ($m - 3\sigma$) load level and at 2g's are still within 73% of that level. These data are pertinent to a given gross weight, altitude and CG position and would change at other operating conditions. Further analysis needs to be performed to examine the impact of these considerations; however, the test has shown that a control system of this type can be an extremely powerful means of maintaining low fatigue loads.

The design rotor diameter of the XV-15 Tilt Rotor Research Aircraft is 7.6 m (25 ft.). If the Boeing 7.9 m (26 ft.) rotor were to be flown on that aircraft, a reduction of tip clearance of 75.2 cm (6 in.) could result. A run was made to assess the impact of tip clearance on blade loads by fitting a "scab-on" bulge on the side of the model fuselage to reduce the tip clearance. The loads measured with and without the bulge fitted are shown in Figure 24 and no effect on load level is in evidence.

During the development of the XV-15, model tests discovered the presence of an unstable yaw derivative at small yaw angles

in cruise which contributed to the decision to use an H tail. Figures 25, 26 and 27 show yaw derivatives for the model tested in this program and show a stable slope at all conditions.

The preceeding data and discussion is by no measure a complete evaluation of the test data obtained on the program reported in this and the appendix volumes; however, it does serve to provide an overview of the extent and quality of the experimental data obtained.

NORMAL FORCE DUE TO CYCLIC PITCH

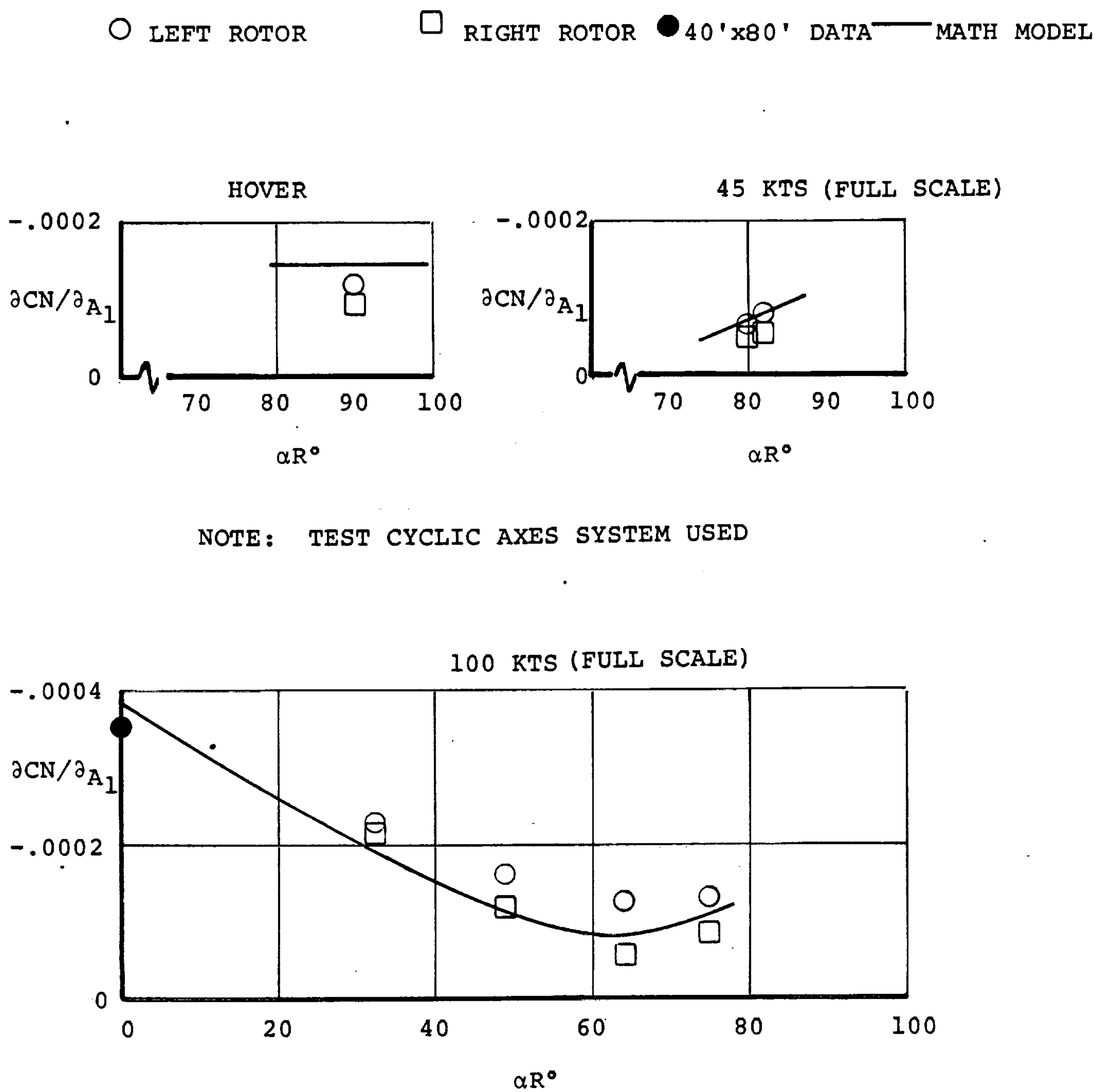

Figure 1. Rotor Normal Force Due to A_1 Cyclic in Hover, 45 and 100 Knots.

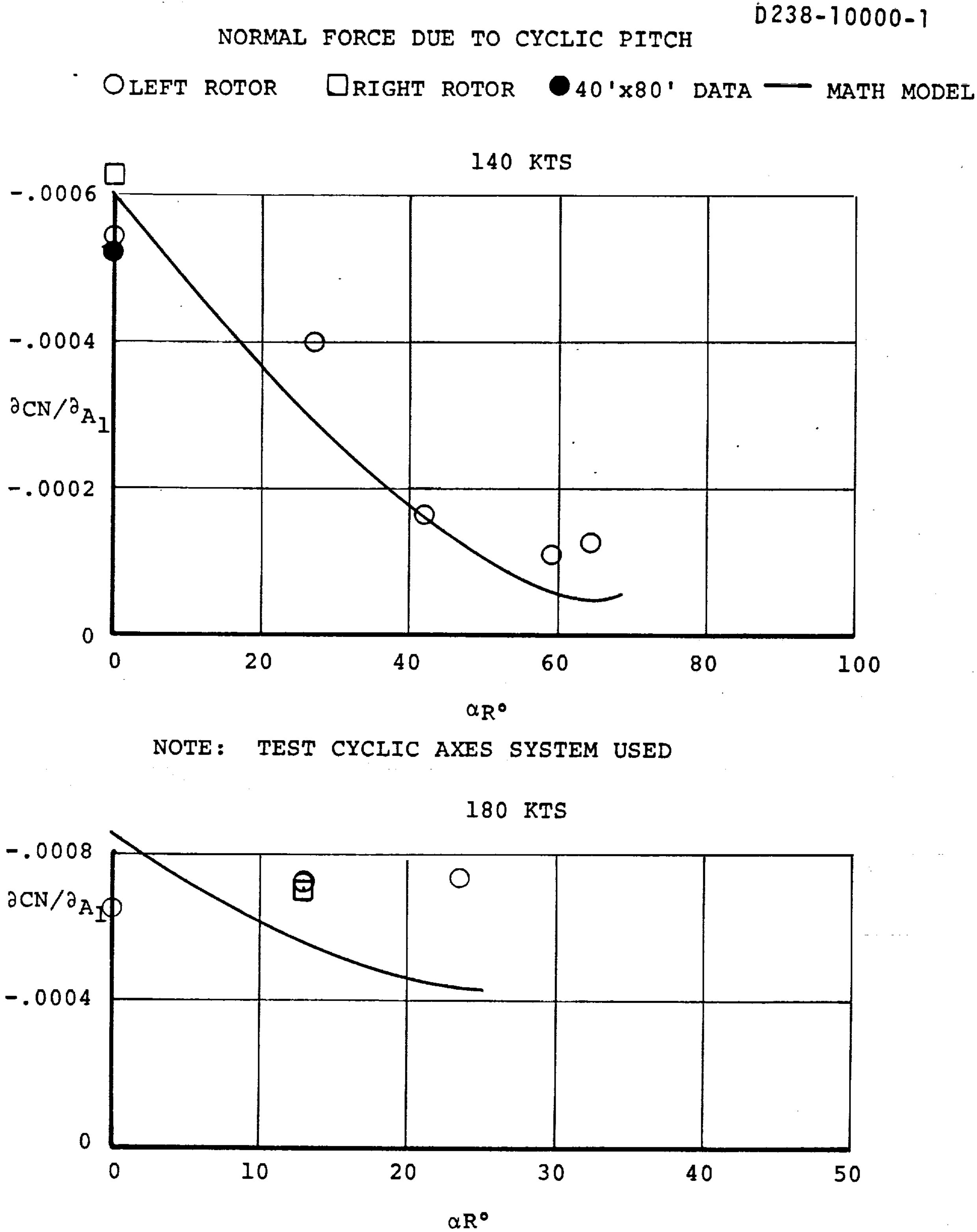

Figure 2. Rotor Normal Force Due to A_1 Cyclic at 140 and 180 Knots in Transition.

NORMAL FORCE DUE TO CYCLIC PITCH

$\partial CN/\partial A_1$

○ LEFT ROTOR □ RIGHT ROTOR ● 40'x80' DATA —— MATH MODEL
△ SIDE FORCE DATA

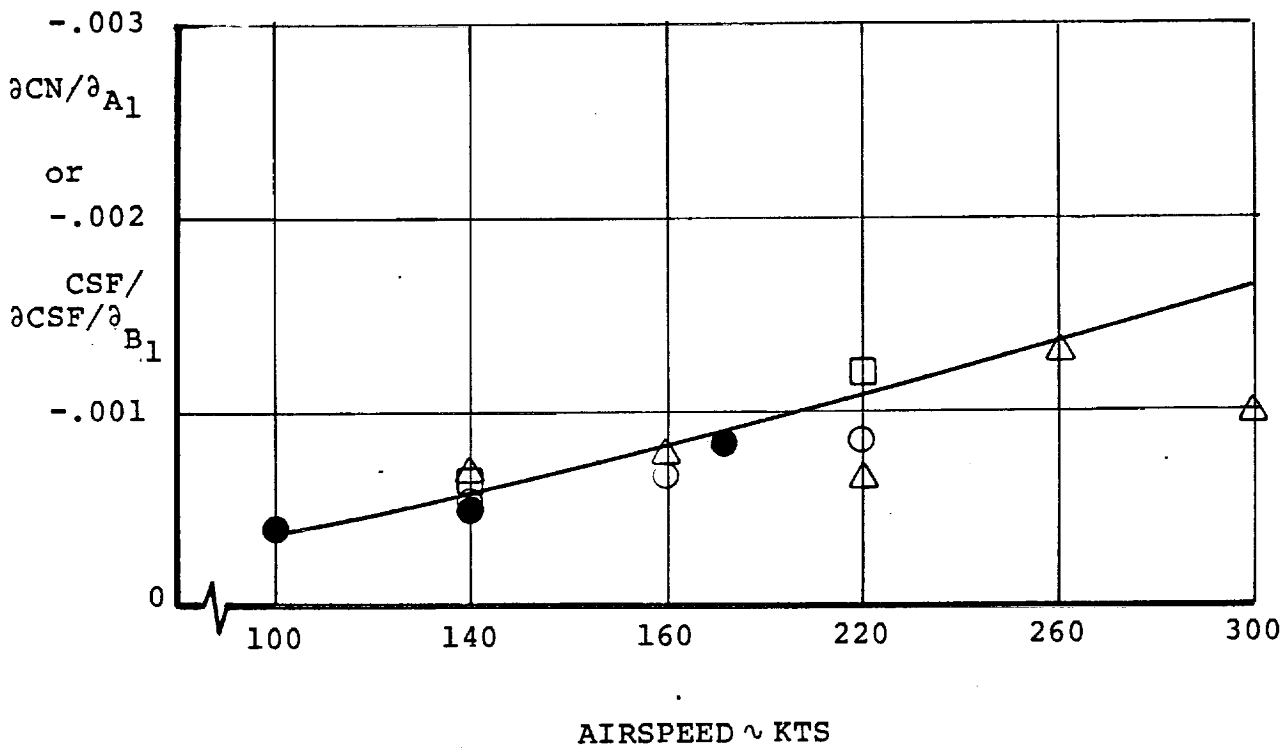

NOTE: TEST CYCLIC AXES SYSTEM USED

Figure 3. Rotor Normal Force Due to A_1 Cyclic and Blade Force Due to B_1 Cyclic in Cruise.

NORMAL FORCE DUE TO CYCLIC PITCH $\partial CN/\partial_{B_1}$

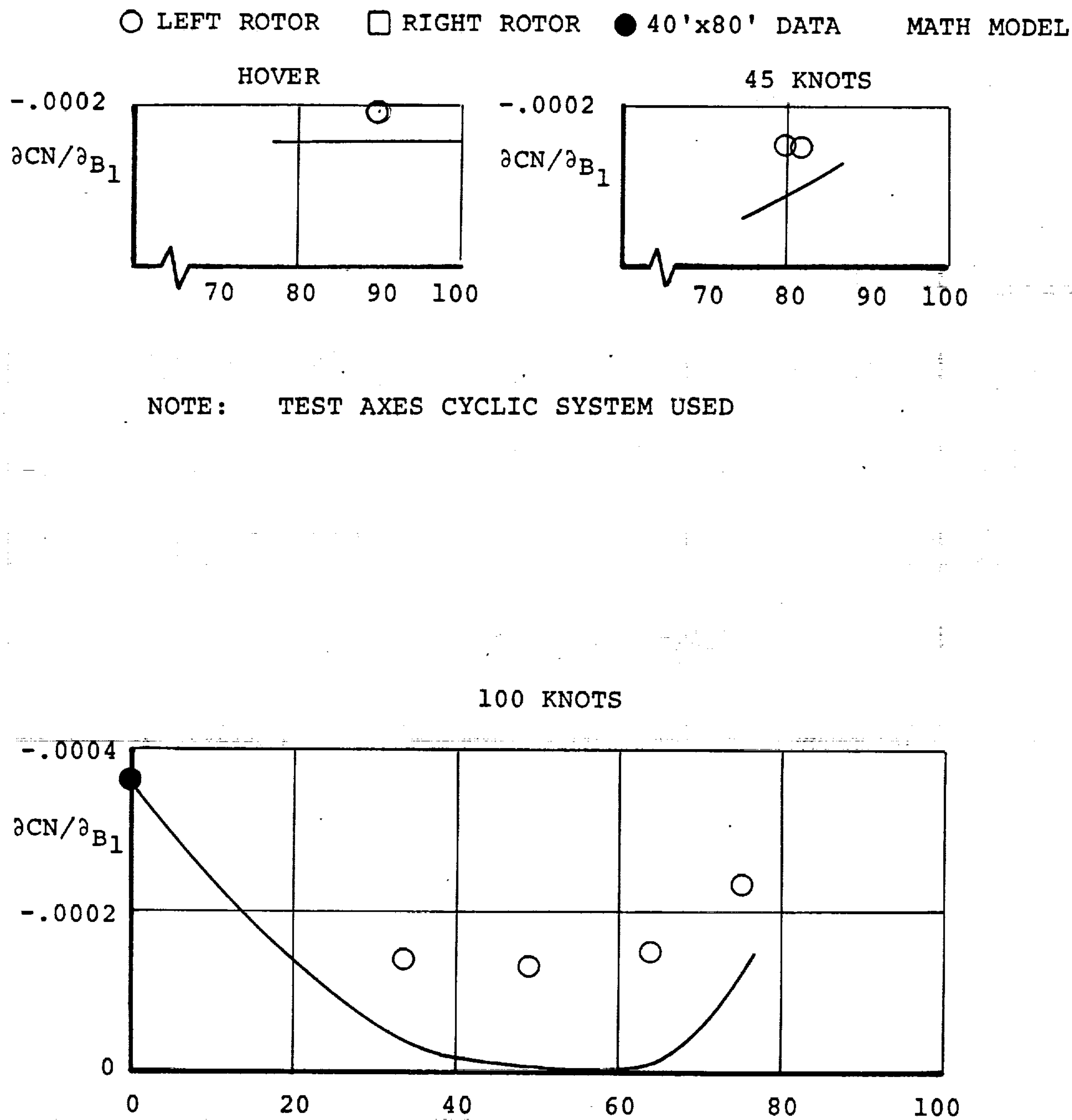

Figure 4. Rotor Normal Force Due to B_1 Cyclic Pitch in Hover and Transition.

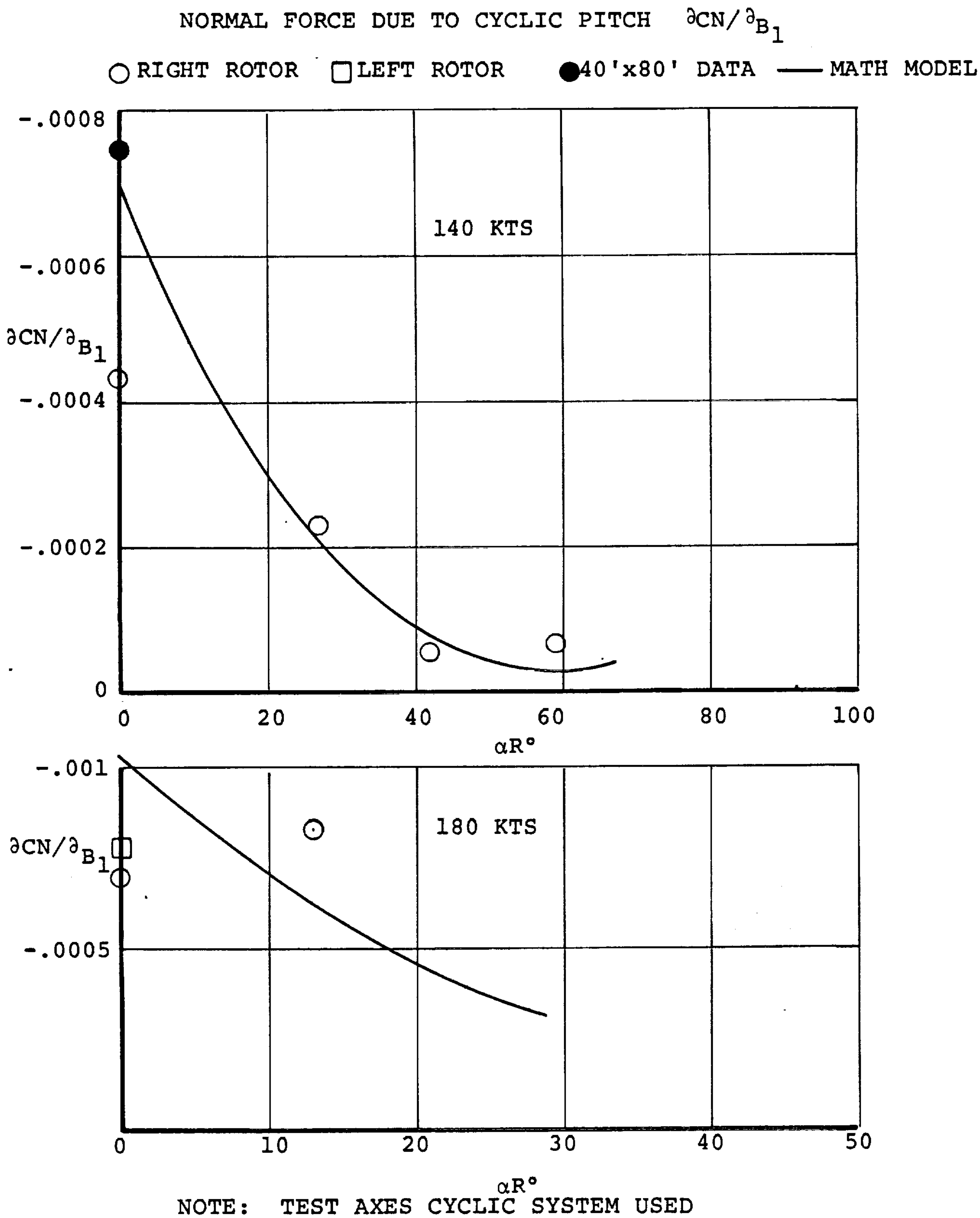

Figure 5. Rotor Normal Force Due to B_1 Cyclic Pitch in Transition.

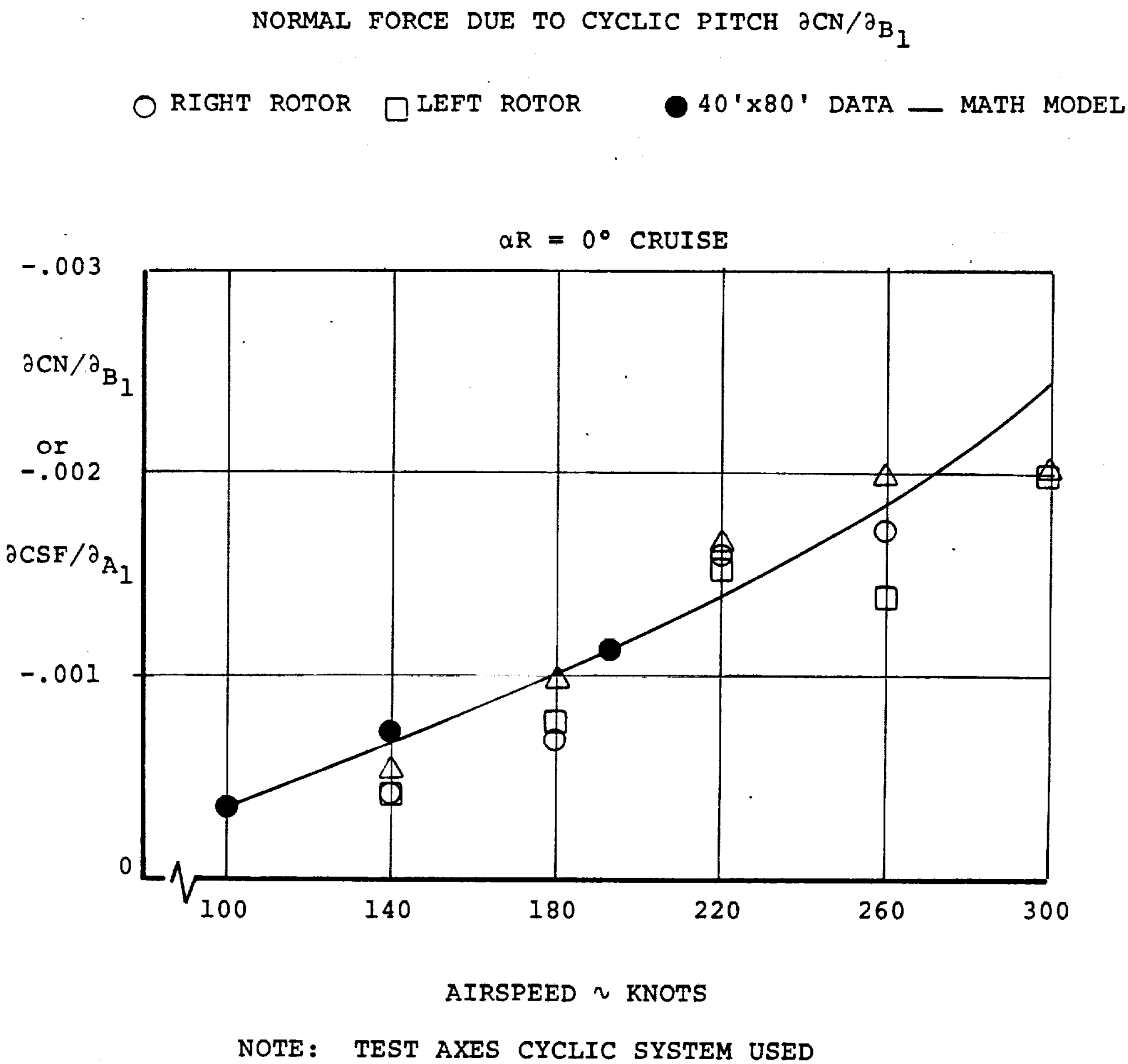

Figure 6. Rotor Normal Force Due to B_1 Cyclic and Side Force Due to A_1 Cyclic in Cruise.

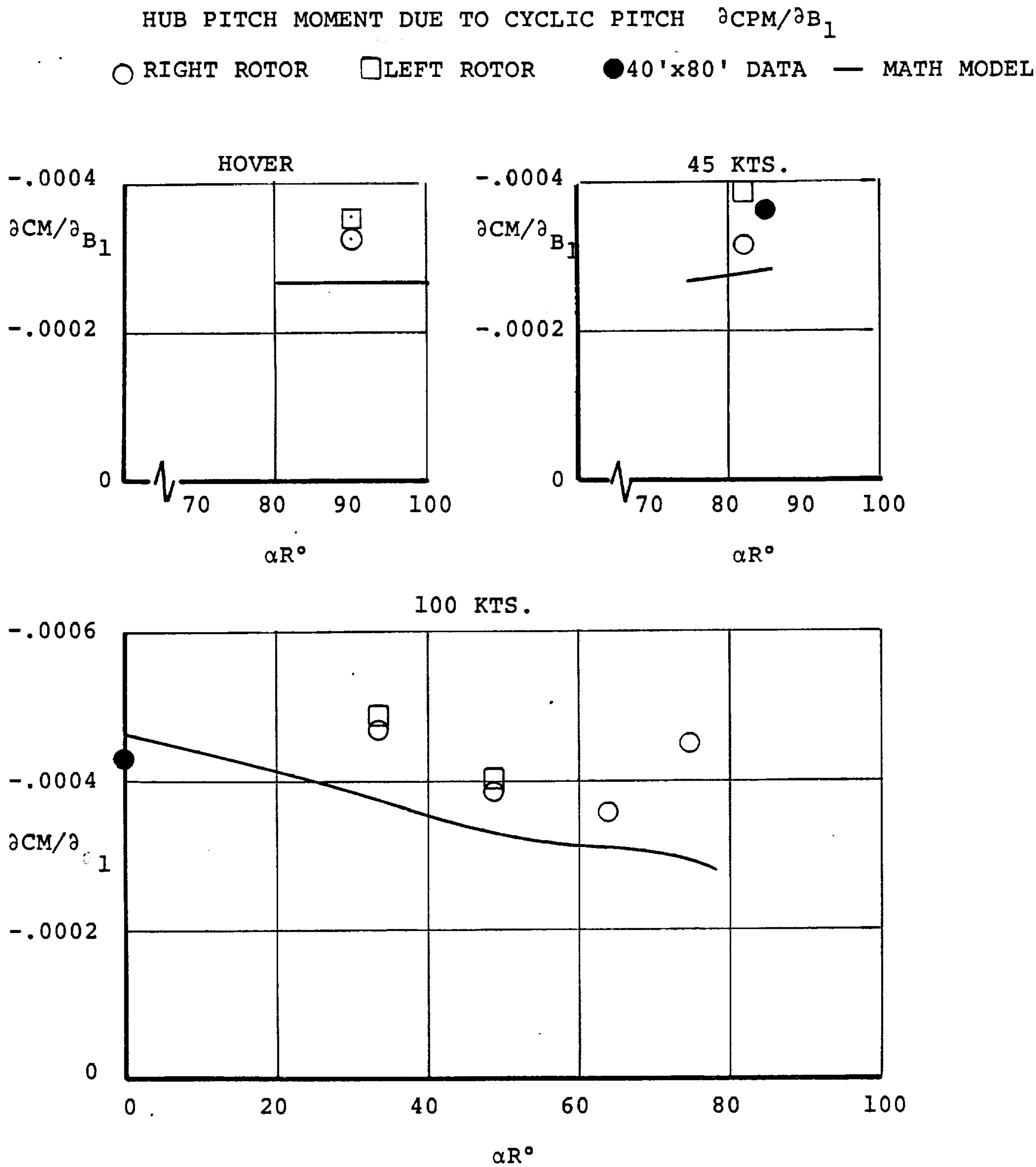

NOTE: TEST AXES CYCLIC SYSTEM USED

Figure 7. Rotor Hub Pitching Moment Due to B_1 Cyclic in Hover and Transition.

HUB PITCH MOMENT DUE TO CYCLIC PITCH $\partial CPM/\partial_{B_1}$

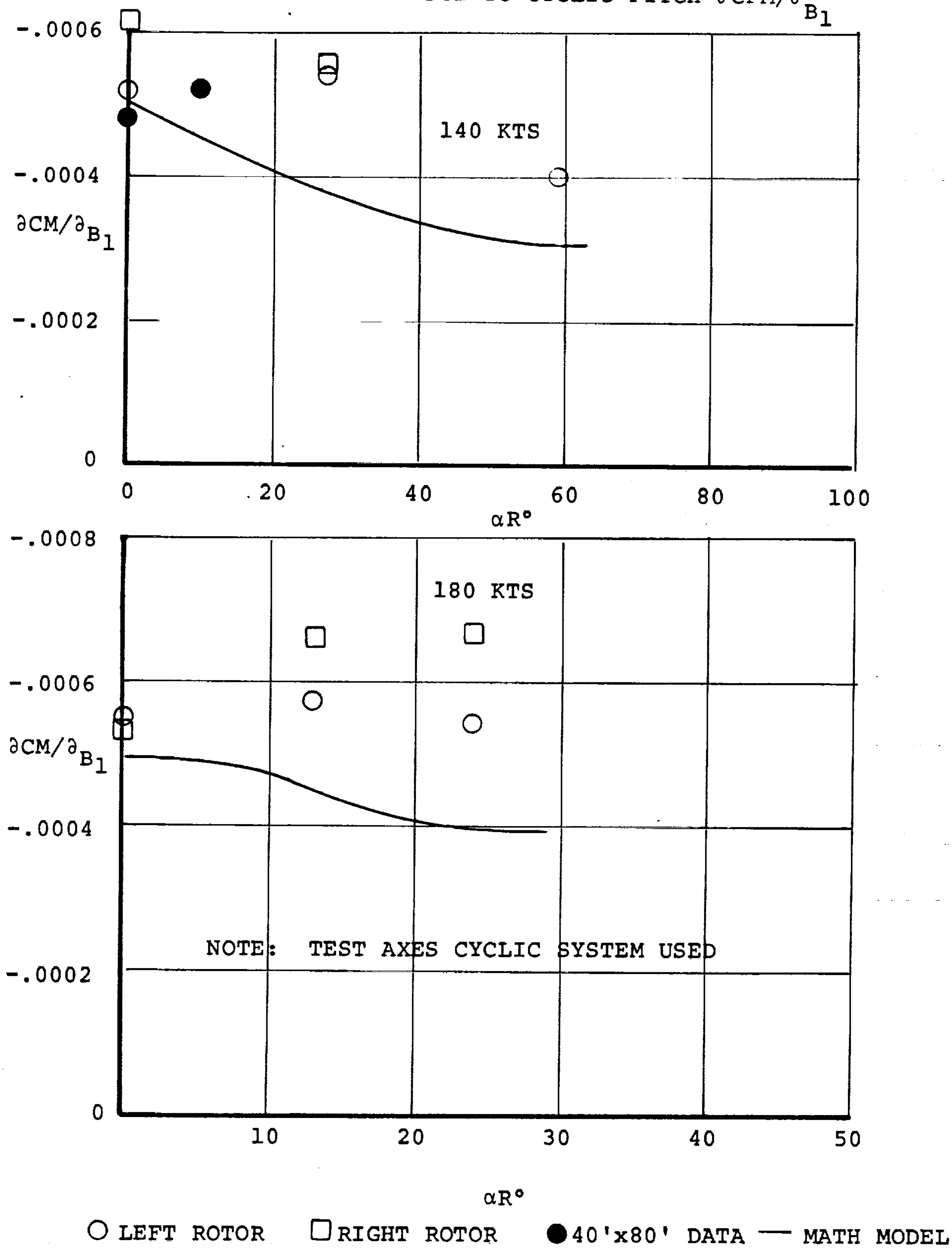

Figure 8. Rotor Hub Pitching Moment Due to B_1 Cyclic in Transition.

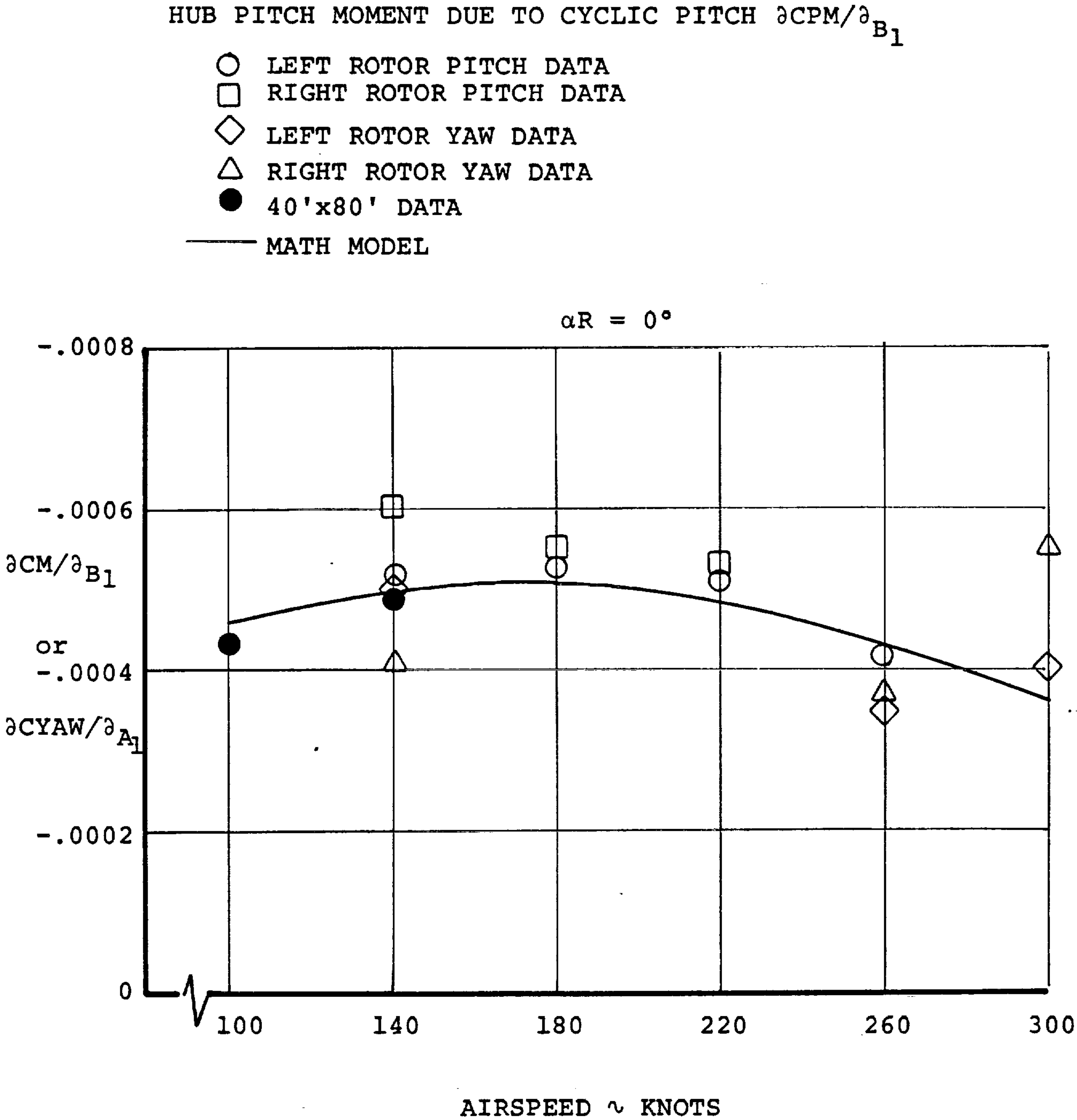

NOTE: TEST AXES CYCLIC SYSTEM USED

Figure 9. Rotor Hub Pitch Moment Due to B_1 Cyclic and Yaw Moment Due to A_1 Cyclic in Cruise.

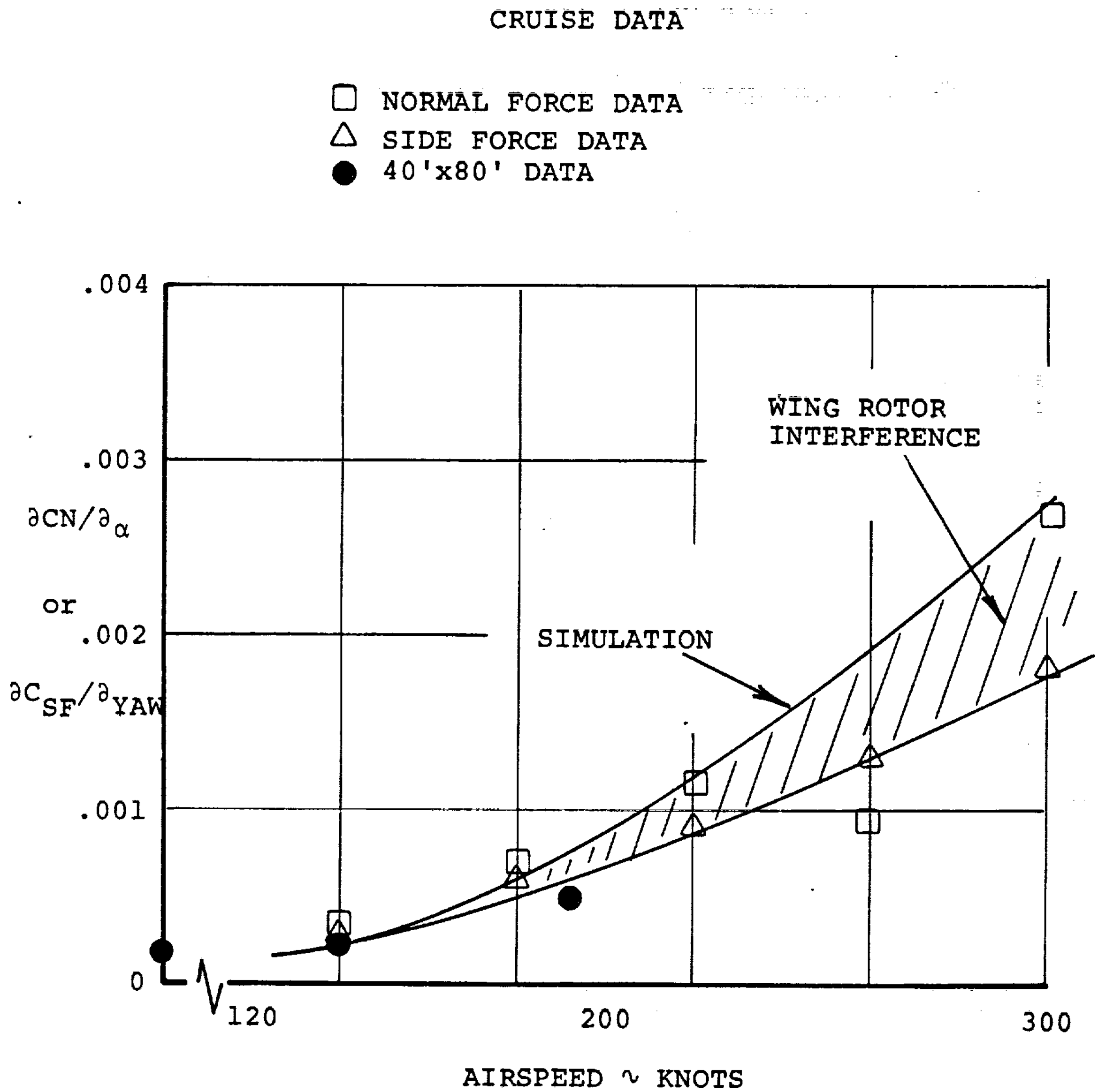

NOTE: TEST AXES CYCLIC SYSTEM USED

Figure 10. Rotor Normal Force Due to α and Side Force Due to Yaw Angle in Cruise.

CRUISE DATA

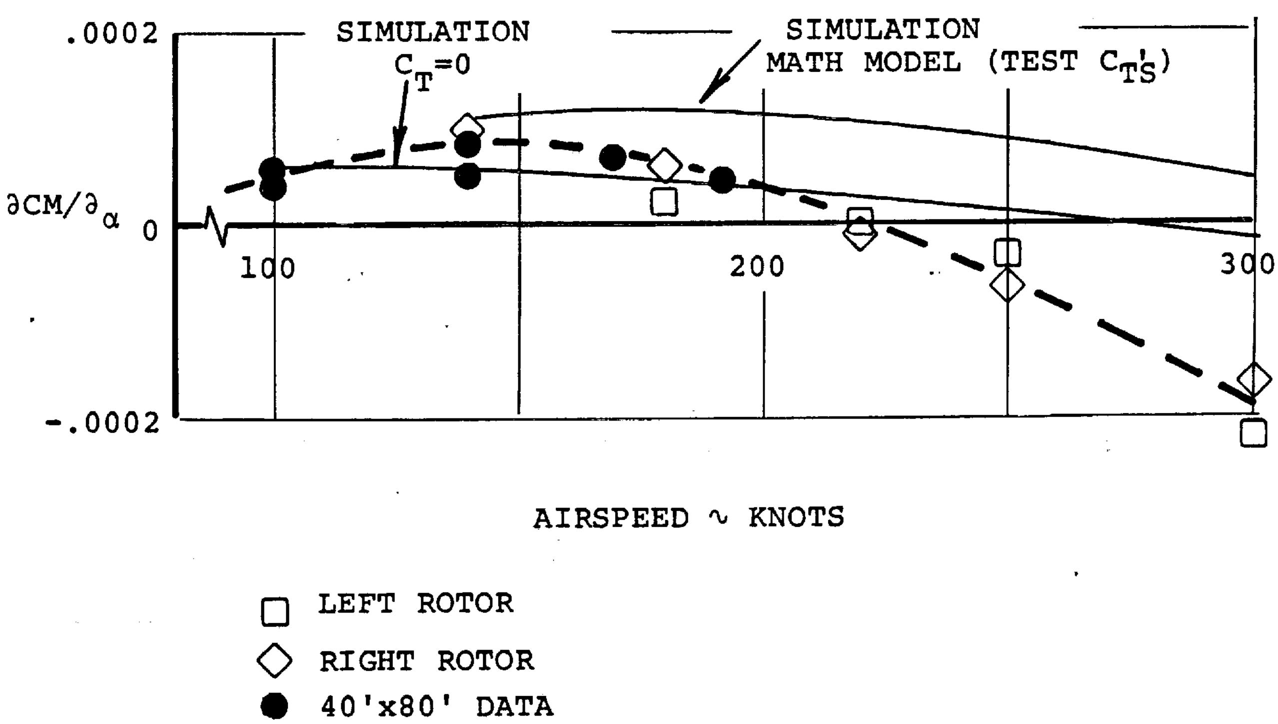

NOTE: TEST ACES CYCLIC SYSTEM USED

Figure 11. Rotor Hub Pitching Moment Due to Angle of Attack.

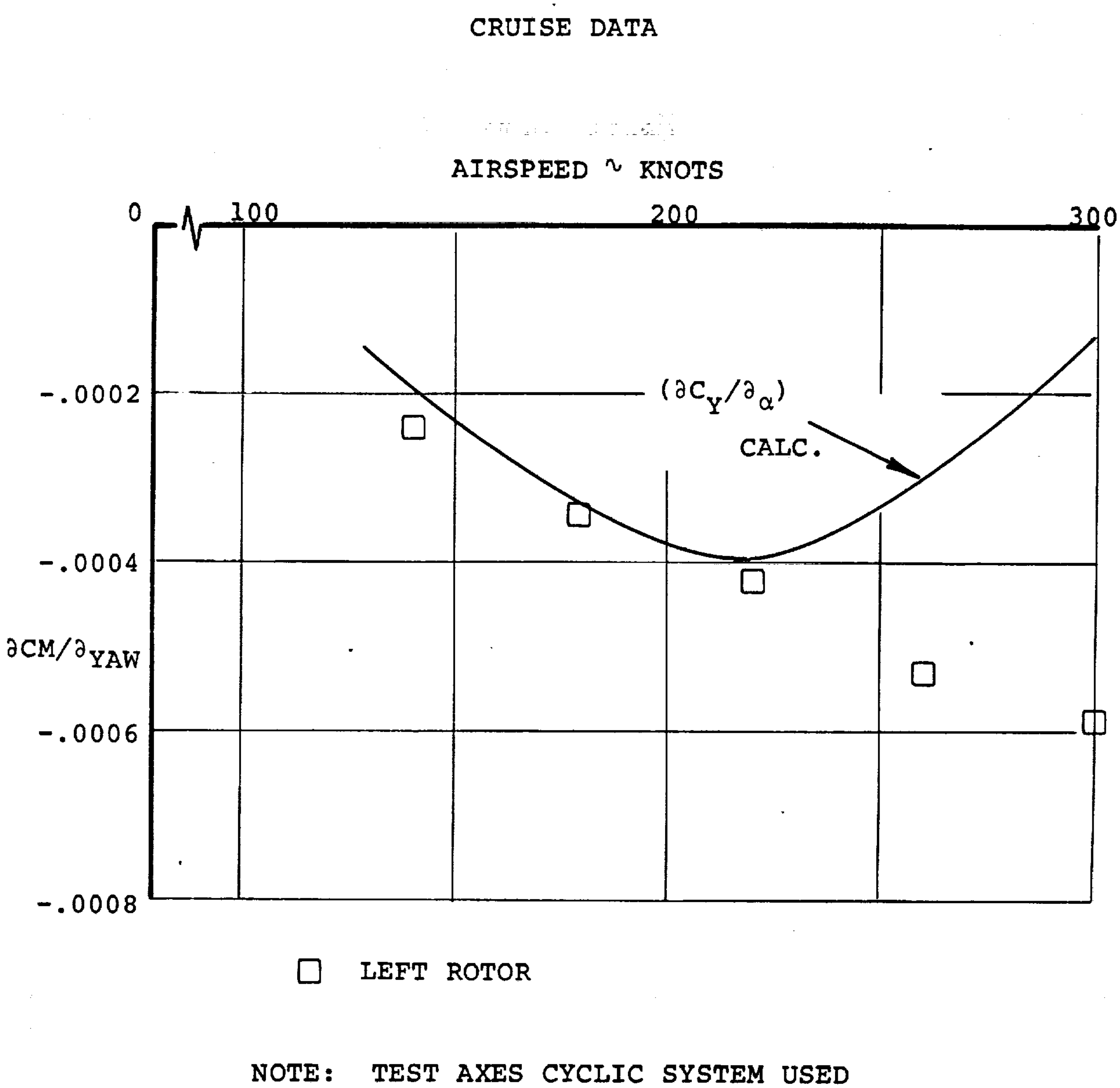

Figure 12. Rotor Hub Pitch Moment Due to Yaw Angle.

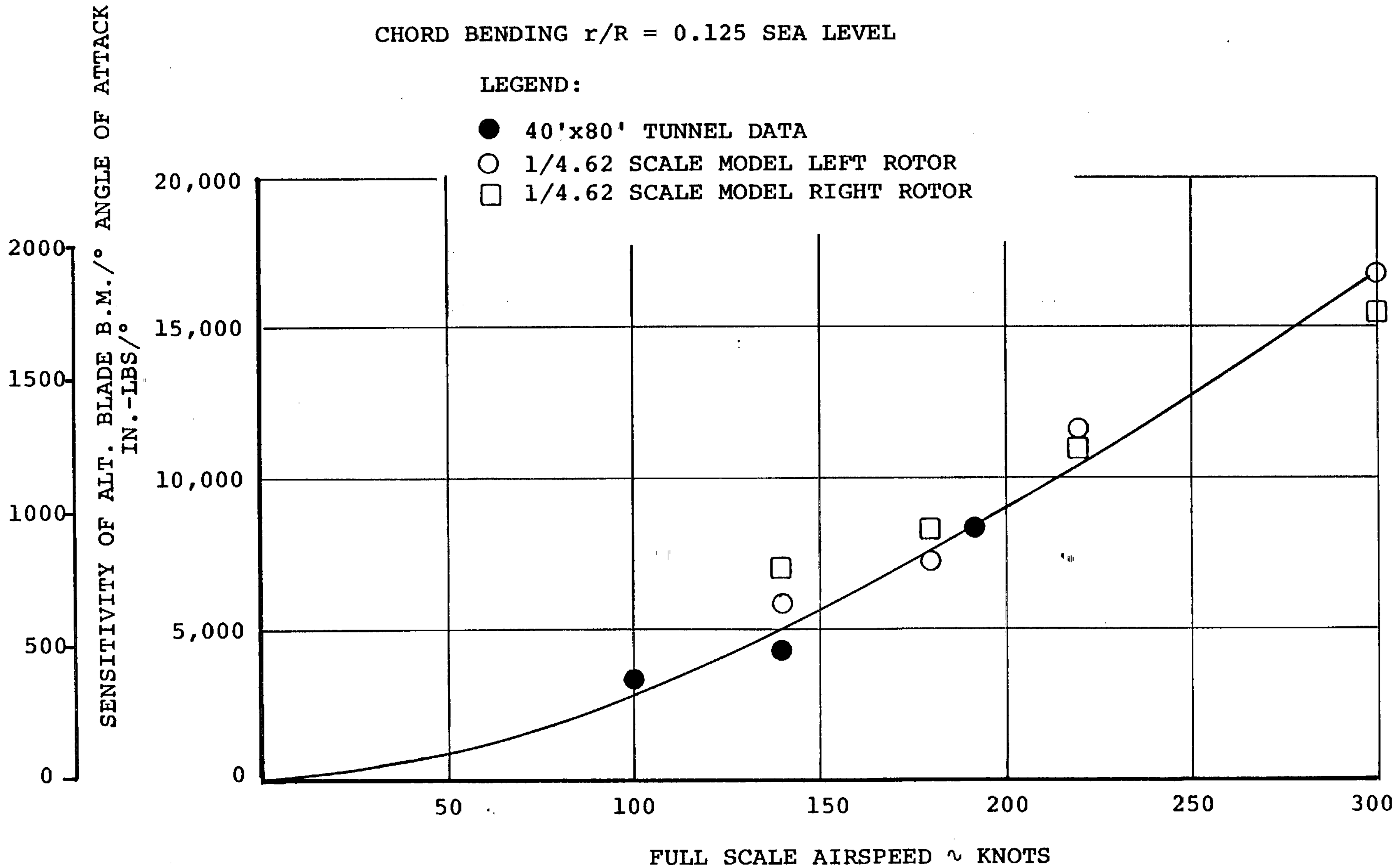

Figure 13. Sensitivity of Alternating Blade Chord Bending Moments to Angle of Attack in Cruise.

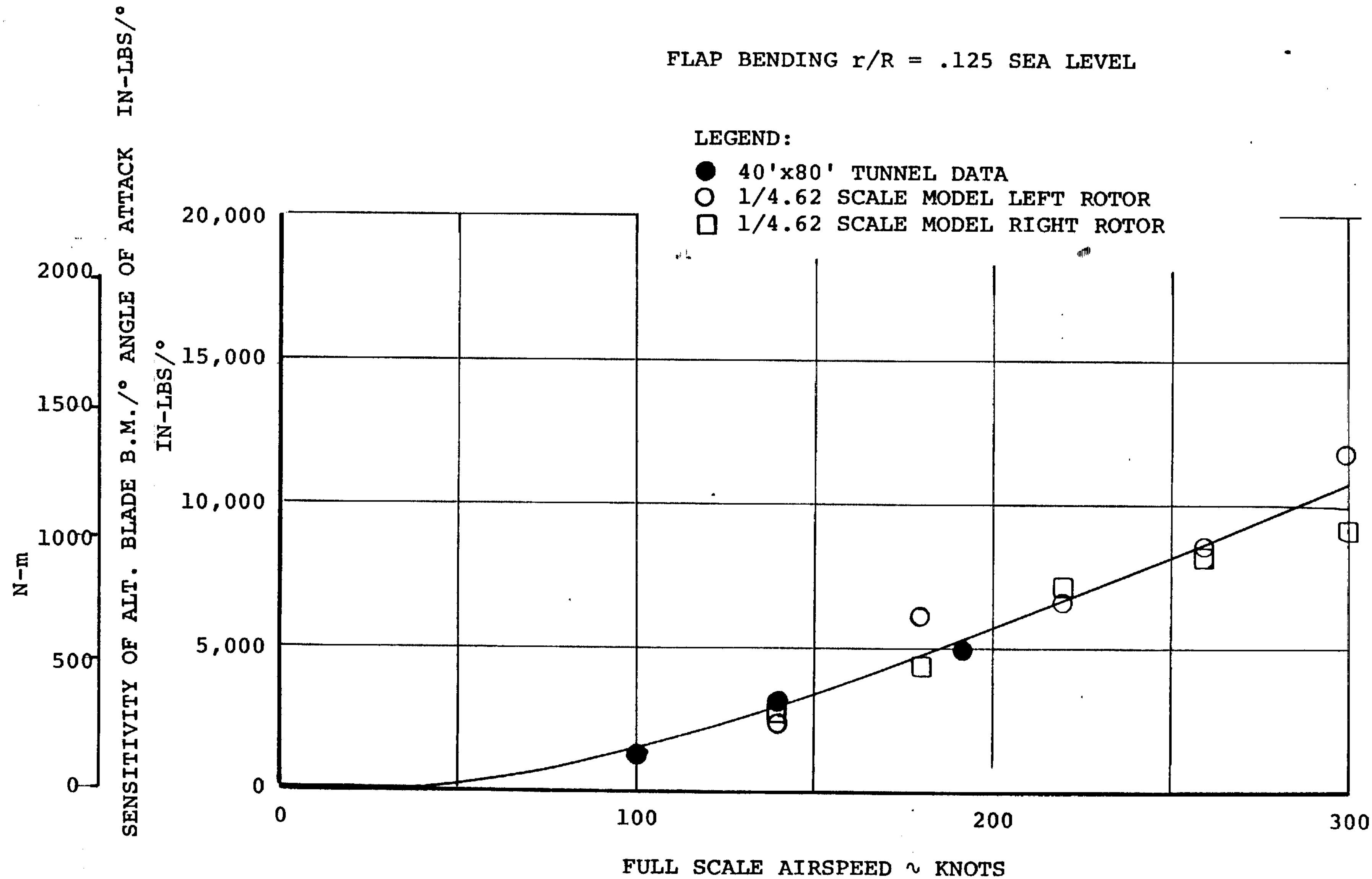

Figure 14. Sensitivity of Blade Flap Bending Moments in Cruise.

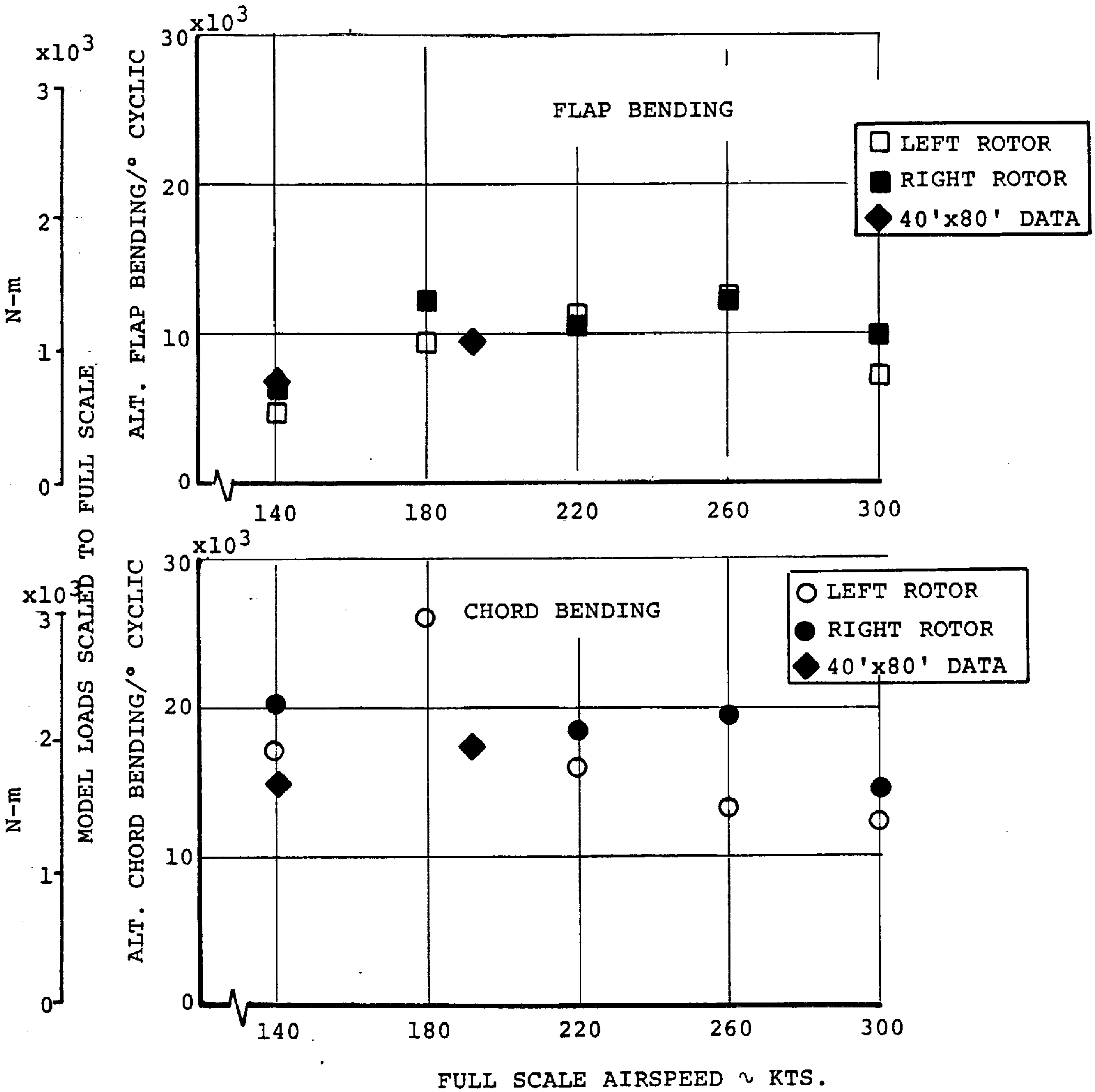

Figure 15. Sensitivity of Blade Bending Loads to Cyclic Pitch - Cruise.

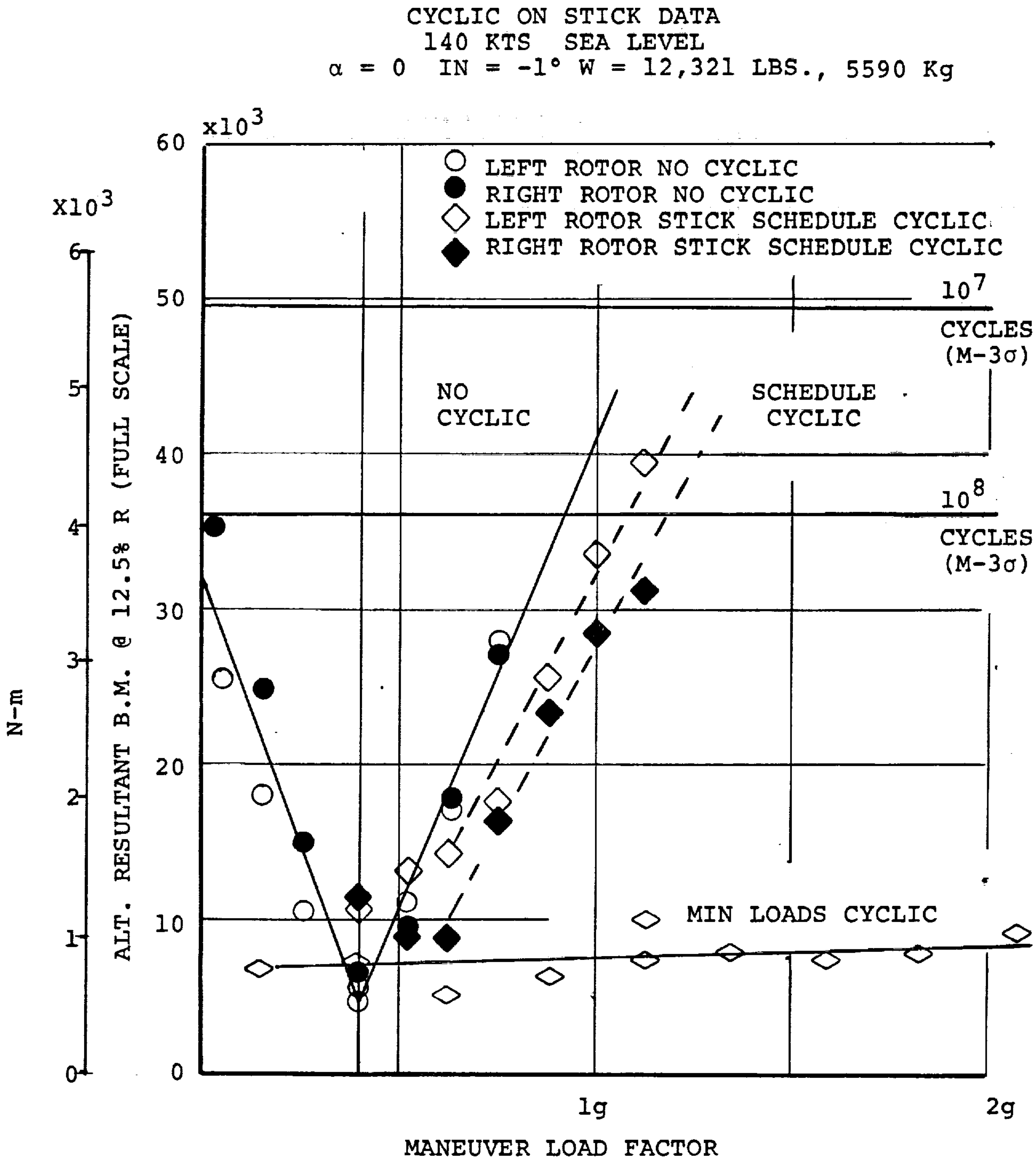

Figure 16. Alternating Blade Loads in Cruise With and Without Cyclic Pitch at 140 Knots (Full Scale).

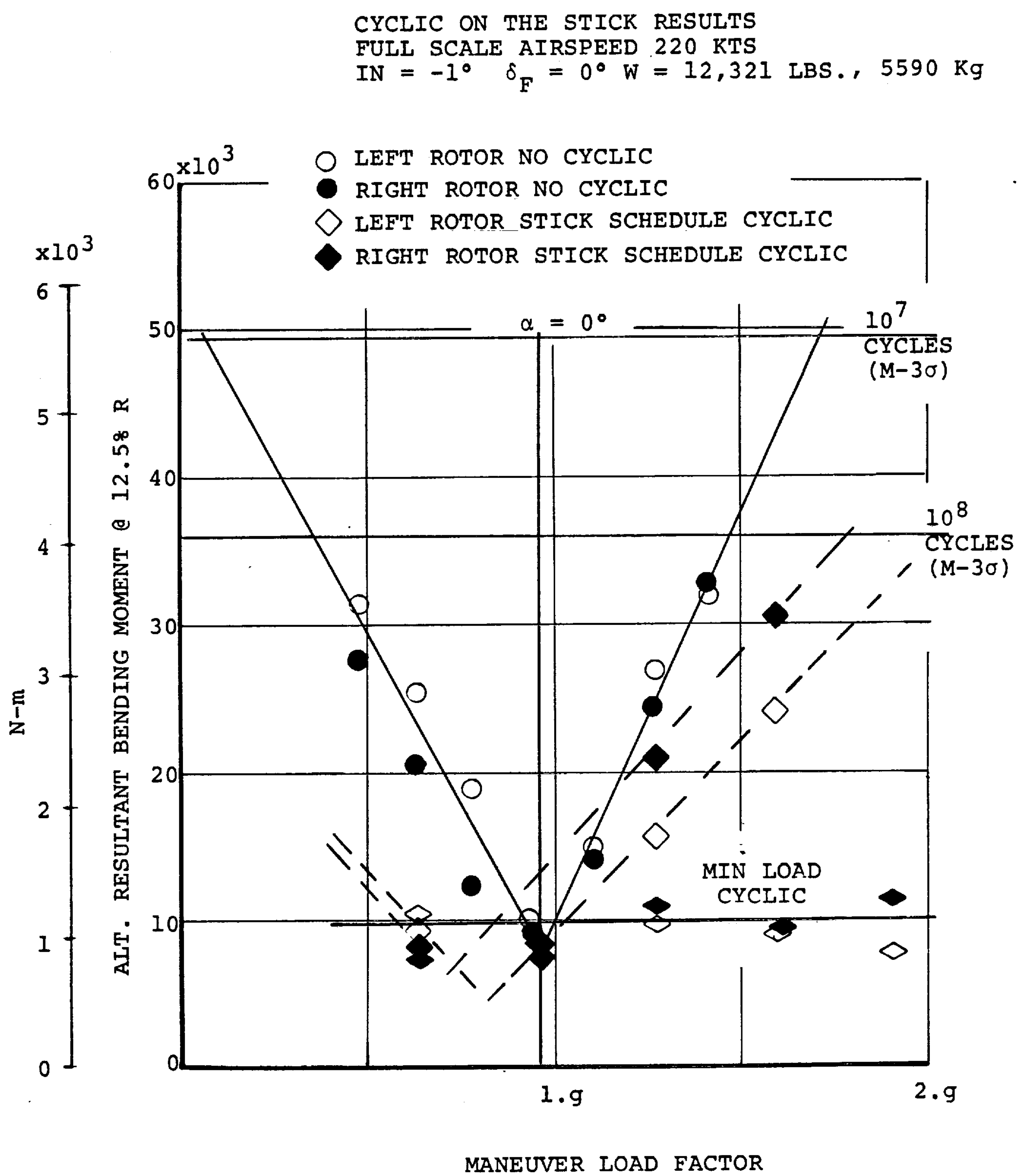

Figure 17. Alternating Blade Loads in Cruise With and Without Cyclic Pitch at 220 Knots (Full Scale).

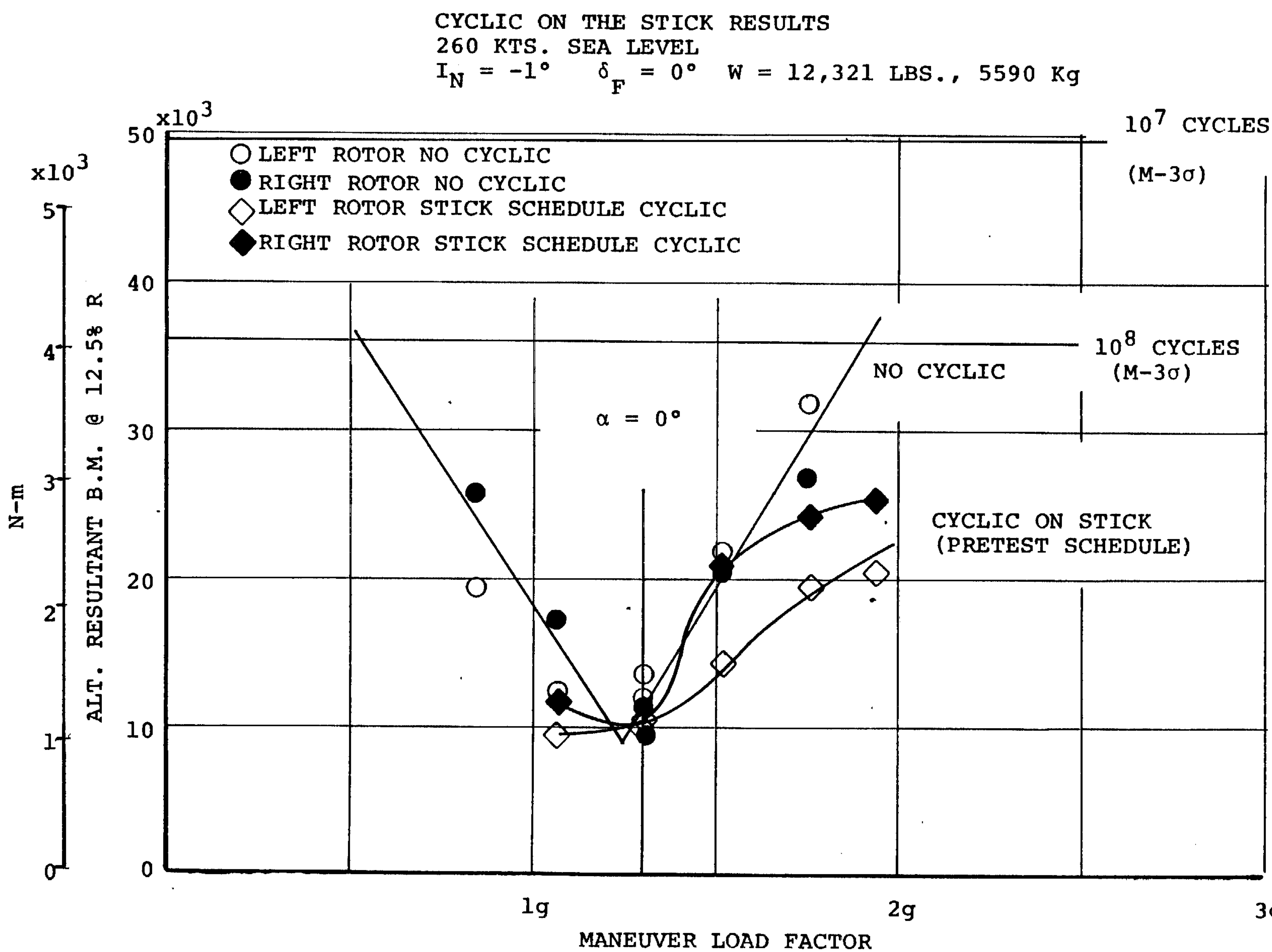

Figure 18. Alternating Blade Loads in Cruise With and Without Cyclic Pitch at 260 Knots (Full Scale).

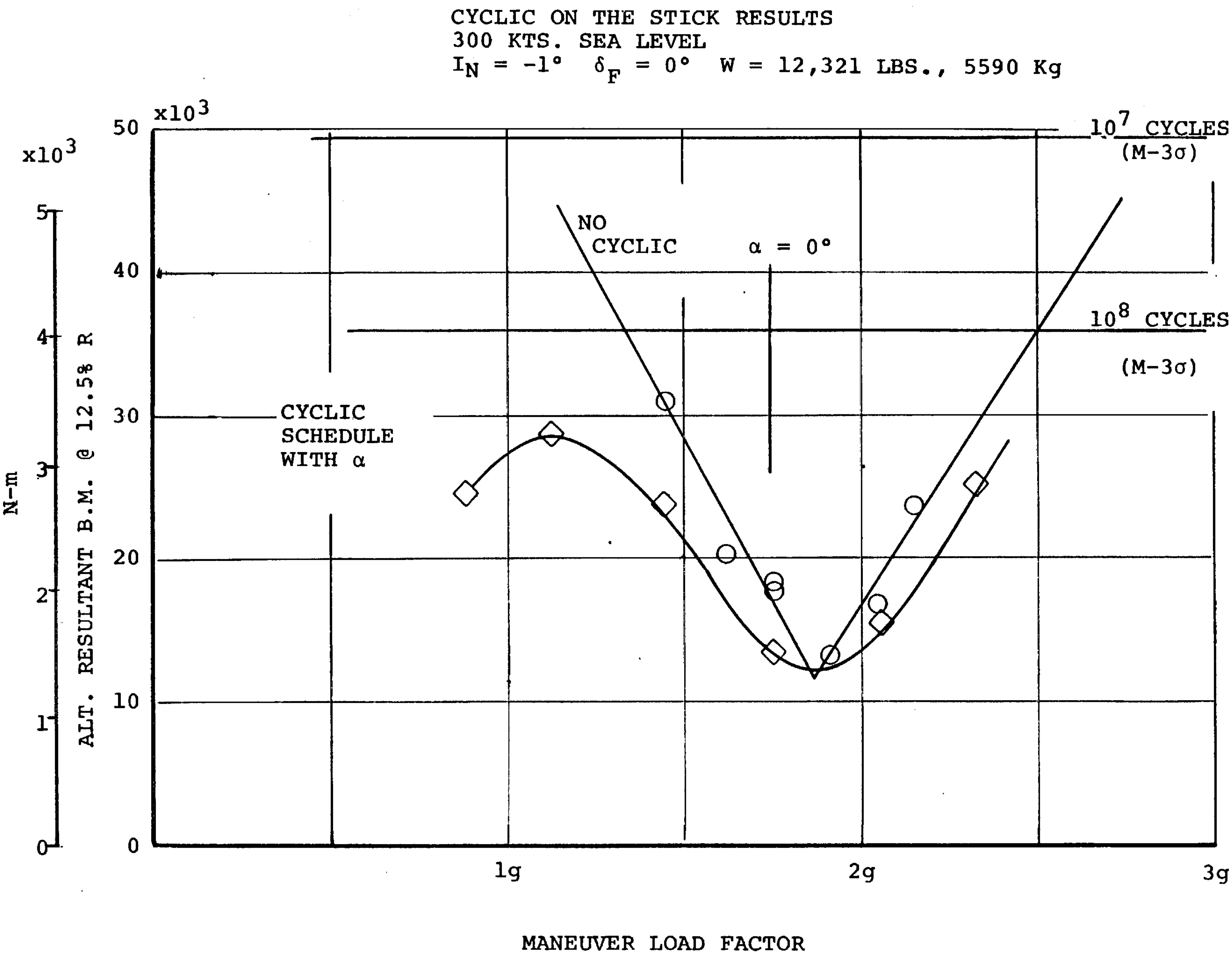

Figure 19. Alternating Blade Loads in Cruise With and Without Cyclic Pitch at 300 Knots (Full Scale).

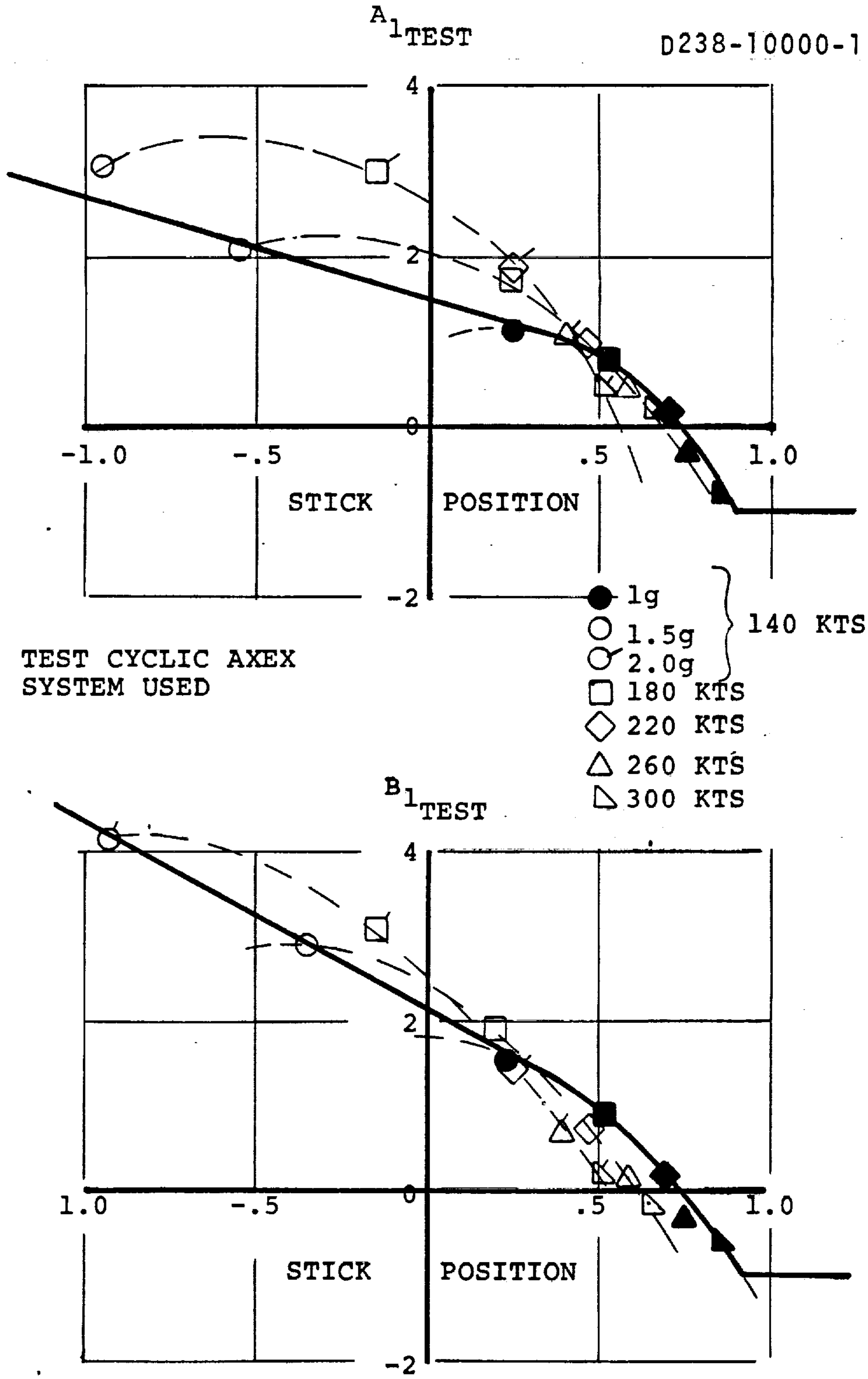

NOTE: TEST CYCLIC AXEX SYSTEM USED

Figure 20. Cyclics Required for Minimum Loads in Cruise.

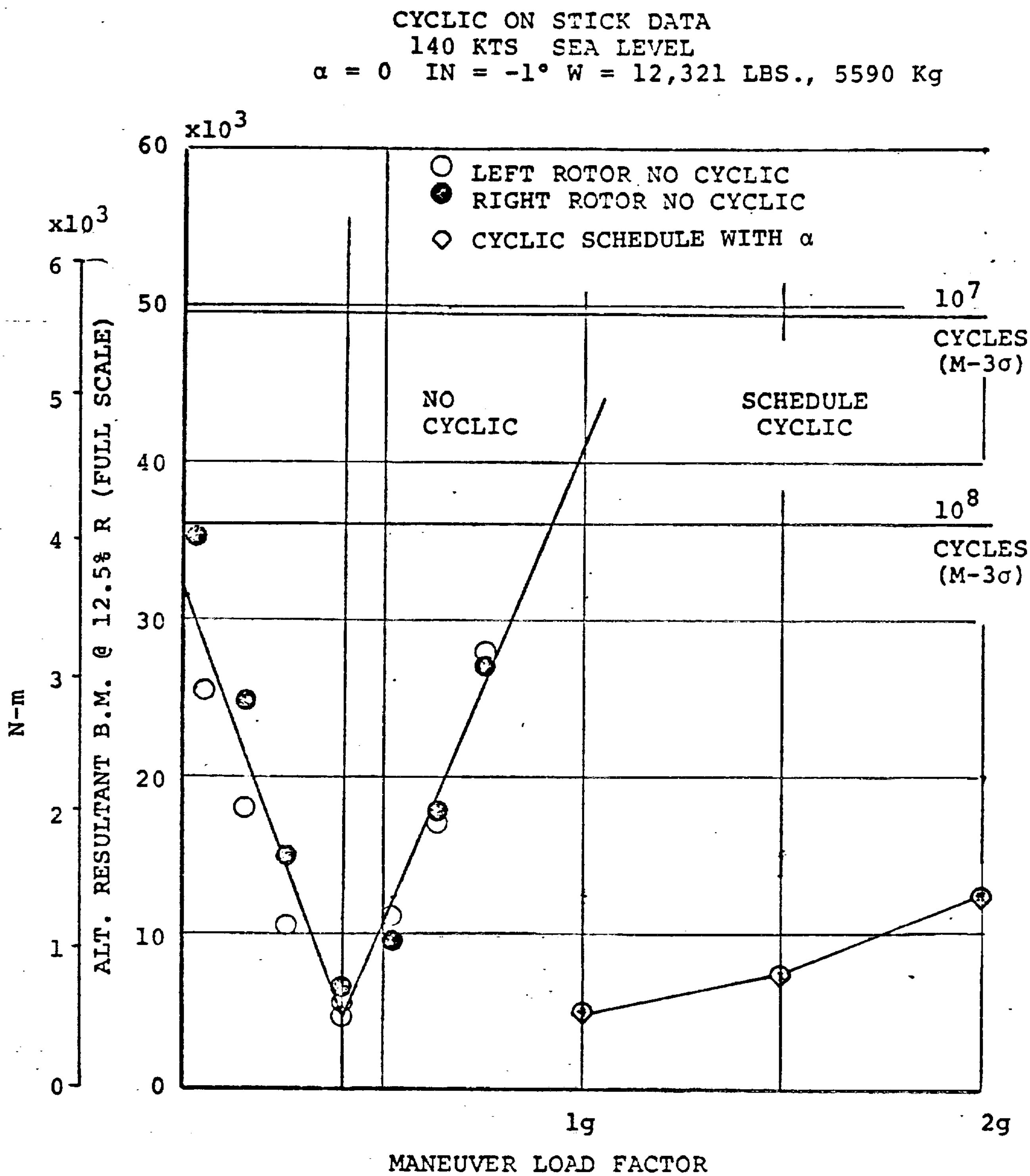

Figure 21. Loads With Test "Cyclic On Stick" 140 Knots Full Scale.

CYCLIC ON THE STICK RESULTS
FULL SCALE AIRSPEED 220 KTS
IN = -1° δ_F = 0° W = 12,321 LBS., 5590 Kg

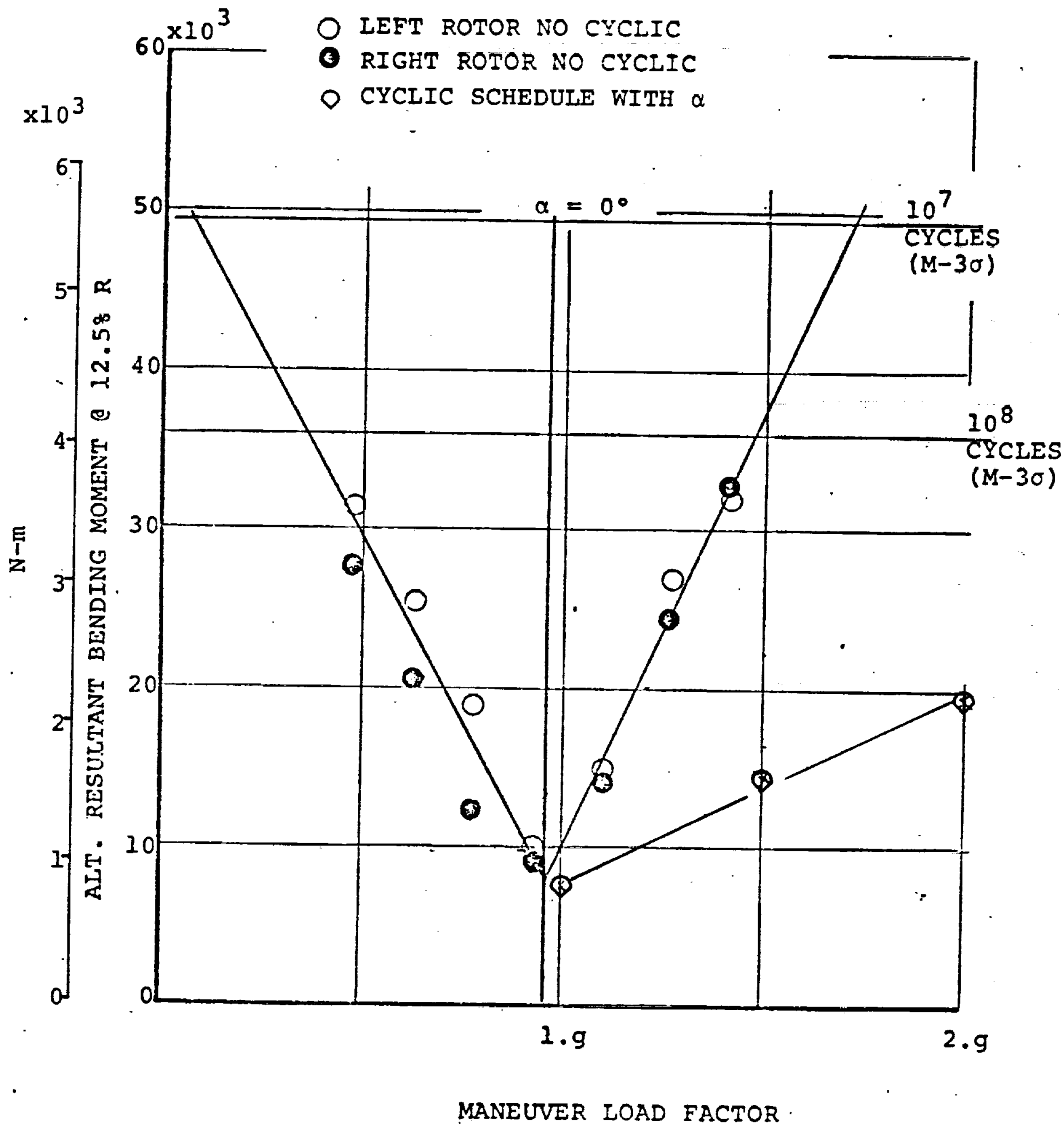

LOADS WITH TEST "CYCLIC ON STICK"

Figure 22. Loads With Test "Cyclic on Stick" 220 Knots Full Scale.

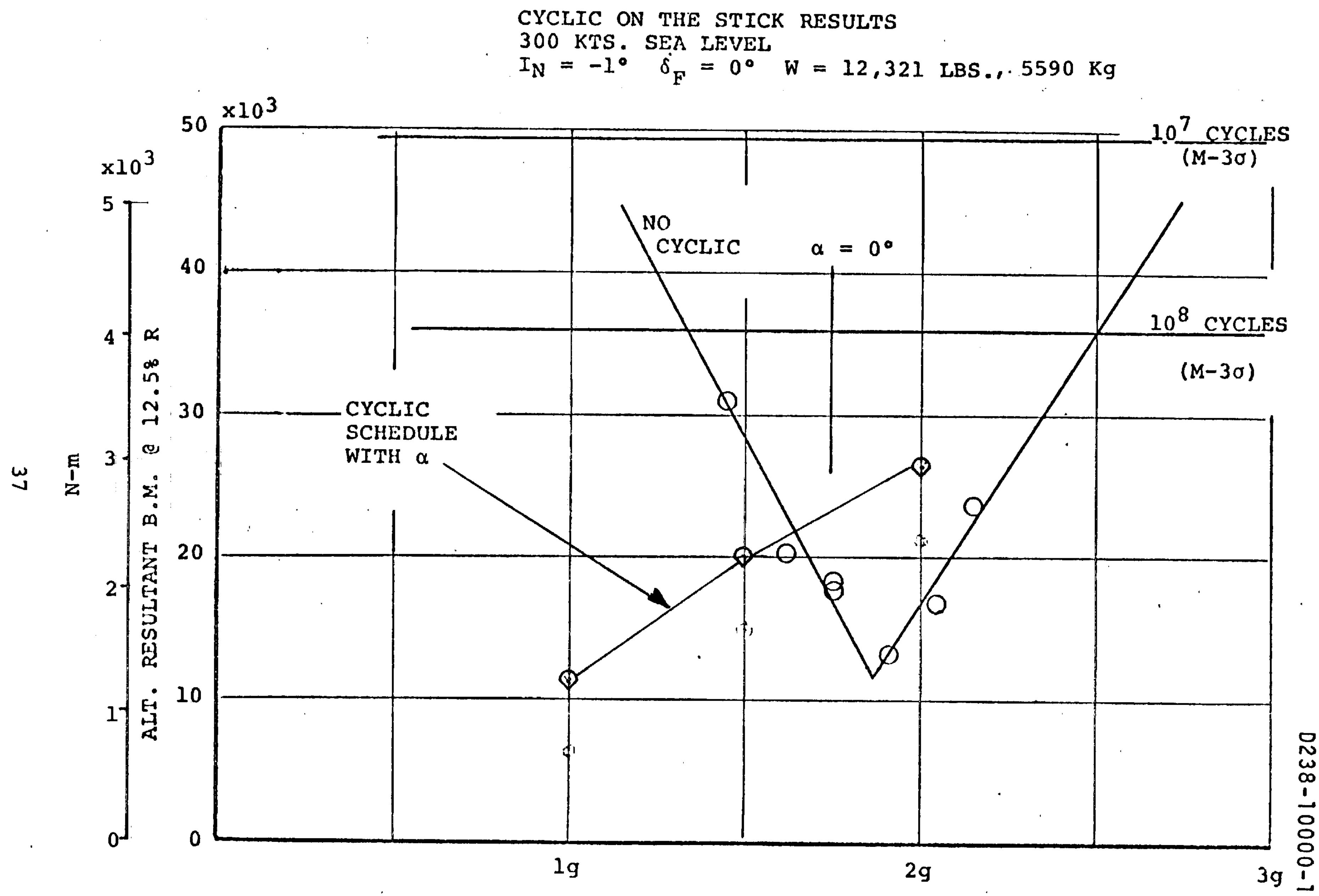

Figure 23. Loads With Test "Cyclic On Stick" 300 Knots Full Scale.

ALTERNATING BLADE BENDING MOMENTS
@ 0.125R CRUISE $\delta_F = 0°$

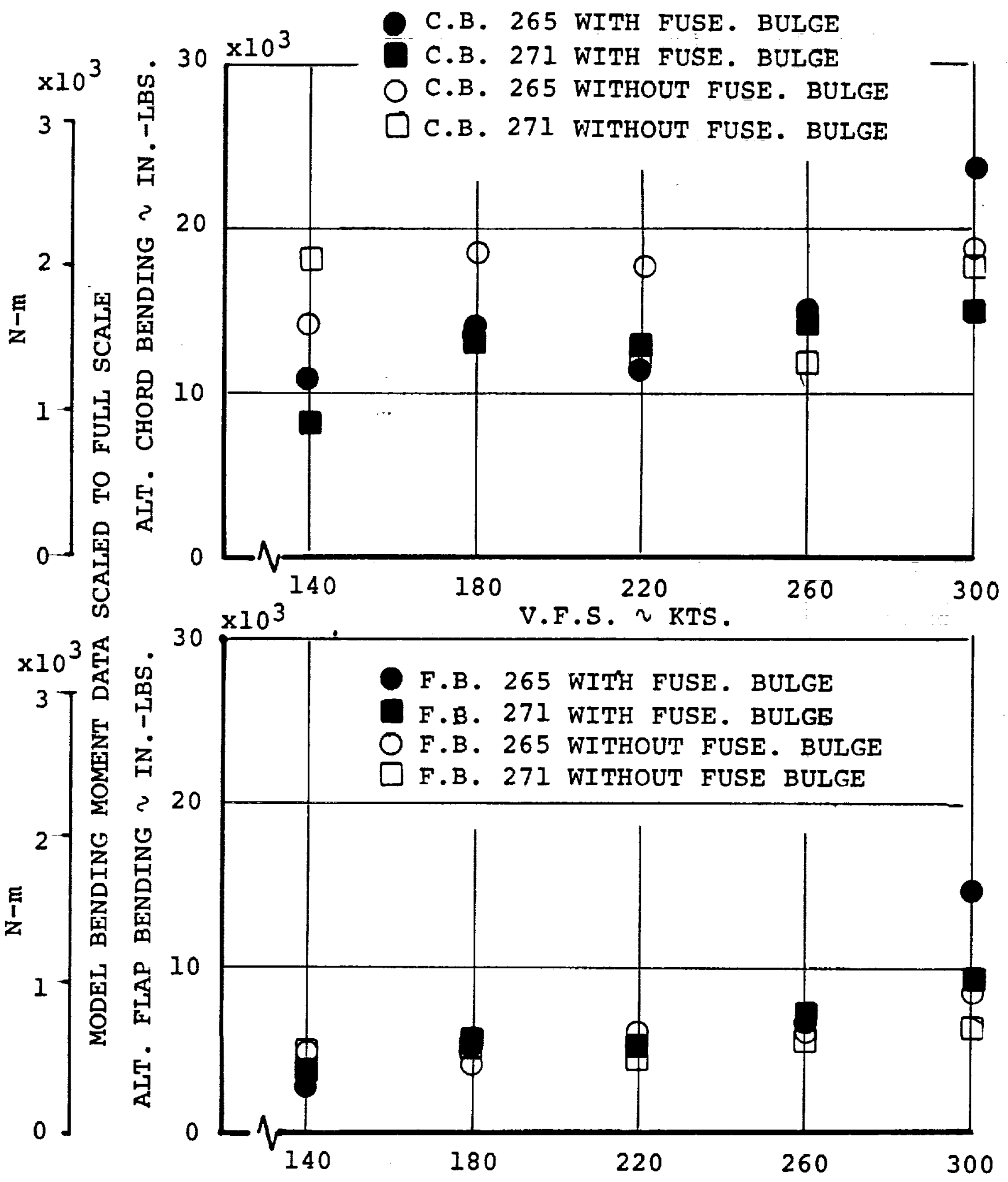

Figure 24. The Effect of Fuselage - Blade Tip Clearance on Alternating Blade Loads in Cruise.

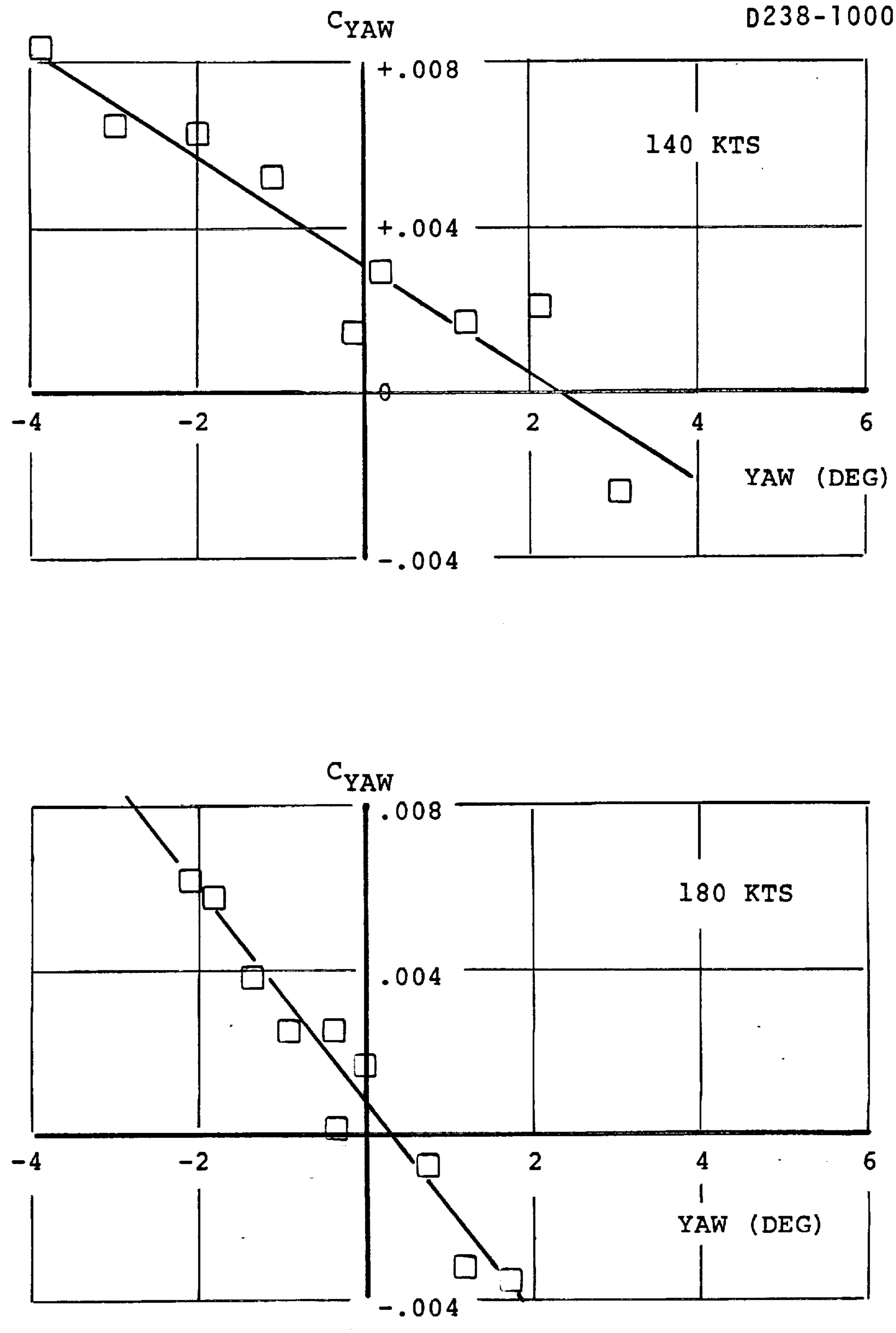

Figure 25. Aircraft Yaw Moment Coefficient as a Function of Yaw Angle in Cruise at 140 and 180 Knots Full Scale.

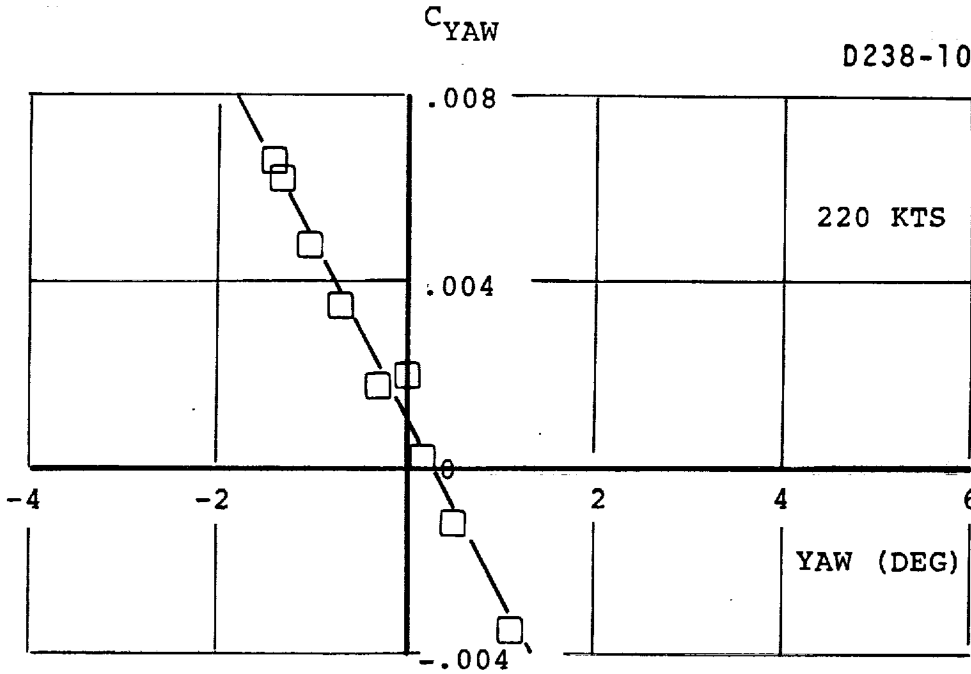

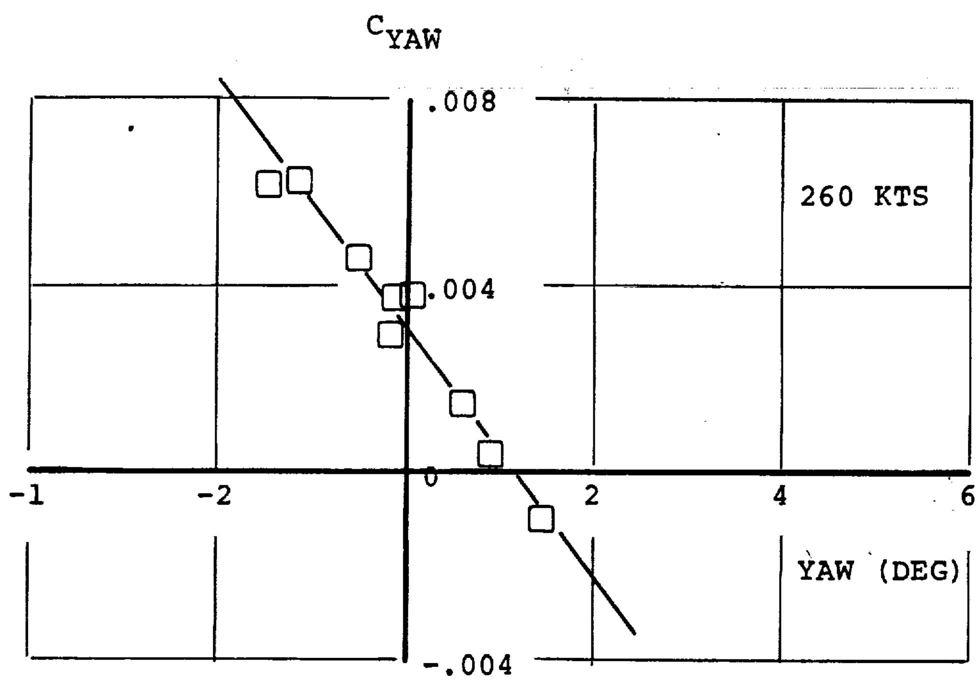

Figure 26. Aircraft Yaw Moment Coefficient as a Function of Yaw Angle in Cruise at 220 and 260 Knots Full Scale.

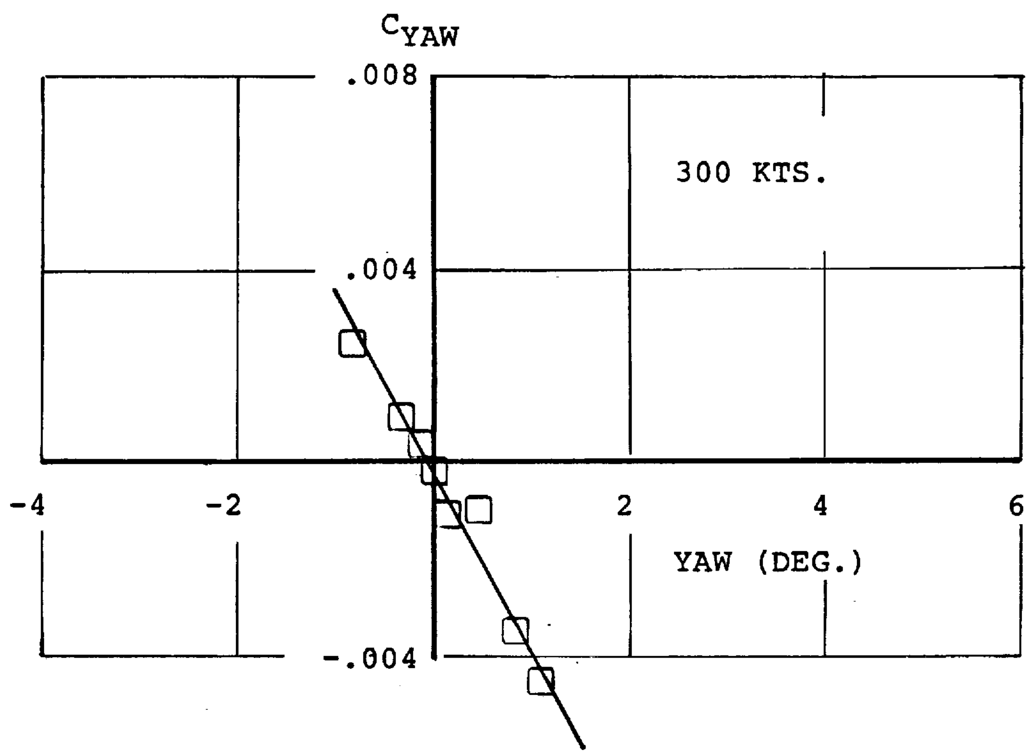

Figure 27. Aircraft Yaw Moment Coefficient as a Function of Yaw Angle in Cruise at 300 Knots Full Scale

3.0 TEST EQUIPMENT AND INSTALLATION

This section of the report serves to document the details of the test model, the model mount in the wind tunnel, the sign conventions and scale factors which apply to the test, the instrumentation and the data reduction procedures adopted.

3.1 Model Description and Instrumentation

The model tested is a 1/4.622 scale full span, powered configuration that is Froude scaled of the Model 222 Tilt Rotor Research aircraft. This model, shown in Figure 28 was provided by Boeing/Vertol for this test program and has the following major dynamically-scaled components.

1. Two 3-bladed rotors
2. Two nacelles
3. Full span wing
4. Fuselage
5. Tail

Photographs of the model in hover, transition and cruise flight conditions are shown in figures 29, 30 and 31.

Basic model dimensions are shown in Table 1.

The nacelles are joined to the wing by a pivot and have remote pitch actuation.

The wing is crown mounted and has full span flaps and leading edge umbrellas for download alleviation. Flaps are used during transition to provide additional lift and the outboard section

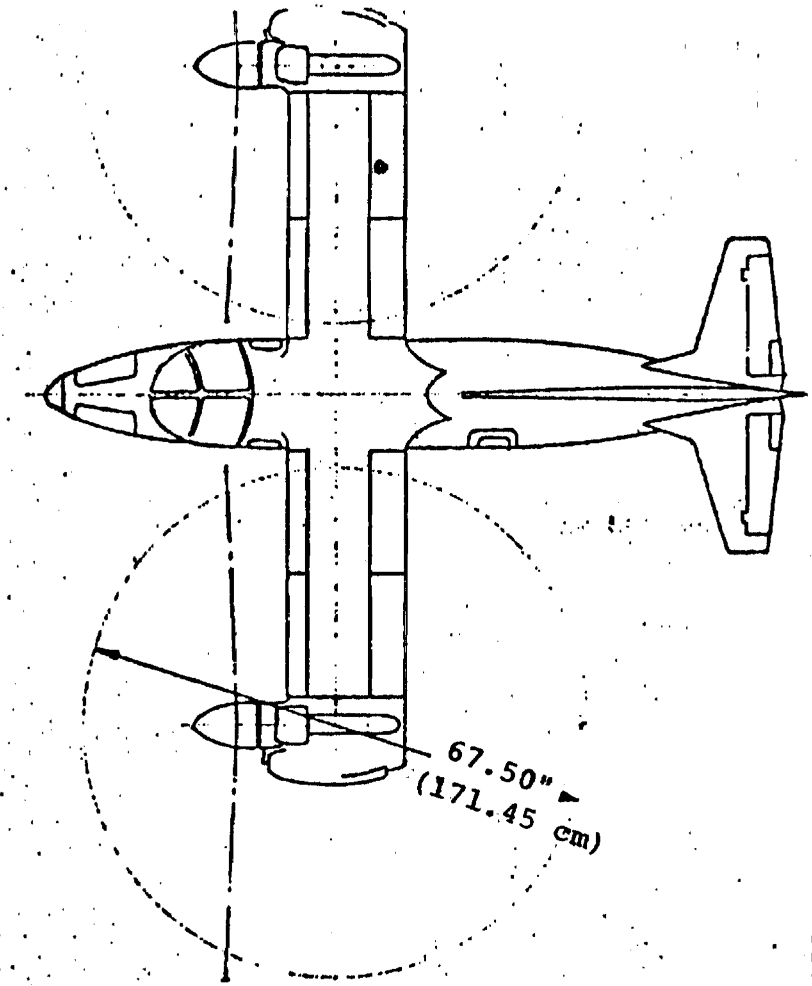

ROTOR

Diameter	67.50 In.	(171.45 cm)
Solidity	.115	
No. Blades	3	

WEIGHTS

Design Gross Wt	122 Lbs	(55.35 Kg)

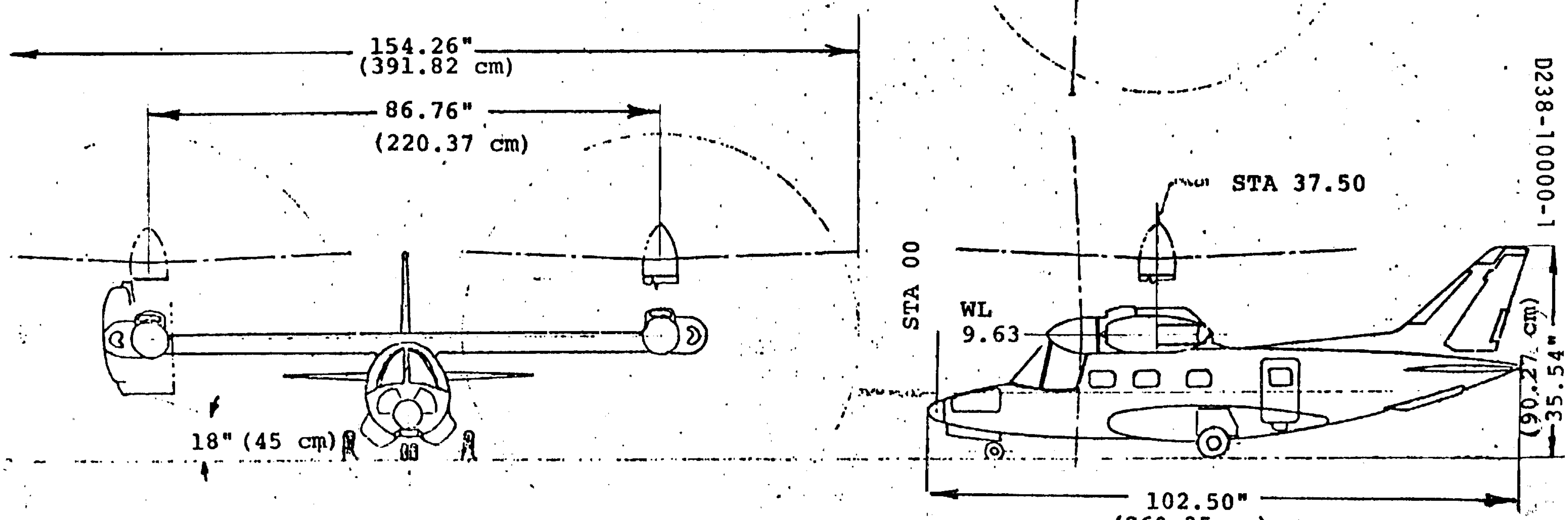

Figure 28. 1/4.622 FROUDE SCALE WIND TUNNEL MODEL.

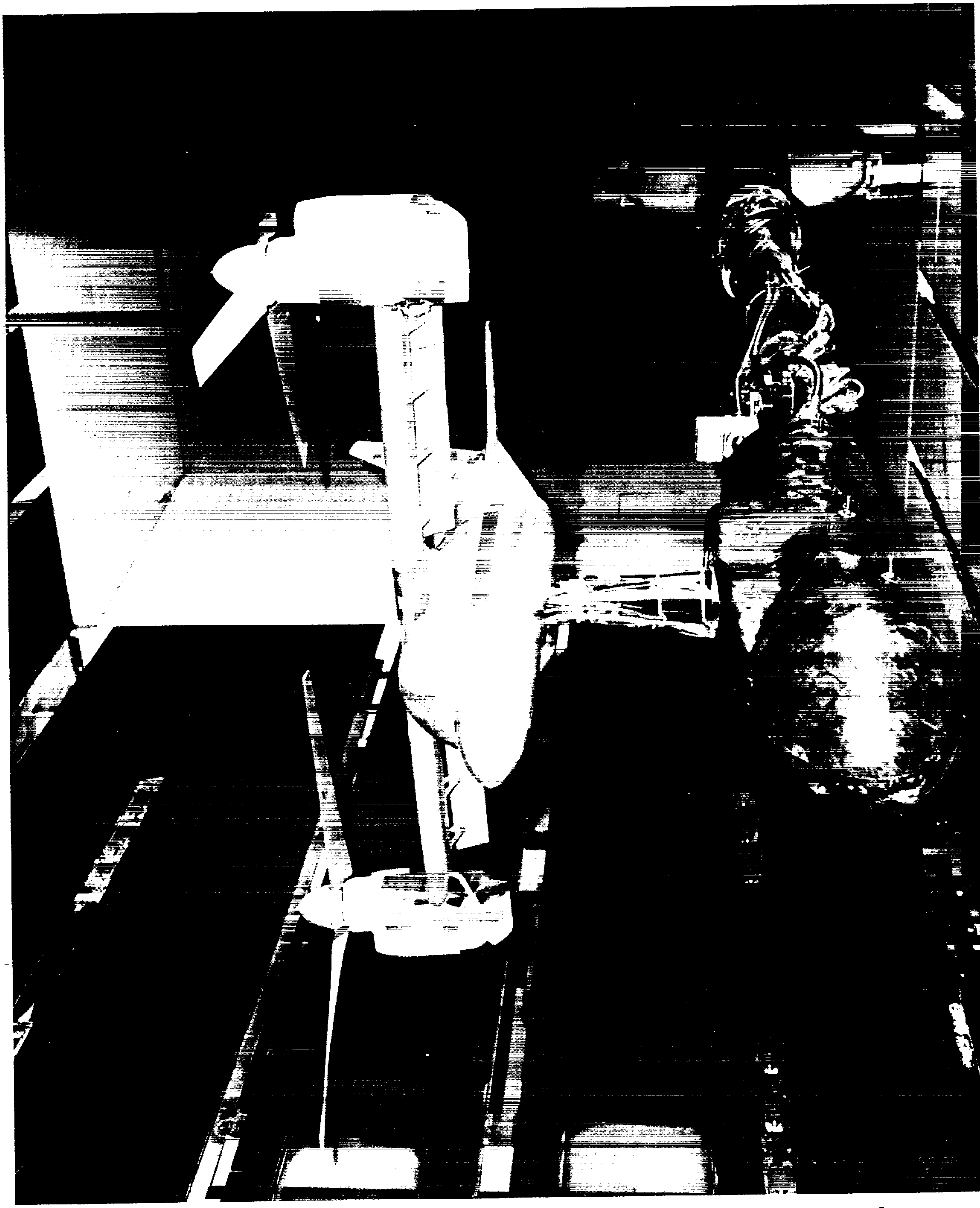

Figure 29. 1/4.622 Scale Model Installed in the Wind Tunnel Test Section (Hover)

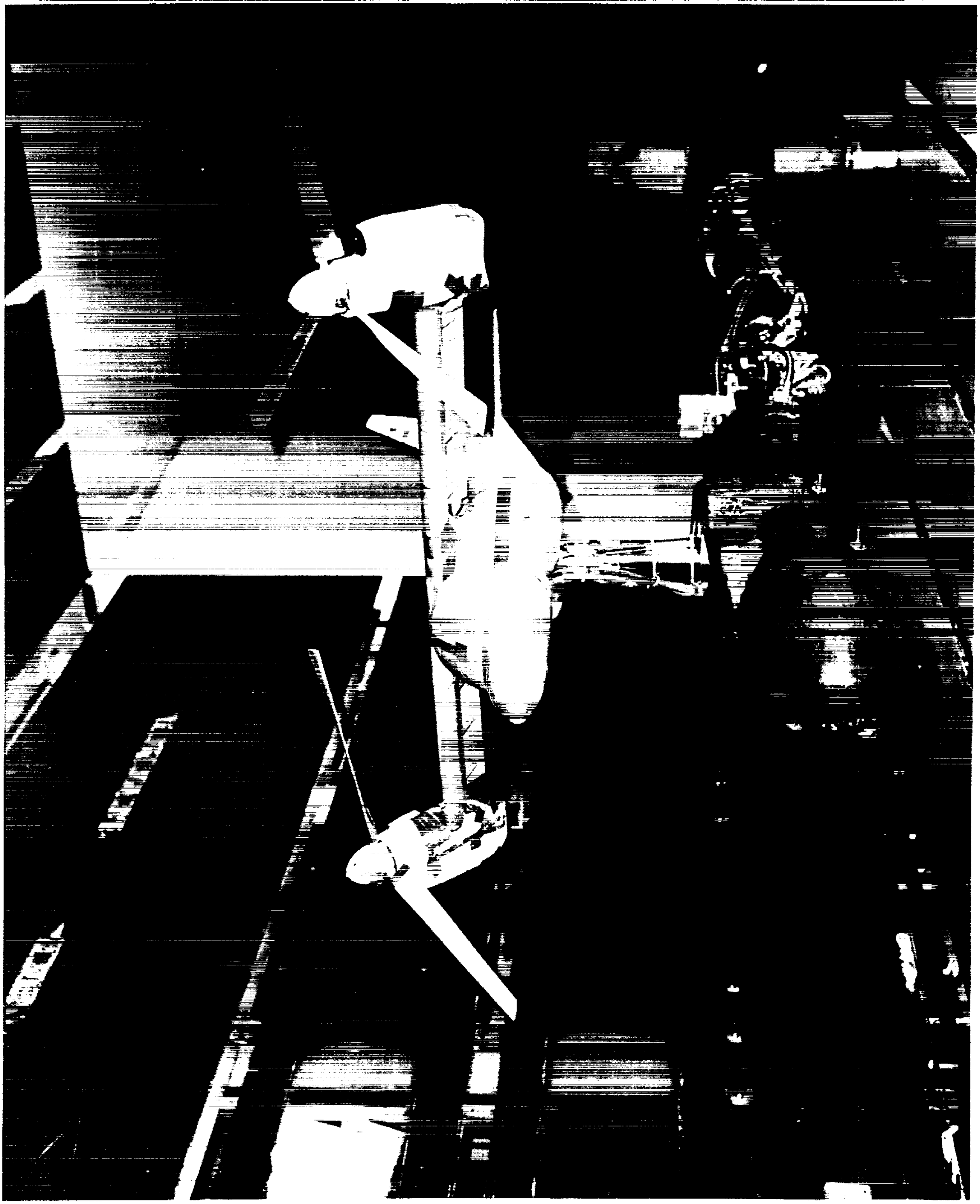

Figure 30. 1/4.622 Scale Model Installed in the Wind Tunnel Test Section (Transition)

Figure 31. 1/4.622 Scale Model Installed in the Wind Tunnel Test Section (Cruise)

TABLE 1

MODEL DIMENSIONS

ROTOR	
Number of Blades	3
Radius	33.75 IN. (85.72 cm)
Chord	4.078 IN. (10.35 cm)
Twist	42.5 DEG.
Airfoil Section	23021/23010-1.58
Solidity	0.115
Rotor Speed (Hover)	1185 RPM
Rotor Speed (Cruise)	825 RPM
Collective Pitch Available	-5 to 65 DEG.
Cyclic Pitch Available	± 10 DEG.
NACELLE	
Nacelle Pivot Position (in % of Wing Chord)	40%
Rotor Disc Nacelle Pivot Distance	12.33 IN. (31.31 cm)
WING	
Airfoil Section	63_4221 Modified
Span (Rotor ℄ to Rotor ℄)	86.76 IN. (220.37 cm)
chord	15.53 IN. (39.44 cm)
Area	9.36 FT.^{2} (.869 M^2)
Aspect Ratio	5.61
Flap in % of Chord	30%
Wing Incidence	2 DEG.
Thickness - Chord Ratio	0.21
FUSELAGE	
Diameter	14.69 IN. (37.31 cm)
Length	102.50 IN. (260.35 cm)
TAIL - HORIZONTAL	
Area	2.73 FT.^{2} (.253 M^2)
Span	10.89 IN. (27.66 cm)
Aspect Ratio	4.25
Taper Ratio (C_{TIP}/C_{ROOT})	.384
Root Chord	14.05 IN. (35.68 cm)
Airfoil Section	64A010
Elevators in % of Chord	44.1%

TABLE 1 (continued)

TAIL - VERTICAL

Area	2.03 FT^2	(.185 M^2)
Span	22.75 IN.	(57.78 cm)
Aspect Ratio	1.77	
Taper Ratio (C_{TIP}/C_{ROOT})	.35	
Root Chord	20.98 IN.	(58.29 cm)
Airfoil Section	64A008	
Rudder in % of Chord	50.6	

of the flap is used as an aileron for control in conjunction with outboard spoilers.

The wing, fuselage, and empennage are dynamically scaled from the Model 222 tilt rotor aircraft and the rudder and elevator and flaps are remotely controlled.

The model is powered by a 20 HP, 11,375 RPM electric motor manufactured by Task Corporation. The motor drives a 3.04:1 reduction gear box in the center fuselage which is connected by cross shafts in the wing to a 3.09:1 reduction gear box in each nacelle. This provides a total gear reduction from the electric motor to rotor of 9.39:1.

The model control station is shown schematically in figure 32 as comprised potentiometer controls and beep switches with analogue meters for readout in the format depicted.

The rotor controls provided collective and two axes of cyclic pitch on each rotor driven by potentiometers at the control station using simple position feedback control, the actuator follow up potentiometer output being used to provide readout to the operator.

The position of the actuators in the rotor azimuth together with the 18.4° between the pitchlink rod end and the blade 1/4 chord defines the cyclic pitch control axes as shown in figure 33. Thus for a longitudinal or B_1 input the maximum

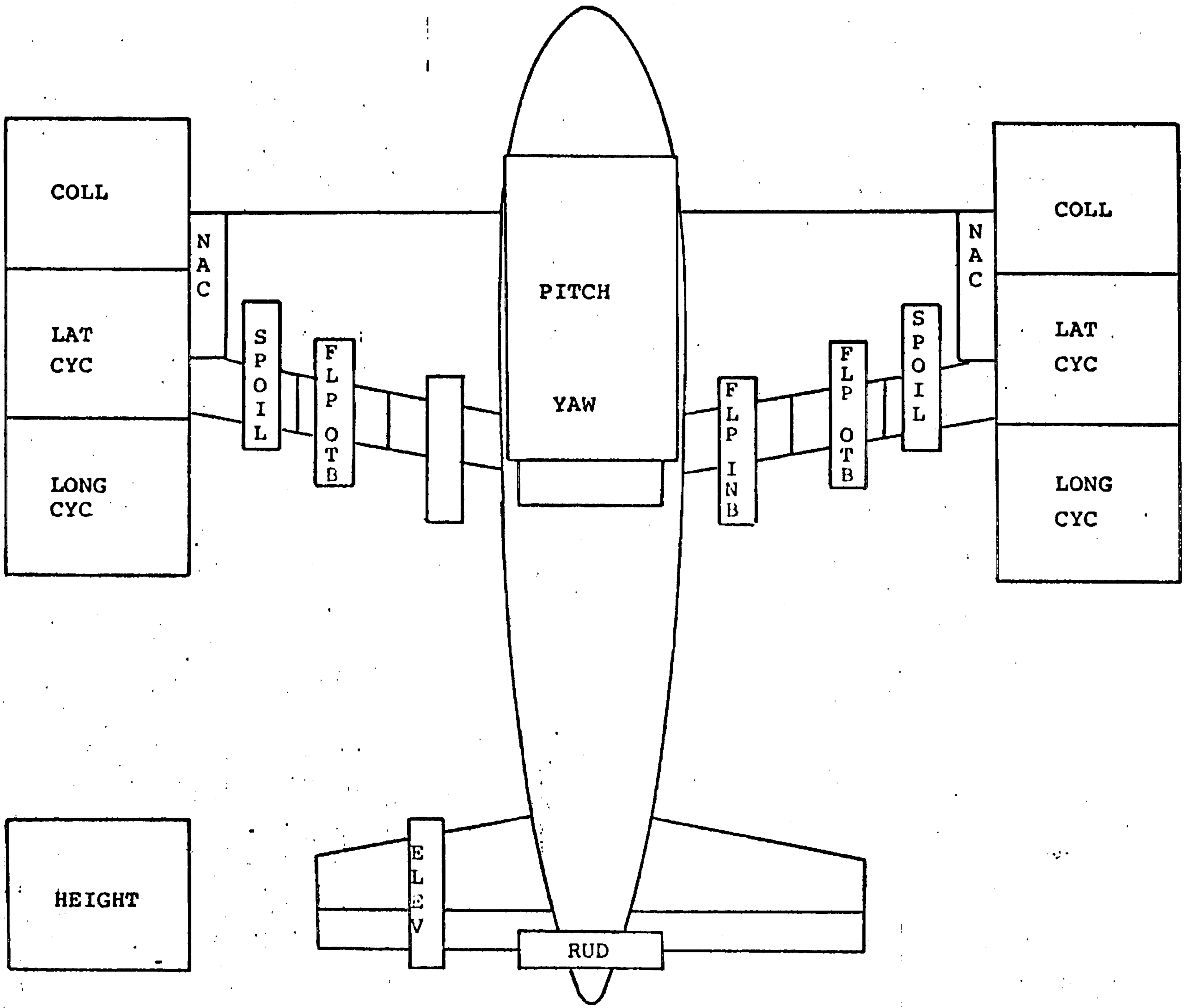

Figure 32. MODEL 222 CONTROL DISPLAY

blade angle occurs at 150.4° and 330.4° azimuth. The lateral or A_1 axis is orthoganal to B_1. When a positive B_1 command is made the maximum blade angle is at $\psi = 330.4^{\circ}$ and a positive A_1 command gives rise to a maximum blade angle at $\psi = 240.4^{\circ}$.

Classical helicopter rotation defines cyclic pitch inputs by the law

$$\Delta\theta = - A_1 \cos \psi - B_1 \sin \psi$$

For this test the cyclic blade angle is defined as

$$\Delta\theta = - A_{1_{TEST}} \cos (\psi - 60.4) - B_{1_{TEST}} \sin (\psi - 60.4)$$

The transformation of test cyclics to classical axis is thus

$$\begin{bmatrix} A_1 \\ B_1 \end{bmatrix} = \begin{bmatrix} .4939 , & - .8696 \\ .8696 , & .4939 \end{bmatrix} \begin{bmatrix} A_1 \text{ TEST} \\ B_1 \text{ TEST} \end{bmatrix}$$

The data presented in this document and the Appendix volumes (References 4 , 5 and 6) are given in terms of test cyclic axes unless otherwise noted.

The instrumentation used on the model included three six component strain gage balances, one in each nacelle to measure rotor hub forces and moments and one total aircraft balance. The positions of the balances in relation to each other and with respect to the hub centers and aircraft reference CG locations are shown in figure 34 . The nacelle balances were calibrated about the hub center, and the total loads balance about the reference CG.

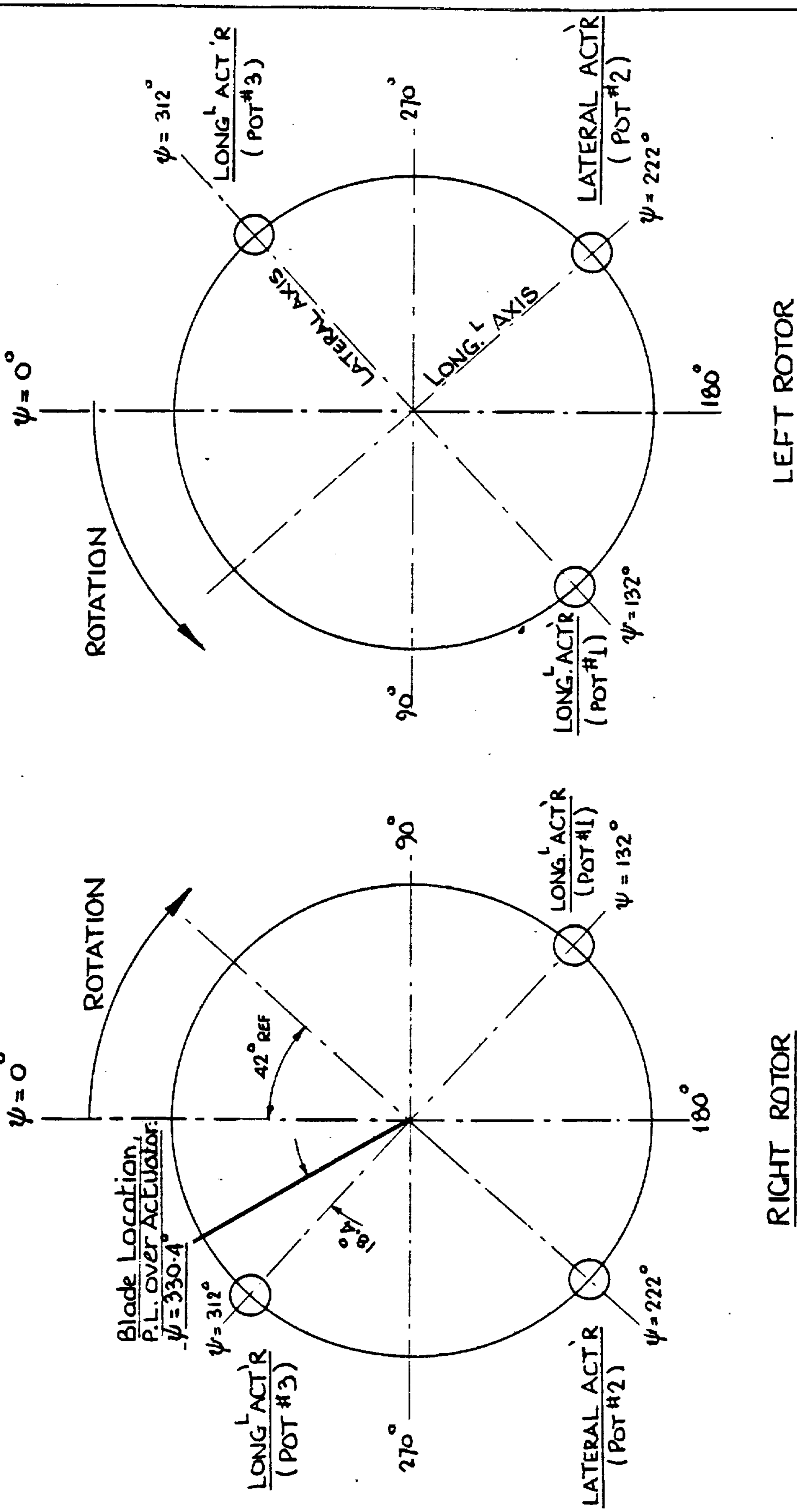

FRONT VIEW ON MODEL, $i_N = 0°$

VR 095 Q-1 1/4.622 SCALE TILT ROTOR MODEL

CONTROL SYSTEM ARRANGEMENT

Figure 33.

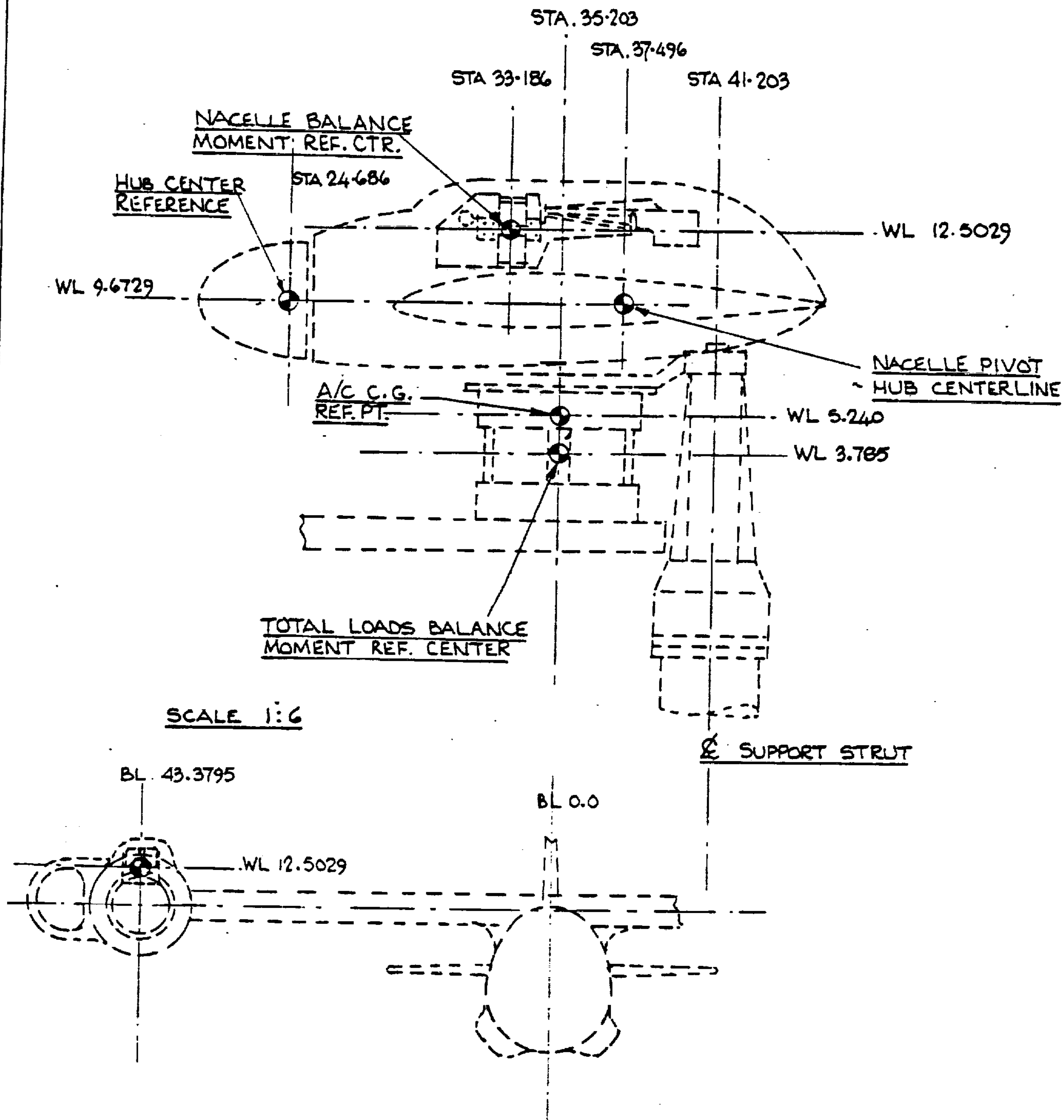

VR 095 Q-1 . 1/4.622 SCALE TILT ROTOR MODEL

Figure 34. RELATIVE BALANCE LOCATIONS & MODEL REFERENCES

In addition to the strain gage balances, the blades were instrumented to provide chord and flap bending at 0.125R and also pitchlink loads and the rotor RPM and 1/rev signals were also generated. The blade positions when the 1/rev market fires are shown in figure 35.

The rotor power was obtained from strain gages on the rotor shaft aligned to measure torque.

The positions of the collective and cyclic controls, wing flap setting and nacelle incidence were obtained from the appropriate control channel follow up potentiometer and provided as analogue and digital displays and inputs made to the data reduction computer on line.

Thermocouples were used to provide safety monitoring of critical motor, gearbox and cross shaft bearing temperatures. Three accelerometers were also mounted in each nacelle and used to monitor the aeroelastic stability of the wing modes.

All of the primary instrumentation channels were available on a patch panel such that any channel could be patched to a digital volt meter and a spectral analyzer on line. This instrumentation enabled the stability of the aeroelastic modes to be monitored and in some instances provided appropriate diagnostic information for model problem resolution on test.

The rotors used on the model were 85.72 cm (33.75 ins) radius and were a soft inplane hingeless rotor configuration having

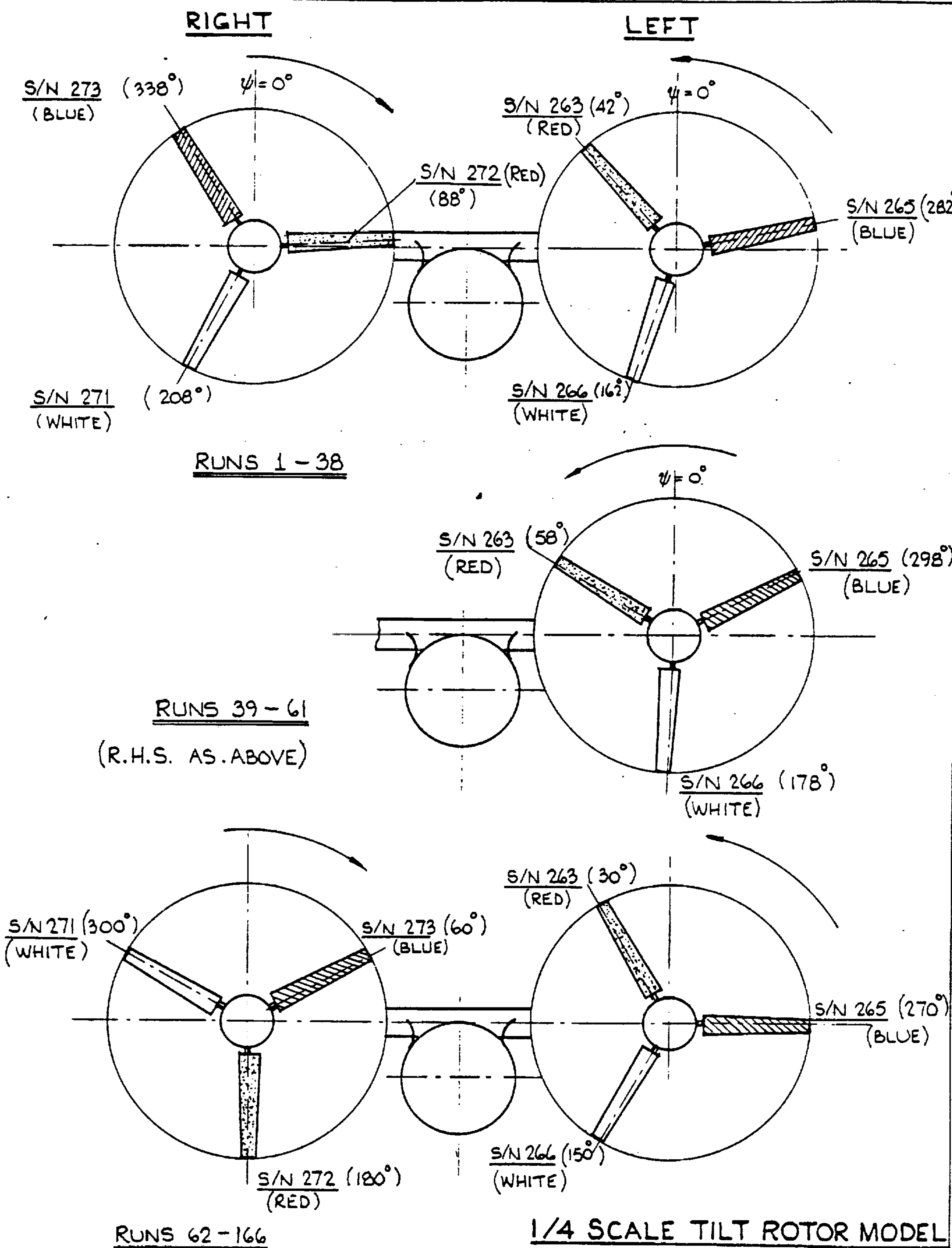

Figure 35. 1/4 SCALE TILT ROTOR MODEL ROTOR ORIENTATION AT 1/REV 'BLIP'

FORM 46284 (2/66)
KEF
5-27-76

three blades and a solidity of 0.115. The aeroelastic properties of the blades were scaled from the 7.9 m (26 ft.) diameter rotor designed, built and tested under NASA Contract NAS2-6505.

The properties of the model rotor blades are shown in figures 36 to 44.

FIGURE 36. FROUDE SCALE MODEL 222 PITCHING INERTIA DISTRIBUTION

R = 33.75 IN., C = 4.078 IN., P.A. = .952 IN.
85.72 CM 10.35 CM 2.41 CM

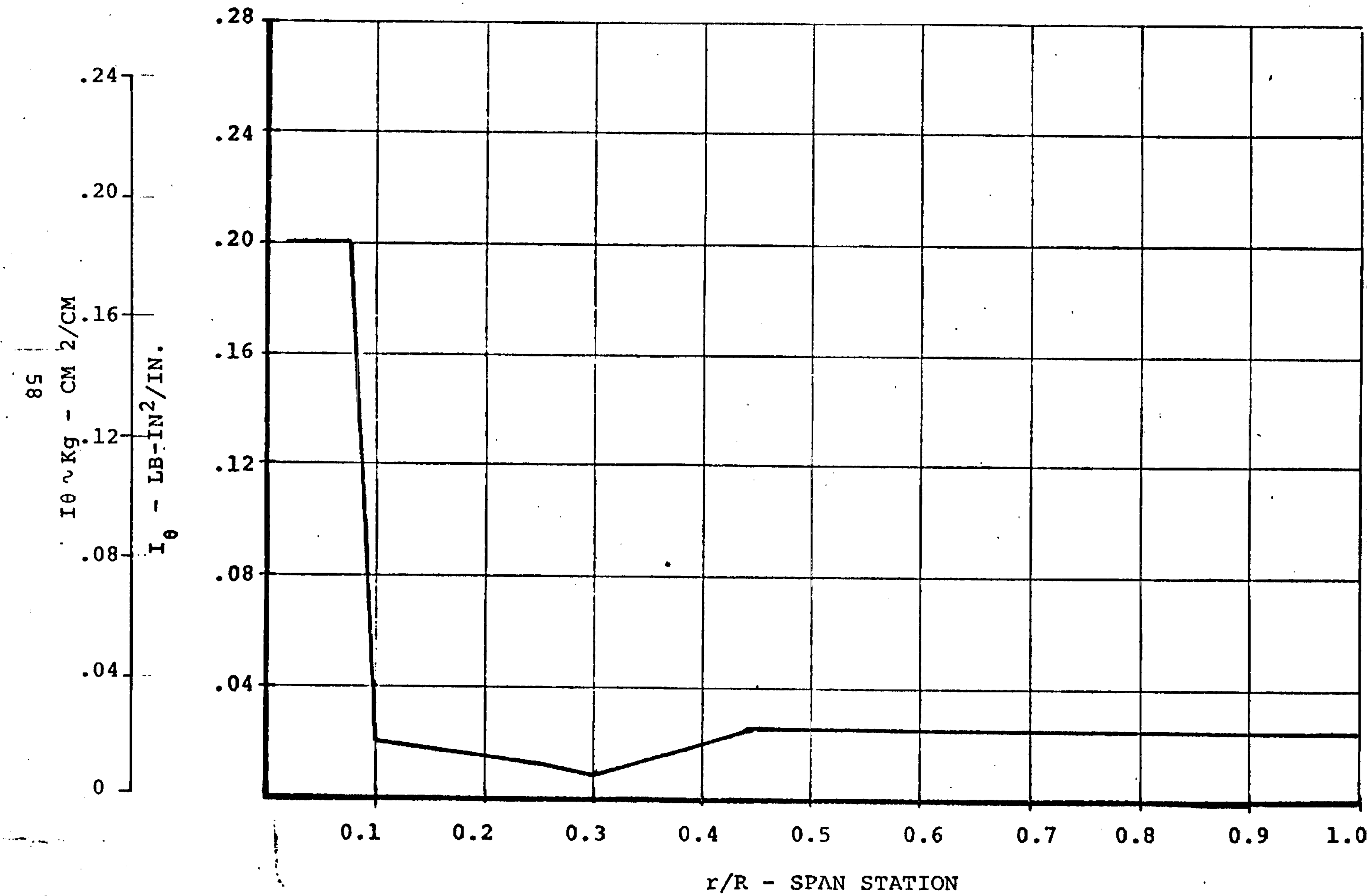

FIGURE 37. FROUDE SCALE MODEL 222 TORSIONAL STIFFNESS DISTRIBUTION - R = 33.75 IN., 85.72 CM
C = 4.078 IN., 10.35 CM
E_θ = .141 IN. .358 CM

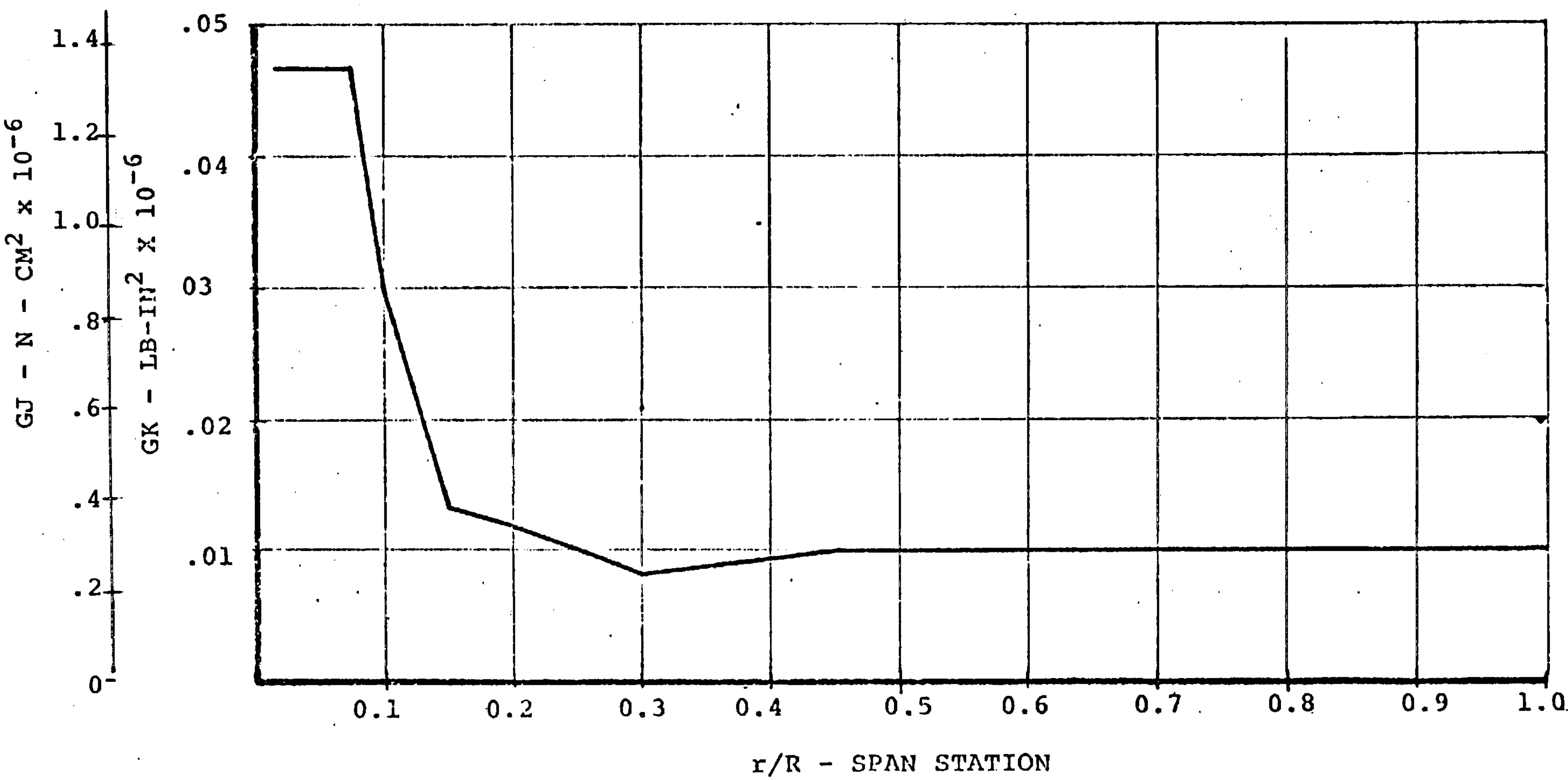

FIGURE 38. FROUDE SCALE MODEL 222 CHORDWISE STIFFNESS DISTRIBUTION

R = 33.75 IN., C = 4.078 IN.
85.72 CM 10.35 CM

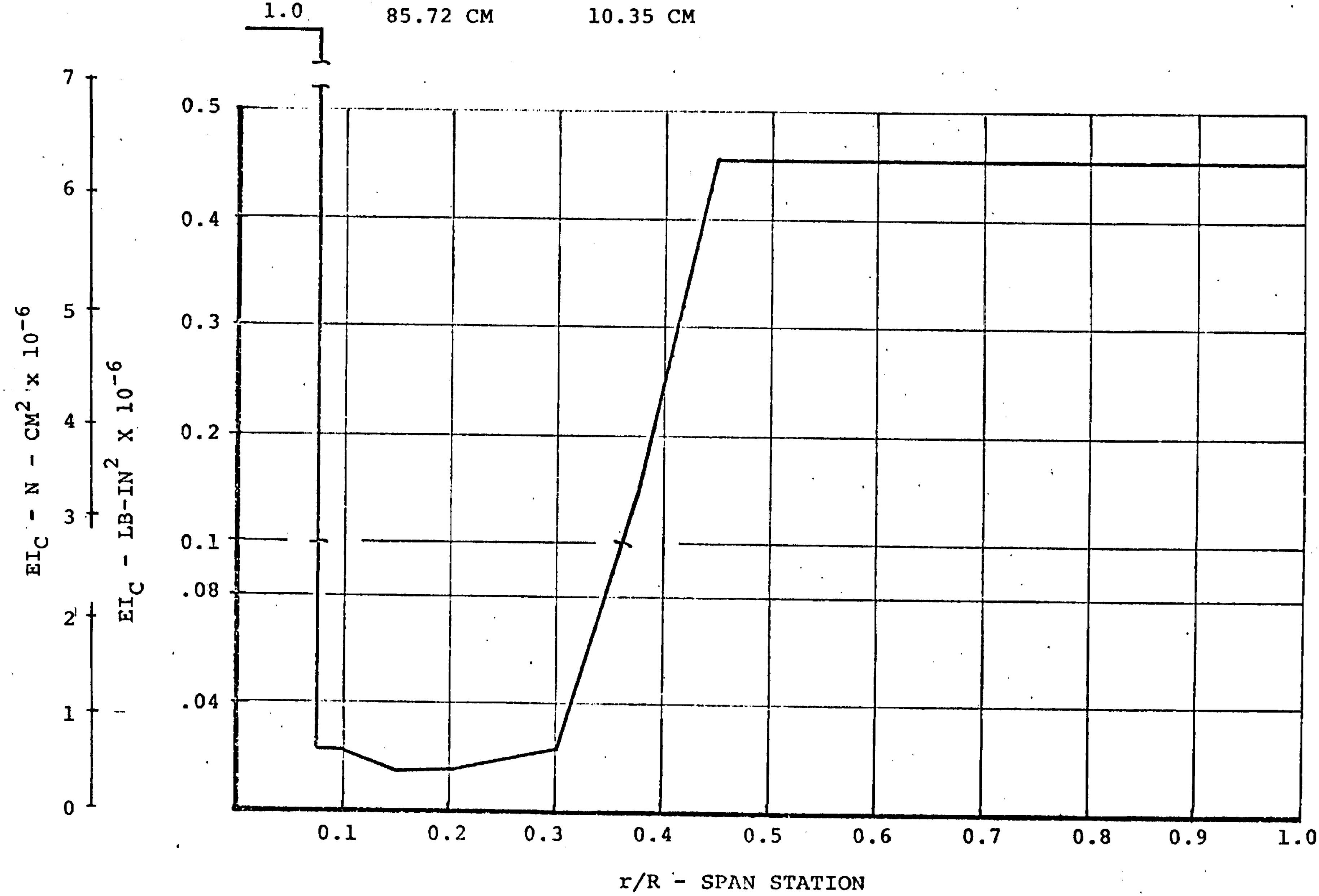

FIGURE 39. FROUDE SCALE MODEL 222 - FLAPWISE STIFFNESS DISTRIBUTION

$R = 33.75$ IN., $C = 4.078$ IN., $\beta_o = 2.5^o$
85.72 CM 10.35 CM

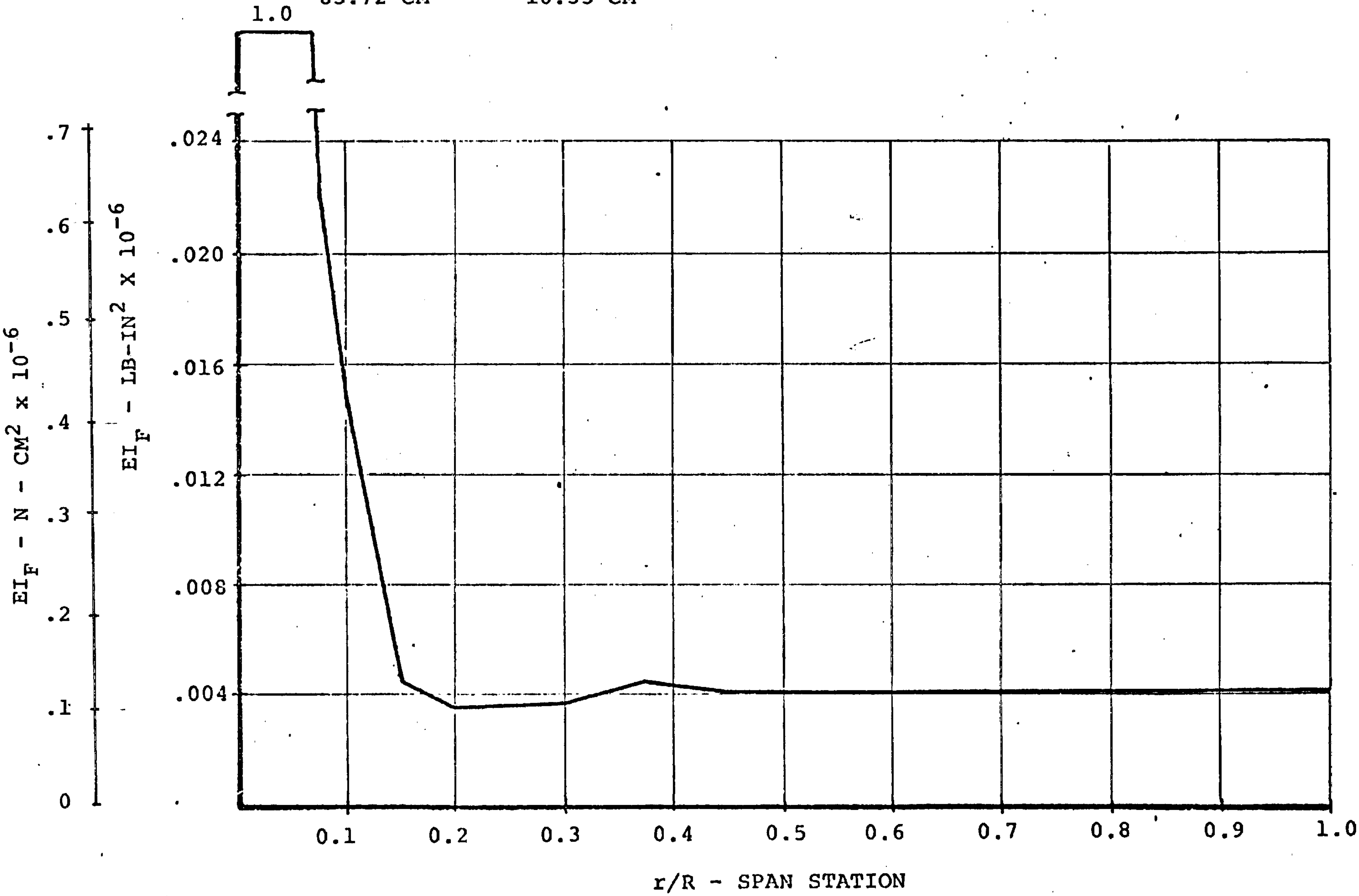

FIGURE 40. FROUDE SCALE MODEL 222 CENTRIFUGAL FORCE DISTRIBUTION

R = 33.75 IN., C = 4.078 IN.

85.72 CM 10.35 CM

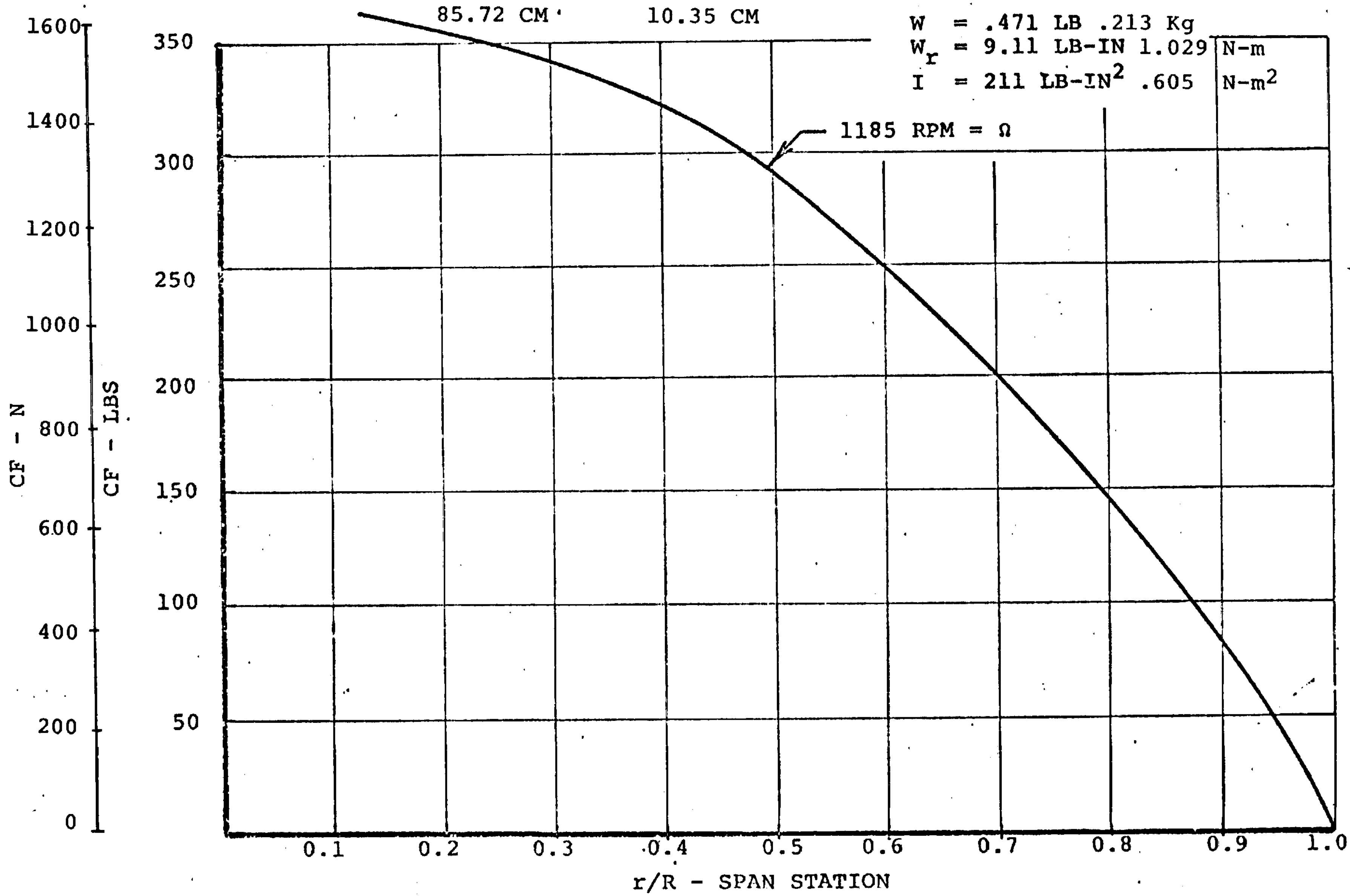

FIGURE 41. FROUDE SCALE MODEL 222 NEUTRAL AXIS DISTRIBUTION - R = 33.75 IN., 85.72 CM
C = 4.078 IN. 10.35 CM

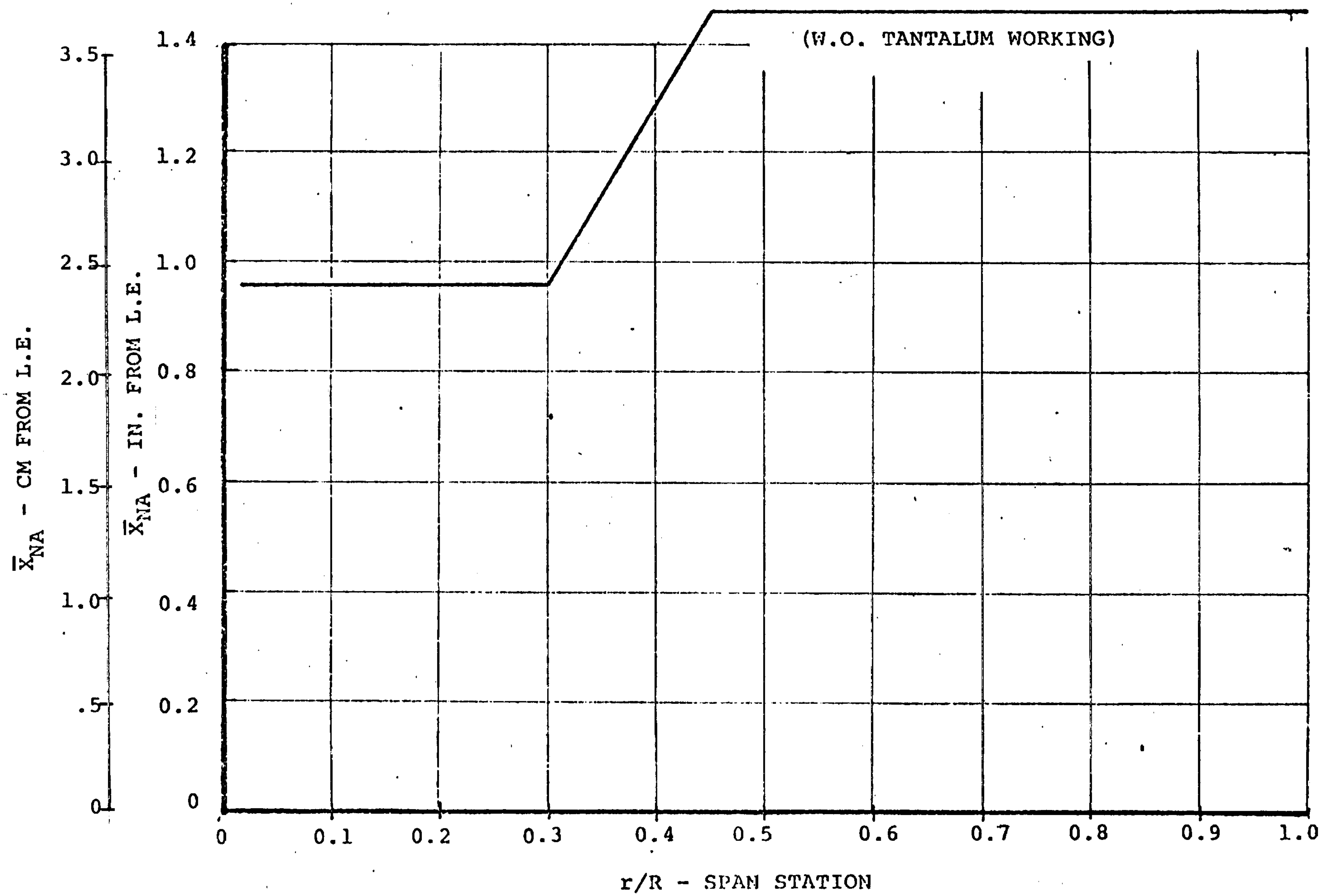

FIGURE 42. FROUDE SCALE MODEL 222 CENTROIDAL AXIS DISTRIBUTION - R = 48.0 IN., 121.92 CM
C = 4.078 IN. 10.35 CM

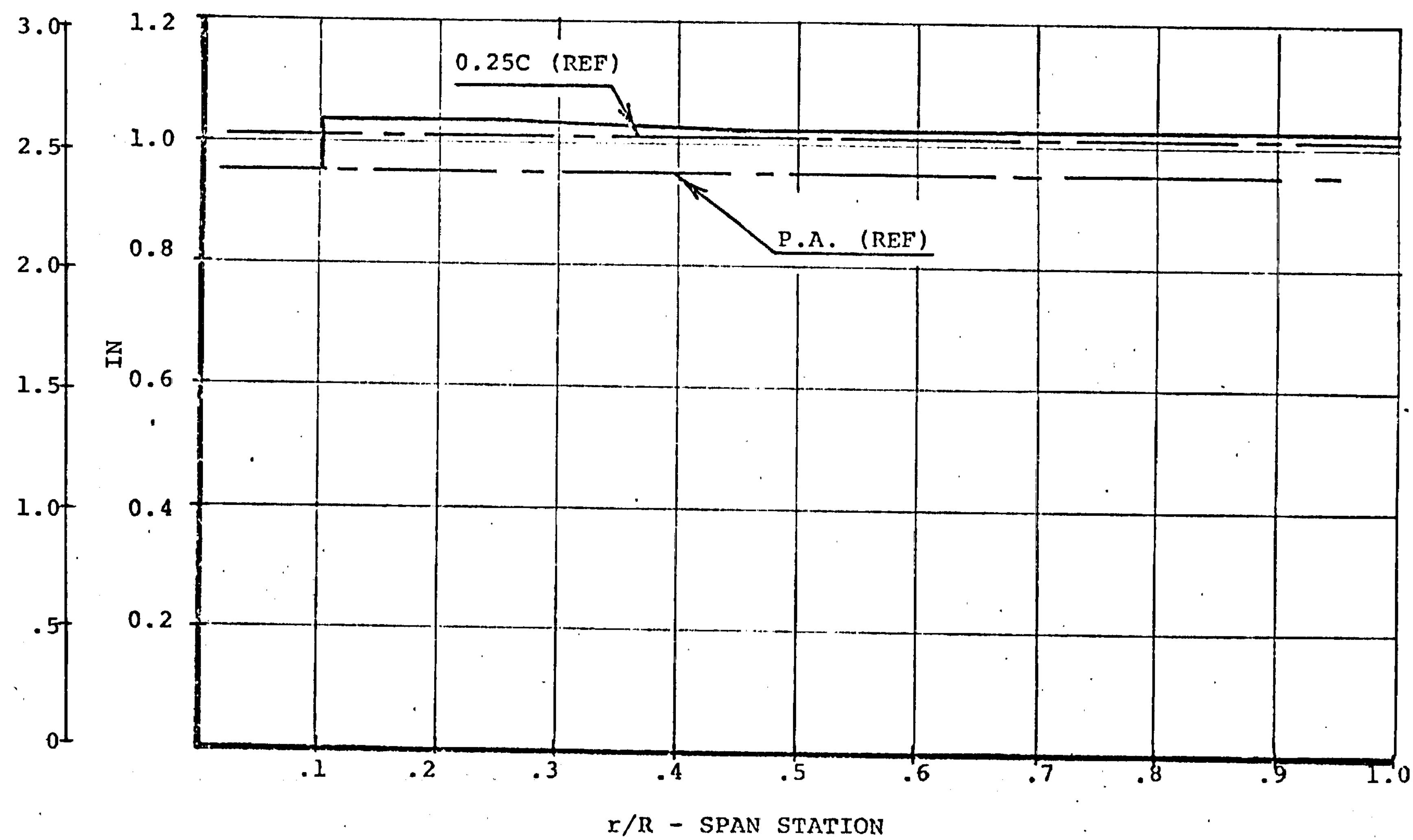

FIGURE 43. FROUDE SCALE MODEL 222 WEIGHT DISTRIBUTION - R = 33.75 IN., 85.72 CM
C = 4.078 IN. 10.35 CM

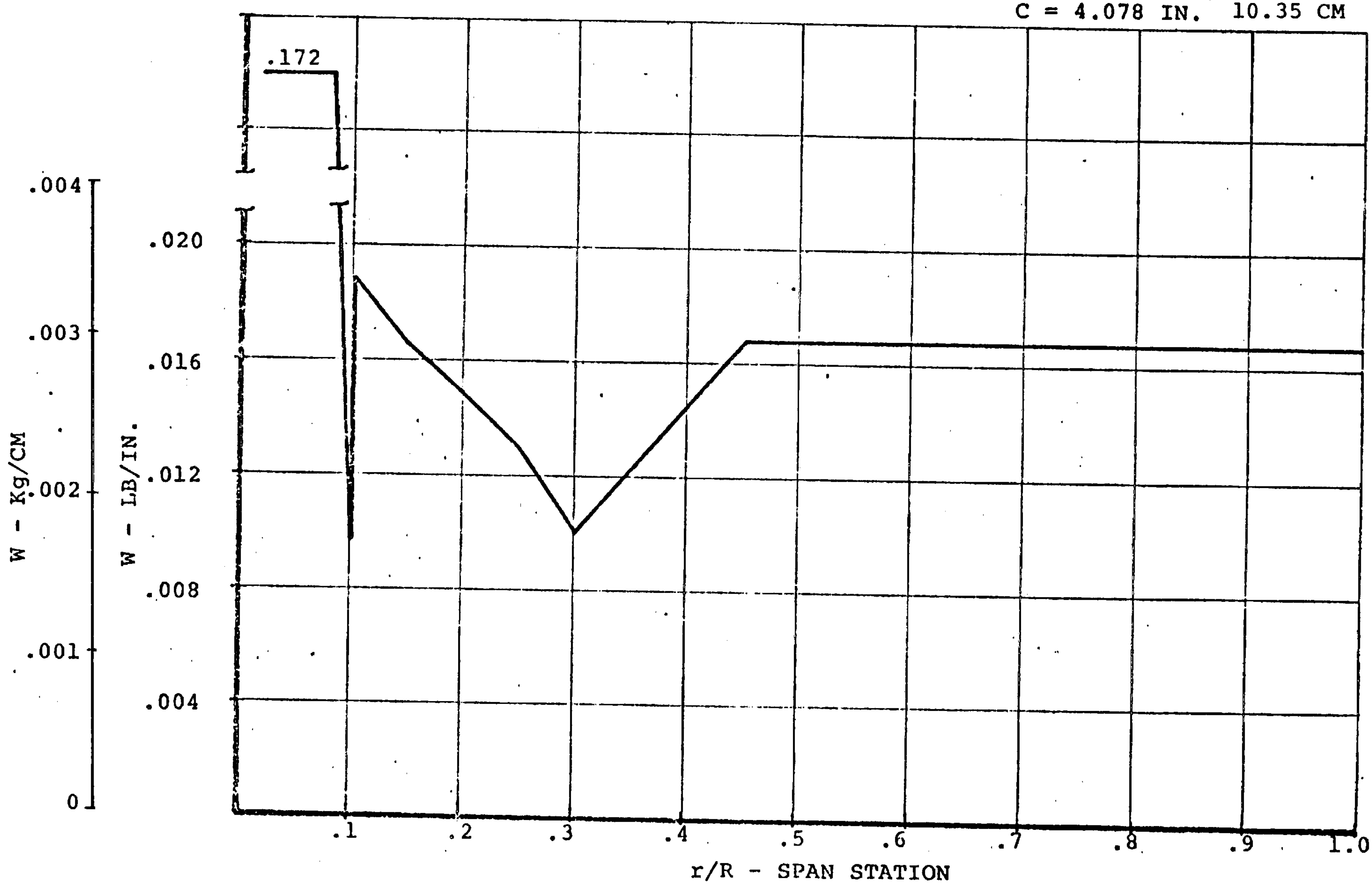

FIGURE 44. FROUDE SCALE MODEL 222 TWIST DISTRIBUTION - R = 33.75 IN., 85.72 CM
C = 4.078 IN. 10.35 CM

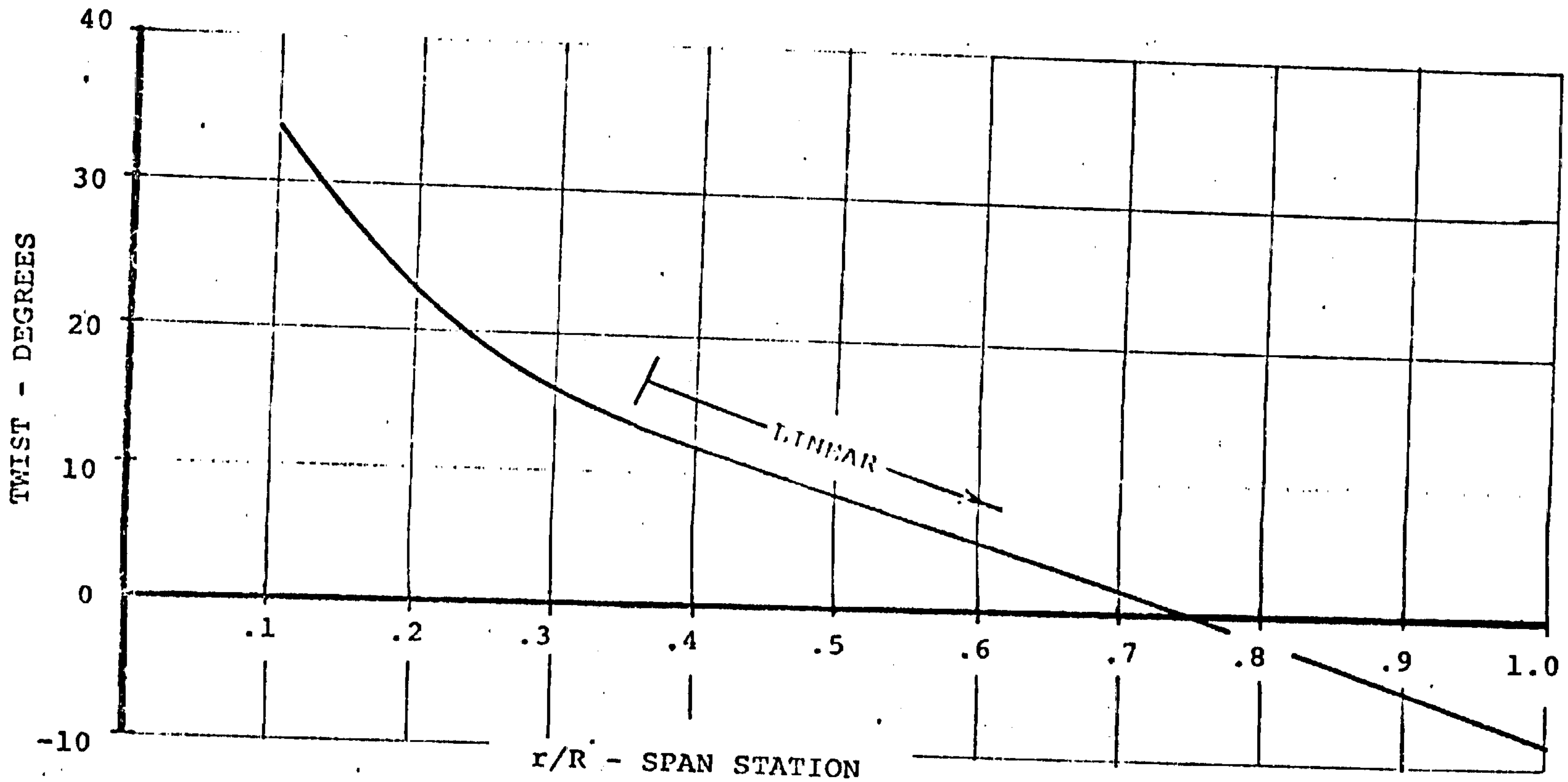

3.2 Model Installation and Wind Tunnel Data

The model was mounted in the wind tunnel on the SRH test stand which itself mounts on the wind tunnel sting. The test stand provides for remote actuation of pitch and yaw attitudes of the model and is shown in figure 45. The model was mounted on a pedestal support from the test stand.

The test stand usually incorporates a six component balance located where "Spacer A" is indicated. For the first 26 test runs this was replaced by a dummy balance since a total loads balance exists in the model. Ground resonance difficulties were observed and deduced to be due to the coalescence of the lower blade lag mode and the total loads balance pitch axis flexure frequency. The model balance was locked out by a stiffener and the spacer replaced by the SRH balance in order to measure loads. Further difficulties were encountered and eventually determined to be the fore and aft motion of the vertical pedestal whose frequency was similar to the original pitch axis frequency. These problems were eventually solved by removing the SRH balance and shortening the vertical pedestal thus increasing the frequency of the mode. The model total loads balance lock was removed and lead weights added to the fuselage nose and tail internally. Sufficient increase in pitch inertia was obtained to decrease the model balance pitch mode frequency and provide a stable mode. This configuration was used for the remainder of the test program.

FIGURE 1

* FOR RUNS 1-26 SPACER 'A' WAS 20" LONG ('DUMMY' SRH BALANCE).
FOR RUNS 27-35 SPACER REPLACED BY SRH BALANCE (20" LONG).
FOR RUNS 36-166 SPACER 'A' FITTED AS DRAWN (2" LONG).

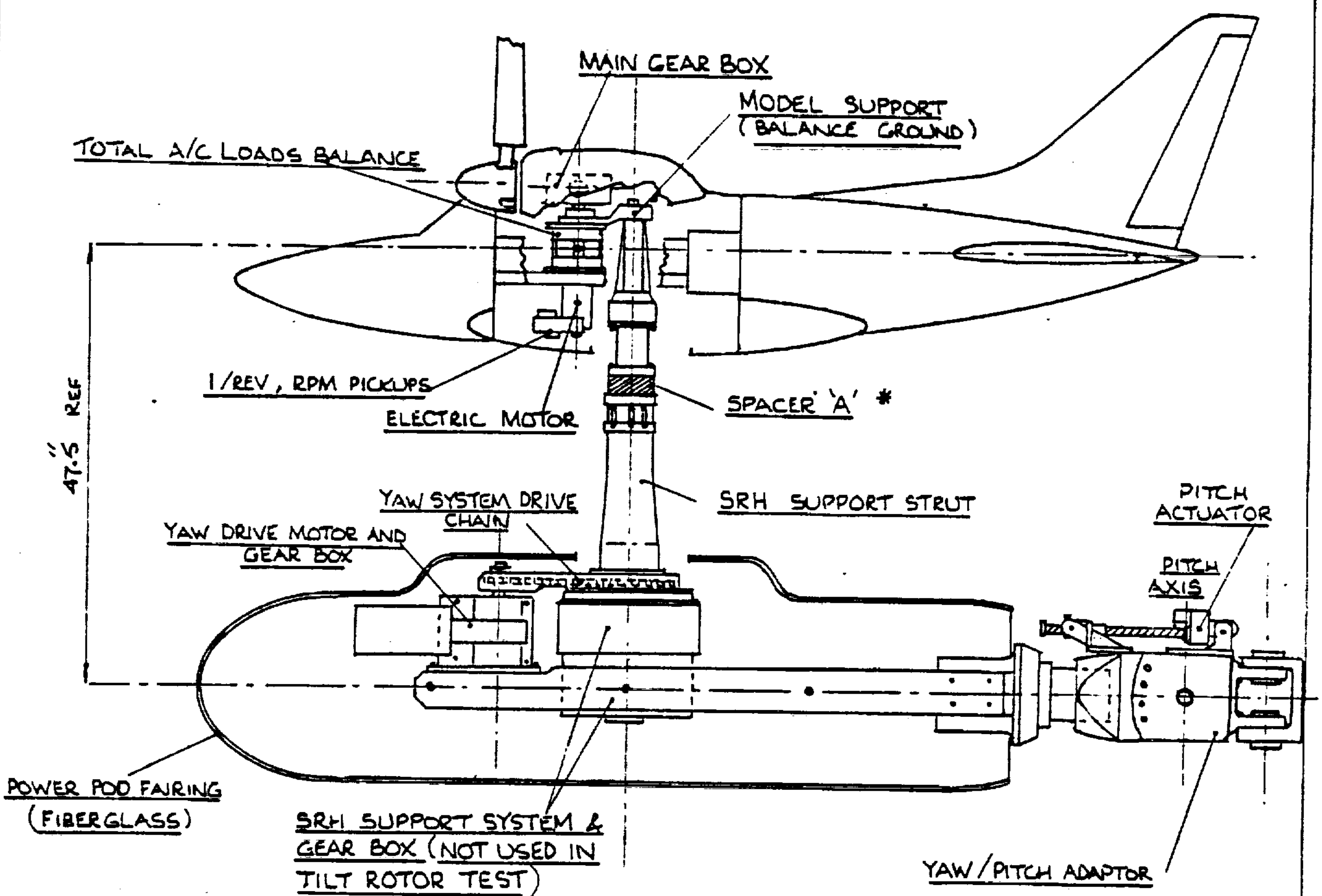

SCALE : 1/20

VR 095Q-1 ~ 1/4.622 SCALE TILT ROTOR MODEL

Figure 45. GENERAL ARRANGEMENT AND INSTALLATION ON SRH TEST STAND

KEF
6-1-76

No instabilities were encountered for the duration of the test; however, it became apparent that the model wing/wing-nacelle pitch frequency was close to 1/rev in cruise conditions and was lower than anticipated. This was thought to be due to the stiffness of the nacelle/wing interface since stiffening the wing and the nacelle balance had little or no effect. The structure of the interface is fairly complex and did not provide an easy means of stiffening so it was decided to increase the inertia and drop the frequency to avoid incorrect amplification of the rotor loads in cruise due to hub motion. This was felt to be an acceptable solution since aeroelastic considerations did not enter into the test objectives. Details of the weight added are shown in Figure 46.

Throughout the test the model was tested at the tunnel centerline.

The tunnel is a closed circuit, continuous flow facility and contains nine fixed-pitch blades, 11.9 m (39 feet) in diameter, which provide wind speeds up to 240 knots. The fan is powered by a 15,000 horsepower motor package consisting of two separate motors located in a nacelle. Air travels through the 226 m (742 foot) closed circuit tunnel and is turned by vanes into the test section which is 6 m (20 feet) wide, 6 m (20 feet) high and 13.7 m (45 feet) long. The tunnel is equipped with an air exchange system which reduces tunnel temperature and

FIGURE 3

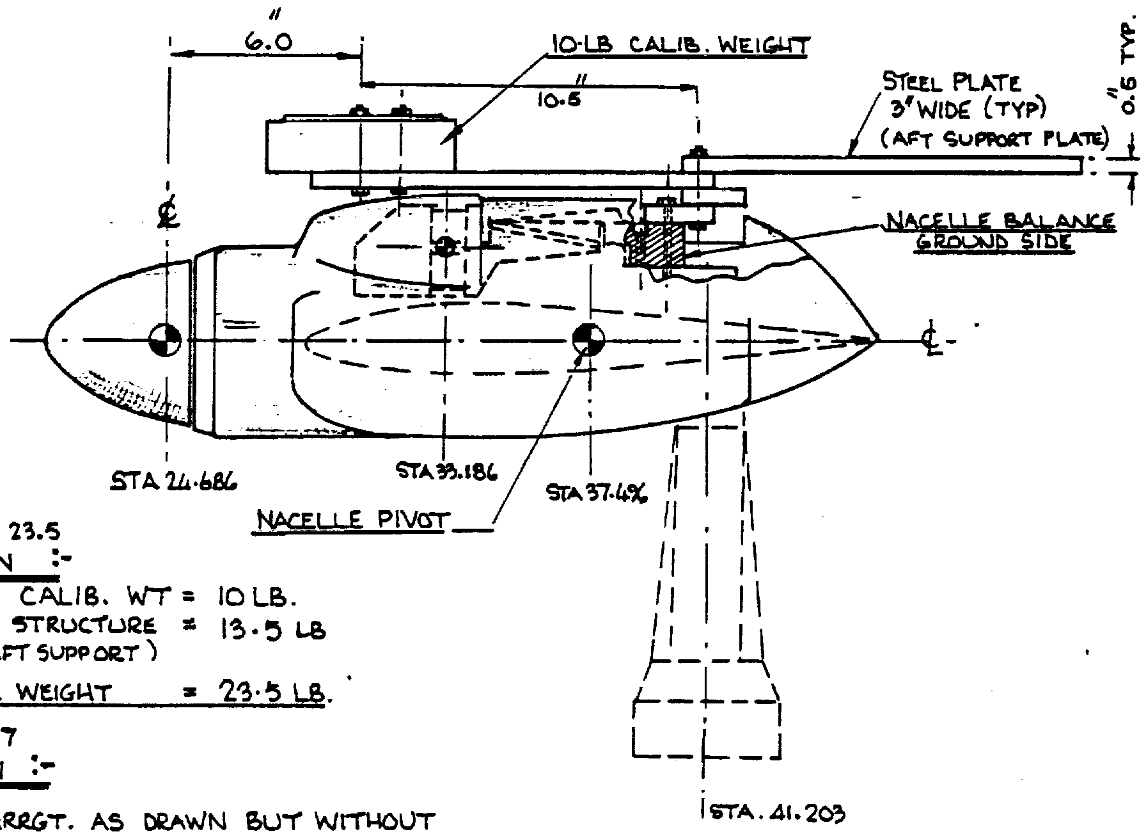

$W_N^{23.5}$:-

CALIB. WT = 10 LB.
WT. OF STRUCTURE = 13.5 LB
(INC. AFT SUPPORT)
TOTAL WEIGHT = 23.5 LB.

W_N^{17} :-

ARRGT. AS DRAWN BUT WITHOUT
AFT SUPPORT PLATE
TOTAL WEIGHT = 17 LB.

SCALE : 1/6 MODEL SCALE

VR 095 Q-1 1/4.622 SCALE TILT ROTOR

Figure 46. DETAILS OF TUNING WEIGHT ADDED TO NACELLES

KEF 6/9/76

also removes the turbulent air boundary layer before it enters the test section. New air is pulled into the wind tunnel through the inlet section of the air exchange system located downstream from the test section. Pertinent wind tunnel data are shown in Table 2 and the wind tunnel general arrangement is shown in figure 47.

TABLE 2. BOEING V/STOL WIND TUNNEL PERTINENT DATA

CIRCUIT DIMENSIONS

Length (overall)	105 m (347 feet) (approx. square in cross section)
Width (overall)	36.5 m (120 feet)
Height (ground)	15.2 m (50 feet)

TEST SECTION DIMENSIONS

Closed	6 m (20 feet) square by 13.7 m (45 feet) long
Slotted	6 m (20 feet) square by 13.7 m (45 feet) long; 10 percent porosity
Open Throat	6 m (20 feet) square by 7 m (23 feet) long
Contraction Ratio	6:1
Diffuser Angle	6 degrees equivalent cone (maximum)

FAN DESCRIPTION

Diameter	11.8 m (39 feet)
Blades	9, fixed pitch
Motors (horsepower)	13,500 AC, 1,500 DC: 15,000 total
Nacelle	5.5 m (18 feet) maximum diameter by 21.9 m (72 feet) long, 272 design rpm

MODEL SUPPORT SYSTEM

Floor Mount	3.6 m (12 feet) by 4.8 m (16 feet) floor insert, custom installation

AUXILIARY SYSTEMS

Data Acquisition	120-channel system using an IBM 1800 computer which operates independently or linked to a central IBM 360 system

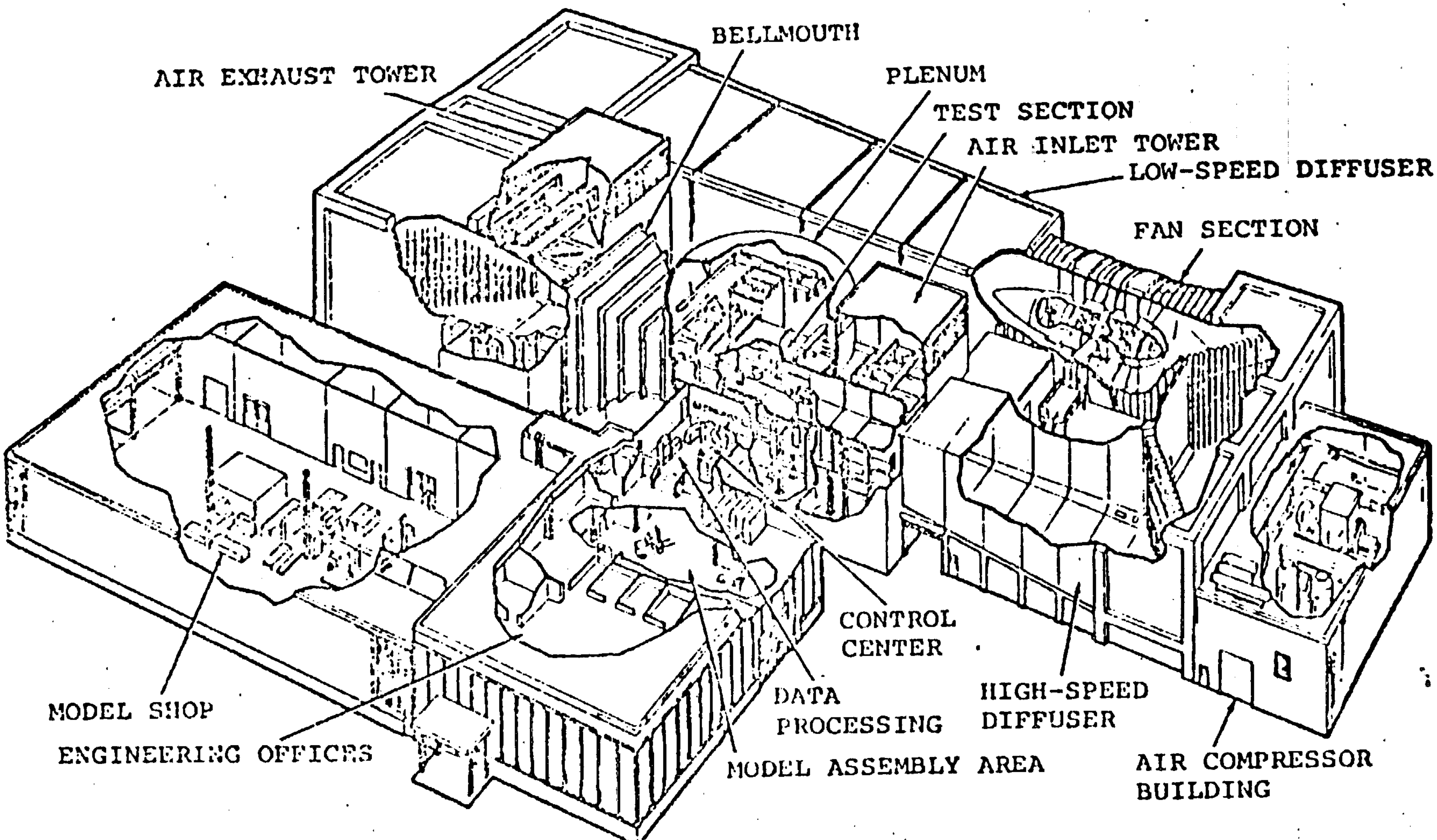

Figure 47. The Boeing V/STOL Wind Tunnel General Arrangement

3.3 Sign Conventions and Scale Factors

The sign conventions for forces and moments maintained throughout the test are depicted in figure 48. The rotor hub force and moment convention is identical to the total loads balance convention in the cruise condition shown. It should be noted however that the rotor hub axes system and sign convention is maintained relative to the rotor shaft axis at all values of nacelle incidence.

For example, this means that rotor yaw moment is in the same sense as aircraft yaw moment at $I_N = 0^o$ but coincides with aircraft roll moment at $I_N = 90^o$. Similarly, rotor normal force at $I_N = 0^o$ is in the same sense as aircraft lift but as the nacelle incidence is increased to $I_N = 90^o$ the normal force acts in the same sense as aircraft drag.

Positive pitch and yaw attitudes are in the same sense as positive aircraft pitch and yaw moments.

The model is a 1/4.622 Froude scale model; therefore, the scale factors to be used in converting from model to full scale are as given below.

	Scale Factor
Linear dimensions	4.622
Mass or weight	98.739
Time	2.15
Frequency	0.46514

	Scale Factor
Velocity	2.15
Viscous Damping	45.927
Stiffness	2109.36
Spring rate	21.363
Mass Moment of Inertia	2109.36
Force	98.739
Strain	1.0
Moment or Torque	456.373
Power	212:278
Per rev frequency	1.0
Disc loading	4.622
Mach No.	2.1498
Froude No.	1.0
Lock No.	1.0

Companions of model and full scale blade Mach No. and Re. No. in hover are shown in figures 49 and 50.

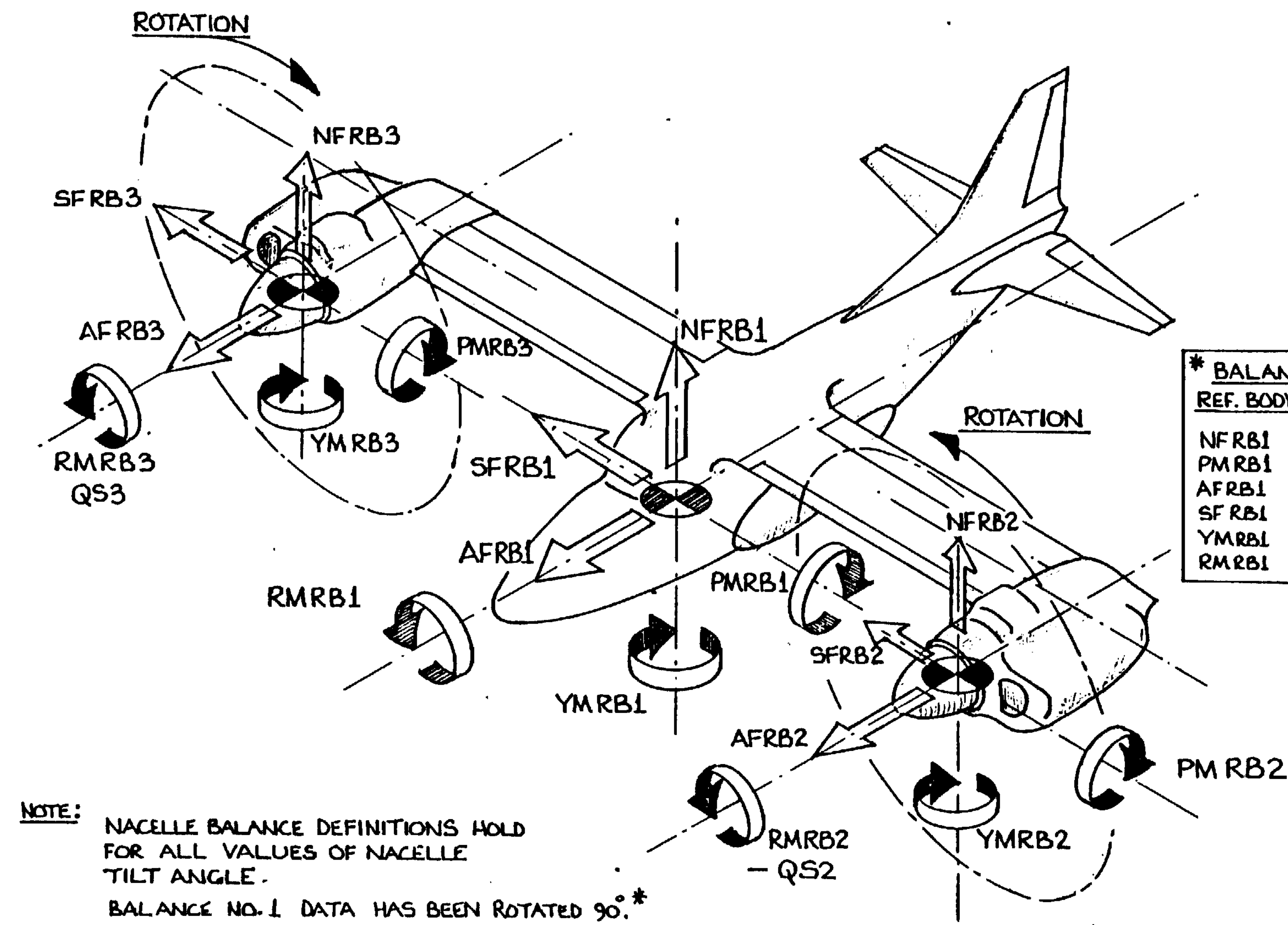

* BALANCE 1 DATA	
REF. BODY	BALANCE
NFRB1	+ AFBAL1
PMRB1	+ PMBAL1
AFRB1	− NFBAL1
SFRB1	+ SFBAL1
YMRB1	− RMBAL1
RMRB1	+ YMBAL1

NOTE: NACELLE BALANCE DEFINITIONS HOLD FOR ALL VALUES OF NACELLE TILT ANGLE.
BALANCE NO. 1 DATA HAS BEEN ROTATED 90°.*

VR 095 Q-1 1/4.622 SCALE TILT ROTOR MODEL

Figure 48. DEFINITION OF MODEL FORCES & MOMENTS REFERRED TO REF. BODY AXES

Ver 1
6-4-76
FORM 46284 (2/66)

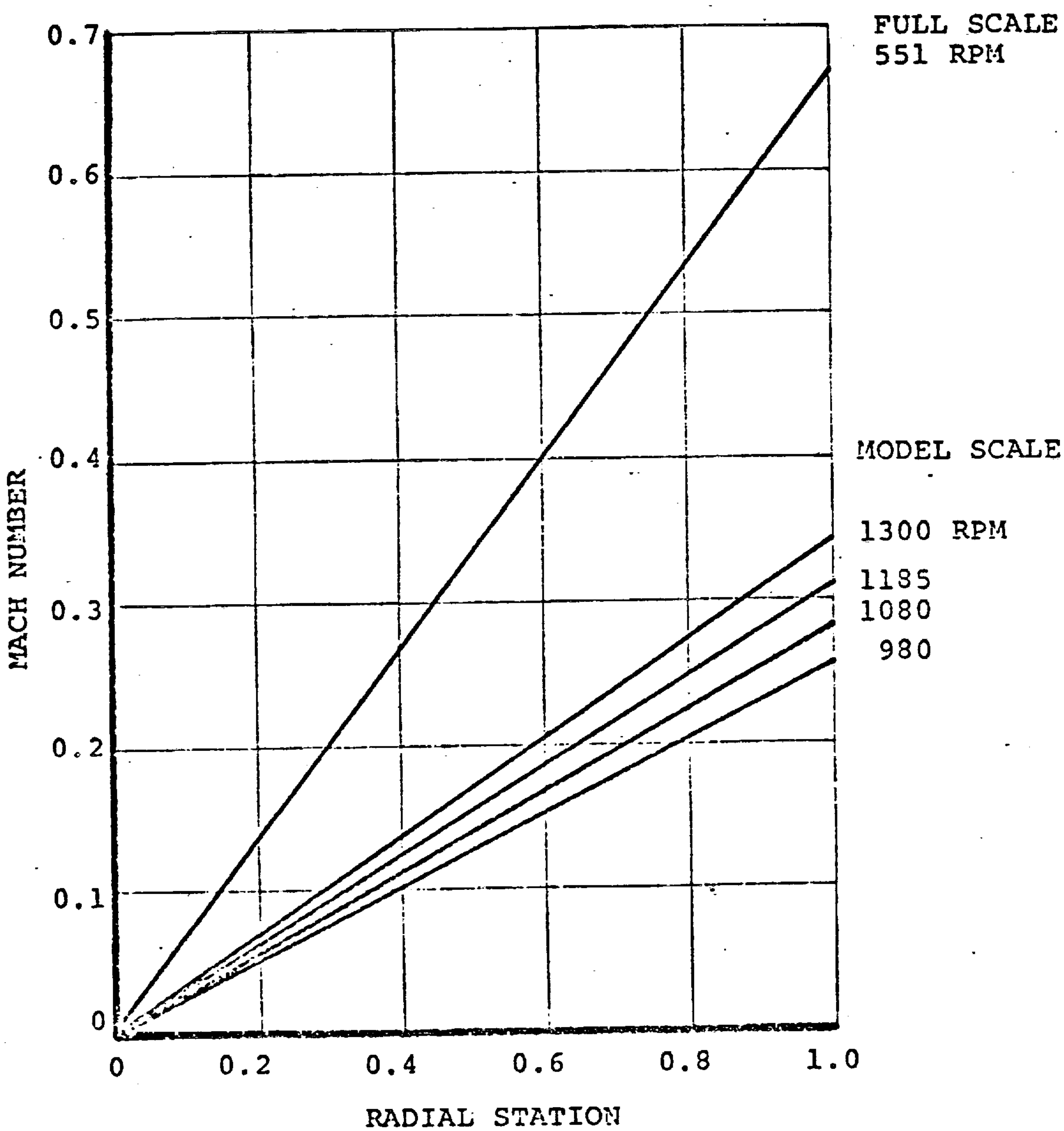

FIGURE 49. COMPARISON OF MODEL SCALE AND FULL SCALE BLADE MACH NUMBER DISTRIBUTIONS.

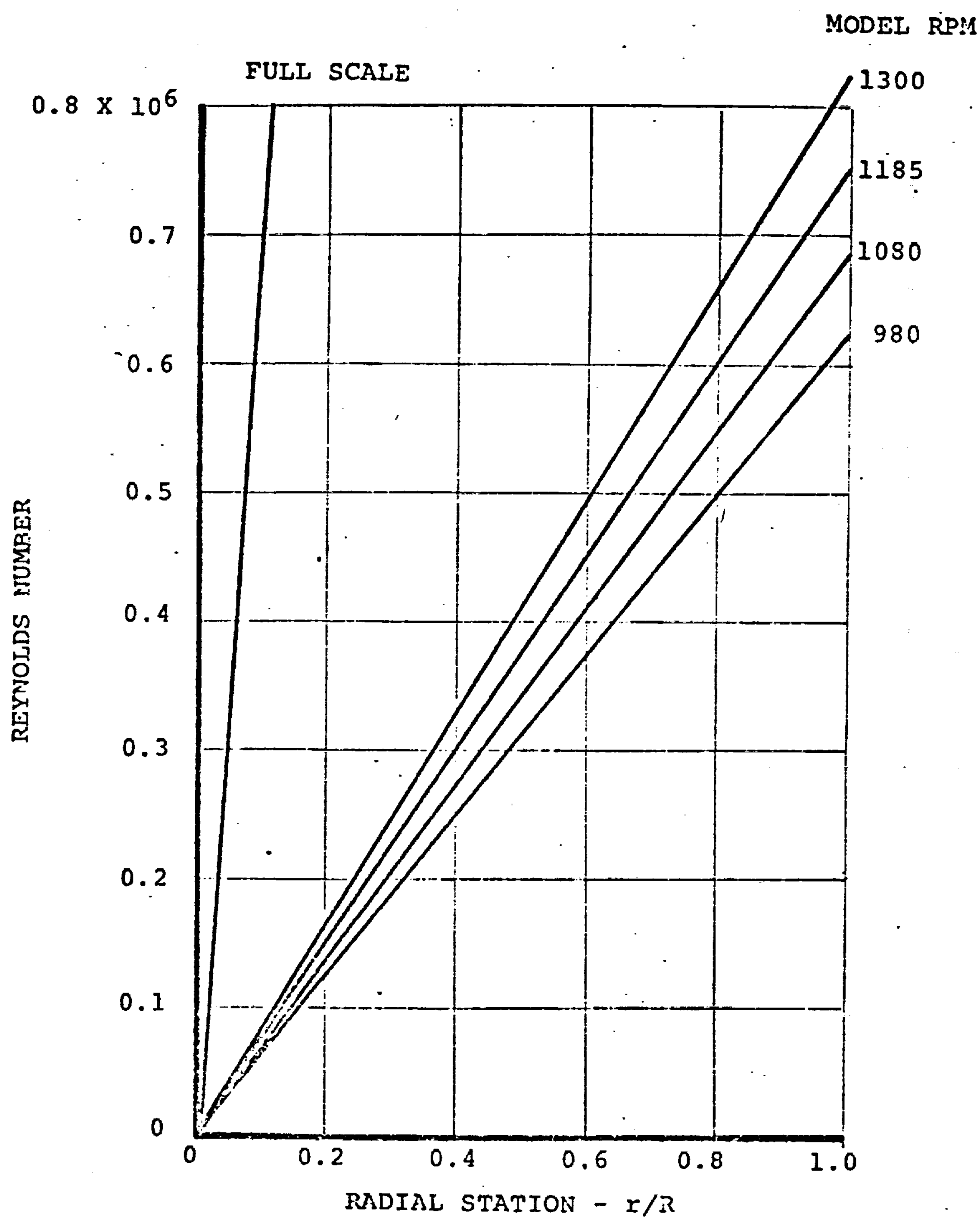

FIGURE 50. COMPARISON OF MODEL SCALE AND FULL SCALE REYNOLDS NUMBER DISTRIBUTIONS.

3.4 Data Reduction

In the early stages of the test a series of runs were made with no blades corresponding to the nacelle incidences, attitudes, RPM's and velocities to be used during the blades on testing. The forces and moments measured on the nacelle balances were divided by dynamic pressure and curve fitted to form the basic hub and spinner tares.

Data taken on the nacelle balances was processed through the balance matrix and corrected for the appropriate hub and spinner tares previously measured at the same operating conditions.

In order to provide an accurate accounting for the rotor shaft incidence the elastic deflections of the model were also used to compute the rotor incidence. This was done by using prior measurements of pitch deflection due to hub moment and normal force.

The summary of the data reduction program is on file at the wind tunnel for BVWT 105. The critical dimensions used as input data for this program are presented in table 3 and a sketch of the balance arrangement is shown in figure 34.

To account for model flexibility in the pitch direction the equations presented below are integrated in the data reduction program.

Wing Pitch Deflections

$$\Delta\alpha w_1 = [NFIMB-(NF_{2RB}+NF_{3RB})\cos i_{N2} - (T2RB+T3RB)\sin i_{N2}]\ K_1$$

$$+[FMIMB+.29AFIMB+.591(T2RB-T3RB)\cos i_{N2} + .408(T2RB+T3RB)\sin i_{N2}$$

$$-PM2RB=PM3RB-(NF2RB+NF3RB)\sin i_{N2}(.375+.365\ \sin i_{N2})$$

$$-(NF2RB+NF3RB)\cos i_{N2}(.365\ \cos i_{N2}-.192)]K_2$$

Nacelle Pitch Deflections

$$\Delta\alpha i_{N2} = (K3=K4\cos i_{N2})NF2RD+K5PM2RB$$

$$-K6T2RB\ \cos i_{N2} + \Delta\alpha w_1$$

$$\Delta\alpha i_{N3} = (K3-K4\ \cos i_{N3})NF3RB+K5PM3RB$$

$$-K6T3RB\ \cos i_{N3} + \Delta\alpha w_1$$

$$i_{N2}\ corr = i_{N2} + \Delta\alpha i_{N2}$$

$$i_{N3}\ corr = i_{N3} \quad \Delta\alpha i_{N3}$$

K_1 = wing rotation due to pitching moment applied by the wing

K_2 = wing rotation due to pitching moment applied by the rotor

K_3 = rotor disc rotation due to rotor normal force

The information is thus reduced and printed. Copies of the computer printout results from which the plotted data were made were given to the NASA technical monitor in microfiche form. Table 4 defines the nomenclature used by the data reduction program.

TABLE 3. - WIND TUNNEL DATA REDUCTION INPUT CONSTANTS

RDINC	SYM		UNITS	ALL DIMENSIONS PER PRINT
1	x_2	Horiz. Dist. from Left Nacelle Bal. Axis ℄ to Ref. Body Axis	FT	.7083
2	y_2	Lat. Dist. from Left Nacelle Bal. Axis ℄ to Ref. Body Axis	FT	0.0
3	z_2	Vert. Dist. from Left Nacelle Bal. Axis ℄ to Ref. Body Axis	FT	-.2188
4	x_3	Horiz. Dist. from Right Nacelle Bal. Axis ℄ to Ref. Body Axis	FT	.7083
5	y_3	Lat. Dist. from Right Nacelle Bal. Axis ℄ to Ref. Body Axis	FT	0.0
6	z_3	Vert. Dist. from Right Nacelle Bal. Axis ℄ to Ref. Body Axis	FT	-.2188
7	d_2	Left Torque Directional Sign i.e. CW Rotation (Blade) =-1 — as view from pilot seat		-1
8	d_3	Right Torque Directional Sign i.e. CCW Rotation (Blade) =+1 — as view from pilot seat		+1
9	l_2	Horiz. Dist. from Left Nacelle Ref. Body Axis to Nacelle Pivot Point	FT	-1.0729
10	m_2	Lat. Dist. from Left Nacelle Ref. Body Axis to Nacelle Pivot Point	FT	0.0
11	n_2	Vert. Dist. from Left Nacelle Ref. Body Axis to Nacelle Pivot Point	FT	0.0
12	l_3	Horiz. Dist. from Right Nacelle Ref. Axis to Nacelle Pivot Point	FT	-1.0729
13	m_3	Lat. Dist. from Right Nacelle Ref. Body Axis to Nacelle Pivot Point	FT	0.0
14	n_3	Vert. Dist. from Right Nacelle Ref. Body Axis to Nacelle Pivot Point	FT	0.0
15	e_1	Horiz. Dist. from Aircraft Balance Axis ℄ to Model Body Axis	FT	0.0
16	f_1	Lat. Dist. from Aircraft Balance Axis ℄ to Model Body Axis	FT	0.0

TABLE 3.
INPUT CONSTANTS (continued)

ALL DIMENSIONS PER PRINT

RDINC	SYM		UNITS	
17	g_1	Vert. Dist. from Aircraft Balance Axis ℄ to Model Body Axis	FT	.3908
18	e_2	Horiz. Dist. from Left Nacelle Pivot Axis to Model Body Axis	FT	+.1911
19	f_2	Lat. Dist. from Left Nacelle Pivot Axis to Model Body Axis (neglecting droop and/or bent spar)	FT	+3.6150
20	g_2	Vert. Dis. from Left Nacelle Pivot Axis to Model Body Axis	FT	-.0794
21	e_3	Horiz. Dist. from Right Nacelle Pivot Axis to Model Body Axis	FT	+.1911
22	f_3	Lat. Dist. from Right Nacelle Pivot Axis to Model Body Axis (neglecting droop and/or best spar)	FT	-3.6150
23	g_3	Vert. Dist. from Right Nacelle Pivot Axis to Model Body Axis	FT	-.0794
24	S	Wing Area	FT^2	9.360
25	b	Wing Span	FT	7.230
26	c	Wing Chord	FT	1.294
27	R_2	Left Rotor Radius	FT	2.8125
28	R_3	Right Rotor Radius	FT	2.8125

Table 4.

LIST AND DEFINITION OF PRINTOUT PARAMETERS

1. TUNNEL PARAMETERS

VTUN	Tunnel Velocity	ft/sec
PTOTAL	Tunnel Total Pressure	lb/ft^2
PSTATIC	Tunnel Static Pressure	lb/ft^2
RHOTUN	Tunnel Air Density	$slug/ft^3$ ($lb\ sec^2/ft^4$)
TSTATIC	Tunnel Temperature	°F
QTUN	Tunnel Dynamic Pressure	lb/ft^2

2. BALANCE PARAMETERS

2.1 General

NF	Normal Force	lb.
PM	Pitching Moment	ft. lb.
AF	Axial Force	lb.
SF	Side Force	lb.
YM	Yawing Moment	ft. lb.
RM	Rolling Moment	ft. lb.
	Torque	ft. lb.

2.2 Balance Parameters, Interactions, Weight Tares Applied Torque Corrections Applied

Fuselage (Total Loads) Balance	Left Nacelle Balance	Right Nacelle Balance
NFBAL1	NFBAL2	NFBAL3
PMBAL1	PMBAL2	PMBAL3
AFBAL1	AFBAL2	AFBAL3
SFBAL1	SFBAL2	SFBAL3
YMBAL1	YMBAL2	YMBAL3
RMBAL1	RMBAL2	RMBAL3

2.3 Nacelle Balance Data Transferred to Rotor Reference Body Axes

NFRB2R	Left rotor normal force, perpendicular to hub axis
PMRB2R	Left rotor pitching moment about hub ref. point (℄)
TRB2R	Left rotor thrust, along hub axis

2.3 Nacelle Balance Data Transferred to Rotor Reference Body Axes (Cont'd)

SFRB2R Left rotor side force, perpendicular to hub axis
YMRB2R Left rotor yawing moment about hub ref. point (¢) (plane perpendicular to NFRB2R)
RMRB2R Left rotor rolling moment about hub ref. point (¢) (plane perpendicular to TRB2R)

QRB2R Left rotor shaft torque

NFRB3R Right rotor normal force, perpendicular to hub axis

etc. etc.

2.4 Nacelle Balance Data Rotor Ref. Body Axes, Corrected for Hub Tares

NFRB2B Left rotor normal force, perp. to hub axis, corr. for hub tares
PMRB2B Left rotor pitching moment about hub ref., corr. for hub tares
TRB2B Left rotor thrust along hub axis, corr. for hub tares
SFRB2B Left rotor side force, perp. to hub axis, corr. for hub tares
YMRB2B Left rotor yawing moment about hub ref. corr. for hub tares
RMRB2B Left rotor rolling moment about hub ref. corr. for hub tares

QRB2B Left rotor torque corrected for hub tares

NFRB3B Right rotor normal force, perp. to hub axis, corr. for hub tares

etc. etc.

2.5 Nacelle Balance Data Referred to Model Body Axes, Hub Tares Not Removed

NFMB-L Left rotor normal force, model body axes
PMMB-L Left rotor pitching moment about body ref. point (A/C C.G.)
AFMB-L Left rotor axial force, model body axes (+ fwd)
SFMB-L Left rotor side force, model body axes
YMMB-L Left rotor yawing moment about body ref. point (A/C C.G.)

2.5 Nacelle Balance Data Referred to Model Body Axes, Hub Tares Not Removed (Cont'd)

RMMB-L Left rotor rolling moment about body ref. point (A/C C.G.)

NFMB-R Right rotor normal force, model body axes

etc. etc.

2.6 Fuselage Balance (Total Loads) Transferred to Model Body Axes

NFMB-AC Total aircraft normal force, body axes
PMMB-AC Total aircraft pitching moment ref. to A/C C.G.
AFMB-AC Total aircraft axial force, body axes (+ fwd)
SFMB-AC Total aircraft sideforce, body axes
YMMB-AC Total aircraft yawing moment, ref. to A/C C.G.
RMMB-AC Total aircraft rolling moment, ref. to A/C C.G.

2.7 Airframe Data Model Body Axes (Corrected for Rotor Effects)

NFMB-AF Airframe normal force, body axes
PMMB-AF Airframe pitching moment ref. to A/C C.G.
DMB -AF Airframe drag, body axes, positive aft
SFMB-AF Airframe sideforce, body axes
YMMB-AF Airframe yawing moment, ref. to A/C C.G.
RMMB-AF Airframe rolling moment, ref. to A/C C.G.

2.8 Fuselage Balance (Total A/C Loads) Transferred to Wind Axes

LW -AC Total aircraft lift, wind axes
PMW-AC Total aircraft pitching moment, ref. to A/C C.G.
AFW-AC Total aircraft axial force, wind axes, positive fwd
SFW-AC Total aircraft sideforce, wind axes
YMW-AC Total aircraft yawing moment, ref. to A/C C.G.
RMW-AC Total aircraft rolling moment, ref. to A/C C.G.

2.9 Airframe Data Wind Axes (Corrected for Rotor Effects)

LW-AF Airframe lift, wind axes
PMW-AF Airframe pitching moment ref. to A/C C.G.
DW-AF Airframe drag, wind axes, positive aft
SFW-AF Airframe side force, wind axes
YMW-AF Airframe yawing moment, ref. to A/C C.G.
RMW-AF Airframe rolling moment, ref. to A/C C.G.

3. NON DIMENSIONAL COEFFICIENTS

3.1 Aircraft

3.1.1 Model Body Axis Coefficients

CNFMB-AC = NFMB-AC / QTUN·S
CPMMB-AC = PMMB-AC / QTUN·S·C
CAFMB-AC = AFMB-AC / QTUN·S
CSFMB-AC = SFMB-AC / QTUN·S
CYMMB-AC = YMMB-AC / QTUN·S·B
CRMMB-AC = RMMB-AC / QTUN·S·B

3.1.2 Wind Axis Coefficients

CLW-AC = LW-AC / QTUN·S
CPMW-AC = PMW-AC / QTUN·S·C
CAFW-AC = AFW-AC / QTUN·S
CSFW-AC = SFW-AC / QTUN·S
CYMW-AC = YMW-AC / QTUN·S·B
CRMW-AC = RMW-AC / QTUN·S·B

3.1.3 Model Body Axis Coefficients (Hover Option)

CNF1-HOV = NFMB-AC / 2π RHOTUN·$R2^2$·$(\text{VTIP-L})^2$
CPM1-HOV = PMMB-AC / 2π RHOTUN·$R2^3$·$(\text{VTIP-L})^2$
CAF1-HOV = AFMB-AC / 2π RHOTUN·$R2^2$·$(\text{VTIP-L})^2$
CSF1-HOV = SFMB-AC / 2π RHOTUN·$R2^2$·$(\text{VTIP-L})^2$
CYM1-HOV = YMMB-AC / 2π RHOTUN·$R2^3$·$(\text{VTIP-L})^2$
CRM1-HOV = RMMB-AC / 2π RHOTUN·$R2^3$·$(\text{VTIP-L})^2$

3.2 Airframe

3.2.1 Model Body Axis Coefficients

CNFMB-AF = NFMB-AF / QTUN·S
CPMMB-AF = PMMP-AF / QTUN·S·C
CDMB-AF = DMB-AF / QTUN·S
CSFMB-AF = SFMB-AF / QTUN·S
CYMMB-AF = YMMB-AF / QTUN·S·B
CRMMB-AF = RMMB-AF / QTUN·S·B

3.2.2 Wind Axis Coefficients

CLW-AF = LW-AF / QTUN·S
CPMW-AF = PMW-AF / QTUN·S·C
CDW-AF = DW-AF / QTUN·S
CSFW-AF = SFW-AF / QTUN·S
CYMW-AF = YMW-AF / QTUN·S·B
CRMW-AF = RMW-AF / QTUN·S·B

3.3 Rotors

3.3.1 Reference Body Axes

$$\text{CNFR-L} = \text{NFRB2R} / \text{RHOTUN}\cdot \text{R2}^2\cdot(\text{VTIP-L})^2\cdot\pi$$
$$\text{CPMR-L} = \text{PMRB2R} / \text{RHOTUN}\cdot \text{R2}^3\cdot(\text{VTIP-L})^2\cdot\pi$$
$$\text{CTR-L} = \text{TRB2R} / \text{RHOTUN}\cdot \text{R2}^2\cdot(\text{VTIP-L})^2\cdot\pi$$
$$\text{CSFR-L} = \text{SFRB2R} / \text{RHOTUN}\cdot \text{R2}^2\cdot(\text{VTIP-L})^2\cdot\pi$$
$$\text{CYMR-L} = \text{YMRB2R} / \text{RHOTUN}\cdot \text{R2}^3\cdot(\text{VTIP-L})^2\cdot\pi$$
$$\text{CRMR-L} = \text{RMRB2R} / \text{RHOTUN}\cdot \text{R2}^3\cdot(\text{VTIP-L})^2\cdot\pi$$
$$\text{CPR-L} = \text{QRB2R} / \text{RHOTUN}\cdot \text{R2}^3\cdot(\text{VTIP-L})^2\cdot\pi$$

$$\text{CNFR-R} = \text{NFRB3R} / \text{RHOTUN R3}^2\ (\text{VTIP-R})^2$$

etc. etc.

Reference Body Axes, Hub Tares Removed

$$\text{CNFB-L} = \text{NFRB2B} / \text{RHOTUN}\cdot \text{R2}^2\cdot(\text{VTIP-L})^2\cdot\pi$$
$$\text{CPMB-L} = \text{PMRB2B} / \text{RHOTUN}\cdot \text{R2}^3\cdot(\text{VTIP-L})^2\cdot\pi$$
$$\text{CTB-L} = \text{TRB2B} / \text{RHOTUN}\cdot \text{R2}^2\cdot(\text{VTIP-L})^2\cdot\pi$$
$$\text{CSFB-L} = \text{SFRB2B} / \text{RHOTUN}\cdot \text{R2}^2\cdot(\text{VTIP-L})^2\cdot\pi$$
$$\text{CYMB-L} = \text{YMRB2B} / \text{RHOTUN}\cdot \text{R2}^3\cdot(\text{VTIP-L})^2\cdot\pi$$
$$\text{CRMB-L} = \text{RMRB2B} / \text{RHOTUN}\cdot \text{R2}^3\cdot(\text{VTIP-L})^2\cdot\pi$$
$$\text{CPB-L} = \text{QRB2B} / \text{RHOTUN}\cdot \text{R2}^3\cdot(\text{VTIP-L})^2\cdot\pi$$

$$\text{CNFB-R} = \text{NFRB3B} / \text{RHOTUN}\cdot \text{R3}^2\cdot(\text{VTIP-R})^2\cdot\pi$$

etc. etc.

4. GENERAL

OMEGA2	Rotational speed, left rotor	$= \pi$RPM1 / 30
OMEGA3	Rotational speed, right rotor	$= \pi$RPM2 / 30
VTIP-L	Tip speed, left rotor	$= \pi$RPM1·R2·/ 30
VTIP-R	Tip speed, right rotor	$= \pi$RPM2·R3·/ 30
MU-LEFT	Advance ratio, left	= VTUN / VTIP-L
MU-RIGHT	Advance ratio, right	= VTUN / VTIP-R
V-KNOTS	Tunnel speed, knots	= 0.5921 VTUN
V-FS	Full scale speed, knots	= 2.14988 V-KNOTS

5. ANGLES

ALPHAW1C	Model angle of attack corrected for initial deflection and rotation due to airframe and rotor loading
ALPHAW2C	Left nacelle incidence (relative to wind axis) corrected for initial deflection and rotation due to rotor loads
ALPHAW3C	Right nacelle incidence (relative to wind axis) corrected for initial deflection and rotation due to rotor loads
NAC-2	Corrected left nacelle incidence, relative to body water line = ALPHAW2C-ALPHAW1C
NAC-3	Corrected right nacelle incidence relative to body water line = ALPHAW3C-ALPHAW1C
BETA	Sideslip angle, positive nose to left.

6. CONTROL SYSTEM

COLL-L	Collective pitch ($\theta_{.75}$ deg.) left rotor
COLL-R	Collective pitch ($\theta_{.75}$ deg.) right rotor
A1C-LEFT	Lateral cyclic pitch, control input, left
A1C-RIGHT	Lateral cyclic pitch, control input, right
B1C-LEFT	Longitudinal cyclic pitch, control input, left
B1C-RIGHT	Longitudinal cyclic pitch, control input, right
A1-LEFT	Lateral cyclic pitch, pure input (ψ=90°), left
A1-RIGHT	Lateral cyclic pitch, pure input (ψ=90°), right
B1-LEFT	Longitudinal cyclic pitch, pure input (ψ=180°), left
B1-RIGHT	Longitudinal cyclic pitch, pure input (ψ=180°), right

3.5 Frequency Data

The analysis and usage of data obtained on a hingeless rotor requires that the frequencies of the blades be known. The static blade frequencies were obtained by bang/tweak tests and the results are provided in table 5. The response of the blade gages at different RPM and collective pitch settings provide a signal input to the spectral analysis methodology and the on line ubiquitous analyzer used on test. This capability allowed us to check the rotating blade frequencies by identifying the peaks on response curves. An example is shown in figure 51.

The rotor blade rotating frequencies in hover at a collective pitch at 8° are shown in figure 52 and in the cruise configuration at a collective pitch of 34° in figure 53.

TABLE 5.

BLADE NATURAL FREQUENCIES FROM BANG/TWEAK TESTS

BLADE S/N	MEASURED NATURAL FREQUENCIES ~ HZ.							
	FLAP		CHORD		TORSION		2ND FLAP	
	1	2	1	2	1	2	1	2
263	5.69 5.69 5.70	5.97*	12.32 12.16 12.24	12.38	88.90 94.28	88.29 87.13	38.70	32.06 31.90
265	5.52 5.60 5.53	5.76*	12.08 12.12 12.0	11.92* 11.83*	95.74 96.00 96.77	87.29 86.45 86.62		33.78 33.82
271	5.51 5.55 5.56	5.54 5.73* 5.86*	11.76 11.68 11.68	11.94 12.06* 12.00*		90.40 90.40	38.46 37.70 35.29	33.57 33.60
273	5.28 5.40 5.43	5.58*	11.92 12.00 11.92	12.03*	96.42	87.23 87.30 87.07	33.33 33.33 33.33	32.61 32.61

1 Original values, blade cuffs fitted

2 Values measured with cuffs removed, 3/23/76

The test set-up was the same in both cases.
An accelerometer was used to define the frequencies, except as defined thus * where a blade strain gauge output was used.

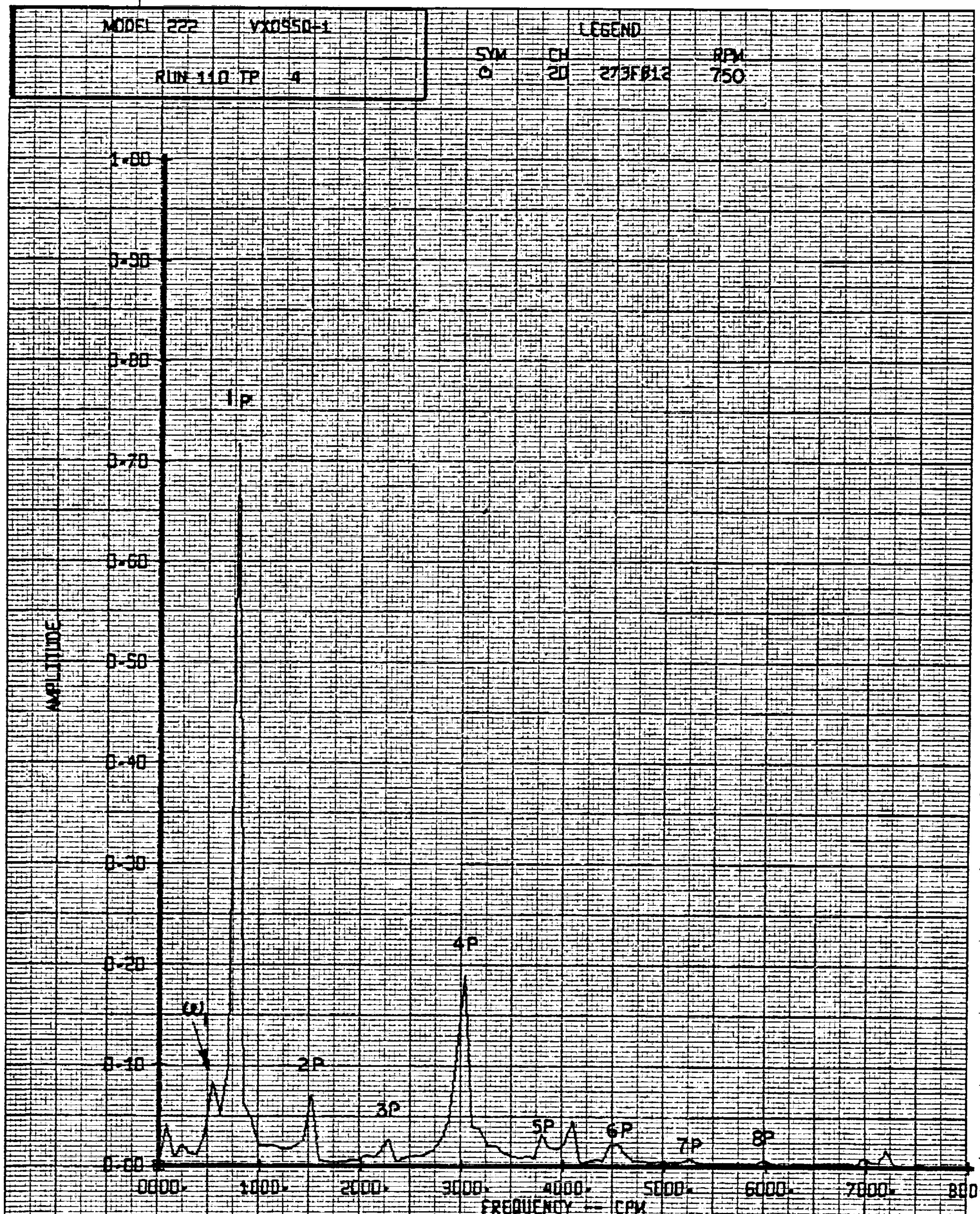

Figure 51. Example of On Line Ubiquitous Analyzer Plot Used on Test

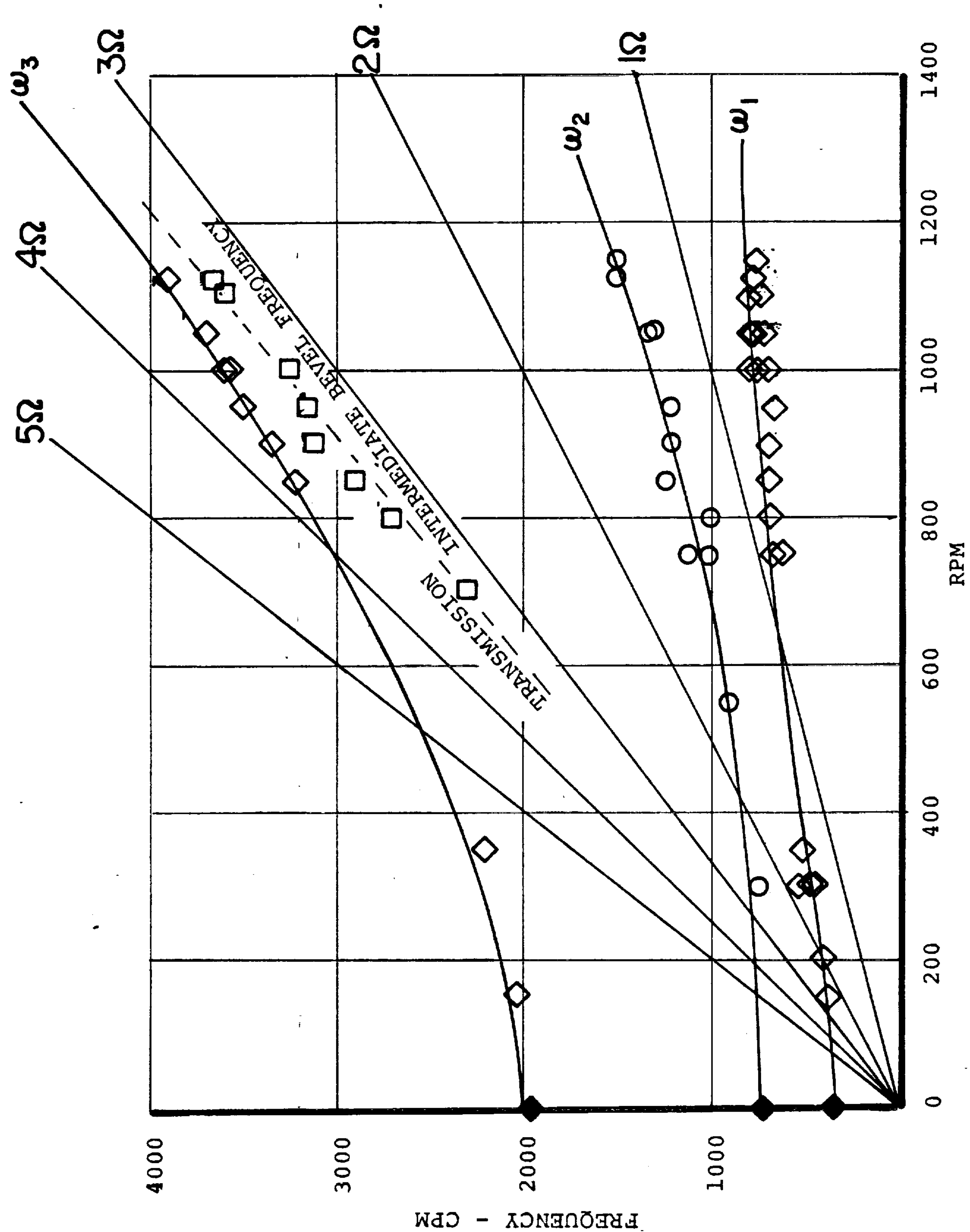

Figure 52. Rotor Blade Rotating Frequencies in Hover (8° Collective Pitch)

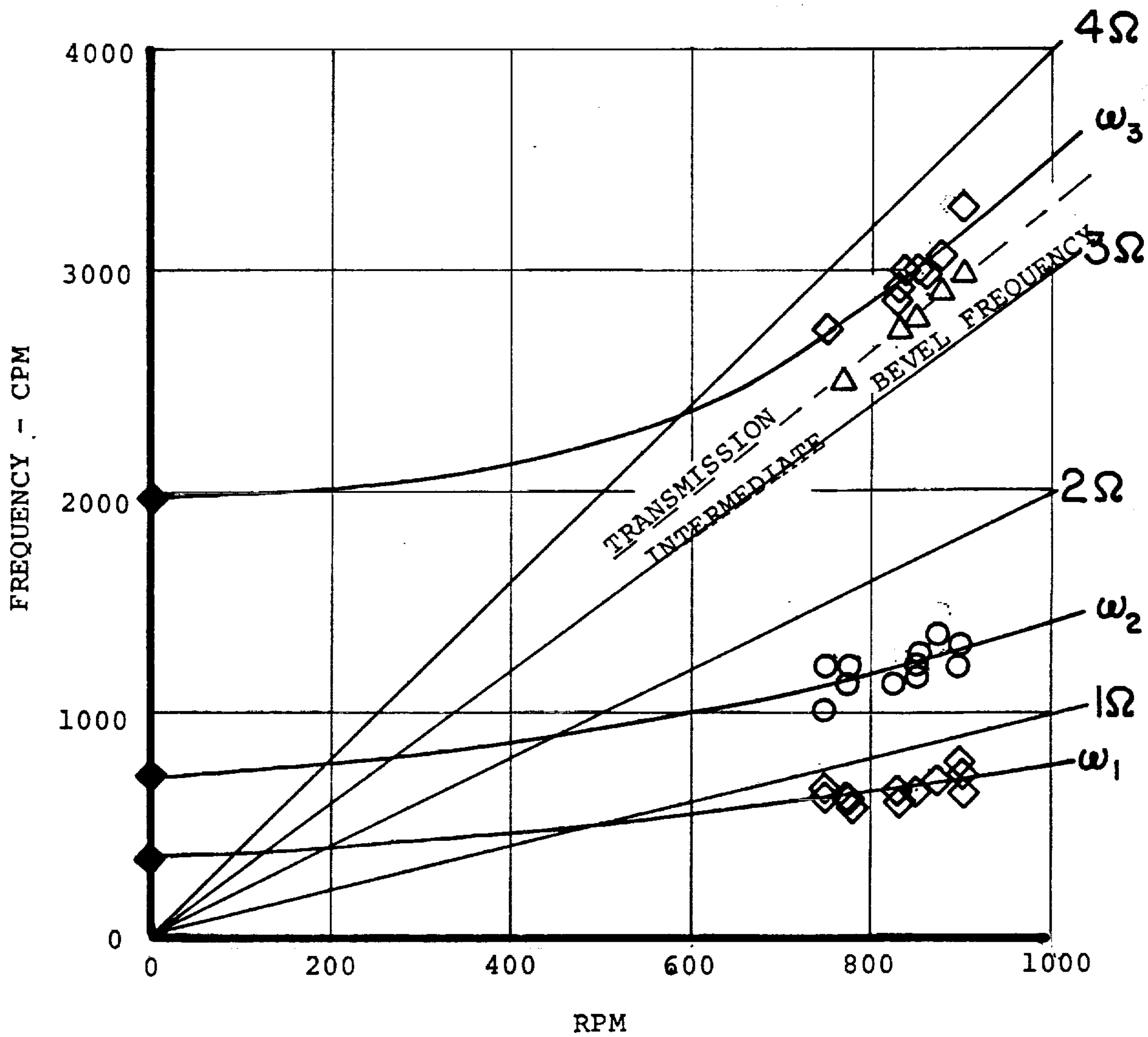

Figure 53. Rotor Blade Rotation Frequencies in Cruise (34° Collective Pitch)

4.0 SCOPE OF TEST AND TEST NOTES

The primary objective of the test program was to develop parametric force, moment and rotor loads data over the anticipated flight envelope of the tilt rotor aircraft. The scope of the test program is depicted in figure 54 which shows the seventeen initial test conditions used on test. These conditions were selected to provide an adequate coverage of the estimated flight envelope and to take advantage of existing full scale data obtained in the NASA Ames 40 x 80 wind tunnel (Reference 2) shown superimposed.

4.1 Test Program and Test Log

The procedure adopted for the data runs was to set up the model at one initial condition with an approximate trim attitude and cyclic pitch for minimum blade loads. From this initial condition the test variables were exercised in turn. In hover (condition 1) Figure 54, the model rotor performance was established, as well as cyclic pitch effectiveness at two thrust levels.

For each of the conditions in transition; i.e., conditions 2 through 12, a sequence of tests was run about each initial condition which involved varying angle of attack, yaw angle, longitudinal and lateral cyclic, collective pitch, wing flap setting and rotor RPM.

The cruise flight data, conditions 13 through 17, were obtained using a different sequence of tests. The nacelles were set to -1° and zero angle of attack and zero yaw established. The

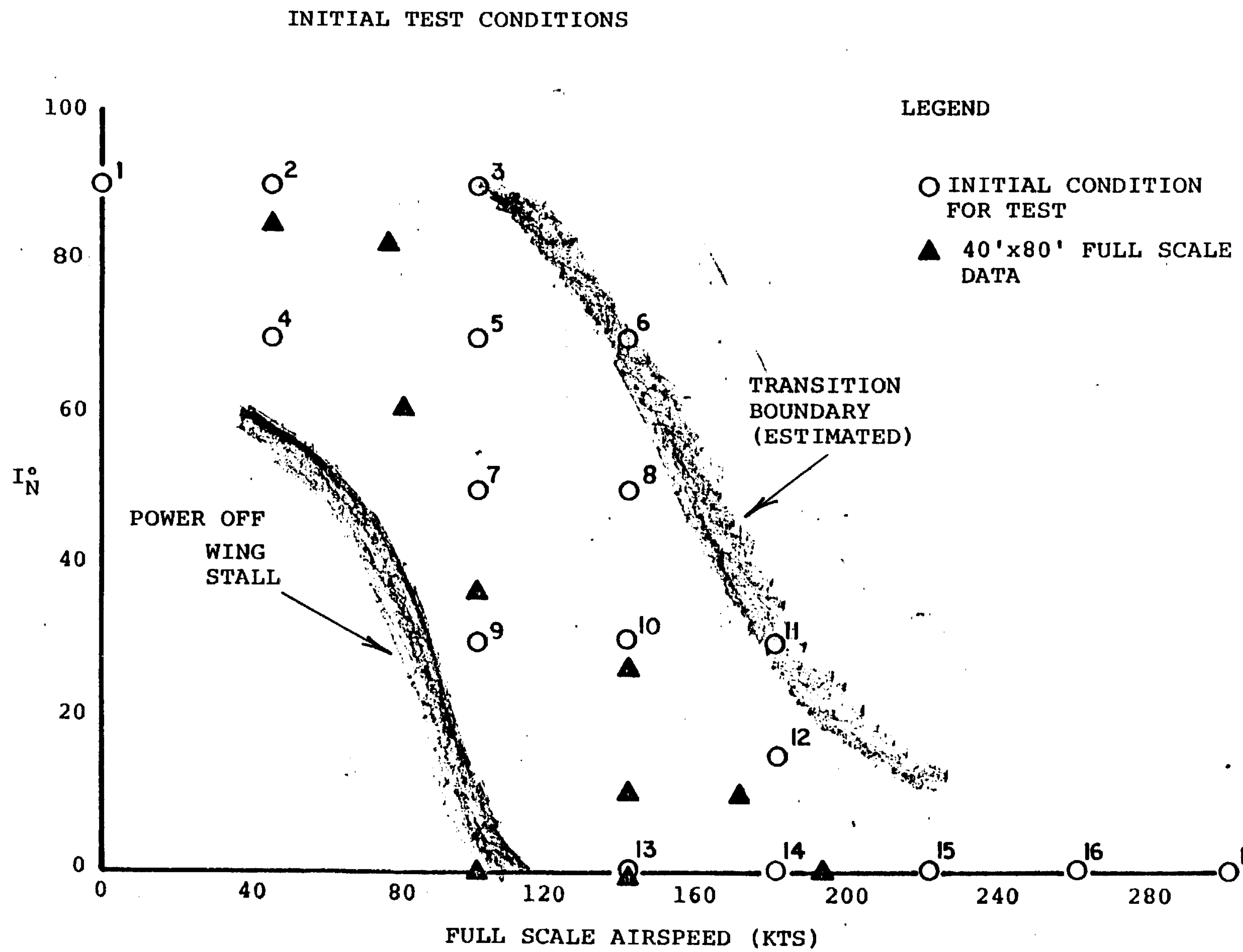

Figure 54. Scope of Test, Initial Test Conditions

cyclic pitch settings were set to minimum loads. The aircraft angle of attack was varied with various wing flap settings establishing the α effects and providing data to determine the effect of wing C_L on the rotor derivatives. The effects of both axes of cyclic pitch were then established and finally α variations made with pre-calculated cyclic schedules and at conditions 13, 14, and 15, α variations with cyclic pitch tuned to minimum loads. These latter runs enable the "cyclic on the stick" data to be deduced.

The test log recorded during the program is provided as table 6. Runs 1 through 23 had no blades fitted and were performed to establish the hub tares required to establish the rotor data on later tests. Weight tares were established before each series of runs at a new configuration.

The test log defines the test configuration by a series of code letters which are summarized in table 7 and detailed explanation of the codes is given in table 8.

RUN NO.	CONFIGURATION	TYPE OF RUN	WT. TARE RUN	RPM	V_{KTS} M/S	V_{KTS}* F/S	i_N°	α_F°	ψ°	$\theta_{.75}$	$A_{1_c}^\circ$	$B_{1_c}^\circ$	δ_F°	DATE / TIME
1	K_1	HUB TARE	1	1185	20.9	45	90	△1	0	–	–	–	0	4/7/76 1135 1150
2	✓	✓	2	✓	20.9	45	✓	✓	✓	–	–	–	✓	1325 1338
3	✓	✓	✓	✓	46.5	100	✓	✓	✓	–	–	–	✓	1340 1346
4	✓	✓	✓	✓	65.1	140	✓			–	–	–	✓	1349 1355
5	✓	YAW SWEEP	✓	✓	✓	✓	✓	0	△2	–	–	–	✓	1356 1403
6	✓	HUB TARE	6	✓	20.9	45	70	△1	0	–	–	–	✓	1424 1435
7	✓	✓	✓	✓	46.5	100	✓	✓	✓	–	–	–	✓	1436 1442
8	✓	✓	✓	✓	65.1	140	✓	✓	✓	–	–	–	✓	1444 1452
9	✓	✓	9	✓	46.5	100	50	✓	✓	–	–	–	✓	1510 1518
10	✓	✓	✓	✓	65.1	140	✓	✓	✓	–	–	–	✓	1520 1525

1. $K_1 = W_1 F_1 N_1 T_1 V_1 H_1$ (BLADES OFF, SPINNERS ON)

△1 : $\alpha_F = -18, -15 \rightarrow +20^\circ \times 5^\circ$'s

* SCALED FULL SCALE FORWARD SPEED ~ KNOTS.

2. REPEAT RUN 1 AS α_F° PROBLEMS.

4. $\alpha_F = 20^\circ$ OMITTED.

5. △2 $\psi = 0, -20^\circ \rightarrow +20^\circ \times 5^\circ$'s   NOTE – FOR THIS RUN α_{GIL} WAS .47° @ $\psi = 20^\circ$
MODEL WOULD BE ROLLED ≈ .16

8. $\alpha_F = 20^\circ$ OMITTED.

10. ✓ ✓ ✓

PREP.	KEF	4/7/76	REVISED	DATE
CHK.				
APPR				

VR 095 Q-1

1/4 SCALE TILT ROTOR MODEL

BVWT

182

FORM 49810 (3/70)

Table 6. 1/4 Scale Test Run Log

RUN NO.	CONFIGURATION	TYPE OF RUN	WT. TARE RUN	RPM	V_{KTS} M/S	V_{KTS} F/S	i_N °	α_F °	ψ °	$\theta_{.75}$ °	A_{1_C} °	B_{1_C} °	δ_F °	DATE / TIME
11	K1	YAW SWEEP	9	1185	65.1	140	50	0	△2	-	-	-	0	4/7/76 1528 1534
12	✓	FLAP SWEEP	✓	✓	✓	✓	✓	✓	0	-	-	-	△3	1536 1543
13	✓	HUB TARE	13	1065	46.5	100	30	△1	✓	-	-	-	0	1549 1558
14	✓	✓	✓	✓	65.1	140	✓	✓	✓	-	-	-	✓	1603 1610
15	✓	✓	✓	✓	83.7	180	✓	△4	✓	-	-	-	✓	1615 1626
17	✓	✓	16	947	✓	✓	15	✓	✓	-	-	-	✓	4/8/76 0908 0920
18	✓	✓	18	830	65.1	140	0	✓	✓	-	-	-	✓	0928 0935
19	✓	YAW SWEEP	✓	✓	✓	✓	✓	0	△2	-	-	-	✓	0936 0941
20	✓	HUB TARE	✓	✓	83.7	180	✓	△4	0	-	-	-	✓	0945 0950
21	✓	✓	✓	✓	102.3	220	✓	△5	✓	-	-	-	✓	1015 1021

12. △3 : $\delta_F = 0° \rightarrow 50° \times 10°$'s

~ DATA @ $\delta_F = 0°$ ONLY COULD NOT MOVE RH. FLAP. RUN ABANDONED.

14. $\alpha_F = 20°$ OMITTED

15. △4 : $\alpha_F = -18 \rightarrow +10 \times 4°$'s

NO RUN 16 DATA. W/T'S UNDER RUN 16.

21. △5 $\alpha_F = -6° \rightarrow +4° \times 2°$'s

PREP.			REVISED	DATE
CHK.				
APPR				

VR 095 Q-1

1/4 SCALE TILT ROTOR MODEL

BVWT

182

FORM 49810 (3/70)

Table 6. (continued)

RUN NO.	CONFIGURATION	TYPE OF RUN	WT. TARE RUN	RPM	V_{KTS} M/S	V_{KTS} F/S	i_N°	α_F°	ψ°	$\theta_{.75}$	$A_{1_C}^\circ$	$B_{1_C}^\circ$	δ_F°	DATE / TIME	
22	K_1	HUB TARE	18	830	120.9	240	0	5 (flag)	0	–	–	–	0	4/8/76	1022 1026
23	✓	✓	✓	✓	139.5	300	✓	✓	0	–	–	–	✓		1038 1034
24	K_2	HOVER FREQ SWEEP	24	6 (flag)	0	0	90	0	0	8	0	0	70	4/15/76	1452 1519
26	✓	✓	✓	✓	✓	✓	✓	✓	✓	✓	✓	✓	✓	4/16/76	
26	✓	✓	✓	✓	✓	✓	✓	✓	✓	✓	✓	✓	✓	✓	
27	✓	HOVER	27	1185	✓	✓	✓	✓	✓	7 (flag)	✓	✓	✓	4/19/76	1043 1137
28	✓	✓	✓	1110	✓	✓	✓	✓	✓	✓	✓	✓	✓		1315 1353
29	✓	✓	✓	✓	✓	✓	✓	✓	✓	FOR C_T = .0499	8 (flag)	0	✓		1407 1430
30	✓	✓	✓	✓	✓	✓	✓	✓	✓	✓	0	9 (flag)	✓		1430 1445
31	✓	✓	✓	✓	✓	✓	✓	✓	.	✓	✓	✓	✓		1600 1625

24. 6 (flag) BLADES FITTED
RPM = 150 → 1185 x 50's ROOF, FLOOR OUT
OMITTED 650 AS 1/R X-OVER, OMITTED 1150, 1165 AS GROUND RESONANCE BDRY ≈ 1135 RPM
ADDED DATA @ 1125.

25. CEC DATA ONLY. FUSE BALANCE (#1) LOCKED OUT. RPM TO 1260.
1) LONG ACCELS RECORDED 2) VERT ACCELS RECORDED.

26. SRH BALANCE (BV 6054) INSTALLED.

27. 7 (flag): $\theta_{.75}$ = 4° → MAX x 2°'s AT 8° GROUND RESONANCE PROBLEM INVESTIGATION, INCL.
(MAX 12°.) RPM SWEEP TO 1195.

29. 8 (flag) A_1 = 0 → 2°, 0 → −2° / .5's $\theta_{.75}$ = 10°

30. 9 (flag) B_1 0 → −2°, 0 RPT. (OMITTED + RANGE – RESONANCE PROBLEM)

31. 2" x 4" SUPPORTS UNDER WING TIPS. WITH RESTRAINING CABLES FROM O/B FLAP BKTS TO FLOOR. FLOOR IN THIS RUN ON. NO MEANINGFUL FUSE. BAL. DATA

$\boxed{K_2} = K_1 + B^{42,162,282}_{2(3,266,265} \; B^{88,208,328}_{272,271,273} + PL1$

Table 6. (continued)

PREP.	KET	4/20/76	REVISED	DATE	VR 095 Q-1	BVWT
CHK.					1/4 SCALE TILT ROTOR MODEL	182
APPR						

RUN NO.	CONFIGURATION	TYPE OF RUN	WT. TARE RUN	RPM	V_{KTS} M/S	V_{KTS} F/S	$i_N°$	$\alpha_F°$	$\psi°$	$\theta_{.75}°$	$A_{1_C}°$	$B_{1_C}°$	$\delta_F°$	DATE / TIME
32	K_2	HOVER B[?] EFF	27	1110	0	0	90	0	0	FNCT = .011	0	9	70	4/20/ 0911 0956
33	✓	FREQ INVEST	✓	→1140	0	0	✓	✓	✓	10	0	0	✓	✓ 1025 1055
34	✓	✓	✓	→1185	✓	✓	✓	✓	✓	6.8	✓	✓	✓	✓ 1530 1559
35	✓	✓	✓	→1185	✓	✓	✓	✓	✓	✓	✓	✓	✓	✓
36	✓	✓	✓	✓	✓	✓	✓	✓	✓	8°-12°	✓	✓	✓	4/23/76
37	✓	CRUISE	37	830	65	140	0	10	0	32	FOR TRIM	CONDITION	0	4-25-76 1334 1433
38	✓	TRANS.	38	1185		45	90	✓	0	9	-.5	+2.75	70	✓
39.	$K_3 + W_F^{23}$	✓	39	✓		✓	✓	✓	✓	✓	FOR TRIM	CONDITION	✓	4/30/76 1355

32. AT COMPLETION CYCLIC SWEEP (B_{1_C}) TOOK RPM TO 1185, TRIMMED CYCLICS. TOOK ANALYSER DATA, ALSO COMPUTER T.P.

33. 2"x4" SUPPORTS AND CABLE BRACES REMOVED THIS RUN. RPM TO 1140. S.A. DATA 1 T.P ON COMPUTER

34. STIFFENING FLEXURES ON L.H. NACELLE BALANCE REMOVED (CALIBS. WILL NOT BE VALID)

35. DUMMY BALANCE L.H. NACELLE. NO BALANCE DATA THIS SIDE.

36. ACTIVE NACELLE BALANCES. SRH TOTAL LOADS BALANCE REMOVED & REDUCED HEIGHT DUMMY BALANCE INSERT FITTED. FUSE. BAL (BV 6019) REACTIVATED BUT IS LOCKED OUT BY MODEL/STRUT STIFFENING PLATE.

No COMPUTER DATA THIS RUN.

37. 10 α_F SWEEP - ABLE TO DO 0, -2, -4, 0, +2 ONLY. PROHIBITIVE LOADS (76 1/2) TOOK DATA AT VARIOUS RPM VALUES COMING DOWN @ $\alpha_F = 0°$ 1750 → 600/25's

38. CONTROL SYSTEM PROBLEM LHS CAUSED GAUGE FAILURE, SWASHPLATE & BEARING DAMAGE. REWORKED

39. 22.77 LBS LEAD WEIGHTS ADDED TO FWD FUSE FRAME AT ≈ 32" FWD C.G. (W_F^{23}) LARGEST ON FUSE. BALANCE REMOVED. REPEAT RUN 38 $\alpha_F = -10° \to 0° \times 1°s$

$\theta_L = 7.9°$ $\theta_R = 9.3°$ ≡ T OF 61 lb.

$\boxed{K_3}$ = K_2 BUT $B_{[?]}^{58,\ 178,\ 298}$ (AFTER RE-WORK)

PREP.	KEF	4/20/76	REVISED	DATE	VR 095 Q-1	BVWT
CHK.					1/4 SCALE TILT ROTOR MODEL	182
APPR						

FORM 49810 (3/70)

Table 6. (continued)

RUN NO.	CONFIGURATION	TYPE OF RUN	WT. TARE RUN	RPM	V_{KTS} M/S	V_{KTS} F/S	i_N°	α_F°	ψ°	$\theta_{.75}^\circ$	$A_{1_C}^\circ$	$B_{1_C}^\circ$	δ_F°	DATE / TIME
40	$K_3 + W_F^{23}$	TRIMS	39	1185		45	90	-10	0	9	FOR TRIM	△11	70	4/30/
41	✓ ✓	✓	✓	✓		✓	✓	✓	✓	✓	△12	FOR TRIM	✓	
42	✓ ✓	✓	✓	✓		✓	✓	0	△13	✓	FOR TRIM	CONDITION	✓	
43	✓ ✓	✓	✓	✓		✓	✓	-10	0	△14	✓	✓	✓	
44	✓ ✓	✓	✓	✓		✓	✓	-10	0	9	✓	✓	△15	1620
45	✓ ✓	✓	✓	△16		✓	✓	✓	✓	✓	✓	✓	70	
46	✓ ✓	✓	46	1185		✓	70	△17	✓	✓	✓	✓	61	5/3/76
47	✓ ✓	✓	✓	✓		✓	✓	12	✓	✓	✓	△11	✓	
48	✓ ✓	✓	✓	✓		✓	✓	✓	✓	✓	*△12	FOR TRIM	✓	
49	✓ ✓	✓	✓	✓		✓	✓	✓	✓	✓	△12	✓	✓	1410

40 △11 B_1 = TRIM $(+5^\circ) \rightarrow +3^\circ \times 1^\circ$S

41 △12 A_1 = TRIM (≈ 0) $\pm 2^\circ \times 1^\circ$S

42 △13 $\psi = 0^\circ \rightarrow +10^\circ, +5^\circ, 0^\circ \rightarrow -10^\circ, -5^\circ, 0^\circ$ RPT

43 △14 $\theta_{.75} = 8^\circ \rightarrow 12^\circ$ (L), $9^\circ \rightarrow 13^\circ$ (R) FREQUENCY LIMIT

44 △15 $\delta_F = 70^\circ \rightarrow 35^\circ \times 5^\circ$S

45 △16 RPM VARIATION 1185 → 1200 → 1150 ATTEMPTED 1125 ~ NO GO, STAB BDRY.

46 △17 $\alpha_F = +6^\circ \rightarrow 20^\circ \times 1^\circ$S $(10^\circ \rightarrow 20^\circ, 0 \rightarrow -6^\circ)$ T_L, T_R AT TRIM = 61 b.

47 B_1 = 5, 4.5, 4.0, 3.5 → 100% BLADE ALLOW.
271CB 273 FB V. SPIKEY RUN # UNCHANGED IN COMPUTER THIS RUN UNDER 46.

48. * INITIAL TRIM POINT ONLY. RH BLADE GAUGES OUT.

49. REPEAT FOR RUN 48. PICKED UP ORIGINAL CB (273 CB 124) AS LOOKED REASONABLE.

PREP.			REVISED	DATE	VR 095 Q-1	BVWT
CHK.					1/4 SCALE TILT ROTOR MODEL	182
APPR						

FORM 49810 (3/70)

Table 6. (continued)

RUN NO.	CONFIGURATION	TYPE OF RUN	WT. TARE RUN	RPM	V M/S	V_{KTS} F/S	i_N°	α_F°	ψ°	$\theta_{.75}^\circ$	A_{1c}°	B_{1c}°	δ_F°	DATE / TIME
50	$K_3 + W_F^{23}$	✓	46	1185		45	70	12	△18	9	FOR CONDITION	TRIM	61	5/3/ 1455
51	✓ ✓	✓	✓	✓		✓	✓	✓	0	△14	✓	✓	✓	
52	✓ ✓	✓	✓	✓		✓	✓	✓	✓	9	✓	✓	△15	
53	✓ ✓	✓	✓	△16		✓	✓	✓	✓	✓	✓	✓	31	
54.	$K_4 + W_F^{23}$	✓	✓	1185	46.5	100	✓	△10	✓	12.5	✓	✓	61	5/5/76 1647
55	✓ ✓	✓	✓	✓	✓	✓	✓	-6	△13	✓	✓	✓	✓	1815
56	✓ ✓	✓	✓	✓	✓	✓	✓	✓	0	✓	△12	✓	✓	5/6/76 0848
57	✓ ✓	✓	✓	✓	✓	✓	✓	✓	✓	✓	FOR TRIM	△11	✓	
58	✓ ✓	✓	✓	✓	✓	✓	✓	✓	✓	△14	✓	FOR TRIM	✓	
59	✓ ✓	✓	✓	✓	✓	✓	✓	✓	✓	12.5	✓	✓	△15	

50: △18 $\psi = 0^\circ \rightarrow -20 \times 2^\circ s, -10^\circ, 0^\circ \rightarrow +20^\circ \times 2^\circ s, +10^\circ, 0^\circ$

52: $\delta_M = 61 \rightarrow 31 \times 5^\circ s$.

53: RPM 1185, 1200, 1225, 1250.

54. LONGER (2") P.L's FITTED (PL2) $\alpha_F = -10^\circ \rightarrow -2^\circ$. RAN UP TO TRIM @ $\alpha_F = -10^\circ$

55 $\psi = 0 \rightarrow -10 \times 2^\circ s, -5, 0 \rightarrow +10 \times 2^\circ s, +5, 0$

56 $A_{1c} = \pm 1.5^\circ$ ABOUT TRIM VALUE (4.28° L, 4.43° R)

57 $B_{1c} = +1^\circ -1.5^\circ$ ABOUT TRIM VALUE (5.7° L&R)

58. $\theta_L = 13.5 \rightarrow 14.5 \rightarrow 10.3$
$\theta_R = 12.4 \rightarrow 13.7 \rightarrow 9.4$

59 $\delta_F = 61^\circ \rightarrow 0^\circ \times 10^\circ s$

$\boxed{K_4} = K_3$ BUT WITH PITCH LINKS PL2 REPLACING PL1 (2" LONGER BARRELS)

PREP.			REVISED	DATE	VR 095 Q-1	BVWT
CHK.						
APPR					1/4 SCALE TILT ROTOR MODEL	152

FORM 49510 (3/70)

Table 6. (continued)

RUN NO.	CONFIGURATION	TYPE OF RUN	WT. TARE RUN	RPM	V_{KT} M/S	V_{KTS} F/S	$i_N°$	$\alpha_F°$	$\psi°$	$\theta_{.75}$ L/R	$A_{1_C}°$	$B_{1_C}°$	$\delta_F°$	DATE / TIME
60	$K_4 + W_F^{23}$	TRANS.	46	16	46.5	100	70	-6	0	13.5/12.3	FOR CONDITION	TRIM	61	5/6/76 1150
61	✓ ✓	✓	61	1185	✓	✓	50	10	✓	16/14.7	✓	✓	42	1135 1232
62	$K_5 + W_F^{23}$	✓	✓	✓	✓	✓	✓	-1	13	✓	✓	✓	✓	5/10/76 1350
63	✓ ✓	✓	✓	✓	✓	✓	✓	✓	0	14	✓	✓	✓	
64	✓ ✓	✓	✓	✓	✓	✓	✓	✓	✓	16.3/15	12	✓	✓	
65	✓ ✓	✓	✓	✓	✓	✓	✓	✓	✓	✓	FOR TRIM	11	✓	
66	✓ ✓	✓	✓	✓	✓	✓	✓	✓	✓	✓	✓	FOR TRIM	15	
67	✓ ✓	✓	✓	16	✓	✓	✓	✓	✓	✓	✓	✓	42	1605
68	✓ ✓	✓	✓	1185	65	140	✓	10	✓	22.6/20.7	✓	✓	✓	
69	✓ ✓	✓	✓	✓	✓	✓	✓	-8	13	✓	✓	✓	✓	

60 RPM = 1185, 1200, 1212, 1185, 1150, 1125 .. RUN No. NOT CHG'D IN COMPUTER THIS RUN.

61. $\alpha_F = -1° \to +6°, -1° \to -8°$ x 1°s, BLADE LOADS LIMIT

62. REWORKED GEARBOX FROM THIS RUN. NEW BLADE AZIMUTH LOCATIONS. THIS RUN ET. SEQ.

$\psi = 0° \to -10, -5, 0 \to +10, +5, 0.$

$\boxed{K5} = K_? + B^{30,\,150,\,270}_{263,\,266,\,265}\ B^{60,\,180,\,300}_{273,\,272,\,271}$ PL2

67. POWER LIMIT @ 1220 RPM. MIN 1125 (STAB. BDRY?)

68. TRIM @ $\alpha_F = -8°$ α_F $-8 \to -5, -8 \to -11°$

69. $\psi = 0 \to -5, -3, 0 \to +4, +2, 0$

PREP.			REVISED	DATE	VR 095 Q-1	BVWT
CHK.					1/4 SCALE TILT ROTOR MODEL	182
APPR						

FORM 49510 (3/70)

Table 6. (continued)

RUN NO.	CONFIGURATION	TYPE OF RUN	WT. TARE RUN	RPM	V_{KT} M/S	V_{KT} F/S	i_N°	α_F°	ψ°	$\theta_{.75}$ L/R	A_{1c}°	B_{1c}°	δ_F°	DATE / TIME
70	K5 + W_F^{23}	TRANS.	61	1185	65	140	50	-8	0	22.6/20.7	12	FOR TRIM	42	5/10/76
71	✓ ✓	✓	✓	✓	✓	✓	✓	✓	✓	✓	FOR TRIM	11	✓	
72	✓ ✓	✓	✓	✓	✓	✓	✓	✓	✓	14	✓	FOR TRIM	✓	5/11/76 0909 1005
73	✓ ✓	✓	✓	✓	✓	✓	✓	✓	✓	22.3/20.3	✓	✓	15	1100
74	✓ ✓	✓	✓	16	✓	✓	✓	✓	✓	✓	✓	✓	42	1210
75	✓ ✓	✓	75	1185	✓	✓	70	10	✓	18.2/17.3	✓	✓	61	
76	✓ ✓	✓	✓	✓	✓	✓	✓	-11	13	✓	✓	✓	✓	
77	✓ ✓	✓	✓	✓	✓	✓	✓	✓	0	✓	12	✓	✓	
78	✓ ✓	✓	✓	✓	✓	✓	✓	✓	✓	✓	FOR TRIM	11	✓	
79	✓ ✓	✓	✓	✓	✓	✓	✓	✓	✓	14	✓	FOR TRIM	✓	

72. 265 FPB 124 OUT AFTER LAST TP. POWER LIMIT UPPER END. T VARIATION OF +5 -10 lb ABOUT TRIM POINT

73. $\delta_F = 42^\circ \rightarrow 12^\circ \times 10$'s COULD NOT INCREASE RH FLAP ABOVE 42°.

74. RPM = 1185, 1200, 1210 (POWER LIMIT) → 1185, 1175, 1150, 1125. (STAB BDRY.). SPURIOUS RH ROTOR THRUST VALUES SEEN IN MONITOR THIS RUN AND LAST. INVESTIG'N FOUND SFBAL3 GOING INTO PERIODIC SATURATION. PROBLEM FOUND IN BALANCE PLUG. REPAIRED PRE-RUN 75.

75. $-11, -10 \rightarrow -14 \times 1^\circ$s.

76. $T_L = T_R \doteq 48$ lb @ $\alpha_F = -11$
$\psi = 0 \rightarrow -8^\circ \times 1^\circ$s, -4°, $0^\circ \rightarrow +6 \times 1^\circ$s, $+3$, 0

77. $A_1 =$

78. $B_1 =$ COLL TRIMMED RHS AFTER 1ST T.P. TRIM POINT RETAKEN TP #2.

79. DECREASE COLLECTIVE ONLY FROM TRIM VALUES. ANY INCREASE - POWER LIMIT

Table 6. (continued)

PREP.			REVISED	DATE	VR 095 Q-1	BVWT
CHK.					1/4 SCALE TILT ROTOR MODEL	182
APPR						

FORM 49810 (3/70)

RUN NO.	CONFIGURATION	TYPE OF RUN	WT. TARE RUN	RPM	V_{KT} M/S	V_{KT} F/S	i_N°	α_F°	ψ°	$\theta_{.75}$ L/R	A_{1c}°	B_{1c}°	δ_F°	DATE / TIME
80	$K5 + W_F^{46}$	TEMS	75	1185	65	140	70	-11	0	18.2/17.3	FOR COND-	TRIM -ITION	15	5/11/76
81	✓ ✓	✓	✓	16	✓	✓	✓	✓	✓	✓	✓	✓	61	✓ 1725
82	✓ ✓	✓	39	1185	46.5	100	90	10	✓	12.1/11.3	✓	✓	70	5/12/76 0940
83	✓ ✓	✓	✓	✓	✓	✓	✓	-15	3	12.1/11.4	✓	✓	✓	
84	✓ ✓	✓	✓	✓	✓	✓	✓	✓	0	✓	12	✓	✓	
85	✓ ✓	✓	✓	✓	✓	✓	✓	✓	✓	✓	FOR TRIM	11	✓	
86	✓ ✓	✓	✓	✓	✓	✓	✓	✓	✓	14	✓	FOR TRIM	✓	
87	✓ ✓	✓	✓	✓	✓	✓	✓	✓	✓	12.2/11.2	✓	✓	15	
88	✓ ✓	✓	✓	16	✓	✓	✓	✓	✓	✓	✓	✓	70	

80. δ_F = 61° → 10° × 10's, 61° RPT, 71°,
81. RPM = 1185 → 1135 × 10's, 1185 RPT. COULD NOT GO HIGHER THAN 1185 ~ POWER LIMIT
82. -15 → -12 (LOAD LIMIT), -15° → -18° (OPERATIONAL, (STING & CAPABILITY) LIMIT)
83. ψ = 0° → -9°, -5°, 0 → +9°, 0° RPT.
84. A_{1c} = ± 1.5 ABOUT TRIM (4.1 L, 5.1 R)
85. B_{1c} = +1°, -1.5° ABOUT TRIM (6.3 L, 6.6 R)
86. $\theta_{.75}$ TO GIVE T = +15#, -5# FROM TRIM VALUE (74#)
87. δ_F = 70° → 10° × 10's, + 80°
88. RPM: 1185, 1200, 1212 (POWER & STAB. LIMIT COINCIDENT), 1185, 1175 → 1135 × 10's
ENCOUNTER INSTABILITY BDRY ≈ RPM 1132

PREP.			REVISED	DATE	VR 095 Q-1	BVWT
CHK.						
APPR					1/4 SCALE TILT ROTOR MODEL	182

FORM 49810 (3/70)

Table 6. (continued)

RUN NO.	CONFIGURATION	TYPE OF RUN	WT. TARE RUN	RPM	V_{KT} M/S	V_{KT} F/S	i_N°	α_F°	ψ°	$\theta_{.75}$ L/R	$A_{1_C}^\circ$	$B_{1_C}^\circ$	δ_F°	DATE / TIME
89	$K5 + W_F^{46}$	TRANS.	89	1065	46.5	100	30	10	0	20.7/18.2	FOR TRIM	CONDITION	31	5/12/76 1545
90	✓ ✓	✓	✓	✓	✓	✓	✓	3.5	13	✓	✓	✓	✓	
91	✓ ✓	✓	✓	✓	✓	✓	✓	✓	0	✓	12	✓	✓	
92	✓ ✓	✓	✓	✓	✓	✓	✓	✓	✓	✓	FOR TRIM	11	✓	
93	✓ ✓	✓	✓	✓	✓	✓	✓	✓	✓	14	✓	FOR TRIM	✓	
94	✓ ✓	✓	✓	✓	✓	✓	✓	✓	✓	20.7/18.2	✓	✓	15	
95	✓ ✓	✓	✓	16	✓	✓	✓	✓	✓	✓	✓	✓	31.	1807
96	✓ ✓	TRANS.	89	1065	65.1	140	30	10	0	29/26.9	FOR TRIM	CONDITION	31	5/13/76 1123
97	✓ ✓	✓	✓	✓	✓	✓	✓	-3	13	✓	✓	✓	✓	
98	✓ ✓	✓	✓	✓	✓	✓	✓	✓	0	✓	12	✓	✓	

89. FURTHER LEAD WEIGHTS (APPROX 23 LB) FITTED INSIDE REAR FUSE., FWD. OF HORZ. TAIL. TRIM @ 3.5° α_F
α_F = 3.5 → 9.5°, 3.5° → -3.5° (LOADS LIMIT BOTH ENDS) 3.5° RPT.

90. ψ = 0, -1, -2 → -9°, -5°, 0° +1, +2, → 9°, +5°, 0°.

91. A_1 = ± 1.5° ABOUT TRIM POINT (2.9° L, 3.8° R)

92. B_1 = ± 1.5 ✓ ✓ ✓ (3.4° L, 3.6° R)

93. $\theta_{.75}$ FOR T VARIATION +20#, -10# ABOUT TRIM VALUE (≈20#)

94. δ_F 31°, 21°, 11°, 31° → 91°, 31° RPT.

95. RPM 1065 → 960, 1065, → 1180, 1065

96. α_F = -3° → 0°, -3 → -5° x 1°5, +1° ADDED @ END. (BLADE LOADS LIMITS)

97. ψ = 0 → -4, -2, 0 → +4°, +2°, 0°

98. A_1 = ± 1° ABOUT TRIM VALUES (4.4° L, 5.1° R)

PREP.	KEF		REVISED	DATE	VR 095 Q-1	BVWT
CHK.					1/4 SCALE TILT ROTOR MODEL	182
APPR						

FORM 49810 (3/70)

Table 6. (continued)

RUN NO.	CONFIGURATION	TYPE OF RUN	WT. TARE RUN	RPM	V_{KT} M/S	V_{KT} F/S	i_N°	α_F°	ψ°	$\theta_{.75}^\circ$	$A_{1_C}^\circ$	$B_{1_C}^\circ$	δ_F°	DATE / TIME
99	$K5 + W_F^{46}$	TRANS	89	1065	65.1	140	30	-3	0	29/27	FOR TRIM	11	31	5/13/
100	✓ ✓	✓	✓	✓	✓	✓	✓	✓	✓	14	✓	✓	✓	
101	✓ ✓	✓	✓	✓	✓	✓	✓	✓	✓	✓	✓	✓	15	
102	✓ ✓	✓	✓	16	✓	✓	✓	✓	✓	✓	✓	✓	31	
103	$K6 + W_F^{46}$	CRUISE	103	830	65.1	140	0	10	0	35/34	FOR CONDITION	TRIM TION	0	5/14 1350 2355
104	✓ ✓	✓	✓	✓	✓	✓	✓	✓	✓	✓	✓	✓	10	5/15
105	✓ ✓	✓	✓	✓	✓	✓	✓	✓	✓	✓	✓	✓	21	
106	✓ ✓	✓	✓	✓	✓	✓	✓	0	13	✓	✓	✓	0	
107	✓ ✓	✓	✓	✓	✓	✓	✓	✓	0	✓	12	✓	✓	
108	✓ ✓	✓	✓	✓	✓	✓	✓	✓	✓	✓	FOR TRIM	11	✓	

99
100 T RANGE $+10^{\#}$ $-15^{\#}$ ABOUT TRIM (20 #)
101 δ_F = 31° → 11°, 31° → 71° × 10's.
102 RPM : 1065 → 1125 (POWER LIMIT) → 1065 → 980 .
103 α_{FUS} : -3° → +3° × 1°Δ
104 α_{FUS} -3° → 2° × 1°Δ
105 α_{FUS} -3 → 2° × 1°Δ
106 ψ : 0, 1, -2, -2.8, 0, 1, 2, 3, 0 RUN 106 APPEARS UNDER RUN 105 IN THE COMPUTER PRINT OUT

$\boxed{K6} = K_1 + B^{30,\,150,\,270}_{263,\,266,\,265}\ B^{60,\,180,\,300}_{273,\,272,\,271}\ PL_{2.1}$

($PL_{2.1}$ IS PL_2 WITH PITCH ARM ROTATED 20° TO PROVIDE INCREASED COLLECTIVE CAPABILITY)

PREP.		REVISED	DATE	VR 095Q-1	BVWT
CHK.				1/4 SCALE TILT ROTOR MODEL	182
APPR					

FORM 49810 (3/70)

Table 6. (continued)

RUN NO.	CONFIGURATION	TYPE OF RUN	WT. TARE RUN	RPM	V_{KTS} M/S	V_{KTS} F/S	i_N°	α_F°	ψ°	$\theta_{.75}^\circ$	A_{1c}	B_{1c}	δ_F	DATE / TIME
109	$K_6 + W_F^{46}$	CRUISE	103	830	65.1	140	0	19	0	35/34	FOR CONDITION	TRIM. CONDITION	0	5/15
110	✓ ✓	✓	✓	16	✓	✓	✓	0	✓	✓	✓	✓	✓	✓ 0255
111	✓ ✓	✓	89	1065	83.7	180	30	10	✓	32.2/32.3	✓	✓	31	5/17 2202
112	✓ ✓	✓	✓	✓	✓	✓	✓	-6	13	✓	✓	✓	✓	
113	✓ ✓	✓	✓	✓	✓	✓	✓	✓	0	✓	12	✓	✓	
114	✓ ✓	✓	✓	✓	✓	✓	✓	✓	✓	✓	FOR TRIM	11	✓	
115	✓ ✓	✓	✓	✓	✓	✓	✓	✓	✓	14	✓	FOR TRIM	✓	
116	✓ ✓	✓	✓	✓	✓	✓	✓	✓	✓	32.2/32	✓	✓	15	5/18, 0045
117	✓ ✓	✓	✓	16	✓	✓	✓	✓	✓	✓	✓	✓	31	

109: α_{FUS} 3, 4, 5, 6, 8, 10, 12, AT TRIM

110 RPM 830, 800, 775, 750, 850, 900, 875, 830

111 $\alpha_F = -6^\circ \rightarrow -8.5^\circ, -6^\circ R \rightarrow -4.5 \times 0.5^\circ s, -6^\circ R$

112 $\psi = 0^\circ \rightarrow -3^\circ, 0 \rightarrow \times 1^\circ s, 0^\circ R.$

113 $A_1 = +1.5^\circ, -1.0$ ABOUT TRIM (6.0°)

114 $B_1 = \pm 1.0^\circ$ ABOUT TRIM $(5^\circ L, 5.3^\circ R)$

115 T VARIATION ≈ 22# → 0#

116 $\delta_F = 31^\circ \rightarrow 0^\circ, \rightarrow 31^\circ \rightarrow 41^\circ \times 10's$

117 RPM = 1065, 1100, 1115 (POWER LIMIT) 1065, 1040, 1020, 1000.

PREP.			REVISED	DATE
CHK.			.	.
APPR				

VR 095 Q-1

1/4 SCALE TILT ROTOR MODEL

BVWT 192

FORM 49810 (3/70)

Table 6. (continued)

RUN NO.	CONFIGURATION	TYPE OF RUN	WT. TARE RUN	RPM	V_{KT} M/S	V_{KT} F/S	i_N°	α_F°	ψ°	$\theta_{.75}$	$A_{1_C}^\circ$	$B_{1_C}^\circ$	δ_F°	DATE / TIME
118	$K_6 + W_F^{46}$	CRUISE	118	947	83.7	180	15	10	0	37.5/37.8	FOR TRIM CONDITION		20	5/19/76 1921
119	✓ ✓	✓	✓	✓	✓	✓	✓	-2	13	✓	✓	✓	✓	
120	✓ ✓	✓	✓	✓	✓	✓	✓	✓	0	✓	12	✓	✓	
121/122	✓ ✓	✓	✓	✓	✓	✓	✓	✓	✓	✓	FOR TRIM	11	✓	
123	✓ ✓	✓	✓	✓	✓	✓	✓	✓	✓	14	FOR TRIM CONDITION		✓	
124	✓ ✓	✓	✓	✓	✓	✓	✓	✓	✓	37.6/37.7	✓	✓	15	
125	✓ ✓	✓	✓	16	✓	✓	✓	✓	✓	✓	✓	✓	20	2200
126	✓ ✓	✓	126	830	✓	✓	-1	10	✓	42.3/42.5	✓	✓	0	2335 0035
127	✓ ✓	✓	✓	✓	✓	✓	✓	✓	✓	✓	✓	✓	✓	
128	✓ ✓ $+ W_N^{17}$	✓	128	✓	✓	✓	✓	✓	✓	✓	✓	✓	0	5/20/ 2150.

2248

118. $\alpha_F = -2 \rightarrow -.5$, $-2 \rightarrow -4 \times 0.5$'s

119. $\psi = 0^\circ \rightarrow -2^\circ, 0^\circ \rightarrow +2^\circ \times 0.5$'s, 0 RPT.

120. A_{1_C}: $\pm 1^\circ$ ABOUT TRIM PT OF 4.2° L, 4.3° R.

121/122 B_{1_C}: $\pm 1^\circ$ ✓ ✓ ✓ ✓ 3.6° L, 3.9° R (RUN 122: ARE — VALUES FROM TRIM)

123. $\theta_{.75}$ FOR TRIM THRUST + 7 lb, − 14 lb (20 LB → 0 LB)

124. $\delta_F = 20^\circ, 10^\circ, 0^\circ$, 20 R, 30, 38, FLAP ACT. STALLED, 20 R.

125 RPM: 947, 925, 900, 947, 960, 965 (POWER LIMIT), 947 R

126 α_F° TRIM = 0°. $\alpha_F = 0 \rightarrow -1$, $0 \rightarrow +1.5$ EXCESSIVE 2/REV. CB LOADS. SHUT DOWN TO INVESTIGATE.

128 W_N^{17}: NACELLE WITH 10 LB WEIGHT CANTILEVERED FROM REAR (GROUND SIDE) OF NACELLE BALANCE, EXTENDING FWD TO JUST AFT ROTOR DISC PLANE. OVER TOP OF FAIRING:

$\alpha_F = 0 \rightarrow -1.5, 0 \rightarrow 2^\circ \times 0.5$'s,

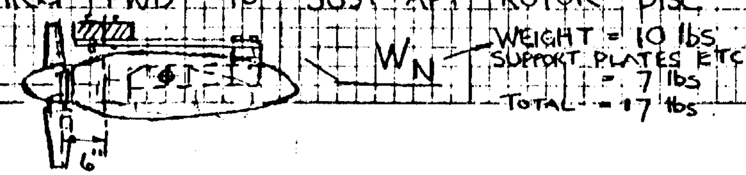

Table 6. (continued)

PREP.			REVISED	DATE	VR 095 Q-1	BVWT
CHK.					1/4 SCALE TILT ROTOR MODEL	182
APPR						

FORM 49810 (3/70)

RUN NO.	CONFIGURATION	TYPE OF RUN	WT. TARE RUN	RPM	V_{KTS} M/S	V_{KTS} F/S	$i_N°$	$\alpha_F°$	$\psi°$	$\theta_{.75}°$	$A_{1_C}°$	$B_{1_C}°$	$\delta_F°$	DATE / TIME
129	$K_6 + W_F^{46} + W_N^{17}$	CRUISE	128	830	83.7	180	-1	10	0	41.5 / 42.2	FOR TRIM CONDITION		10	6/20/
130	✓ ✓	✓	✓	✓	✓	✓	✓	✓	✓	✓	✓	✓	20	
131	✓ ✓	✓	✓	✓	✓	✓	✓	✓	✓	✓	✓	✓	✓	
132	✓ ✓	✓	✓	✓	✓	✓	✓	0	13	✓	✓	✓	0	
133	✓ ✓	✓	✓	✓	✓	✓	✓	✓	0	✓	12 FT	✓	✓	
134	✓ ✓	✓	✓	✓	✓	✓	✓	✓	✓	✓	FOR TRIM	11 FT	✓	0055
135	✓ ✓ $+ W_N^{23.5}$	✓	135	✓	✓	✓	✓	10	✓	41.4 / 42.2	✓	FOR TRIM	✓	6/21 1953 2017 2040
136	✓ ✓ ✓	✓	✓	✓	✓	✓	✓	17	✓	✓	17	17	✓	
137	✓ ✓ ✓	✓	✓	✓	✓	✓	✓	10	✓	✓	FOR TRIM AT EACH α_F		✓	2230

129 $\alpha_F = 0 \to -1.5, 0 \to +2 \times 0.5$ s

130 $\alpha_F = 0 \to -1.5, 0 \to +1.5° \times 0.5$ s THIS RUN DOUBTFUL AS RH FLAP SETTING IN DOUBT. REPEATED BELOW AS 131

131 $\alpha_F = 0 \to -1.5°, 0 \to +1.5$

132 $\psi = 0 \to -2°, 0 \to +2° \times 0.5°$s

133 LH ROTOR EXCURSION ONLY (RH CB GAUGE TOO SPIKEY)
$A_1 = -.75° + 1.0$ ABOUT TRIM OF $-.5°$

134 LH ROTOR EXCURSION ONLY

135 $W_N^{23.5}$: WEIGHT AS W_N^{17} WITH AN ADDITIONAL PLATE & PACKING PIECE (PROVISION FOR POSSIBLE AFT WEIGHT ADDITION RQMT.) - EXTENDING AFT FROM BALANCE GROUND SIDE.
SHUT DOWN TO INVESTIGATE LOSS OF CB GAUGE RHS. PATCHED IN 273 CB 124 - OK
$\alpha_F = 0 \to -1.5, 0 \to +2° \times 0.5$s

136 17 $\alpha_F, A_1 B_1$ SCHEDULE

137 LOADS MINIMISED WITH A_1, B_1 @ EACH α_F
$\alpha_F = 5 \to 10°, 5 \to 0 \times 1°$s

α_F: 0°, 1°, 2° USING ZERO CYCLICS AS DATUM
2°, 3°, 4°, 5° ✓ TRIM VALUES FOR 2° AS DATUM
5° TRIMMED AT 5°.

Table 6. (continued)

PREP.		REVISED	DATE	VR 095 Q-1	BVWT
CHK.				1/4 SCALE TILT ROTOR MODEL	182
APPR					

FORM 49810 (3/70)

RUN NO.	CONFIGURATION	TYPE OF RUN	WT. TARE RUN	RPM	V_{KTS} M/S	V_{KTS} F/S	i_N°	α_r°	ψ°	$\theta_{.75}^\circ$	A_{1c}°	B_{1c}°	δ_F°	DATE / TIME
138	$K6 + W_F^{46} + W_N^{23.5}$	CRUISE	135	830	102.3	220	−1	10	0	47.1 / 48.1	FOR CONDITION	TRIM	0	5/21 2338
139	✓ ✓ ✓	✓	✓	✓	✓	✓	✓	✓	✓	✓	✓	✓	5	
140	✓ ✓ ✓	✓	✓	✓	✓	✓	✓	✓	✓	✓	✓	✓	10	
141	✓ ✓ ✓	✓	✓	✓	✓	✓	✓	0	13	✓	✓	✓	0	
142	✓ ✓ ✓	✓	✓	✓	✓	✓	✓	✓	0	✓	12	✓	✓	
143	✓ ✓ ✓	✓	✓	✓	✓	✓	✓	✓	✓	✓	FOR TRIM	11	✓	5/22 0125
144	✓ ✓ ✓	✓	✓	✓	✓	✓	✓	17	✓	✓	17	17	✓	5/24 2238 2312
145	✓ ✓ ✓	✓	✓	✓	✓	✓	✓	10	✓	✓	TRIM EACH	AT α_F	✓	5/25
146	✓ ✓ ✓	✓	✓	✓	120.9	260	✓	✓	✓	52/53.3	FOR TRIM CONDITION		✓	
147	✓ ✓ ✓	✓	✓	✓	✓	✓	✓	✓	✓	✓	✓	✓	5	

138 $\alpha_F = 0^\circ \rightarrow -1.5, 0 \rightarrow +1.5^\circ \times 0.5^\circ$/s 273 FB WENT OUT BEFORE DATA. 271 FB PATCHED. IN FOR RUN.

139 $\alpha_F = 0^\circ \rightarrow -1.5, 0 \rightarrow +1.0 \times 0.5^\circ$/s

140 $\alpha_F = 0^\circ \rightarrow -1^\circ, 0^\circ \rightarrow +1.0 \times 0.5^\circ$/s

141 $\psi = 0 \rightarrow -1.5, 0^\circ, \rightarrow +1.5^\circ$

142 $A_1 = \pm 1^\circ$ ABOUT TRIM $\times 0.25^\circ$/s APPROX.

143 $B_1 = -1^\circ$ ABOUT TRIM (BOTH ROTORS) & $+1^\circ$ ABOUT TRIM L.H.S. ONLY AS 273 CB 124 WENT BAD.

144 LOST PIECE OF FUSE SHELL MID WING UPPER SURFACE. SHUT DOWN, FIXED WITH TAPE & CARDBOARD. DATA @ $\alpha_F = 0^\circ, 1^\circ, 2^\circ, -1^\circ$ CYCLIC SCHEDULE.

145 $\alpha_F = -1^\circ \rightarrow +3^\circ \times 1^\circ$/s. BLADE LOADS TRIMMED EACH α_F.

146 $\alpha_F = 0, -.5^\circ, -1^\circ, 0, +.5^\circ, +1.0^\circ$, 0 RPT

147 $\alpha_F = 0^\circ, -.5^\circ, -1.0^\circ$, 0 RPT, $0.5^\circ, 1.0^\circ$, 0 RPT.

PREP.			REVISED	DATE	VR 095 Q-1	BVWT
CHK.						
APPR					1/4 SCALE TILT ROTOR MODEL	182

Table 6. (continued)

RUN NO.	CONFIGURATION	TYPE OF RUN	WT. TARE RUN	RPM	V_{KT} M/S	V_{KT} F/S	i_N°	α_F°	ψ°	$\theta_{.75}^\circ$	A_{1c}°	B_{1c}°	δ_F°	DATE / TIME
148	$K_6 + W_F^{46} + W_N^{23.5}$	CRUISE	135	830	120.9	260	-1	0	△13	~~52~~ 53.3	FOR TRIM	CONDITION	0	5/25
149	✓ ✓ ✓	✓	✓	✓	✓	✓	✓	✓	0	✓	△12	✓	✓	
150	✓ ✓ ✓	✓	✓	✓	✓	✓	✓	✓	✓	✓	FOR TRIM	△11	✓	
151	✓ ✓ ✓	·	✓	✓	✓	✓	✓	△17	✓	✓	△17	△17	✓	
152	✓ ✓ ✓	✓	✓	✓	139.5	300	✓	0	✓	~~56.5~~ 58.2	FOR TRIM	CONDITION	✓	D325
153	✓ ✓ ✓	✓	✓	✓	✓	✓	✓	△10	✓	~~56.3~~ 57.8	✓	✓	✓	5/26 / 1945
154	✓ ✓ ✓	✓	✓	✓	✓	✓	✓	0	△13	✓	✓	✓	✓	
155	✓ ✓ ✓	✓	✓	✓	✓	✓	✓	✓	0	✓	△12	✓	✓	
156	✓ ✓ ✓	✓	✓	✓	✓	✓	✓	✓	✓	✓	FOR TRIM	△11R	✓	2100
157	✓ ✓ ✓	✓	✓	✓	✓	✓	✓	△17	✓	✓	△17	△17	✓	2133

148 $\psi = 0^\circ, -.5, -1.0^\circ, -1.4^\circ, 0^\circ, +.5^\circ, +1.0^\circ, +1.5^\circ$, 0 RPT.

149. $A_1 = \pm 1.0^\circ$ ABOUT TRIM PT. OF 0° X 0.25's

150 $B_1 = \pm 1.0$ ABOUT ✓ ✓ ✓ -1.0°(L), -0.4 (R)

151 α_F = 0, .5, 1.0, 1.5, $-.5^\circ$ A_1°, B_1° TO SCHEDULE.

152 $\alpha_F = 0^\circ$ ONLY. STAB EXPLORATORY RUN AT 300 KTS F/S.

153 $\alpha_F = 0 \rightarrow -0.5, 0 \rightarrow +.75^\circ$ X 0.26's

154 $\psi = 0 \rightarrow -1.0^\circ, 0^\circ \rightarrow +1.0^\circ$ BY SMALL INCREMENTS.

155 $A_1 = -.5^\circ + 1.0$ ABOUT TRIM PT.

156 $B_1 = +.5^\circ$ ABOUT TRIM PT. R.H. ROTOR ONLY. TRIM $= -.25^\circ$.
SHUT DOWN - TUNNEL DRIVE COOLING OVERHEATING.

157. $\alpha_F = 0^\circ, .5, 1.0, -.5^\circ, -1.0$. A_1, B_1 TO SCHEDULE.

NOTE:- RUNS 157, 158 PULSE CAMERA MOVIES TAKEN.

PREP.			REVISED	DATE	VR 095 Q-1 / 1/4 SCALE TILT ROTOR MODEL	BVWT / 182
CHK.						
APPR						

FORM 49810 (3/70)

Table 6. (continued)

RUN NO.	CONFIGURATION	TYPE OF RUN	WT. TARE RUN	RPM	V_{KTS} M/S	V_{KTS} F/S	i_N°	α_F°	ψ°	$\theta_{.75}^\circ$	A_{1C}°	B_{1C}°	δ_F°	DATE / TIME
158	$K7 + W_F^{46} + W_N^{23.5}$	CRUISE	135	830	VAR	18	−1	0	0	FOR V_{KTS}.	FOR CONDITION	TRIM	0	5/26/76 0050
159	K6 ✓ ✓	✓	✓	✓	65.1	140	✓	10	✓	33.8 / 34.7	✓	✓	0	0055
160	✓ ✓ ✓	✓	✓	✓	✓	✓	✓	✓	✓	✓	✓	✓	10	
161	✓ ✓ ✓	✓	✓	✓	✓	✓	✓	✓	✓	✓	✓	✓	20	
162	✓ ✓ ✓	✓	✓	✓	✓	✓	✓	0	13	✓	✓	✓	0	
163	✓ ✓ ✓	✓	✓	✓	✓	✓	✓	✓	0	✓	12	✓	✓	
164	✓ ✓ ✓	✓	✓	✓	✓	✓	✓	✓	✓	✓	FOR TRIM	11	✓	
165	✓ ✓ ✓	✓	✓	✓	✓	✓	✓	17	✓	✓	17	17	✓	
166	✓ ✓ ✓	✓	✓	✓	✓	✓	✓	10	✓		TRIM EACH	@ α_F	✓	0255
					END	OF	TEST							

158. $\boxed{K_7}$ = K6 BUT WITH $F_{1.1}$. [$F_{1.1}$ = F_1 WITH LOCAL FUSE. BULGE 10" LONG x 6" WIDE ON LHS, IN ROTOR PLANE; BLADE TIP TO BULGE GAP = 1.25".]

18: V_{KTS} = 140, 180, 220, 260, 300,

159→164: REPEAT OF PREVIOUS 140 KT RUNS 103→108 (NOTE THAT i_N WAS 0° IN THESE RUNS. "BULGE" REMOVED.

α_F = 0 → −3°, 0 RPT → +3°, 0 R x 1°'s.

160. α_F = 0 → −3°, 0 → +3, 0 RPT x 1°'s

161 α_F AS 160

162. ψ = 0° → −4°, 0° → +3° x 1°'s, 0 RPT.

163 A_1 = ± 1° ABOUT TRIM x 0.5°'s (TRIM −.23° L, −.57° R)

164 B_1 = ± 1° ABOUT TRIM x 0.5°'s (−.55° L, +.12° R)

165 α_F = 0° → 6° x 1°'s A_1, B_1 TO SCHEDULE.

166 α_F = 6° → 14°, → 6° → −2° x 2°'s. 0° RPT TRIMMING LOADS EACH α_F°.

PREP.			REVISED	DATE	VR 095 Q-1	BVWT
CHK.					1/4 SCALE TILT ROTOR MODEL	182
APPR						

FORM 49810 (3/70)

Table 6. (continued)

Table 7. Summary of Configurations Tested and Configuration Codes

Code	Configuration
K_1	$W_1\ F_1\ N_1\ T_1\ V_1\ H_1$
K_2	$W_1\ F_1\ N_1\ T_1\ V_1\ H_1\ B^{42,162,282}_{263,266,265}\ B^{88,208,328}_{272,271,273}\ PL_1$
K_3	$W_1\ F_1\ N_1\ T_1\ V_1\ H_1\ B^{58,178,298}_{263,266,265}\ B^{88,208,328}_{272,271,273}\ PL_1$
K_4	$W_1\ F_1\ N_1\ T_1\ V_1\ H_1\ B^{58,178,298}_{263,266,265}\ B^{88,208,328}_{272,271,273}\ PL_2$
K_5	$W_1\ F_1\ N_1\ T_1\ V_1\ H_1\ B^{30,150,270}_{263,266,265}\ B^{60,180,300}_{272,271,273}\ PL_2$
K_6	$W_1\ F_1\ N_1\ T_1\ V_1\ H_1\ B^{30,150,270}_{263,266,265}\ B^{60,180,300}_{272,271,273}\ PL_{2.1}$
K_7	$W_1\ F_{1.1}\ N_1\ T_1\ V_1\ H_1\ B^{30,150,270}_{263,266,265}\ B^{60,180,300}_{272,271,273}\ PL_{2.1}$

Table 8. Configuration Codes Components Description

W_1	Wing
F_1	Basic Fuselage
N_1	Engine Nacelle
T_1	Horizontal Tail
V_1	Vertical Tail
H_1	Basic Hub
W_F^{23}	Lead tuning weight of 23 lb. fitted in front fuselage 32 ins. forward of model C.G. (Sta 40.613, WL 4.404) as defined by weight tares routine.
W_F^{46}	Lead tuning weight as defined by W_F^{23} with an additional lead weight of 23.5 lb. in the rear fuselage 31.5 ins. aft of the model C.G.
W_N^{17}	17 lb. tuning weight fitted to each nacelle, comprising a 10 lb. calibration weight at 6 ins. aft of the hub center-line and 7 lbs. of steel supporting structure. (See Figure)
$W_N^{23.5}$	Tuning weight as W_N^{17}, with 6.5 lb. of additional weight in the form of an aft weight support bracket (See Figure)
PL_1	Basic pitch link arrangement.
PL_2	Pitch link with barrel 2 ins. longer than PL_1.
$PL_{2.1}$	Pitch link PL_2 with pitch arm rotated 20° to obtained higher values of collective pitch.
B_{XXX}^{YYY}	Basic rotor blade. Rotor is defined as: $B_{XXX,YYY,ZZZ}^{AAA,BBB,CCC}$, where XXX, YYY, ZZZ are the blade serial numbers and AAA, BBB, CCC are the respective azimuth locations in cyclic order with respect to the blade 1/rev indication. (In the Config. Descriptions, the left hand rotor is identified first.)

Table 8. Configuration Codes Components Description (Cont'd)

$F_{1.1}$ Fuselage F_1 with local 'Bulge' 10 ins. long x 6 ins. wide added to left hand side of the fuselage in the rotor plane, approximately on the fuselage ℄, to reduce the rotor/fuselage gap to 1.25 ins. (scaled full scale dim'n.).

4.2 Data Notes and Instrumentation Log

As with any test program, the circumstances of the test, condition of instrumentation, etc., have a direct bearing on the interpretation of the experimental data. The data obtained on this test program are contained in seventeen data files; each file containing the information pertaining to the initial condition of the same number as explained in section 4-1. The file reference system is explained in section 5.0 This volume contains data for the first four conditions. The rest of the data can be found in the Appendix. Volumes 2, 3 and 4 References 4, 5 and 6.

The instrumentation log of the test program is provided in table 9. It is the purpose of this section to point out those conditions which are known to have influenced the data.

Blade loads data were obtained from strain gage measurements at 0.125R. At least two blades were instrumented on each rotor although only one blade on each rotor was recorded on each test run. From time to time blade gage instrumentation failures required switching from one blade to another mid run or in order to complete a run sequence. These events are recorded in the log on a run by run basis.

The strain gage balance sensitivities are recorded and also variations in sensitivity made as a result of check calibrations (ETESC, end to end system checks). The total loads balance in

the model (BV-6049) was used for Runs 1 to 25. The SRH balance (BV-6054) was used in Runs 26 to 35 and then replaced by a short adapter and BV-6049 used for the remainder of the test.

Two six component balances were used to measure the rotor forces and moments, one in each nacelle. These balances are designated BV-6047 (left nacelle) and BV-6048 (right nacelle).

On Run 82, the side force channel on the right hand balance was found to be saturating intermittently and causing the right hand rotor data to be spurious after processing through the balance matrix. Subsequent examination of the data showed that this problem occurred earlier and results in the right hand rotor data being invalid between Runs 68 and 96. The right hand rotor data are not plotted for these runs. The nature of the problem was an intermittent connection at the gage itself on one of the side force flexures. This failure was not always apparent under static load and may have resulted in some error prior to Run 68. The right hand rotor data should be interpreted with some caution. If error was present, the yaw moment would be the most seriously affected. From Run 82 to Run 92, the right hand side force sensitivity was set to zero. For these runs the longitudinal force and moment measurements should not be seriously affected. From Run 96 on, the left hand side force channel signal was fed into the computer input for right hand side force with its sign inverted to

preserve sign conventions. For data runs subsequent to Run 96, the test conditions were symmetrical rotor behavior would be expected (e.g., α effects) should yield reasonable data on the right hand side. Where symmetry is not the case, the lateral data from the right hand side must be interpreted with caution.

During the 180 Kt. cruise data runs, the blade gage data contained unexpected harmonics and non integer responses. During investigative work, a flexible coupling in the drive system failed. Replacing the flexible coupling caused the wave forms to return to their expected shape. Similar phenomena were seen in the shaft torque wave forms. Blade loads data for the 180 Kt. cruise condition (Condition #14) are suspect insofar as the residual loads are probably artifically high as a result of the drive system problem.

Table 9. INSTRUMENTATION SUMMARY BVWT-182

PARAMETERS	V_B	GAIN	FILTER	SENSITIVITY	ALLOW EU	ALLOW VOLTS	CEC VCAL	MPX	AMP	COND	SCOPE	CEC	P-P	REMARKS	RUN
BALANCE	BV-6049	(FUSELAGE)													
NFBAL1	-10	1000		27.506				H01 L01	01	01			2*	* TOTAL LOADS ALLOWABLE	1
PMBAL1	-10	1000		67.402				H02 L02	02	02	4		2	PM VS RM ON SCOPE	1
AFBAL1	-15	1000		348.074				H03 L03	33	03			2		1
SFBAL1	-10	1000		81.688				H04 L04	34	04			2		1
YMBAL1	-10	1000		59.064				H05 L05	05	05	4		2	PM VS RM ON SCOPE YMBAL = RM AC.	1
RMBAL1	-5	1000		22.172				H06 L06	06	06			2		1
BALANCE	BV 6047	(LEFT NACELLE)													
NFBAL2	10	1000		14.964				H16 L16	16	16			0*	* TOTAL LOADS ALLOWABLE	1
PMBAL2	6	1000		30.140				H15 L15	15	15			0		1
AFBAL2	10	1000		34.186				H14 L14	14	14			0		1
SFBAL2	10	1000		14.450				H13 L13	13	13			0		1
YMBAL2	6	1000		28.471				H18 L18	18	18			0		1
RMBAL2	6	1000		5.587				H17 L17	17	17			0		1
															1
QS2	5	500		19.447				L32	32	32					1

2

Table 9. INSTRUMENTATION SUMMARY BVWT - 182

PARAMETERS	V_B	GAIN	FILTER	SENSITIVITY	ALLOW EU	ALLOW VOLTS	CEC VCAL	MPX	AMP	COND	SCOPE	CEC	P-P	REMARKS	RUN
BALANCE BV-604B (RIGHT NACELLE)															
NFBAL3	10	1000	1K	15.347				H10 L10	10	10			01*	* TOTAL LOADS ALLOWABLE	1
PMBAL3	6	1000	1K	30.177				H09 L09	09	09			01		1
AFBAL3	10	1000	1K	37.210				H08 L08	08	08			01		1
SFBAL3	10	1000	1K	14.750				H07 L07	07	07			01		1
YMBAL3	6	1000	1K	29.716				H12 L12	12	12			01		1
RMBAL3	6	1000	1K	5.990				H11 L11	11	11			01		1
QS3	5	500		19.364				L31	31	31					1
265CB124	5	200	1K	22.470	± 70	± 3.12		H22	53	22	1(H)		03	L.H.S STEADY ON (P-P) METER	24
265FB124	5	200	1K	19.978	±43.5 / ±15	±2.18 / ±.75		H23	54	23	1(V) / 3(U)		04	" "	24
265PA	5	500	1K	8.625	20 STDY ± 20	± 2.32		H31	55	24	5(U)			"	24
273CB124	5	200	1K	26.200	± 70	± 2.67		H19	50	19	2H		05	RHS STEADY ON (P-P) METER	24
273FB124	5	200	1K	17.895	±43.5 / ±15	±2.43 / ±.84		H20	51	20	2V / 3L		06	" " OUT RUN 48	24
273PA	5	500	1K	8.401	20STDY ± 20	± 2.38		H21	52	21	5L			"	24

3

Table 9. INSTRUMENTATION SUMMARY BVWT-182

PARAMETERS	V_B	GAIN	FILTER	SENSITIVITY	ALLOW EU	ALLOW VOLTS	CEC VCAL	MPX	AMP	COND	SCOPE	CEC	P-P	REMARKS	RUN
LEFT NACELLE TILT ($i_N°$)	2.5	10		24.840				L20	20	26					1
RIGHT NACELLE TILT ($i_N°$)	2.5	10		28.441				L19	19	25					1
LEFT FLAP ANGLE	1.0	5		28.00				L22	22	28					24
RIGHT FLAP ANGLE	1.0	5		28.00				L21	21	27					24
ELEVATOR ANGLE	2.0	10		4.793				L23	23	29					24
ACCELEROMETERS															
LEFT VERT.	10	100	1K	0.6805				H25	56	52				'K' IN g's/VOLT.	24
LEFT LAT.^{L}	10	100	1K	1.0793				H26	57	53				"	24
LEFT LONG.^{L}	10	100	1K	0.6542				H27	58	54				"	24
RIGHT VERT.	10	100	1K	0.6658				H28	59	55				"	24
RIGHT LAT.^{L}	10	100	1K	0.7135				H29	60	56				"	24
RIGHT LONG.^{L}	10	100	1K	0.6873				H30	61	57				"	24
PITCH ANGLE (KNUCKLE)	-	-		-										SHAFT ENCODER DIRECT READOUT.	1
YAW ANGLE (SRH)	5	5		19.633				L24	24	30					1

FORM 46284 (2/66)

Table 9. INSTRUMENTATION SUMMARY BVWT-182

PARAMETERS	V_B	GAIN	FILTER	SENSITIVITY	ALLOW EU	ALLOW VOLTS	CEC VCAL	MPX	AMP	COND	SCOPE	CEC	P-P	REMARKS	RUN
CONTROL SYSTEM															2
RH ACT. #1	-	1		-.1354				L28	65	45					24
RH ACT #2	-	1		-.1379				L29	66	46					24
RH ACT #3	-	1		-.1390				L30	67	47					24
LH ACT #1	-	1		-.1326				L25	62	42					24
LH ACT #2	-	1		-.1351				L26	63	43					24
LH ACT #3	-	1		-.1392				L27	64	44					24
60/REV														PC124	1
1/REV														L.H.	1
SRH BALANCE (BV-6054)															
NF BAL 1	-8	1000	1 KC	218.4598				H01 L01	01	01			2	THIS BALANCE REMOVED AFTER RUN 35 AND	26
PM BAL 1	-5	1000	1 KC	188.2352				H02 L02	02	02	4		2	REPLACED BY 2" HIGH DUMMY.	26
AF BAL 1	-8	1000	1KC	285.0359				H03 L03	33	03			2		26
SF BAL 1	-8	1000	1KC	222.5071				H04 L04	34	04			2		26
YM BAL 1	-5	1000	1KC	187.7934				H06 L05	05	05	4		2		26
RM BAL 1	-5	1000	1KC	156.6695				H06 L06	06	06			2		26

5

Table 9. INSTRUMENTATION SUMMARY BVWT-182

PARAMETERS	V_B	GAIN	FILTER	SENSITIVITY	ALLOW EU	ALLOW VOLTS	CEC VCAL	MPX	AMP	COND	SCOPE	CEC	P-P	REMARKS	RUN
265 PA	5	500	1K	5.59	±20	±3.58		H31	55	24	5U			CHECK CALIB SENS.	27
263 CB124	5	200	1K	23.485	±70	±2.98		H22	53	22	1H			SUBS FOR 265 CB 124	35
271 CB 124	5	200	1K	21.233	±70	±3.30		H19	50	19	2H			SUBS FOR 273 CB 124	35
BALANCE BV-6049 ~ (FUSELAGE)															
NFBAL1	-10	1000	1K	27.506				H 01 L 01	01	01			2	BALANCE REINSTATED LOCKED OUT RUNS 36	37
PMBAL1	-10	1000	1K	67.402				H 02 L 02	02	02	4		2	→ 38. ACTIVE RUN 39 →	37
AFBAL1	-15	1000	1K	348.0743				H 03 L 03	33	03			2		37
SFBAL1	-10	1000	1K	81.688				H 04 L 04	34	04			2		37
YMBAL1	-10	1000	1K	59.064				H 05 L 05	05	05	4		2		37
RMBAL1	-5	1000	1K	22.172				H 06 L 06	06	06			2		37
YAW ANGLE				19.133				L24	24	30				NEW SENS. POT RESET	37
LEFT NACELLE TILT ~ in°				24.752										"	37
RIGHT NACELLE TILT ~ in°				28.80										"	37
263 CB124	5	200	1K	25.394	±70	±2.76		H22	53	22	1H			OUT IN RUN 38	37
271 CB 124	5	200	1K	22.797	±70	±3.07		H19	50	19	2H				37

FORM 46284 (2/66)

Table 9. INSTRUMENTATION SUMMARY BVWT-182

PARAMETERS	V_B	GAIN	FILTER	SENSITIVITY	ALLOW EU	ALLOW VOLTS	CEC VCAL	MPX	AMP	COND	SCOPE	CEC	P-P	REMARKS	RUN
273 PA	5	500	1K	5.225	±20	±3.83		H21	52	21	5L				39
271 CB124	5	200	1K	23.266	±70	±3.01		H19	50	19	2H				39
265 CB124	-5	200	1K	20.224	±70	±3.46		H22	53	22	1(H)			NEW GAUGE. REPLACED 263 CB124	39
265 FB124	5	200	1K	17.288	±43.5 / ±15	2.52 / ±.86		H23	54	23	1(V) / 3(U)			REWORKED GAUGE WENT BAD IN RUN	39
263 FB124	5	200	1K	16.072	±43.5 / ±15	±2.71 / ±.93		H23	54	23	1(V) / 3(U)			REPLACED 265 FB124	39
LEFT NACELLE TILT~i_N°	2.5	10		27.481				L20	20	26				NEW POT, REPLACED BROKEN ONE.	39
271 FB124	5.	200	1K	15.83	±43.5 / ±15	2.74 / .95		H20	51	20	2V / 3L.			REPLACED 273 FB124 (WENT OUT IN RUN 48)	49
273 CB124	5	200	1K	26.2	±70	±2.67		H19	50	19	2H			PICKED UP ORIGINAL GAUGE, REPLACING 271CB	49
RIGHT FLAP ANGLE	1.0	5		26.85				L21	21	27					46
LEFT NACELLE TILT, i_N°	2.5	10		27.522				L20	20	26				REPLACEMENT POT.	54
RIGHT NACELLE TILT, i_N°	2.5	10		29.276				L19	19	25				CHECK CALIB.	54.
RIGHT FLAP ANGLE	1.0	5		29.478				L21	21	27				" "	54

7.

Table 9. INSTRUMENTATION SUMMARY BVWT-182

PARAMETERS	V_B	GAIN	FILTER	SENSITIVITY	ALLOW EU	ALLOW VOLTS	CEC VCAL	MPX	AMP	COND	SCOPE	CEC	P-P	REMARKS	RUN
265CB124	5	200	1K	19.51	±70	±3.59		H22	53	22	1H			NEW GAUGE	54
265FB124	5	200	1K	16.02	±43.5/±25	2.72/1.56		H23	54	23	1V/3U			NEW GAUGE WENT OUT RUN 72	54
273FB124	5	200	1K	15.84	±43.5/±25	2.75/1.58		H20	51	20	2V/3L			NEW GAUGE	54
271CB124	-5	200	1K	21.85	±70	±3.20		H19	50	19	2H			NEW GAUGE. (273 REGAUGED BUT BAD)	54
RIGHT NACELLE TILT i_N°	2.5	10		31.546				L19	19	25				NEW SENS.	56
271CB124	-5	200	1K	20.83	±70	±3.36		H19	50	19	2H			NEW SENS. FROM ETESC.	63
263CB124	5	200	1K	20.856	±70	±3.36		H22	53	22	1H			REPLACED 265CB124 (BAD SPIKING)	72
263FB124	5	200	1K	14.54	43.5/25	±2.99/±1.72		H23	54	23	1V/3U			REPLACED 265 FB124	73
RIGHT NACELLE TILT, i_N°	2.5	10		29.449				L19	19	25				NEW SENS.	82
SFBAL3	10	1000	1K	0				H07 L07	07	07				COMPONENT SATURATING INTERMITTENTLY. SENS. SET TO '0', AMP. OFF	82
SFBAL3	10	1000	1K	− 14.45				H07 L07	07	07				LH SFBAL2 OUTPUT TO SFBAL3 CH. − SENS.	96
265PA	5	500	1K	6.16	±20	3.247		H31	55	24	5U			NEW SENS. (ETESC) (OUT RUN 115)	96
273PA	5	500	1K	6.88	±20	2.907		H21	52	21	5L			" " "	96

8

Table 9. INSTRUMENTATION SUMMARY BVWT-182

PARAMETERS	V_B	GAIN	FILTER	SENSITIVITY	ALLOW EU	ALLOW VOLTS	CEC VCAL	MPX	AMP	COND	SCOPE	CEC	P-P	REMARKS	RUN
LEFT FLAP ANGLE	1.0	5		28.25				L22	22	28				POT RESET TO GIVE $\delta_F = 0°$ READOUT. RECALIB.	103
LEFT NACELLE TILT ~ $i_N°$	2.5	10		0				L20	20	26				BAD POT. SENS SET TO '0'. INTERCEPT OF REQU'D $i_N°$	103
RIGHT NACELLE TILT ~ $i_N°$	2.5	10		28.674				L19	19	25				NEW CALIB.	103
273 CB 124	5	200	1K	20.80	±70	3.37		H19	50	19	2H			NEW SENS.	103
273 FB124	5	200	1K	14.63	±43.5/±25	2.99/1.72		H20	51	20	2V/3L			NEW SENS.	103
263 CB124	-5	200	1K	20.86	±70	±3.36		H22	53	22	1H			REPAIRED GAUGE	103
263 FB124	5	200	1K	14.54	±43.5/±25	2.99/1.72		H23	54	23	1V/3U				103
263 FB124	5	200	1K	12.55	±43.5/±25	±3.47/±1.99		H23	54	23	1V/3U			ADJUSTED SENSITIVITY, FROM ETESC	111
263 FB124	5	200	1K	14.54	±43.5/±25	±2.99/1.72		H23	54	23	1V/3U			"	118
RIGHT NACELLE TILT ~ $i_N°$	2.5	10		0				L19	19	25				SENS. SET TO 0. i_N PUT IN AS INTERCEPT →	118
273 CB124	5	200	1K	18.40	±70	±3.80		H19	50	19	2H			ADJUSTED SENS.	128
271 FB124	5	200	1K	15.83	±43.6/±25	±2.75/±1.58		H20	51	20	2V/3L			REPLACED 273FB124 AS THIS V. NOISY	128
273 FB124	5	200	1K	14.54	±43.5/±26	2.99/1.72		H20	51	20	2V/3L			PICKED UP AGAIN AS 271FB124 OUT. O.K. NOW ~~OUT RUN 138~~	128
271 CB124	5	200	1K	13.78	±70	±5.08		H19	50	19	2H			REPLACED 273 CB124 WENT OUT THIS RUN. NO ~~DATA~~	135
273 CB124	5	200	1K	18.40	±70	±3.80		H19	50	19	2H/5L			PICKED UP AGAIN FOR 271 OUT RUN 143	135

PUT ON SCOPE VS ψ (USING PA SCOPE)

9

Table 9. INSTRUMENTATION SUMMARY BVWT-182

PARAMETERS	V_B	GAIN	FILTER	SENSITIVITY	ALLOW EU	ALLOW VOLTS	CEC VCAL	MPX	AMP	COND	SCOPE	CEC	P-P	REMARKS	RUN
271 FB124	5	200	1K	15.83	±43.5/±25	2.75/1.58		H20	51	20	2V/3L			REPLACED 273 FB124 (OUT BEFORE DATA)	138
265 CB124			1K	17.02	± 70	± 4.11		H22	53	22	1H/5U			NEW GAUGE ADDED TO SCOPE VS ψ	144
265 FB124			1K	14.65	±43.5/±25	2.97/1.70		H23	54	23	1V/3U			NEW GAUGE	144
265 PA			1K	6.16				H31	55	24					144
273 CB124			1K	20.27	± 70	± 3.45		H19	50	19	2H/5L			NEW GAUGE	144
273 FB124			1K	14.54	±43.5/±25	±2.99/±1.72		H20	51	20	2V/3L			NEW GAUGE. THIS WENT OUT ON SETTING UP. NO DATA ON IT.	144
273 PA			1K	6.88				H21	52	21					144
271 FB124			1K	15.0	±43.5/±25	±2.90/±1.67		H20	51	20	2V/3L			NEW GAUGE. REPLACED 273 FB124. GUESS SENS. AS NO CALIBRATION.	144
271 FB124			1K	15.4	±43.5/±25	±2.82/±1.62		H20	51	20	2V/3L			REVISED SENS. AFTER ETESC (cf 15.0 ABOVE)	153

5.0 DATA FILE SYSTEM

The nature of the test program where twenty-four quantities were measured against seven variables at seventeen conditions, was such that the test data produced required a system of filing to allow orderly usage of the information. The data are presented in seventeen data files, each file corresponding to an initial flight condition as shown previously in figure 54.

The data obtained in transition (Conditions 2 through 12) are presented in the order shown in table 10. All of the measured quantities which are comprised of the six components of the left rotor balance, the right rotor balance and the total loads balance followed by the blade data are first plotted against angle of attack $\alpha°$ and then the sequence repeats with yaw angle as the independent variable and so on. This sequence of results is maintained except where data are not presented due to instrumentation difficulties as described in section 4.2.

The hover data in data file 1 are given in a slightly different format. The measured data are in the same order as for the transition information and are first shown as functions of collective pitch followed by cyclic pitch effects at two thrust settings.

In cruise (data files 13 through 17) the measured data are first plotted against α for various flap settings as shown in

TABLE 10. TRANSITION DATA ORGANIZATION

C_T C_P C_{NF} C_{SF} C_{PM} C_{YM}	LEFT ROTOR	VS	α^{o} YAW^{o} B_1^{o} A_1^{o} θ_{75}^{o} δ_F^{o} RPM
C_T C_P C_{NF} C_{SF} C_{PM} C_{YM}	RIGHT ROTOR		
C_L C_{SF} C_{AX} C_{PM} C_{YM} C_{RM}	TOTAL AIRCRAFT		
ALT CHORD BENDING LEFT			
ALT FLAP BENDING LEFT			
ALT PITCH LINK LOAD LEFT			
ALT CHORD BEND RT			
ALT FLAP BEND RT			
ALT PITCH LINK LOAD RT			

table 11, followed by yaw and cyclic pitch variations.

Only the blade loads data and control settings data are given for the combined α and cyclic runs at the end of each file.

The data provided in this volume are in the following files.

Data File 1 $I_N = 90°$ $V_{FULL\ SCALE} = 0$

Data File 2 $I_N = 90°$ $V_{FULL\ SCALE} = 45$ Kts.

Data File 3 $I_N = 90°$ $V_{FULL\ SCALE} = 100$ Kts.

Data File 4 $I_N = 70°$ $V_{FULL\ SCALE} = 45$ Kts.

Volume II presents data files 5 through 8.

Data File 5 $I_N = 70°$ $V_{FULL\ SCALE} = 100$ Kts.

Data File 6 $I_N = 70°$ $V_{FULL\ SCALE} = 140$ Kts.

Data File 7 $I_N = 50°$ $V_{FULL\ SCALE} = 100$ Kts.

Data File 8 $I_N = 50°$ $V_{FULL\ SCALE} = 140$ Kts.

Volume III presents data files 9 through 12.

Data File 9 $I_N = 30°$ $V_{FULL\ SCALE} = 100$ Kts.

Data File 10 $I_N = 30°$ $V_{FULL\ SCALE} = 140$ Kts.

Data File 11 $I_N = 30°$ $V_{FULL\ SCALE} = 180$ Kts.

Data File 12 $I_N = 15°$ $V_{FULL\ SCALE} = 180$ Kts.

The cruise data files 13 through 17 are presented in Volume IV.

Data File 13 $I_N = -1°$ $V_{FULL\ SCALE} = 140$ Kts.

Data File 14 $I_N = -1°$ $V_{FULL\ SCALE} = 180$ Kts.

TABLE 11. CRUISE DATA ORGANIZATION

C_T, C_P, C_{NF}, C_{SF}, C_{PM}, C_{YM}	LEFT ROTOR	VS	α^{0} (VARIOUS δ_F) YAW^{0} A_1^{0} B_1^{0}
C_T, C_P, C_{NF}, C_{SF}, C_{PM}, C_{YM}	RIGHT ROTOR		
C_L, C_{SF}, C_{AX}, C_{PM}, C_{YM}, C_{RM}	TOTAL AIRCRAFT		
ALT CHORD BENDING LEFT			
ALT FLAP BENDING LEFT			
ALT PITCH LINK LOAD LEFT			
ALT CHORD BEND RT			
ALT FLAP BEND RT			
ALT PITCH LINK LOAD RT			

BLADE LOAD AND CYCLIC PITCH DATA VS COMBINED α AND CYCLIC

Data File 15 I_N = -1° $V_{FULL\ SCALE}$ = 220 Kts.

Data File 16 I_N = -1° $V_{FULL\ SCALE}$ = 260 Kts.

Data File 17 I_N = -1° $V_{FULL\ SCALE}$ = 300 Kts.

One further set of information is needed to allow the reader to use the information presented. It is necessary to know the constant values of test variables during each parametric variation. Each of the data plots list the nacelle angle full scale airspeed simulated, fuselage attitude and flap setting on the plot. The other variables (e.g., cyclic settings collective pitch, etc.) can be obtained by reference to tables 12 to 15.

For example, during an angle of attack variation in data set 3, the control settings pertinent to that run can be obtained by reference to table 12 and reading the values of the control parameters as:

$V_{FULL\ SCALE}$	100 Kts.
I_N°	90°
RPM	1183
θ_{75} left rotor	12
A_1 left rotor	4.1°
B_1 left rotor	6.2
δ_F left wing	70°
θ_{75} righ t rotor	11.3°
A_1 right rotor	5.2°
B_1 right rotor	6.8°

δ_F	right wing	70°
β	yaw angle	0

The tables pertinent to the data sets provided in volumes II, III and IV, are reproduced in those volumes for convenience.

CONDITION	PARAMETER VARIED	FIGURES	V	α_{FUSE}	I_N	RPM	θ_{75_L}	A_{1_L}	B_{1_L}	δ_{F_L}	θ_{75_R}	A_{1_R}	B_{1_R}	δ_{F_r}	β	DATA SET
							TEST VARIABLES HELD CONSTANT									
HOVER	$\theta_{.75}$	1-18	0	0	90	1185		-.6	.4	70.0		-.6	-.7	70	0	1 →
I_N = 90°	$\theta_{.75}$	1-18	0	0	90	1110		-.6	.4	70.0		-.6	-.7	70	0	
	LONG. CYC.	19-36	0	0	90	1110	10.0	-.5		70.0	10.0	.1		70	0	
	LAT. CYC.	37-54	0	0	90	1110	10.0		.2	70.0	10.0		-.2	70	0	
TRANSITION	α	1-24	43		90	1185	7.8	-.4	4.7	73.6	9.0	.09	4.9	70	0	2 →
I_N = 90°	YAW ANGLE	25-48	44	0	90	1183	8.0	-.4	5.0	64.0	9.3	.55	5.0	71		
V_{FS} = 45 KTS	LONG. CYC.	49-72	44	-10.0	90	1183	8.0	-.4		73.0	9.0	1.1		70	0	
	LAT. CYC.	73-96	44	-10.0	90	1183	8.0		5.0	71.0	9.3		5.0	71	0	
	$\theta_{.75}$	97-120	44	-9.9	90	1183		.4	4.7	69.0		.43	4.7	71	0	
	δ_{FLAP}	121-144	45	-9.9	90	1185	8.0	-.2	4.8		9.3	.5	4.8	69	.8	
	RPM	145-168	44	-9.9	90		8.1	-.25	4.8	69.0	9.4	.5	4.8	69	.8	
TRANSITION	α	1-24	100		90	1183	12.0	4.1	6.2	70.0	11.3	5.2	6.8	70	0	3 →
I_N = 90°	YAW ANGLE	25-48	100	-15.0	90	1183	12.1	4.1	6.2	70.0	11.3	5.4	6.8	70		
V_{FS} = 100 KTS	LONG. CYC.	49-72	100	-15.0	90	1185	11.8	4.1		70.0	10.9	5.3		70	0	
	LAT. CYC.	73-96	100	-15.0	90	1183	12.2		6.2	70.0	11.4		6.8	70	0	
	$\theta_{.75}$	97-120	100	-15.0	90	1185		4.5	6.5	70.0		5.1	6.5	70	0	
	δ_{FLAP}	121-144	100	-15.0	90	1183	12.0	4.0	6.4		11.2	5.1	6.6	70	0	
	RPM	145-168	100	-15.0	91		12.0	4.0	6.4	70.0	11.2	5.1	6.6	70	0	
TRANSITION	α	1-24	45		70	1185	8.9	-.75	5.0	61.0	10.0	.7	4.9	61	.4	4 →
I_N = 70°	YAW ANGLE	25-48	45	12.0	70	1183	8.9	-.75	5.0	61.0	10.0	.15	5.0	61		
V_{FS} = 45 KTS	LONG. CYC.	49-72	43	12.0	70	1185	8.4	-.8		61.0	9.7	.7		61	.4	
	LAT. CYC.	73-96	44	11.9	70	1185	9.2		5.0	61.0	9.9		5.0	61	.5	
	$\theta_{.75}$	97-120	44	11.9	70	1183		-.5	5.0	61.0		-.45	5.0	61	.1	
	δ_{FLAP}	121-144	44	11.9	70	1185	8.9	-.7	5.0		10.0	.85	5.0		.1	
	RPM	145-168	44	11.9	70		8.9	-.7	5.0	30.0	10.0	.85	5.0	30	.1	

TABLE 12. CONSTANT VALUES OF TEST VARIABLES

IN = 90^{o} HOVER

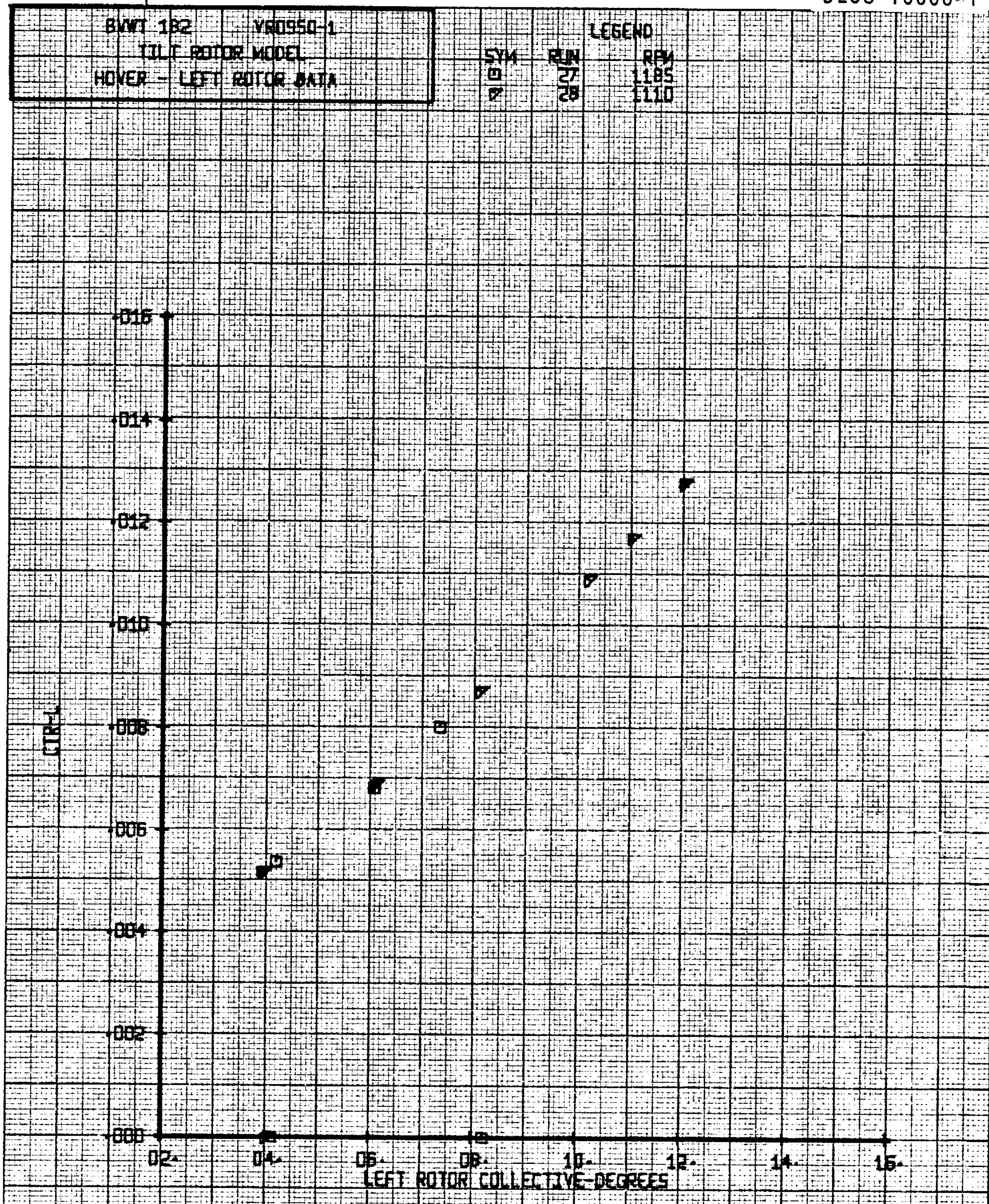

Figure 1-001. Left Rotor Thrust Coefficient Versus Collective Pitch. I_N = 90° Hover.

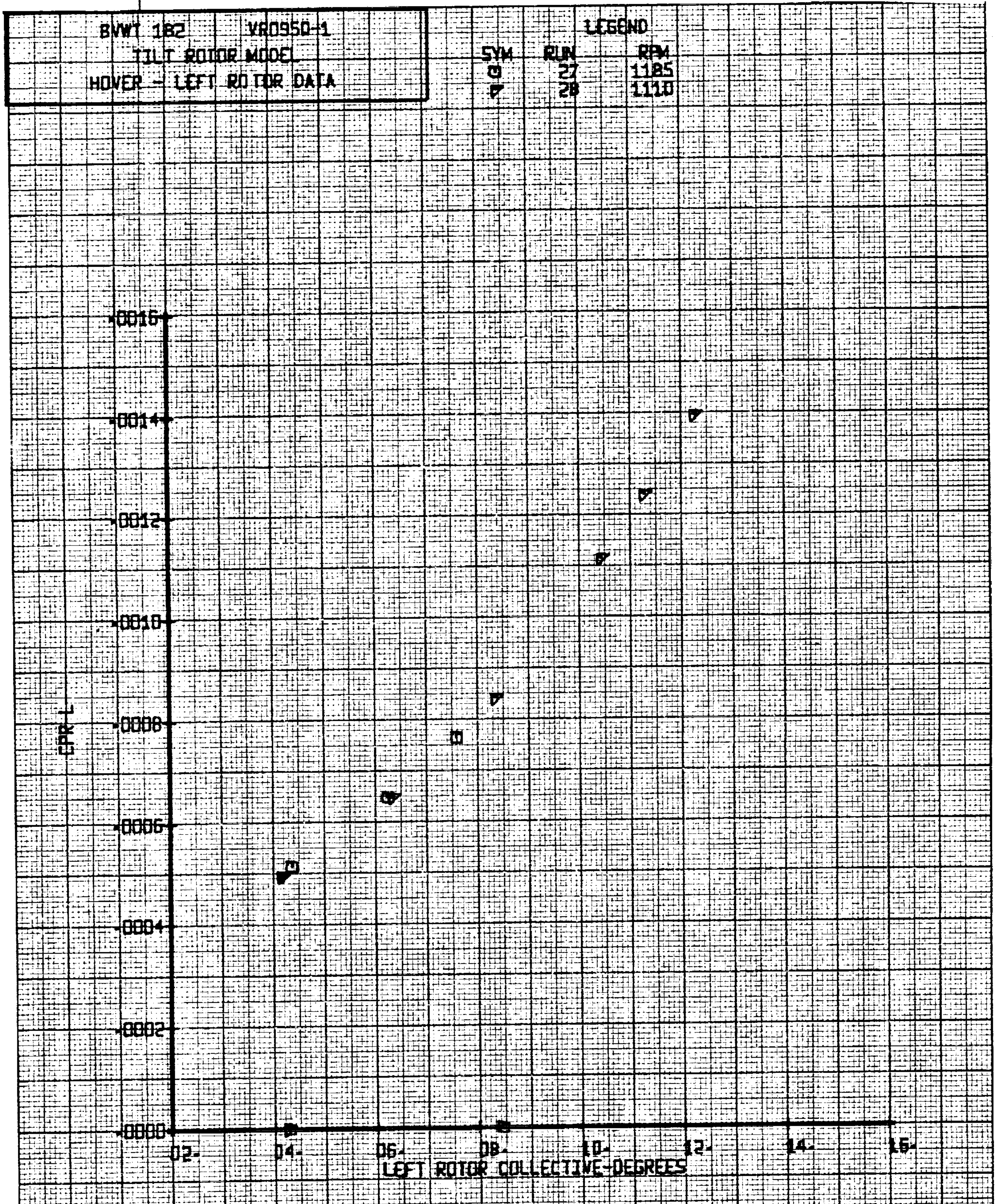

Figure 1-002. Left Rotor Power Coefficient Versus Collective Pitch. I_N = 90° Hover.

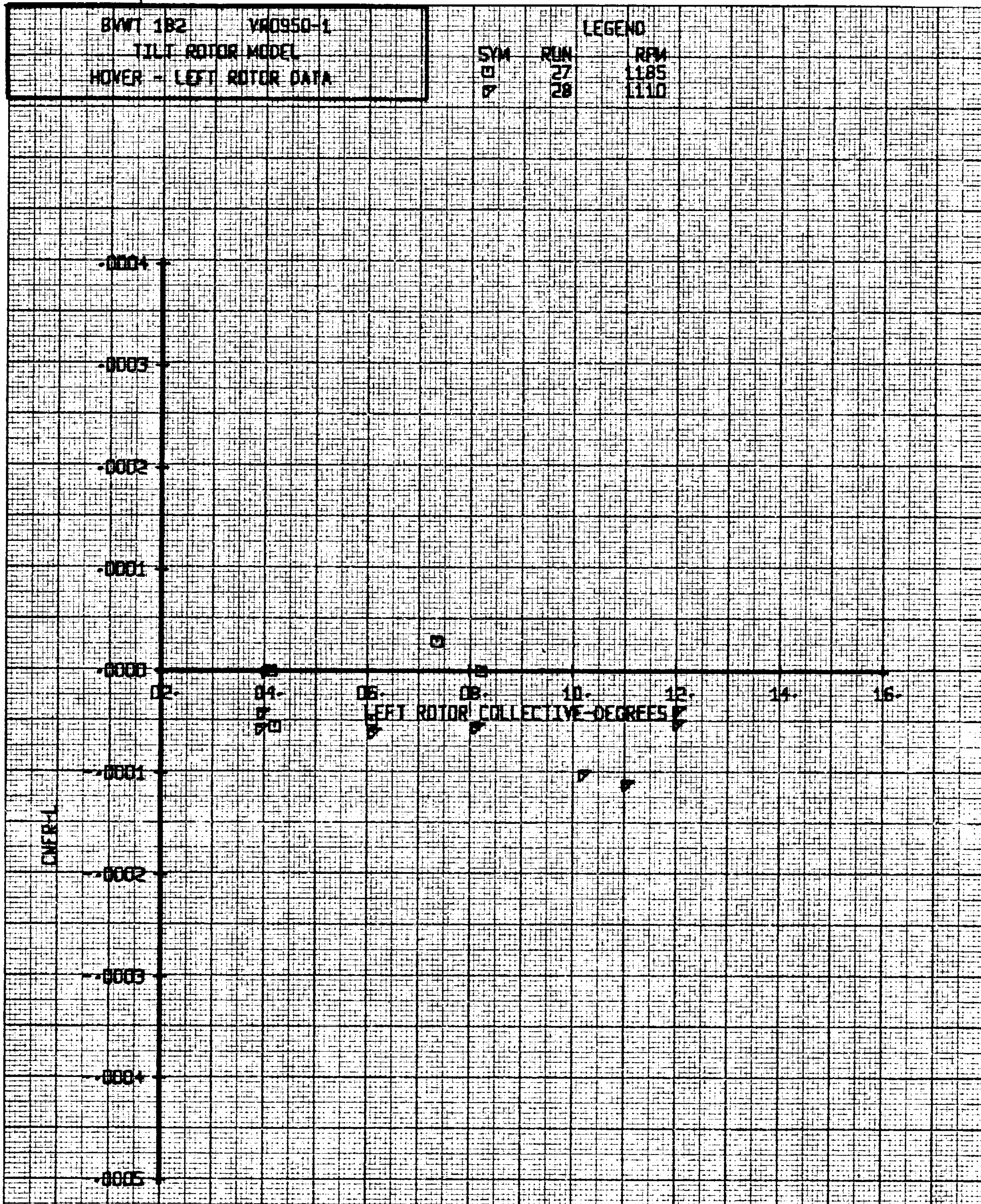

Figure 1-003. Left Rotor Normal Force Coefficient Versus Collective Pitch. $I_N = 90°$ Hover.

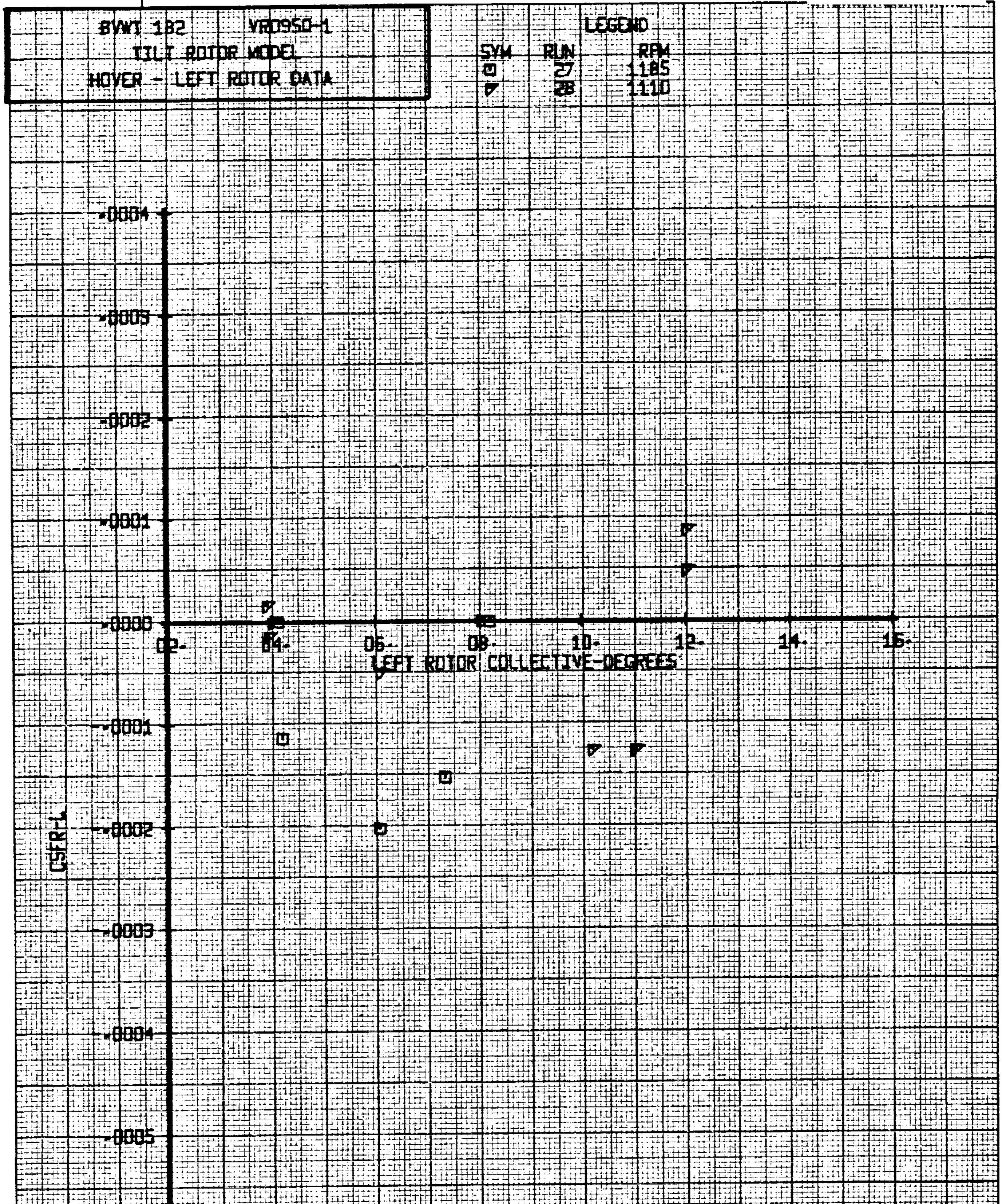

Figure 1-004. Left Rotor Side Force Coefficient Versus Collective Pitch. I_N = 90° Hover.

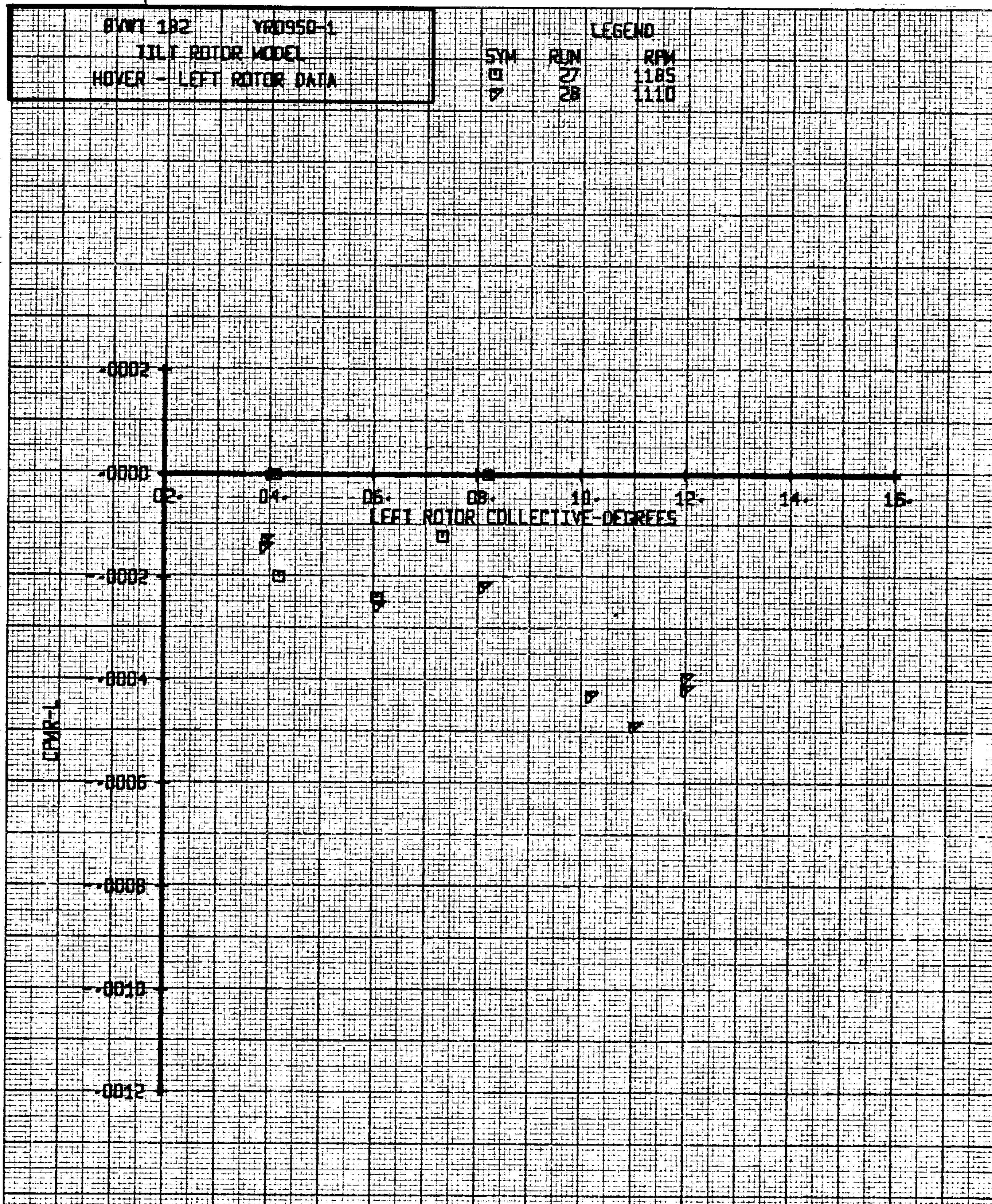

Figure 1-005. Left Rotor Pitching Moment Coefficient Versus Collective Pitch. $I_N = 90°$ Hover.

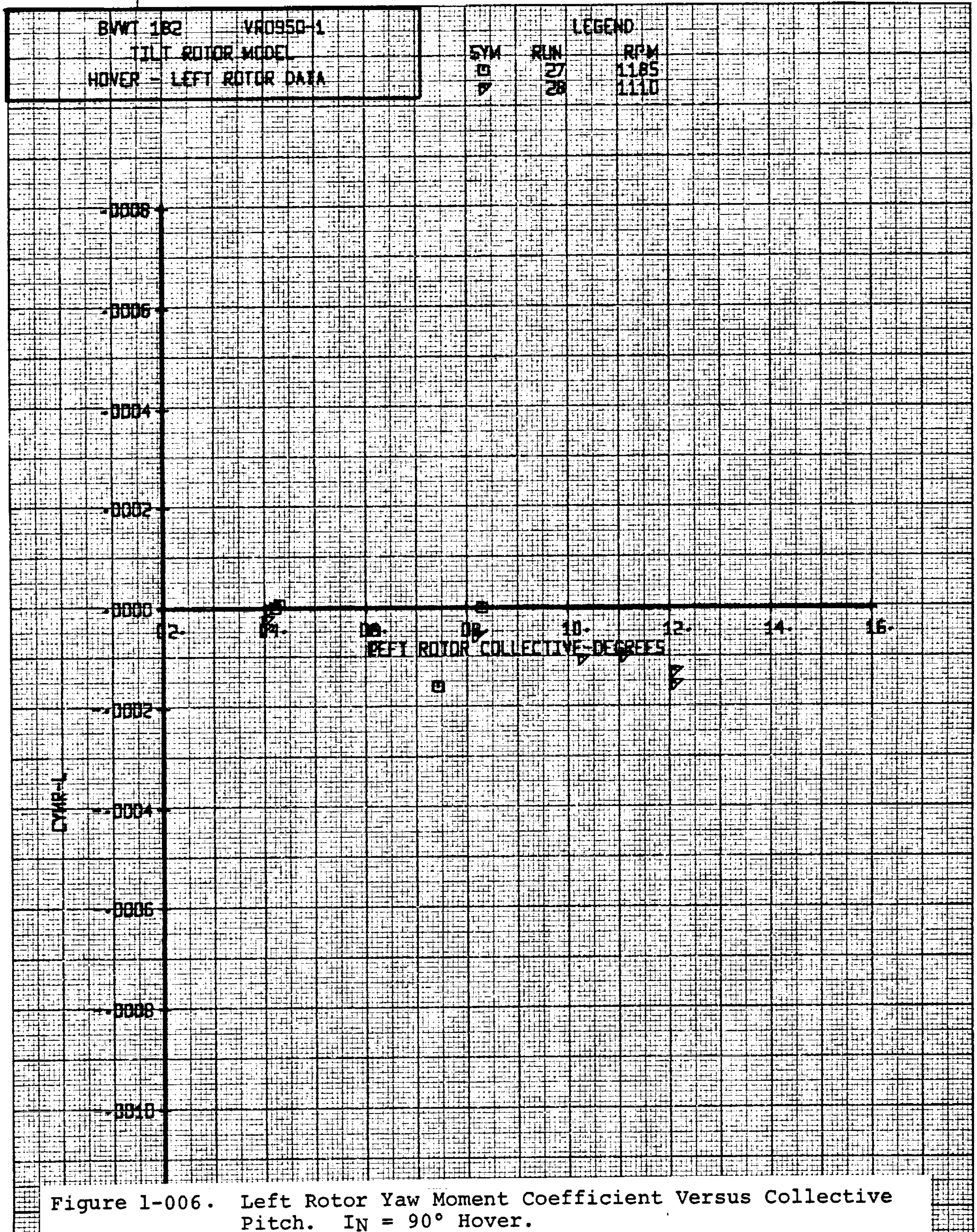

Figure 1-006. Left Rotor Yaw Moment Coefficient Versus Collective Pitch. I_N = 90° Hover.

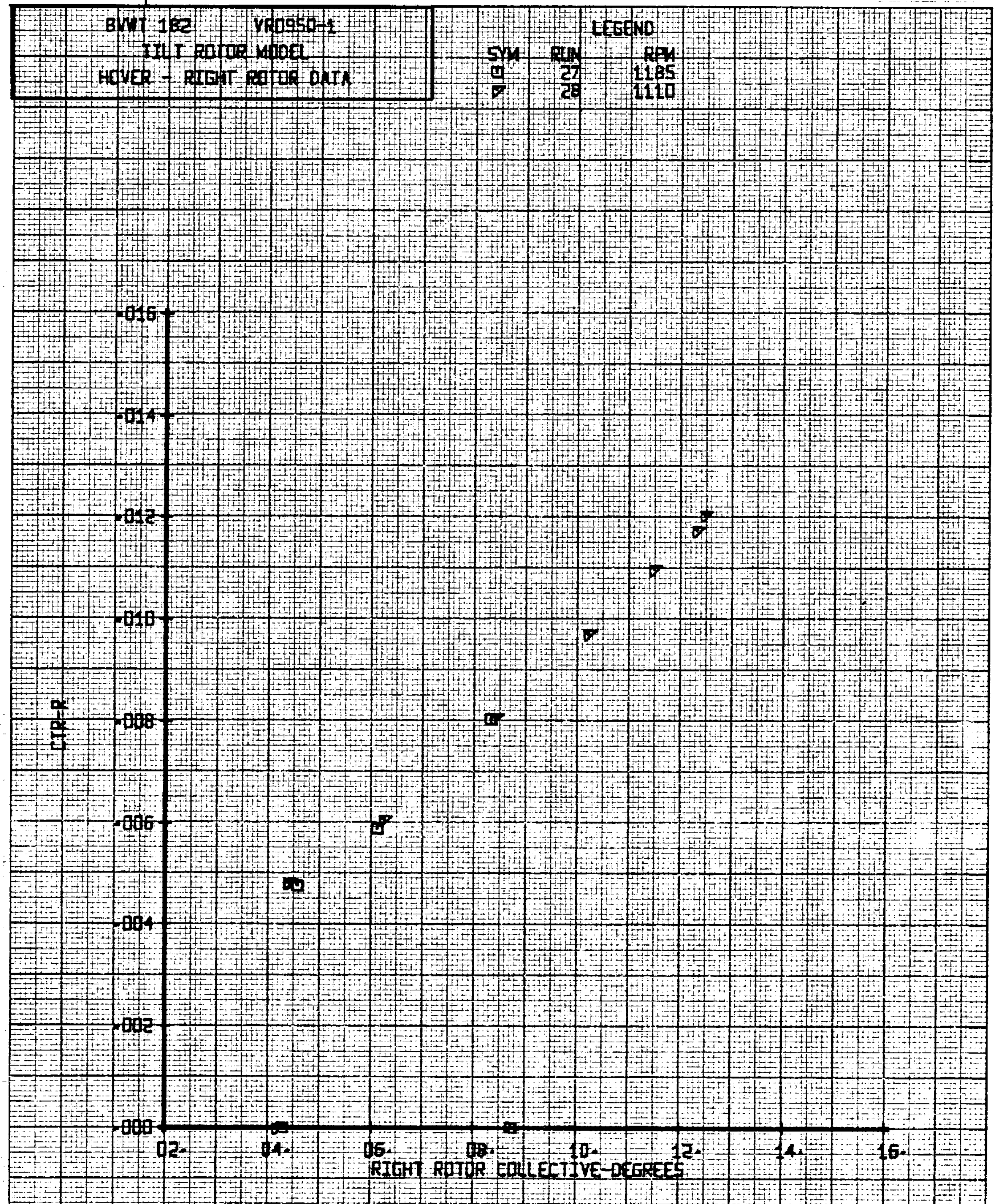

Figure 1-007. Right Rotor Thrust Coefficient Versus Collective Pitch. I_N = 90° Hover.

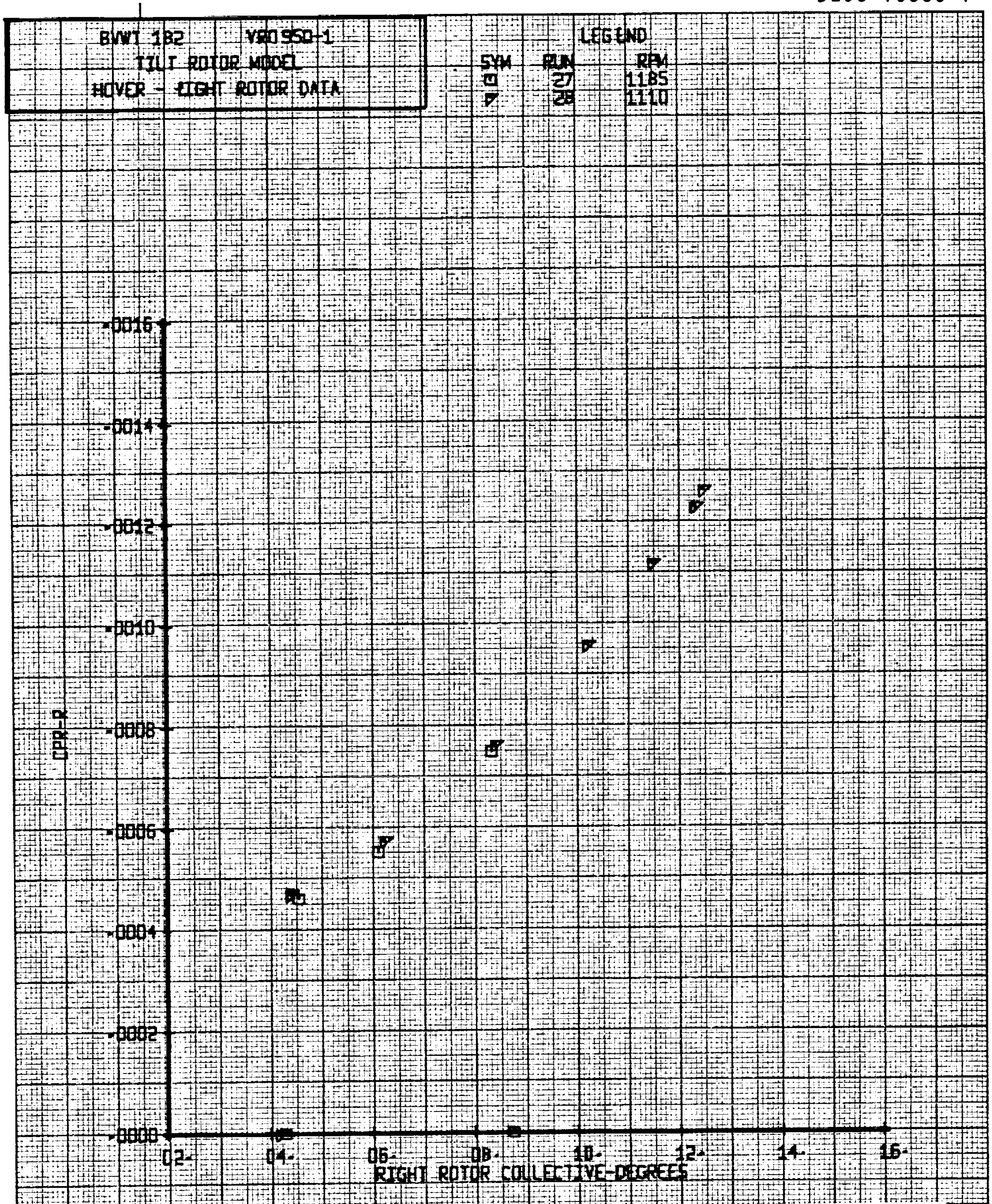

Figure 1-008. Right Rotor Power Coefficient Versus Collective Pitch. $I_N = 90°$ Hover.

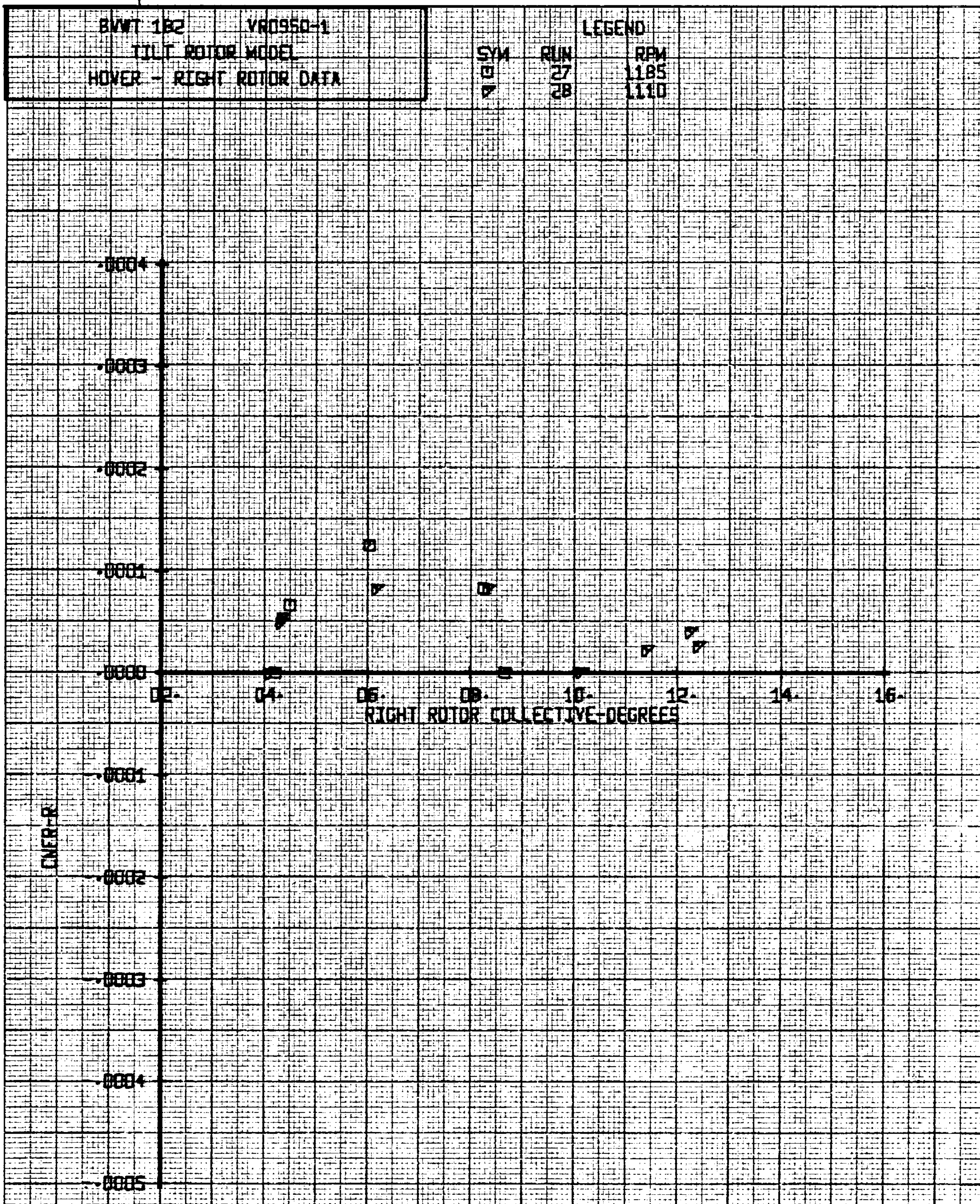

Figure 1-009. Right Rotor Normal Force Coefficient Versus Collective Pitch. I_N = 90° Hover.

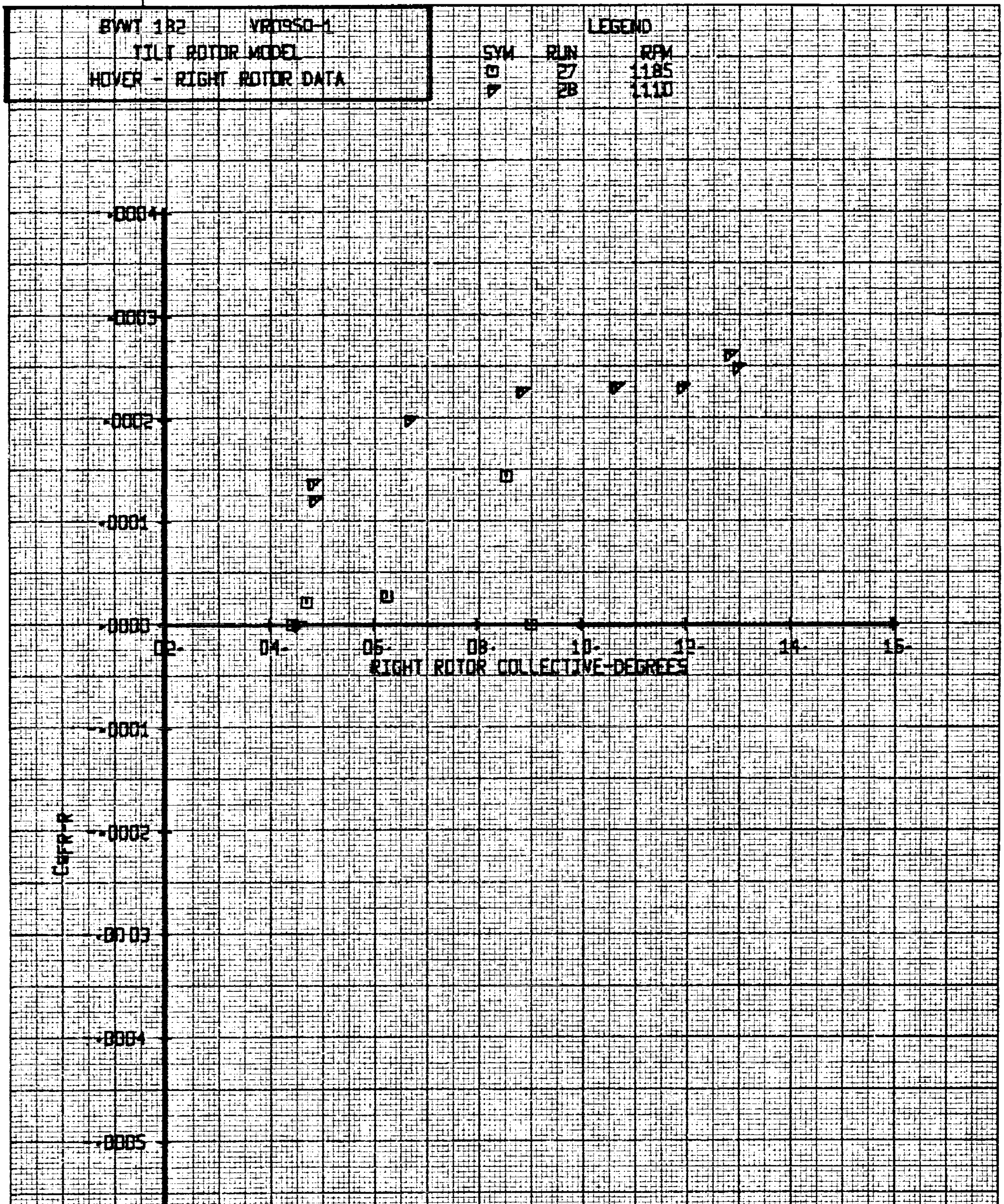

Figure 1-010. Right Rotor Pitch Moment Coefficient Versus Collective Pitch. $I_N = 90°$ Hover.

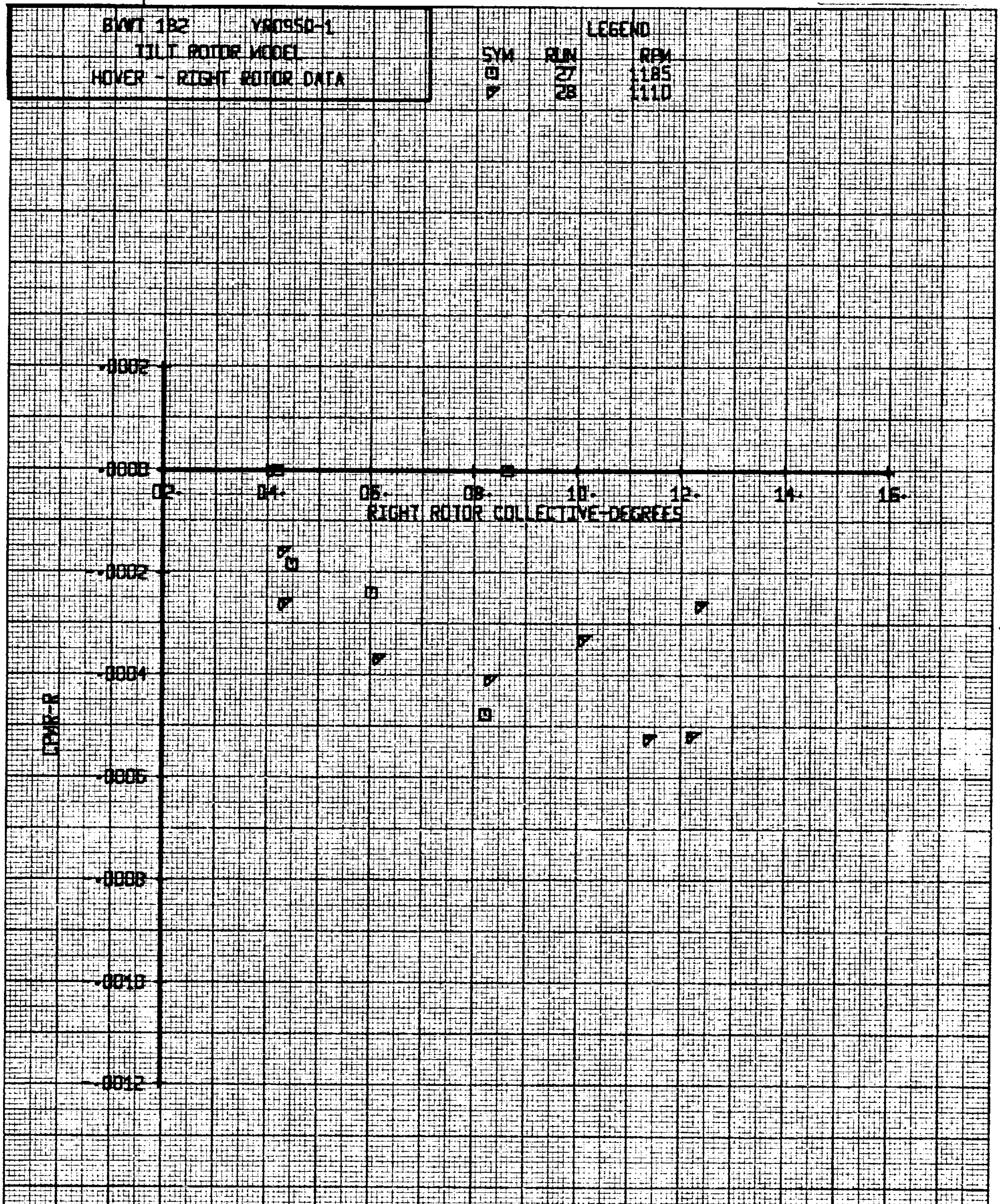

Figure 1-011. Right Rotor Pitch Moment Coefficient Versus Collective Pitch. I_N = 90° Hover.

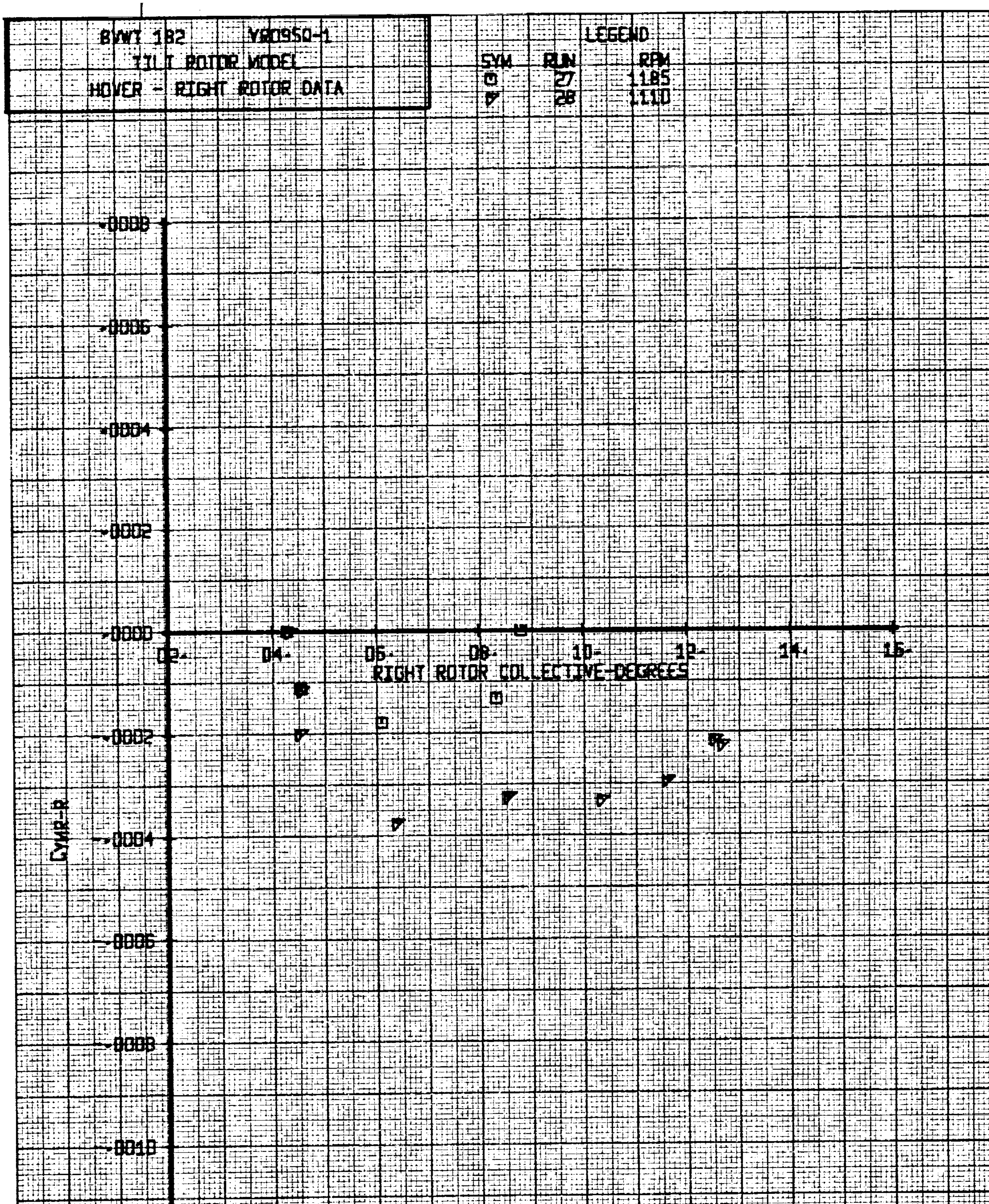

Figure 1-012. Right Rotor Yaw Moment Coefficient Versus Collective Pitch. I_N = 90° Hover.

Figure 1-013. Alternating Blade Chord Bending, Left Rotor, Versus Collective Pitch. I_N = 90° Hover.

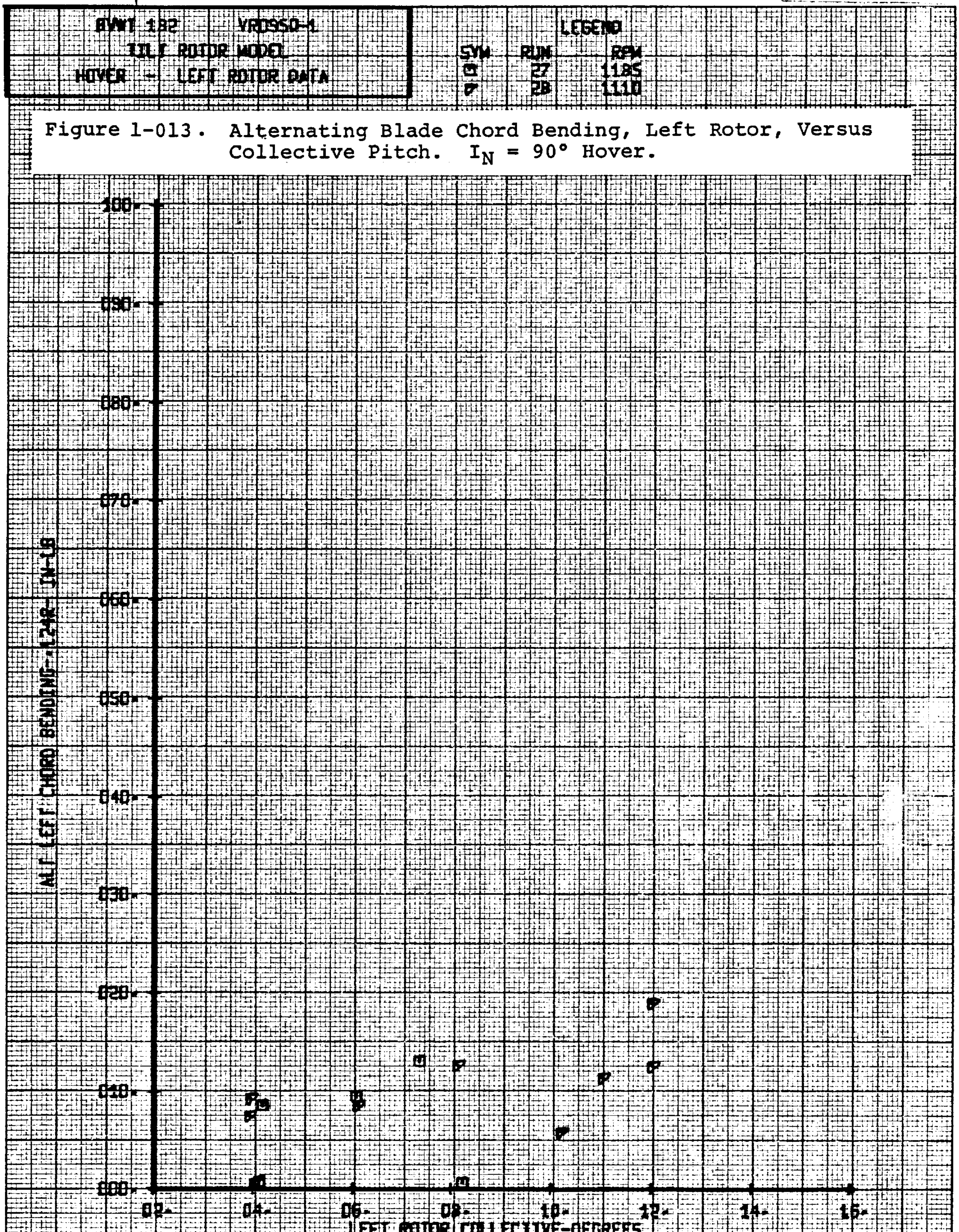

161

Figure 1-014. Alternating Blade Flap Bending, Left Rotor, Versus Collective Pitch. I_N = 90° Hover.

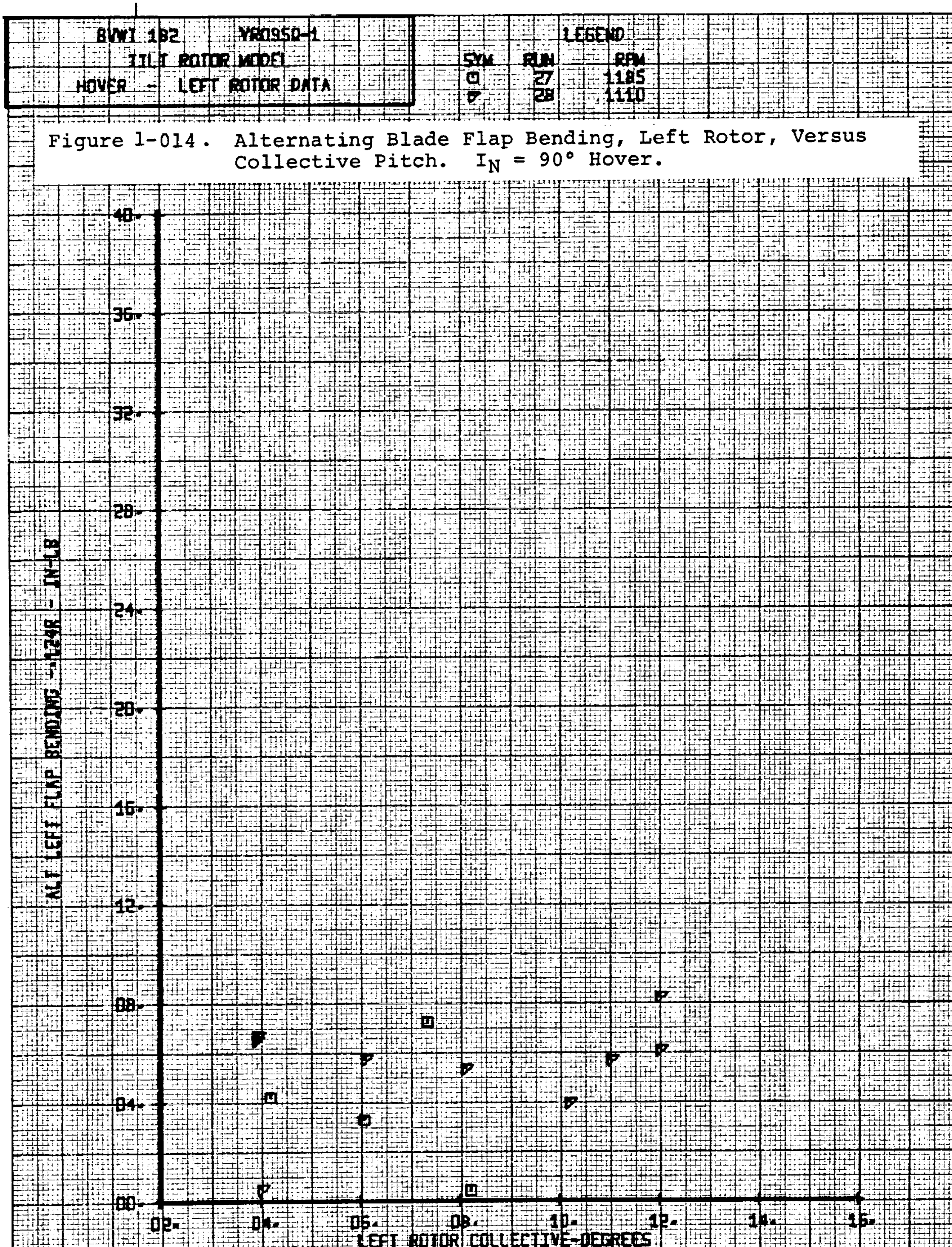

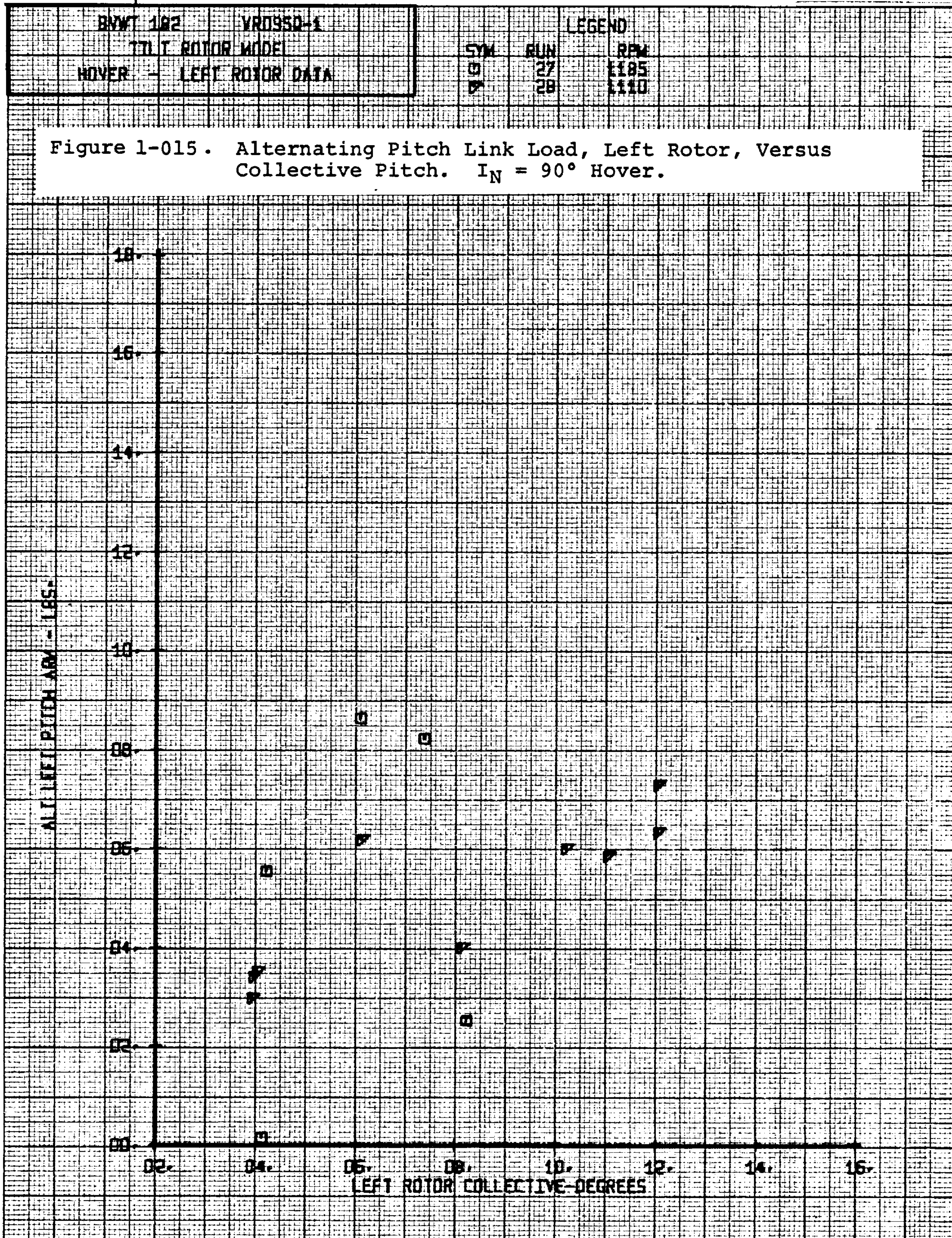

Figure 1-015. Alternating Pitch Link Load, Left Rotor, Versus Collective Pitch. I_N = 90° Hover.

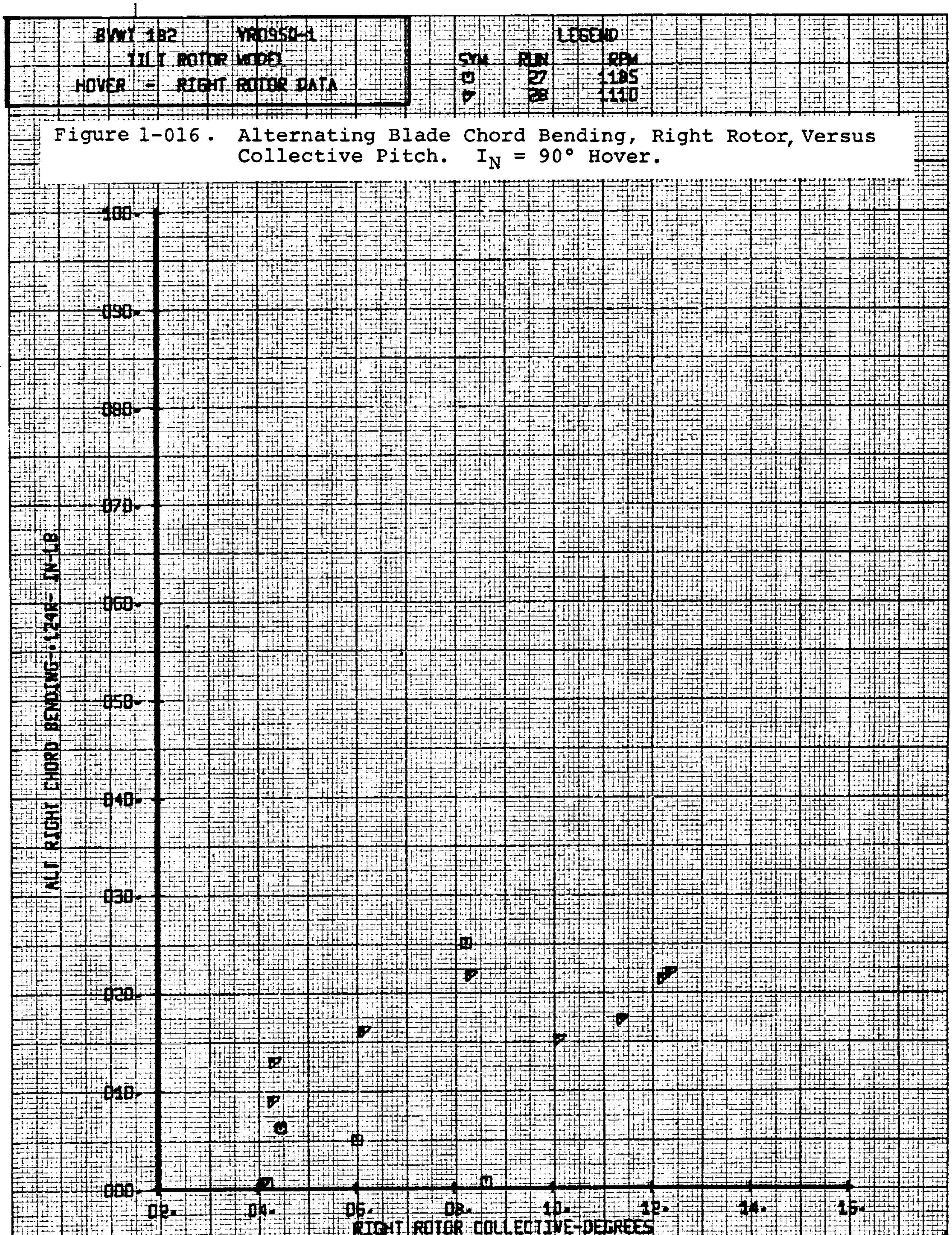

Figure 1-016. Alternating Blade Chord Bending, Right Rotor, Versus Collective Pitch. I_N = 90° Hover.

SET 116
BVWT 182

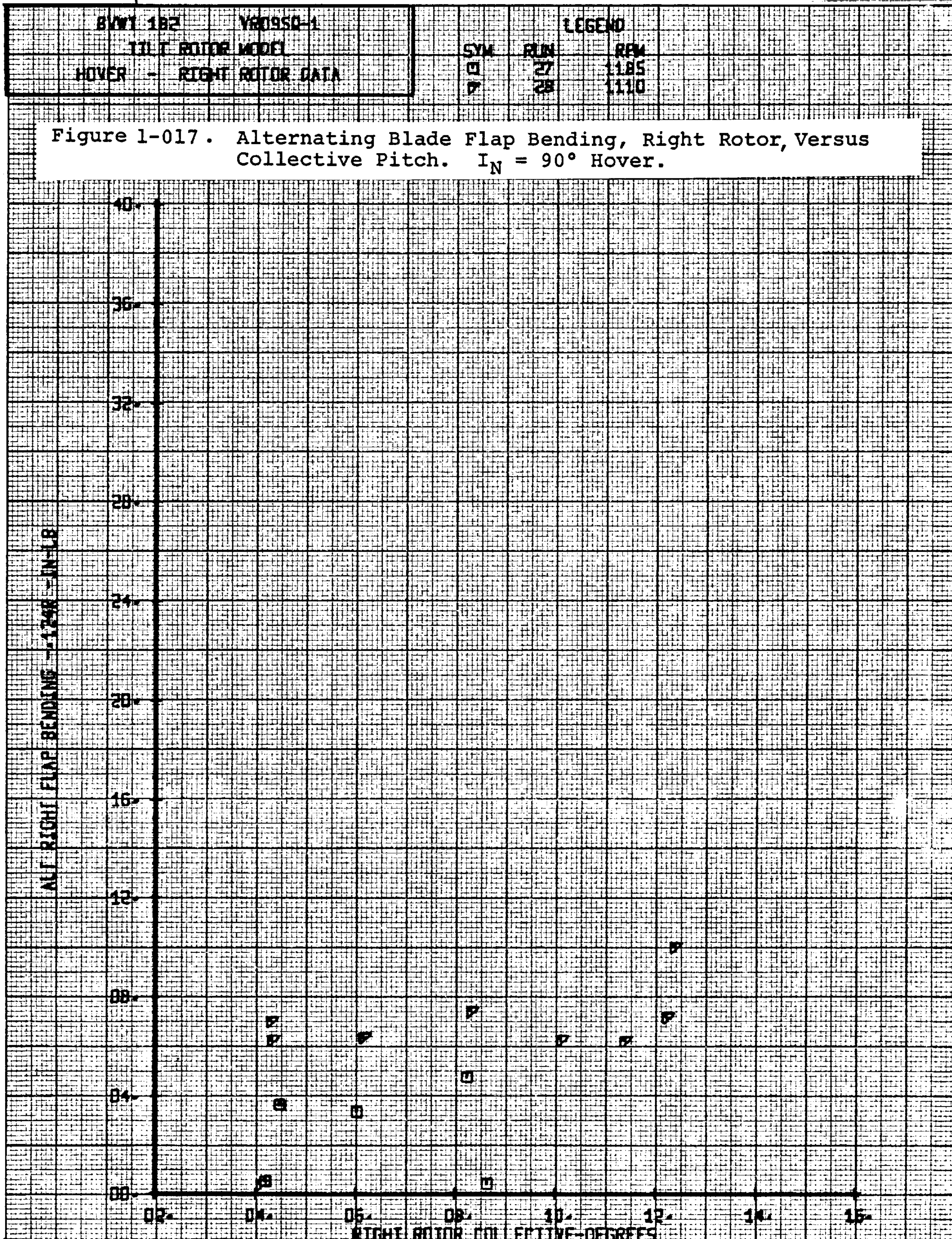

Figure 1-017. Alternating Blade Flap Bending, Right Rotor, Versus Collective Pitch. $I_N = 90°$ Hover.

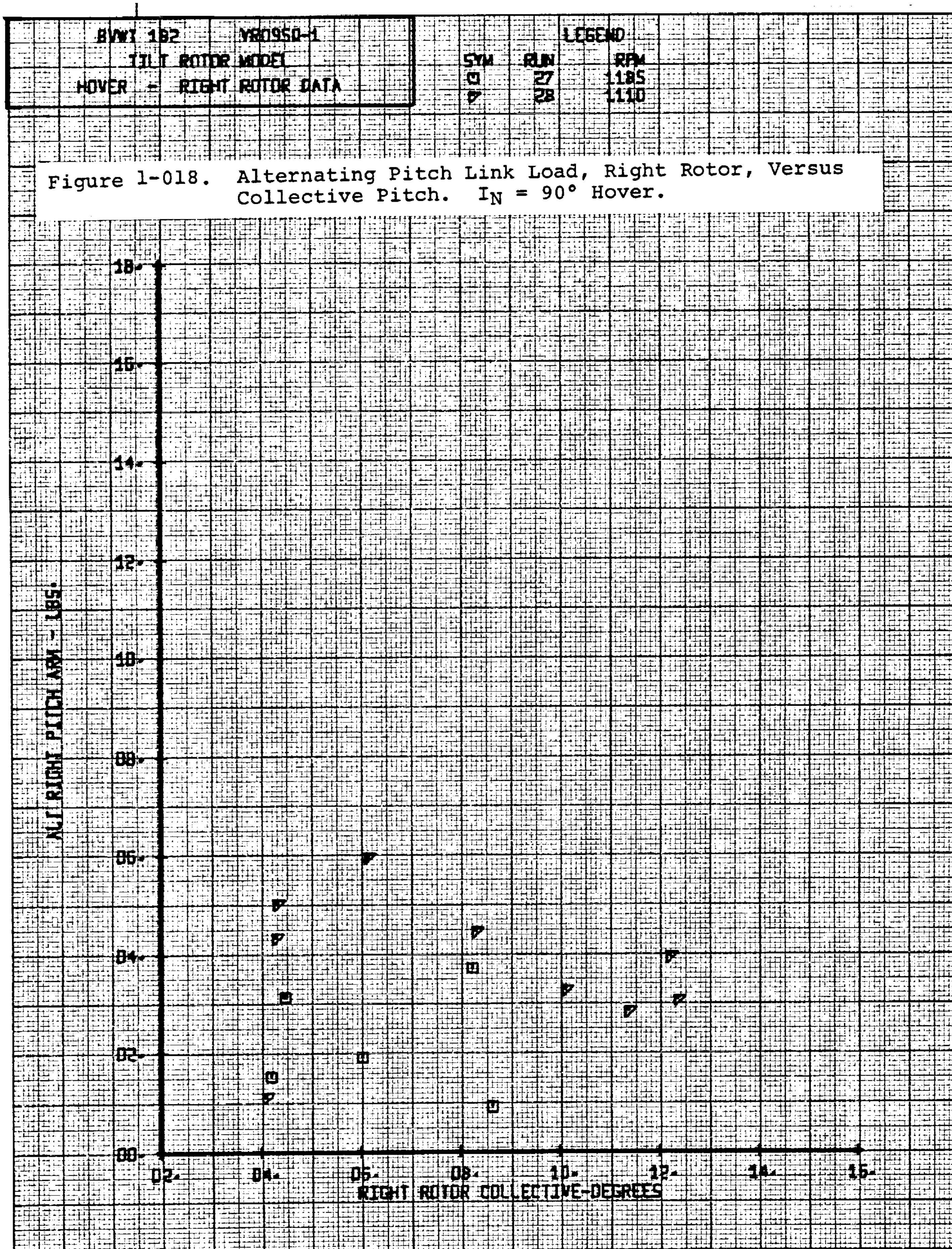

Figure 1-018. Alternating Pitch Link Load, Right Rotor, Versus Collective Pitch. $I_N = 90°$ Hover.

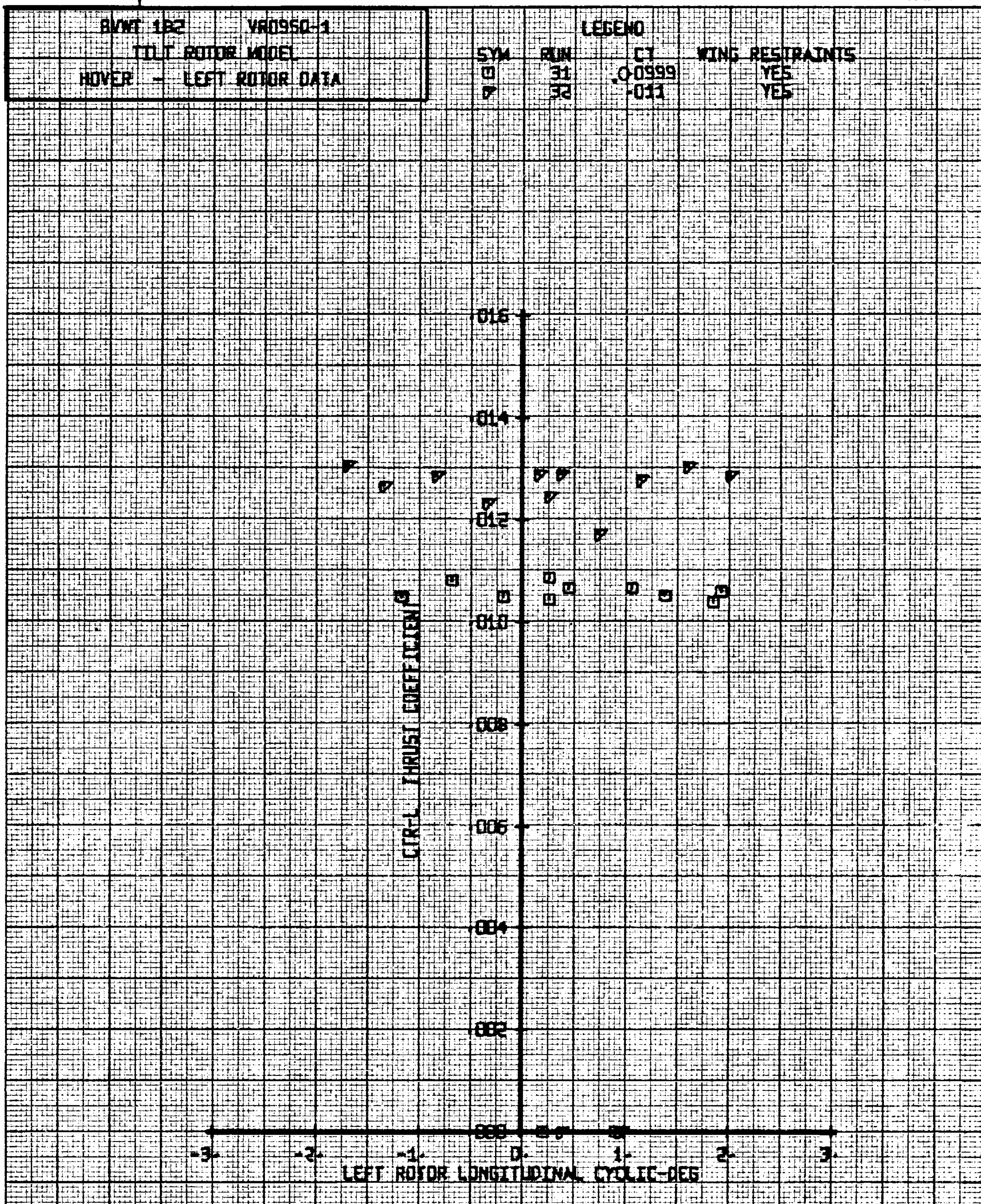

Figure 1-019. Left Rotor Thrust Coefficient Versus Longitudinal Cyclic Pitch. $I_N = 90°$ Hover.

Figure 1-020. Left Rotor Power Coefficient Versus Longitudinal Cyclic Pitch. I_N = 90° Hover.

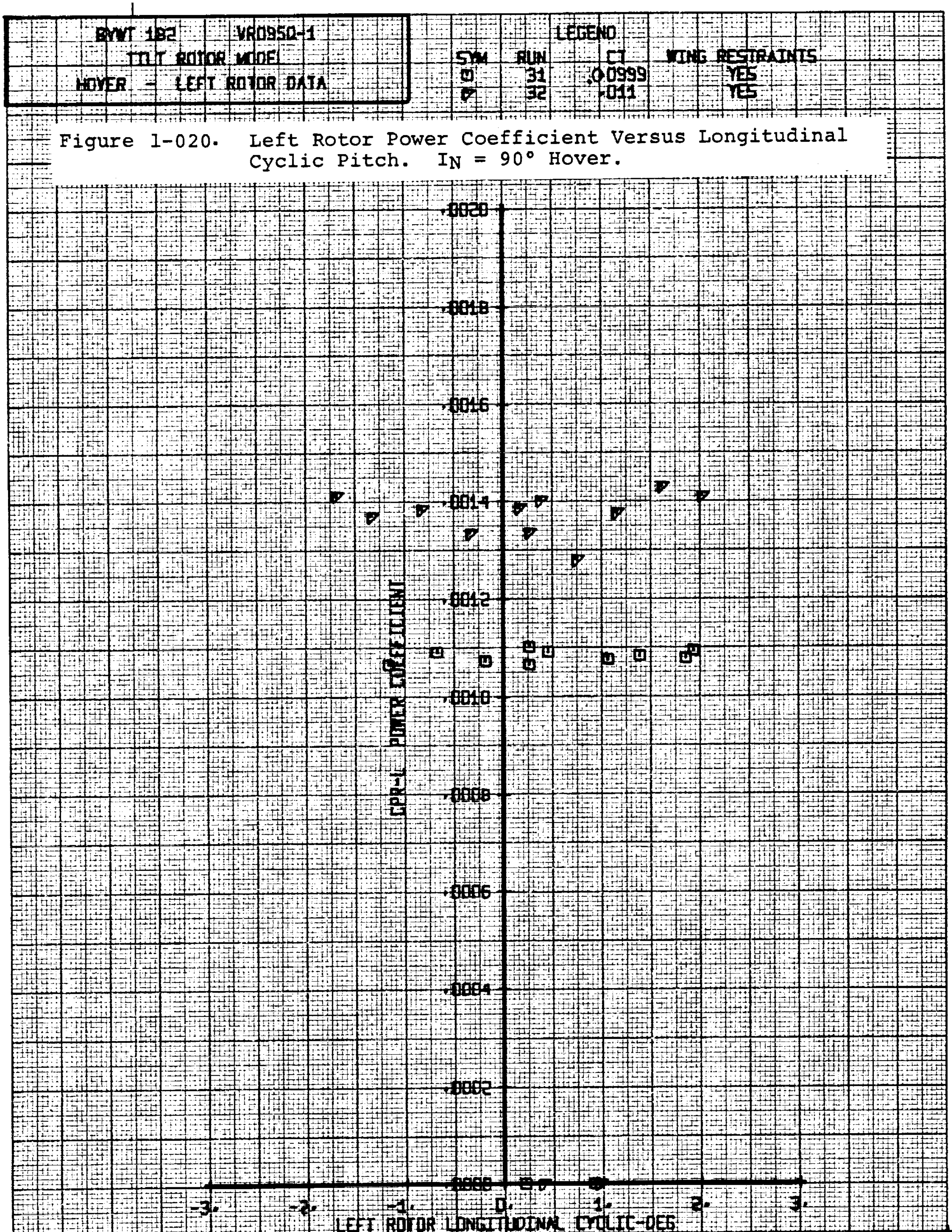

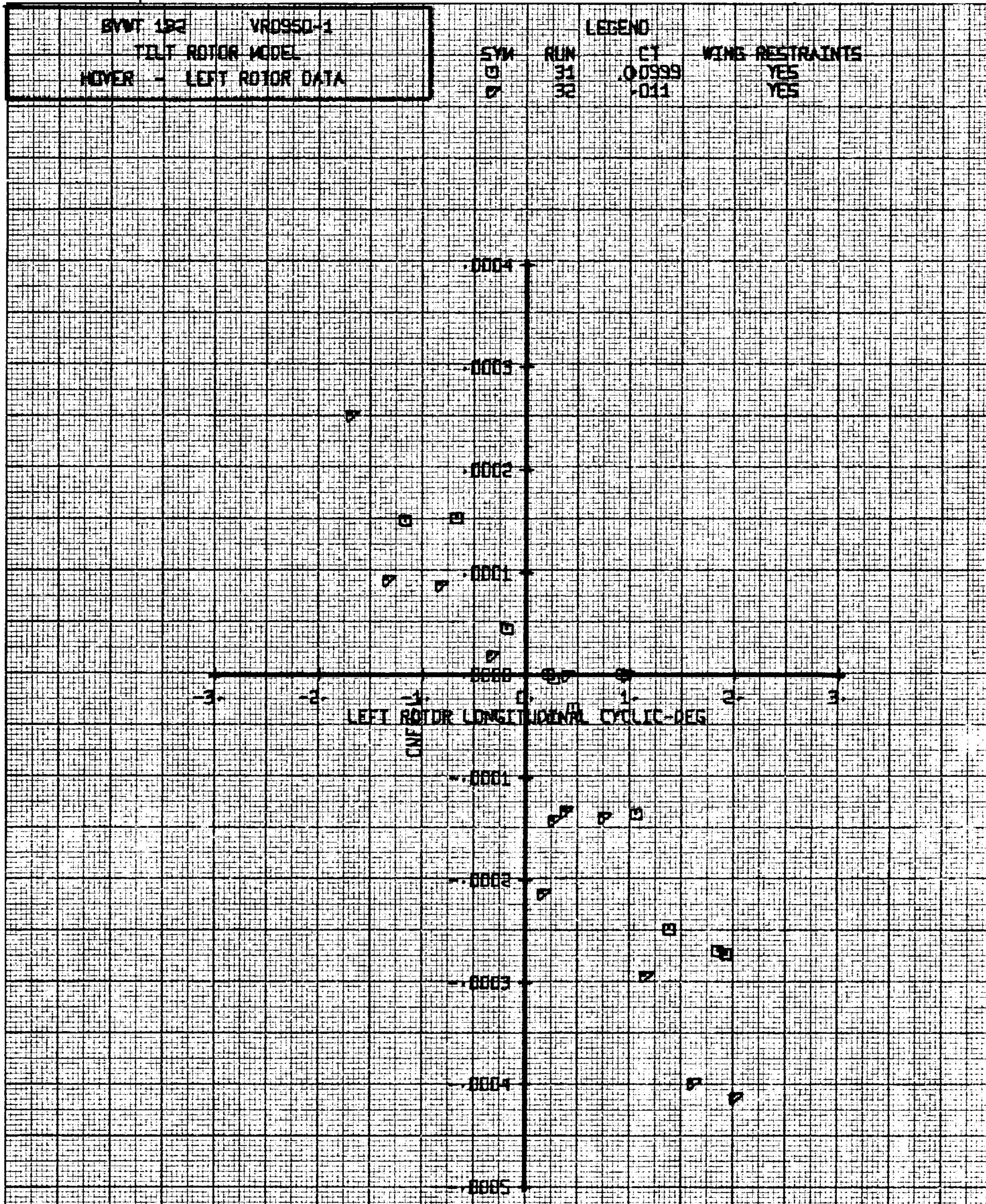

Figure 1-021. Left Rotor Normal Force Coefficient Versus Longitudinal Cyclic Pitch. $I_N = 90°$ Hover.

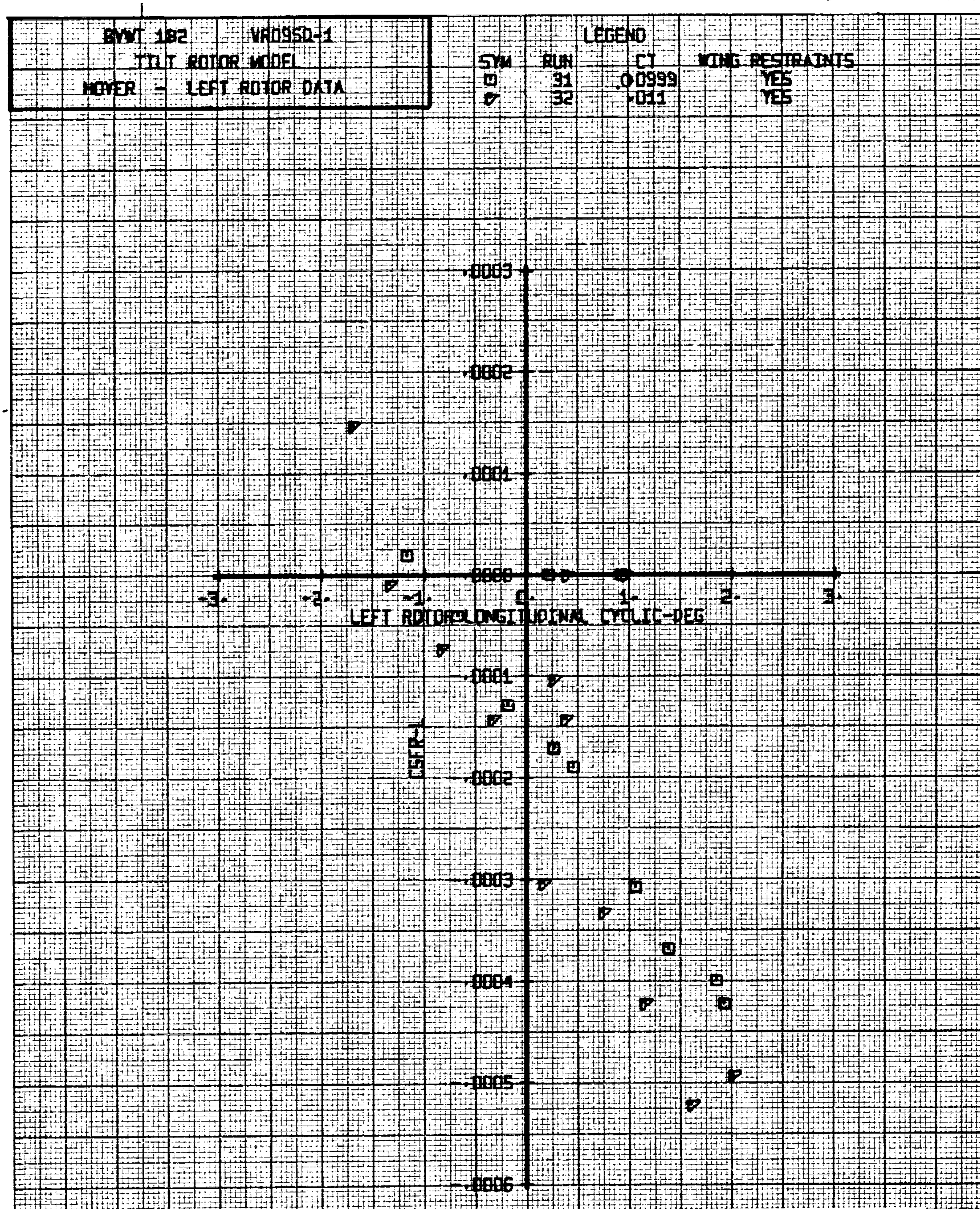

Figure 1-022. Left Rotor Side Force Coefficient Versus Longitudinal Cyclic Pitch. I_N = 90° Hover.

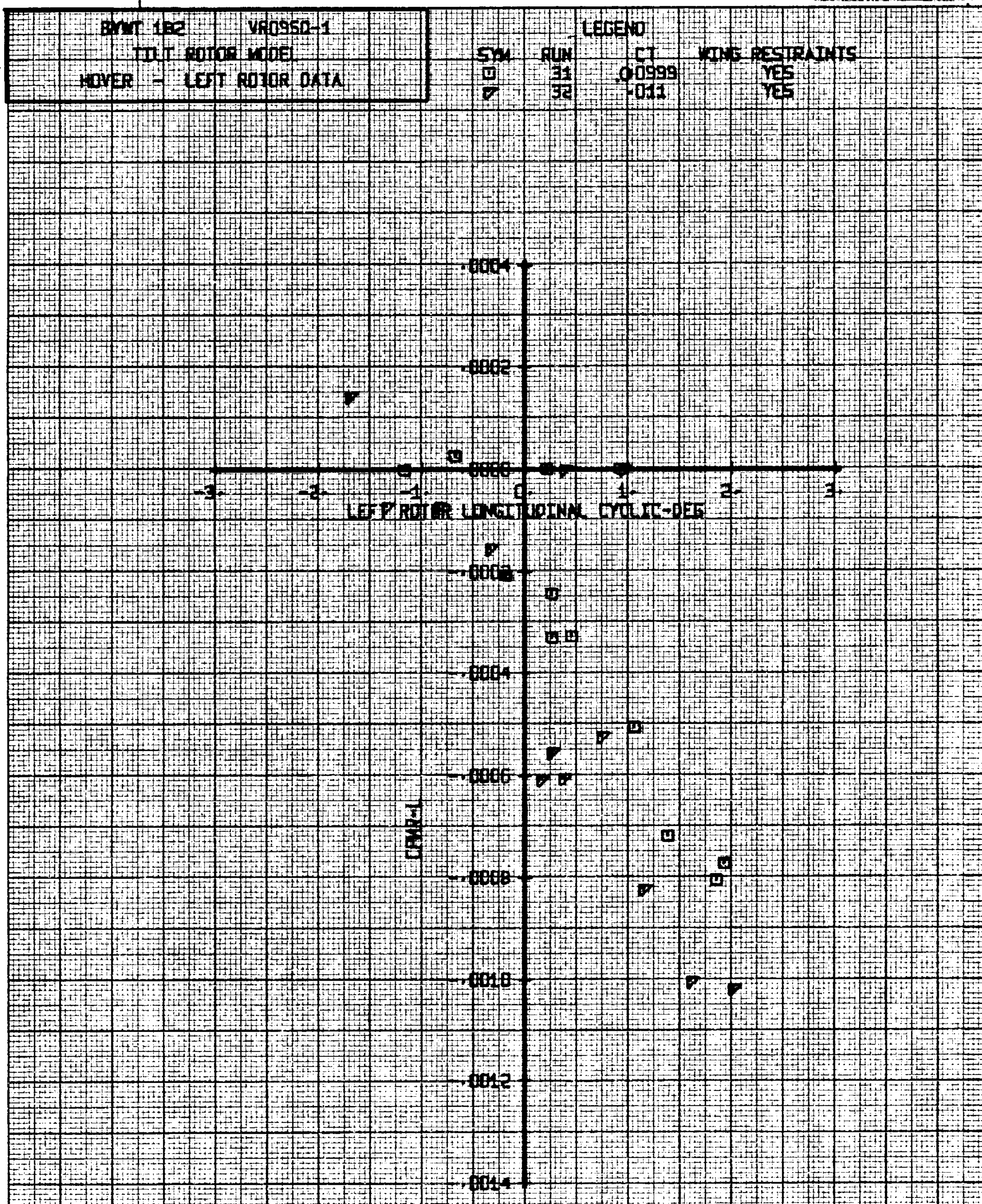

Figure 1-023. Left Rotor Pitch Moment Coefficient Versus Longitudinal Cyclic Pitch. $I_N = 90°$ Hover.

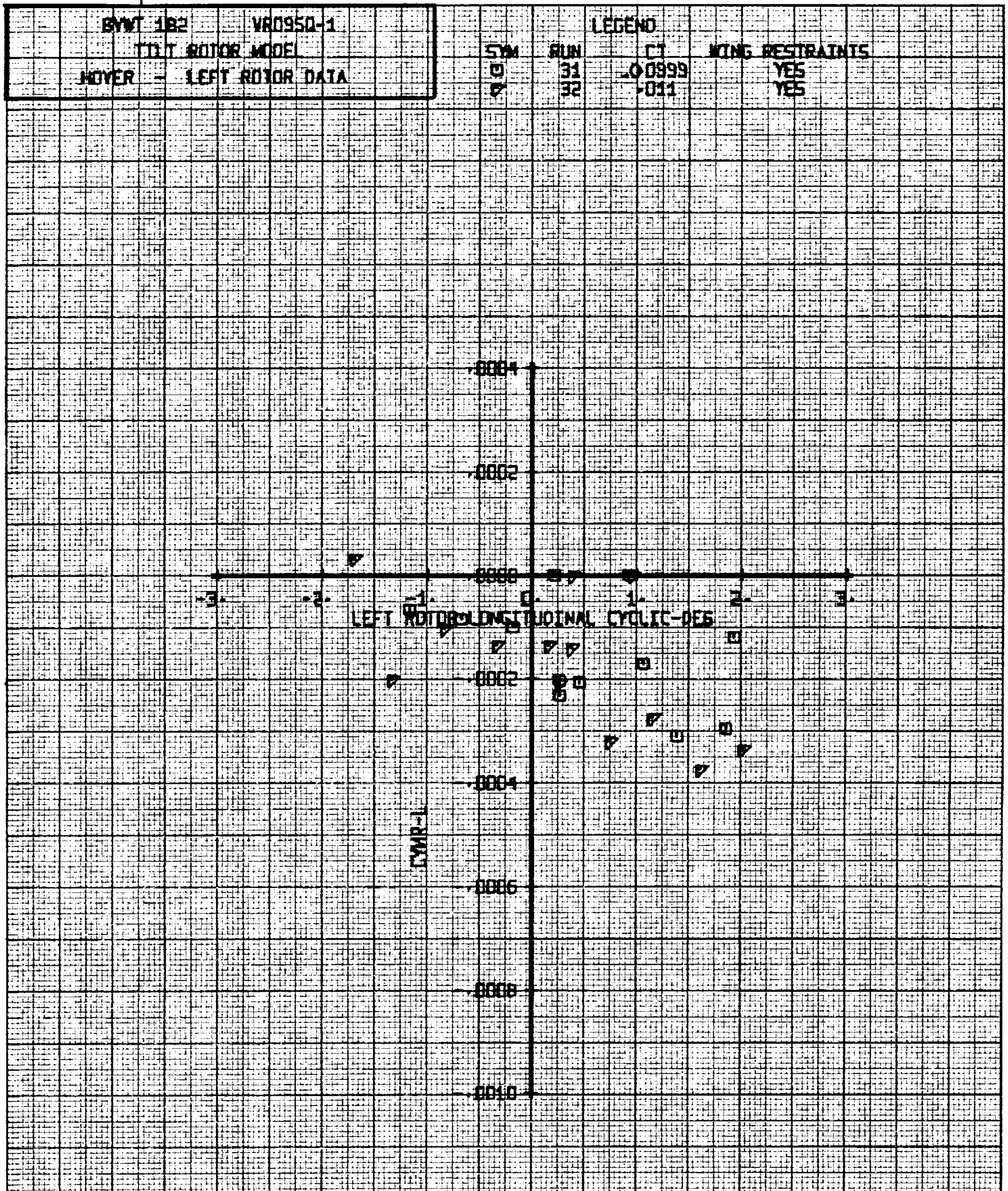

Figure 1-024. Left Rotor Yaw Moment Coefficient Versus Longitudinal Cyclic Pitch. I_N = 90° Hover.

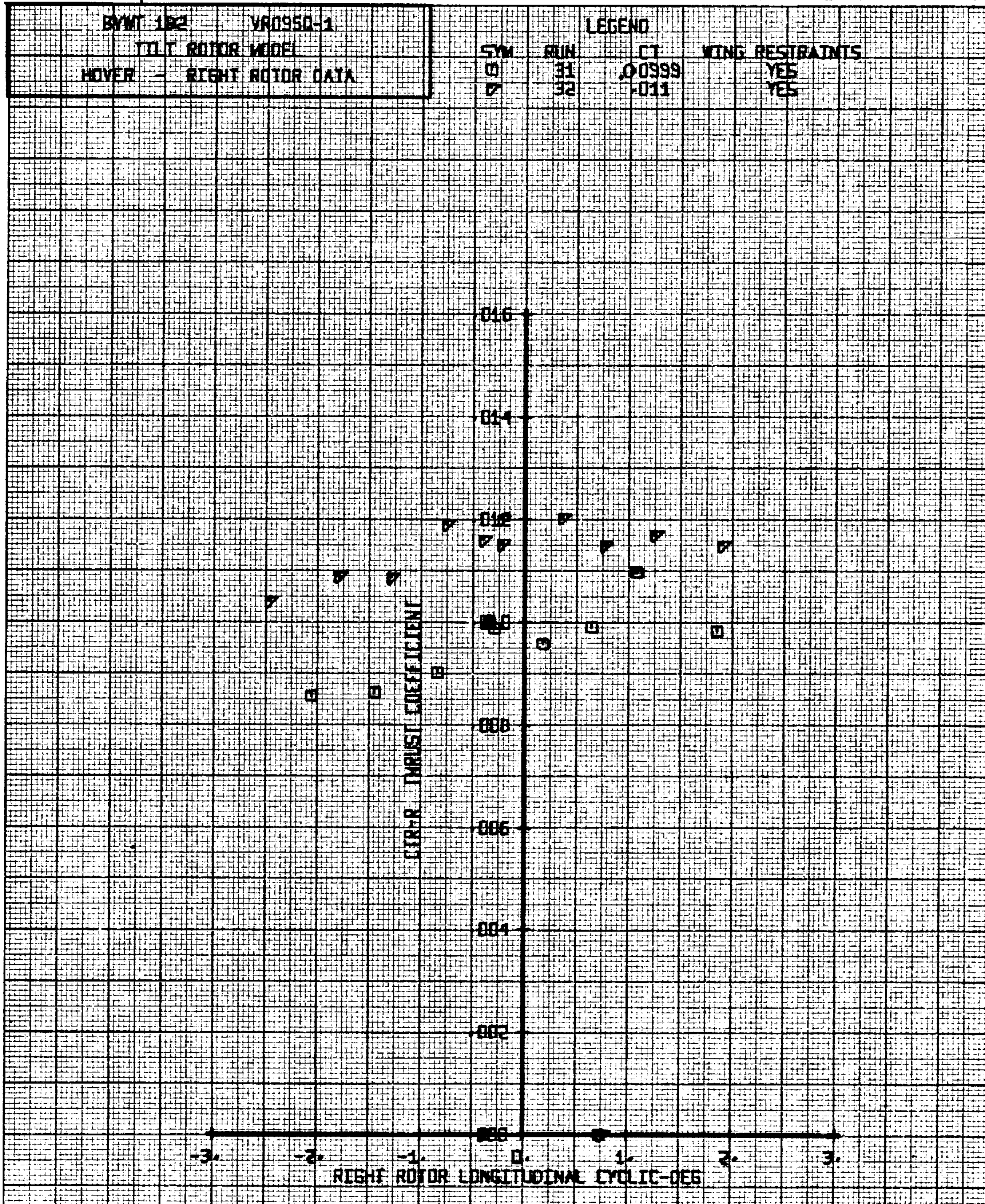

Figure 1-025. Right Rotor Thrust Coefficient Versus Longitudinal Cyclic Pitch. $I_N = 90°$ Hover.

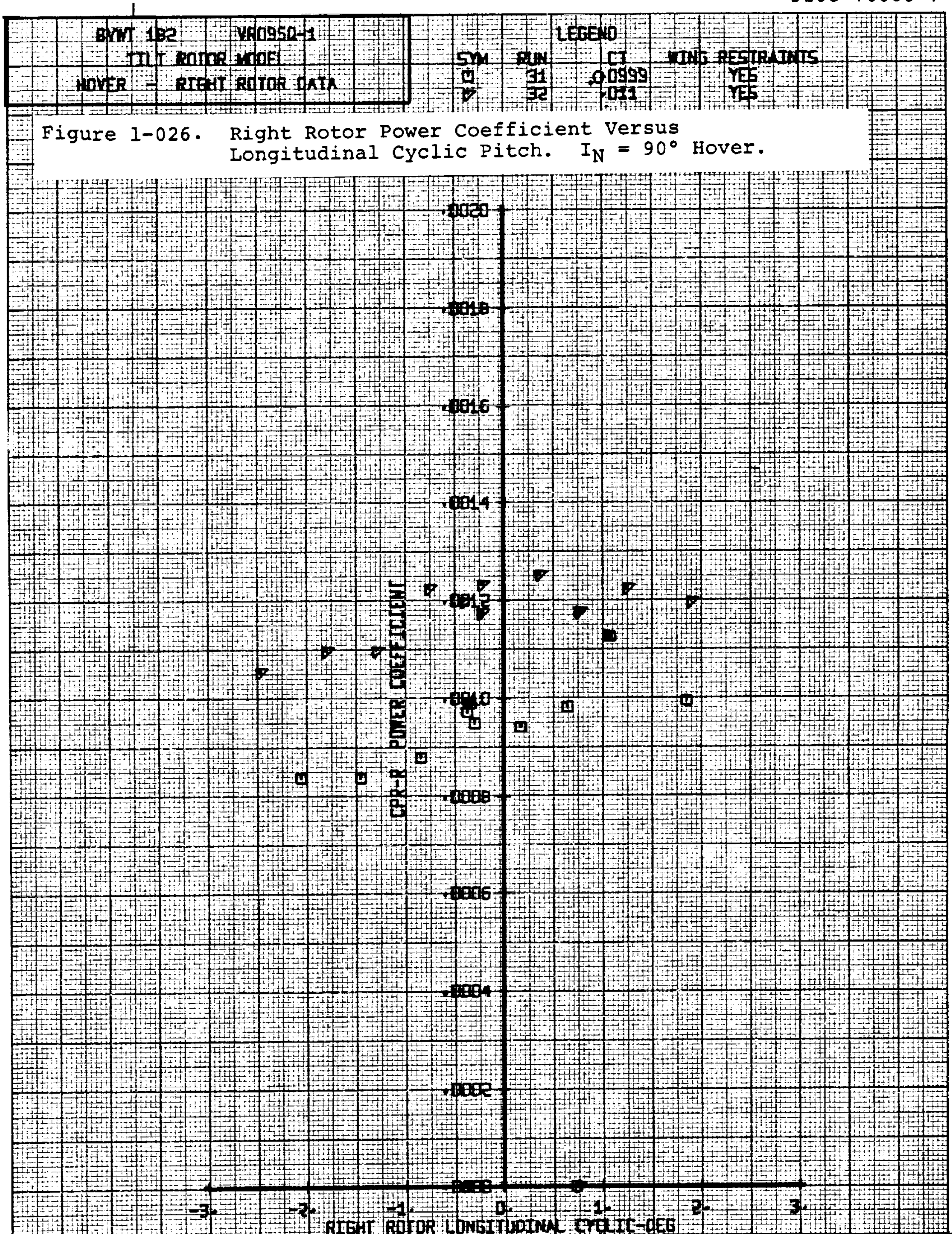

Figure 1-026. Right Rotor Power Coefficient Versus Longitudinal Cyclic Pitch. I_N = 90° Hover.

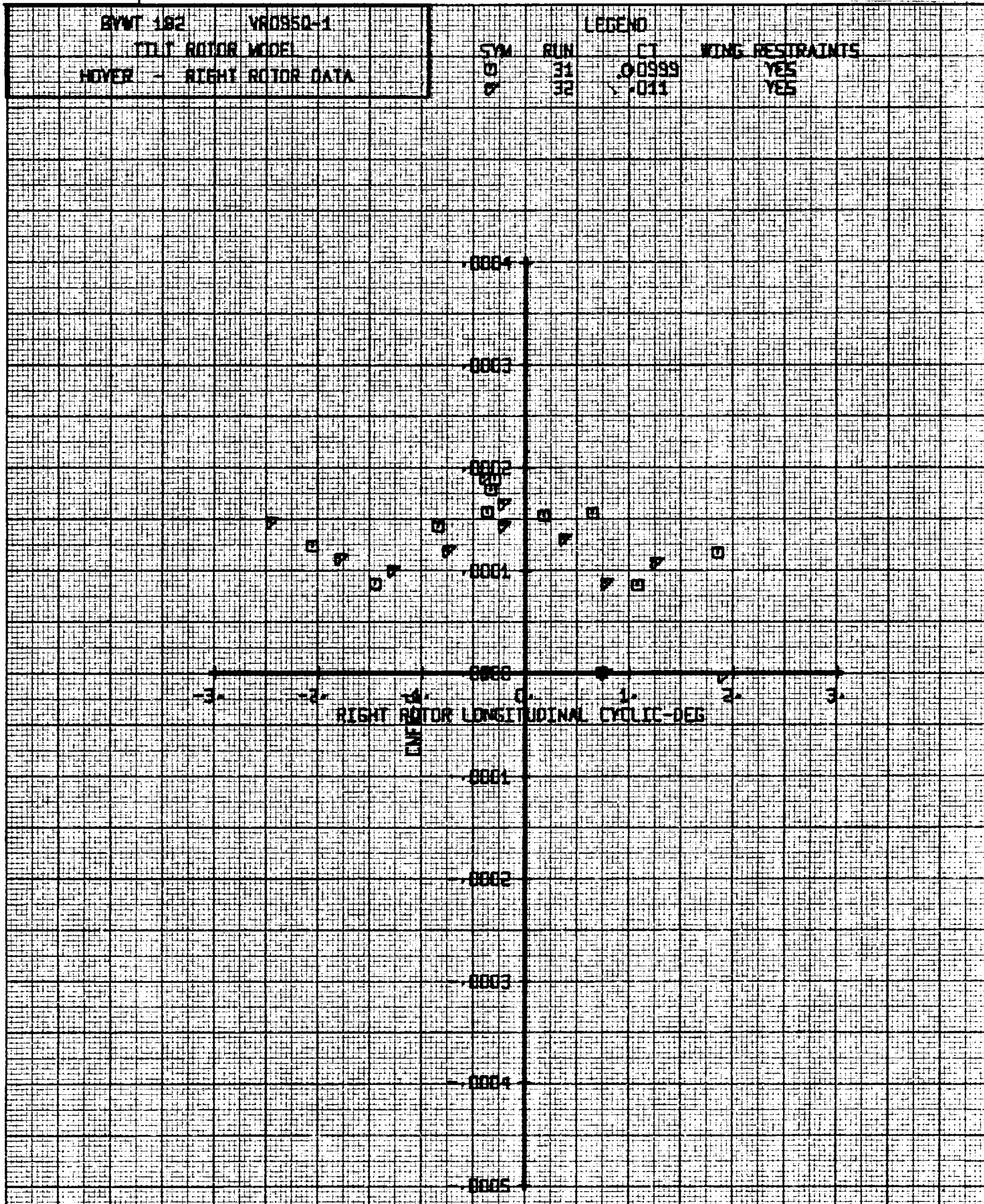

Figure 1-027. Right Rotor Normal Force Coefficient Versus Longitudinal Cyclic Pitch. $I_N = 90°$ Hover.

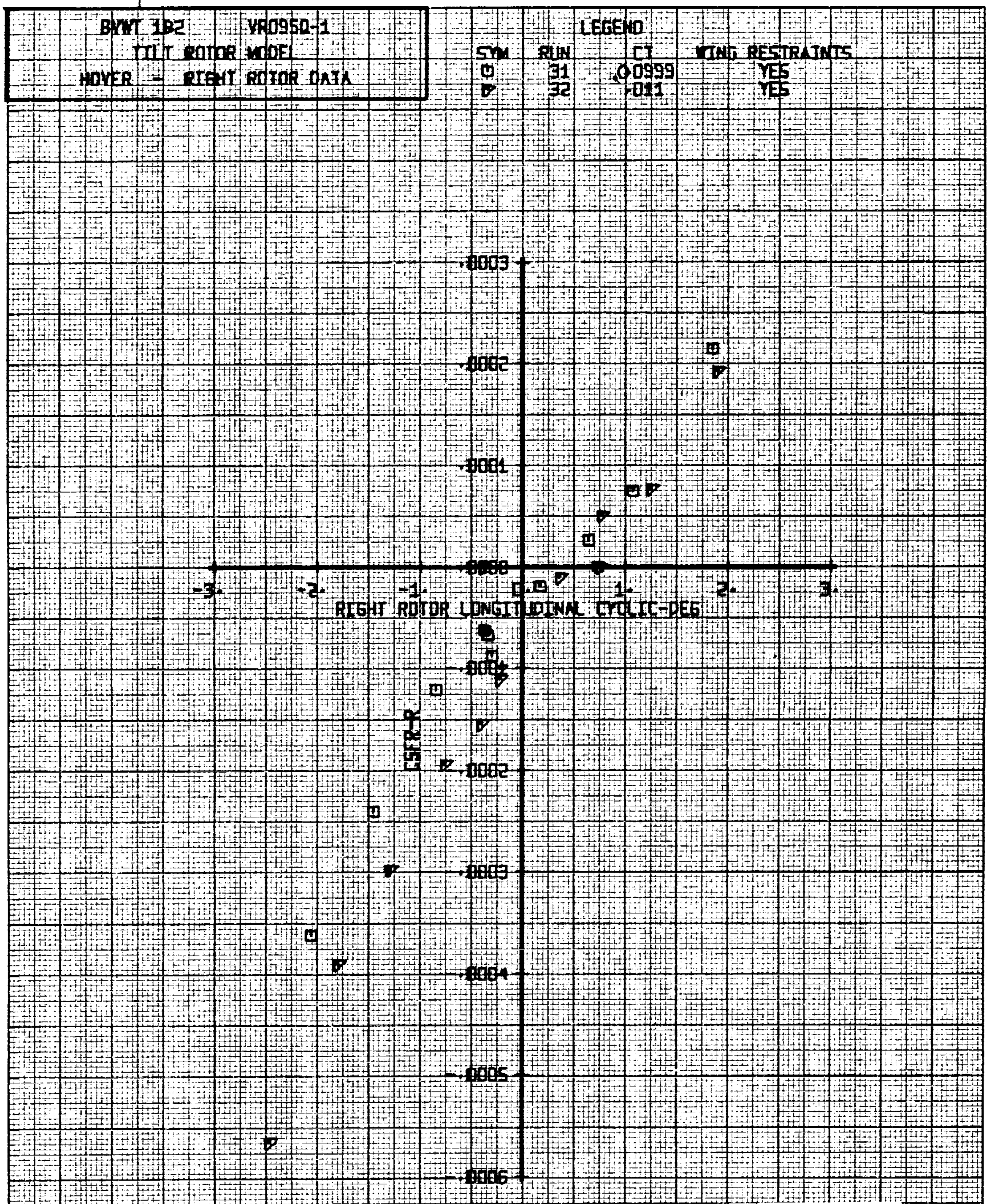

Figure 1-028. Right Rotor Side Force Coefficient Versus Longitudinal Cyclic Pitch. $I_N = 90°$ Hover.

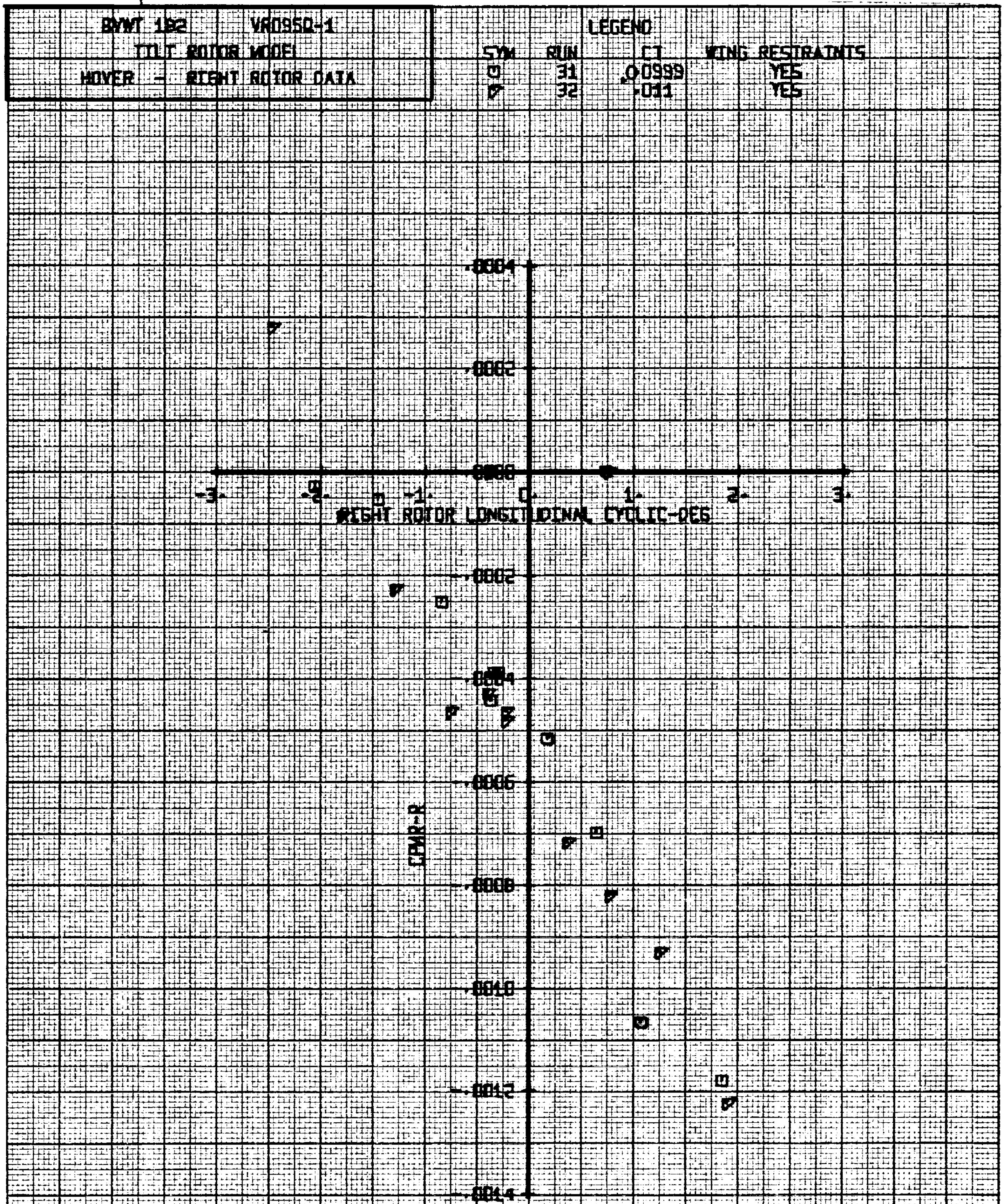

Figure 1-029. Right Rotor Pitching Moment Coefficient Versus Longitudinal Cyclic Pitch. I_N = 90° Hover.

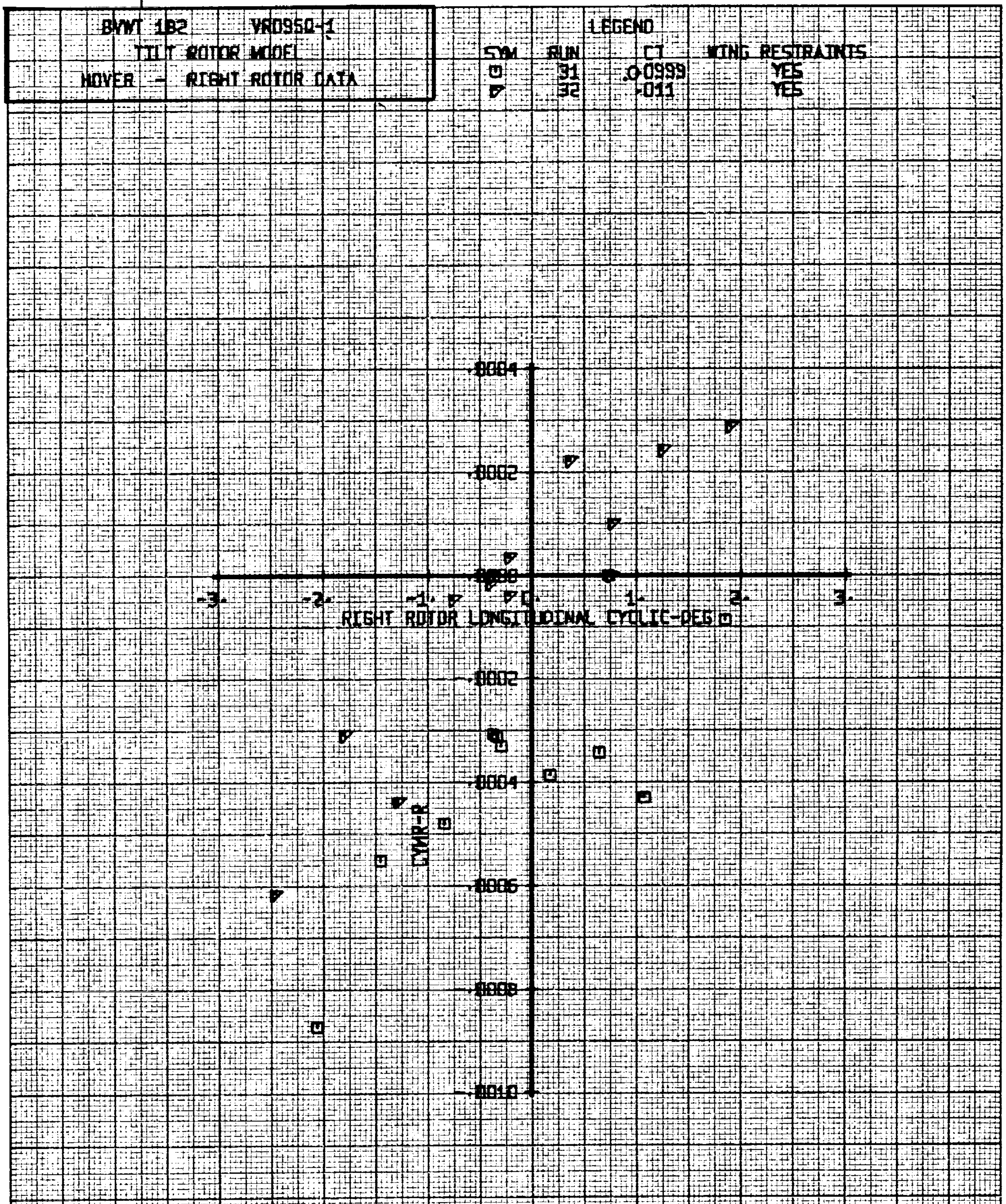

Figure 1-030. Right Rotor Yaw Moment Coefficient Versus Longitudinal Cyclic Pitch. I_N = 90° Hover.

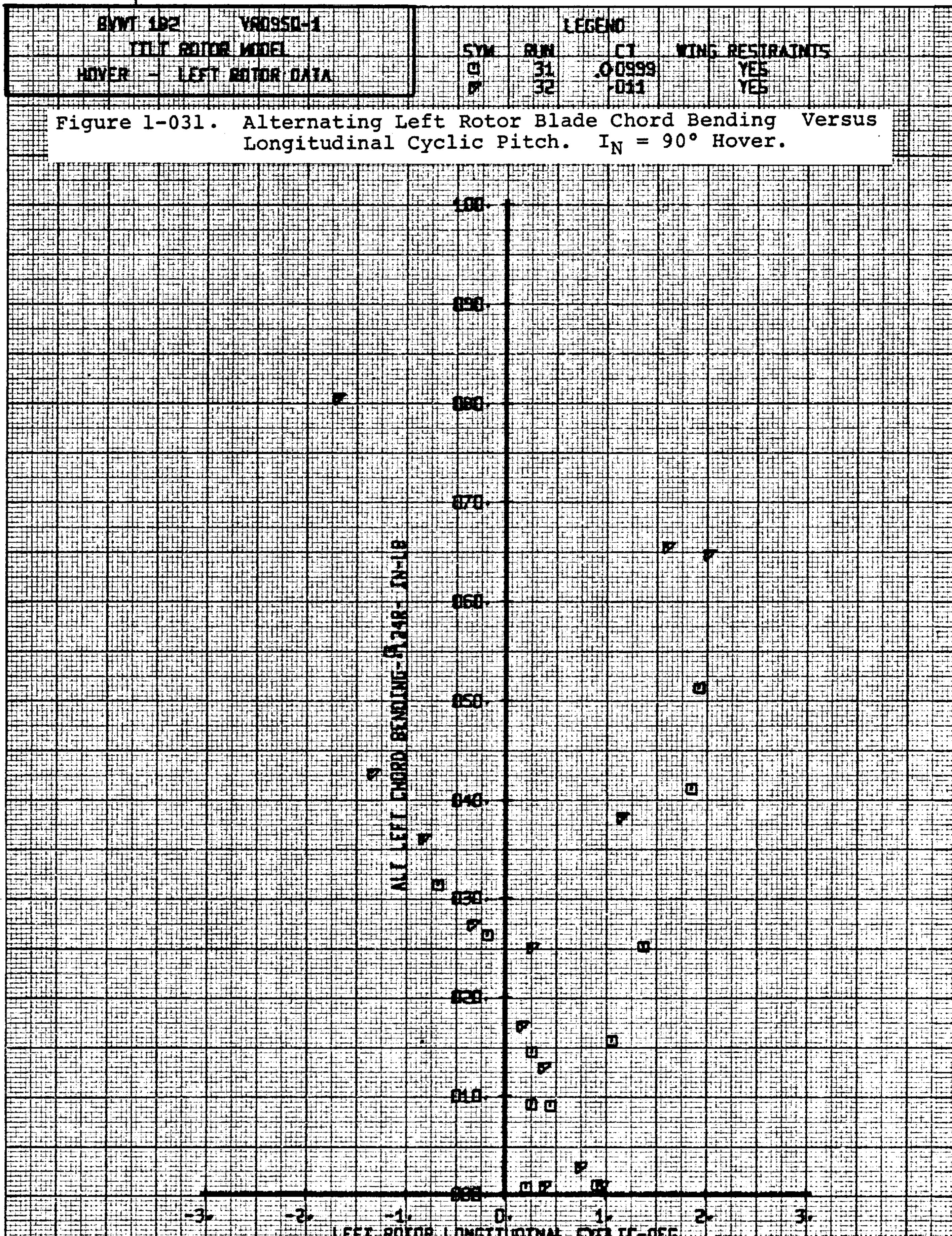

Figure 1-031. Alternating Left Rotor Blade Chord Bending Versus Longitudinal Cyclic Pitch. $I_N = 90°$ Hover.

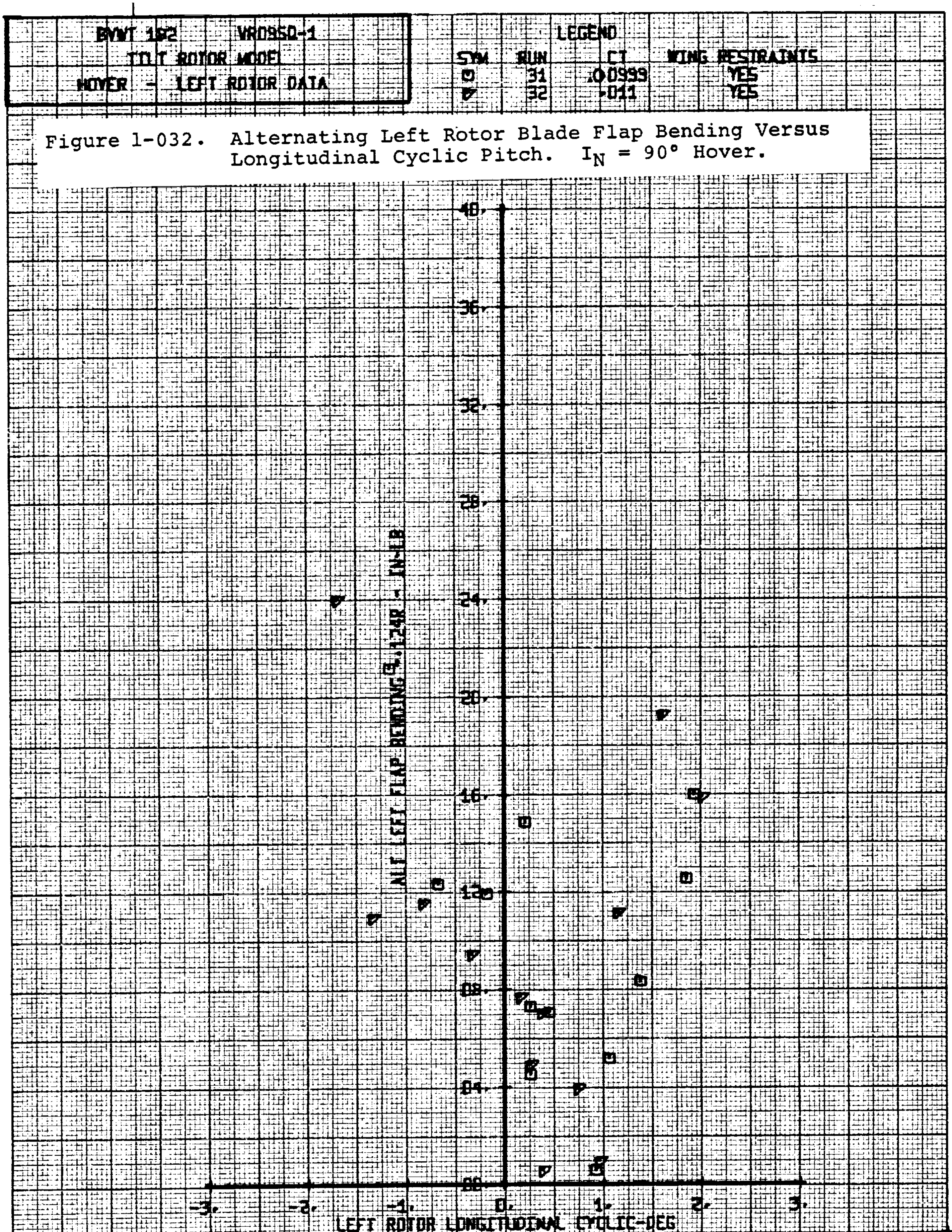

Figure 1-032. Alternating Left Rotor Blade Flap Bending Versus Longitudinal Cyclic Pitch. I_N = 90° Hover.

119
182

SET 119
BVWT 182

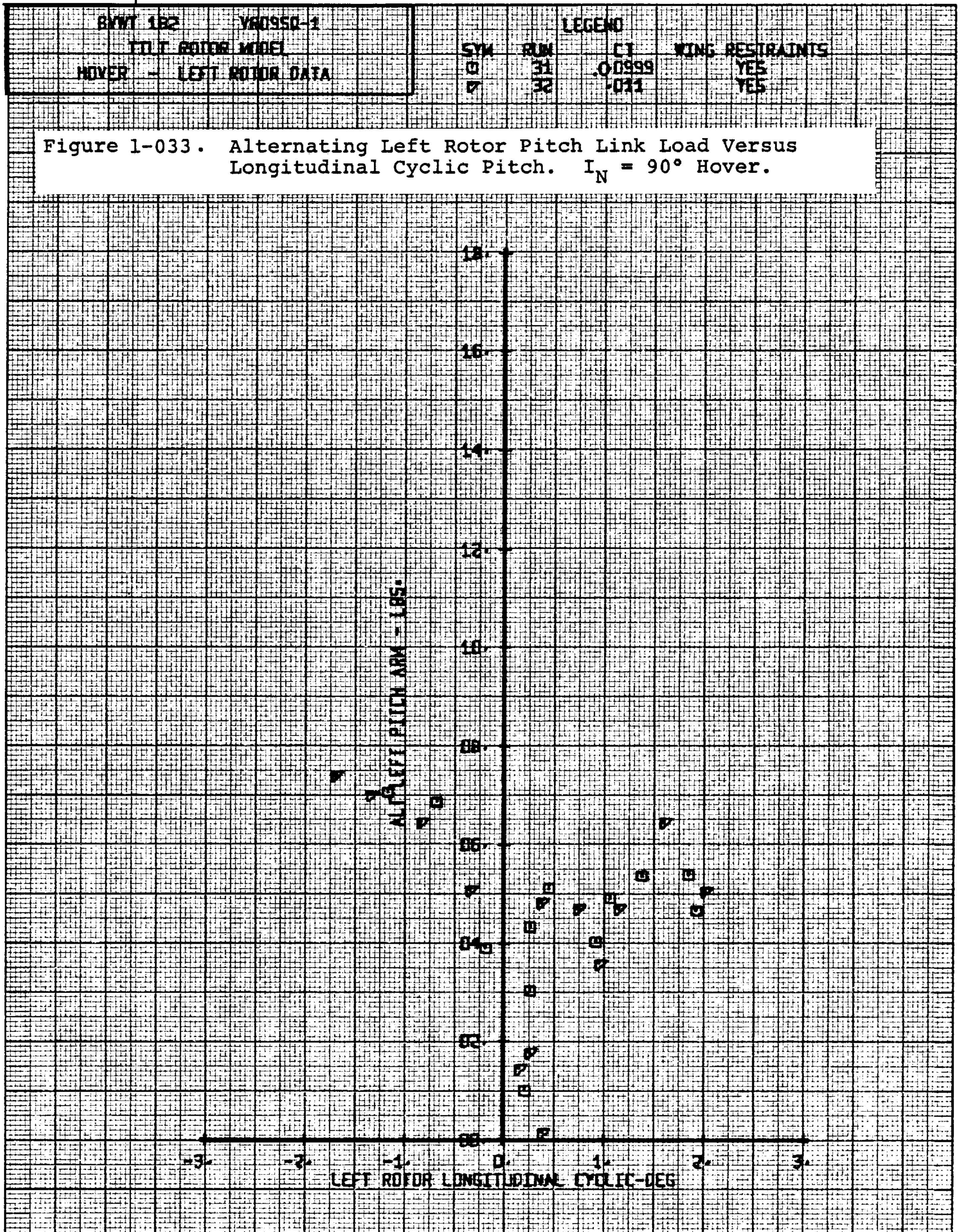

Figure 1-033. Alternating Left Rotor Pitch Link Load Versus Longitudinal Cyclic Pitch. I_N = 90° Hover.

Figure 1-034. Alternating Right Rotor Blade Chord Bending Versus Longitudinal Cyclic Pitch. I_N = 90° Hover.

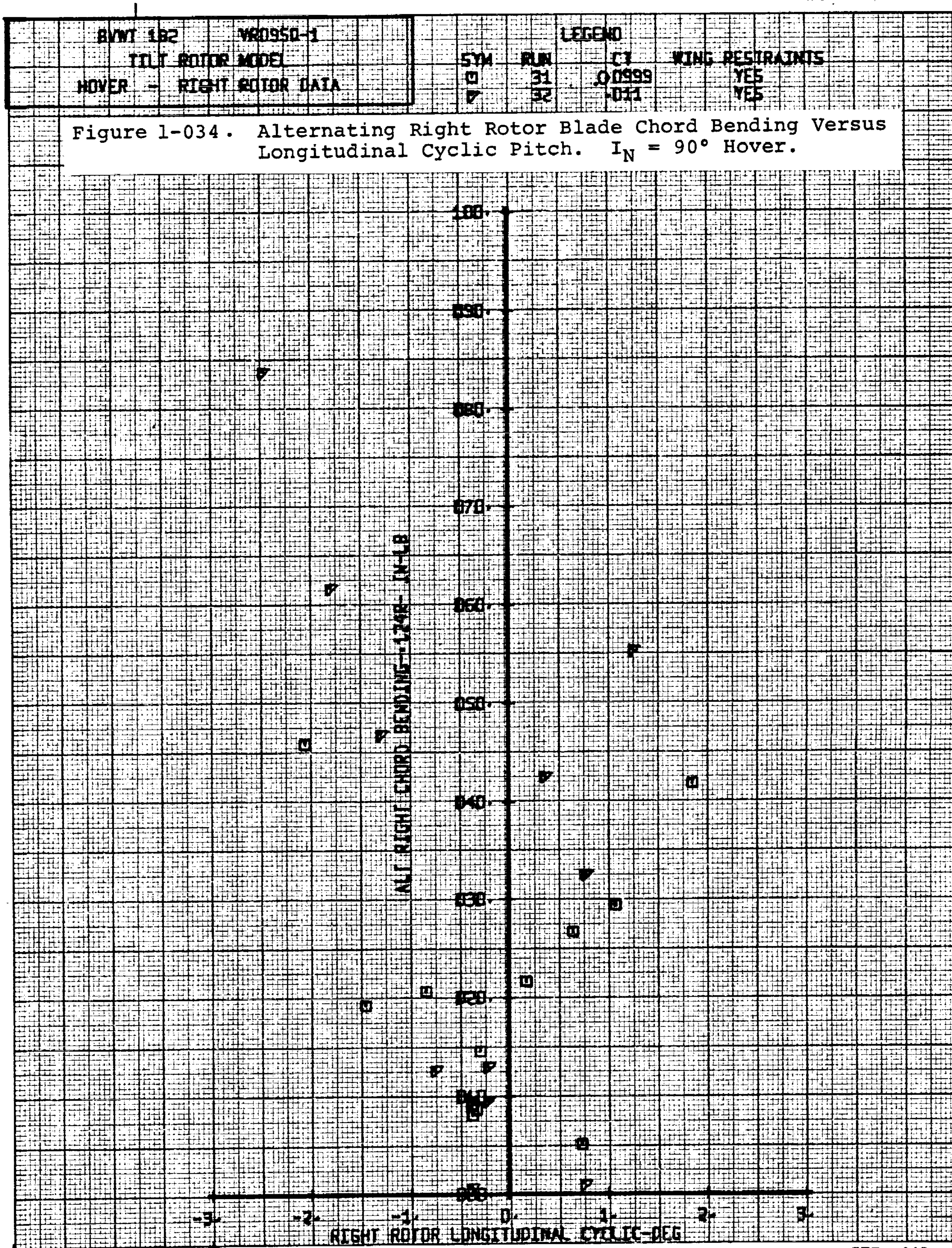

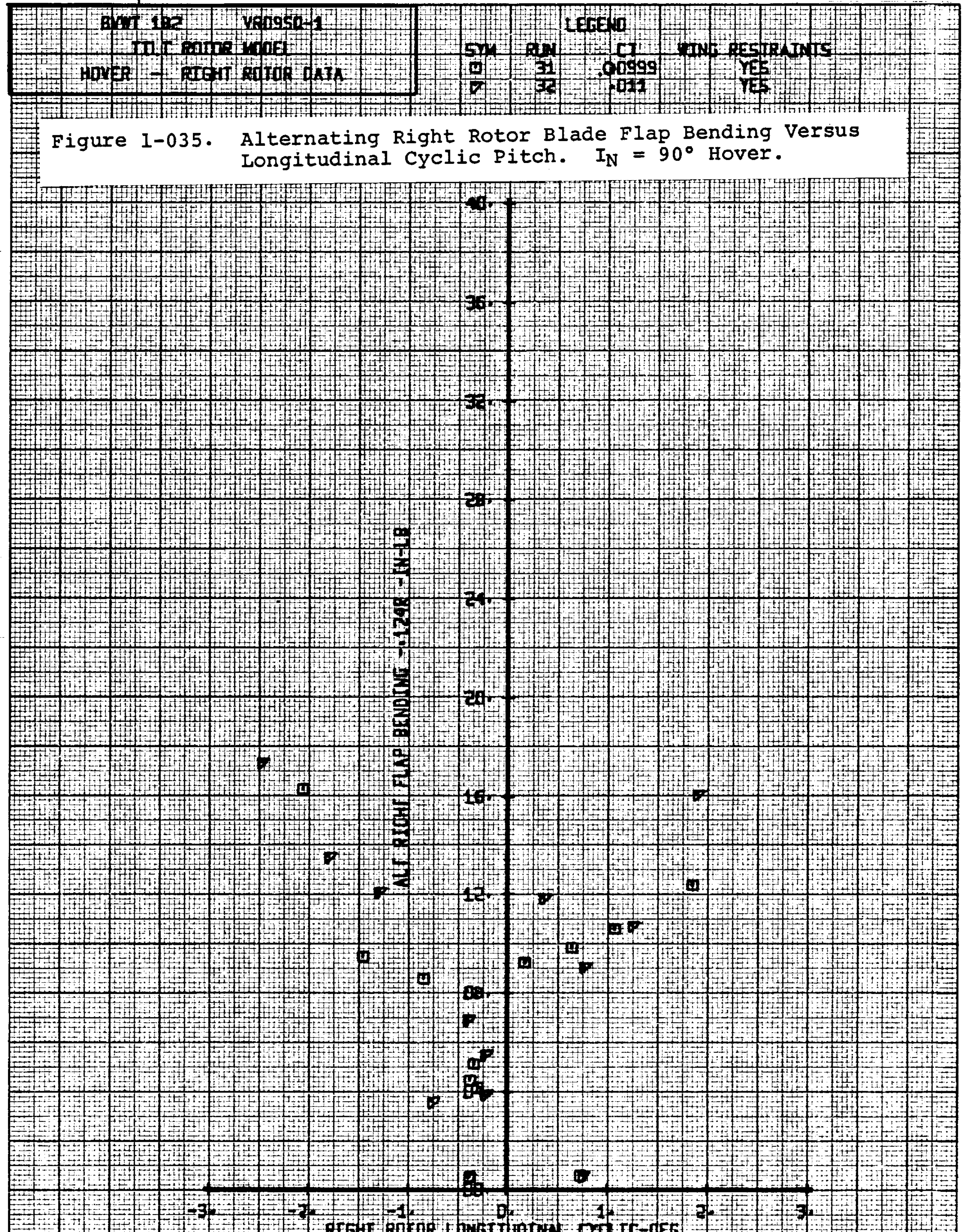

Figure 1-035. Alternating Right Rotor Blade Flap Bending Versus Longitudinal Cyclic Pitch. I_N = 90° Hover.

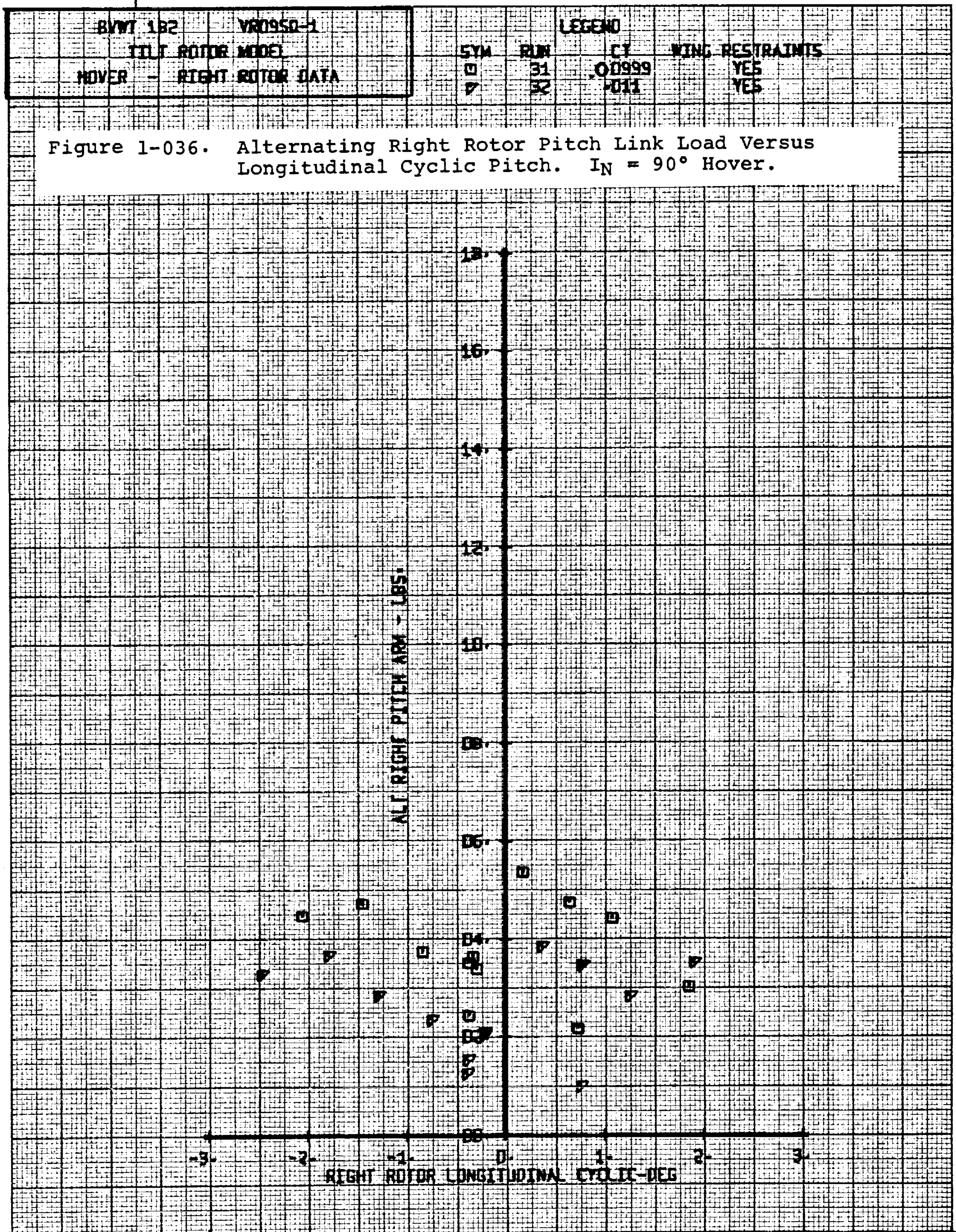

Figure 1-036. Alternating Right Rotor Pitch Link Load Versus Longitudinal Cyclic Pitch. $I_N = 90°$ Hover.

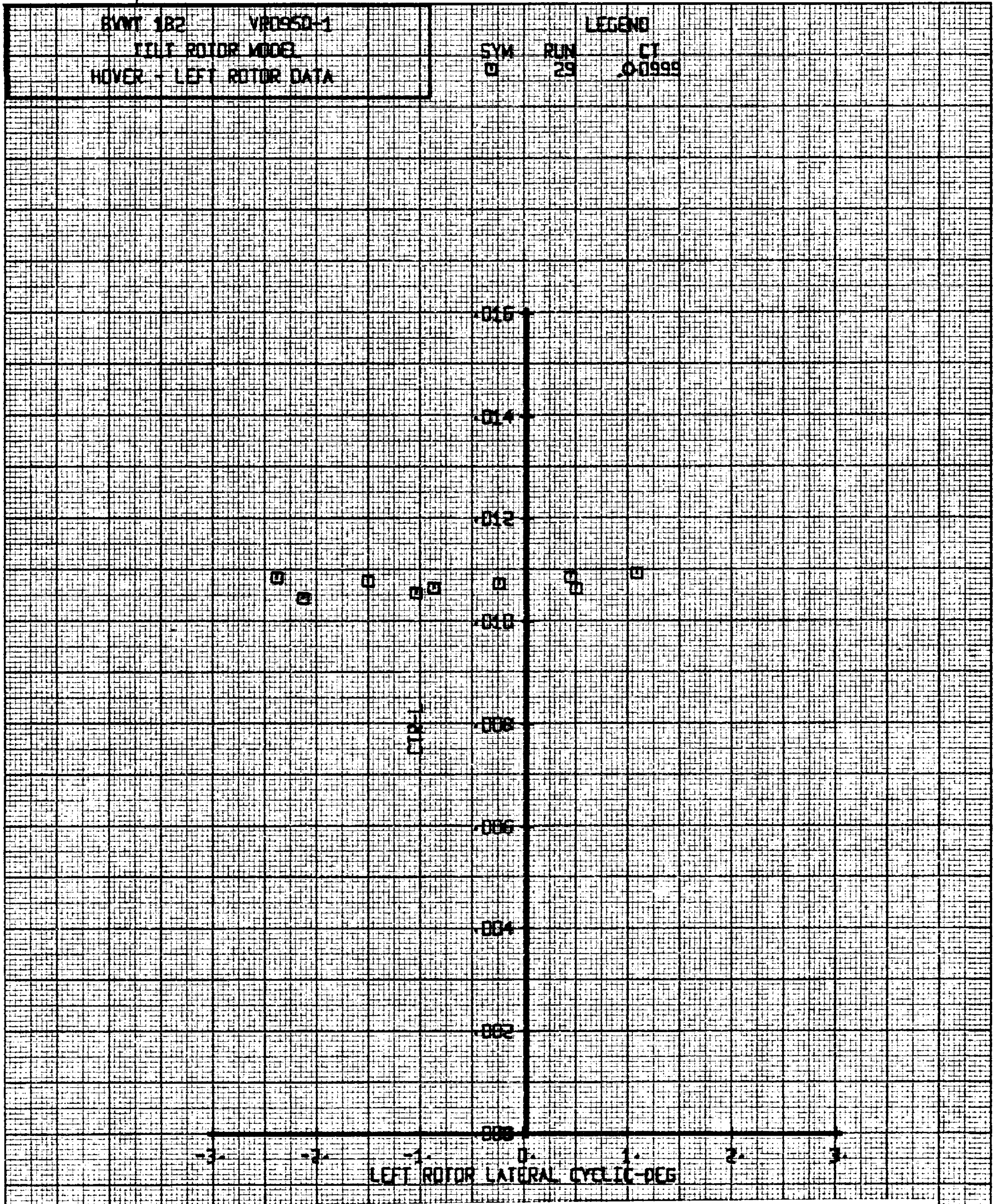

Figure 1-037. Left Rotor Thrust Coefficient Versus Lateral Cyclic Pitch. I_N = 90° Hover.

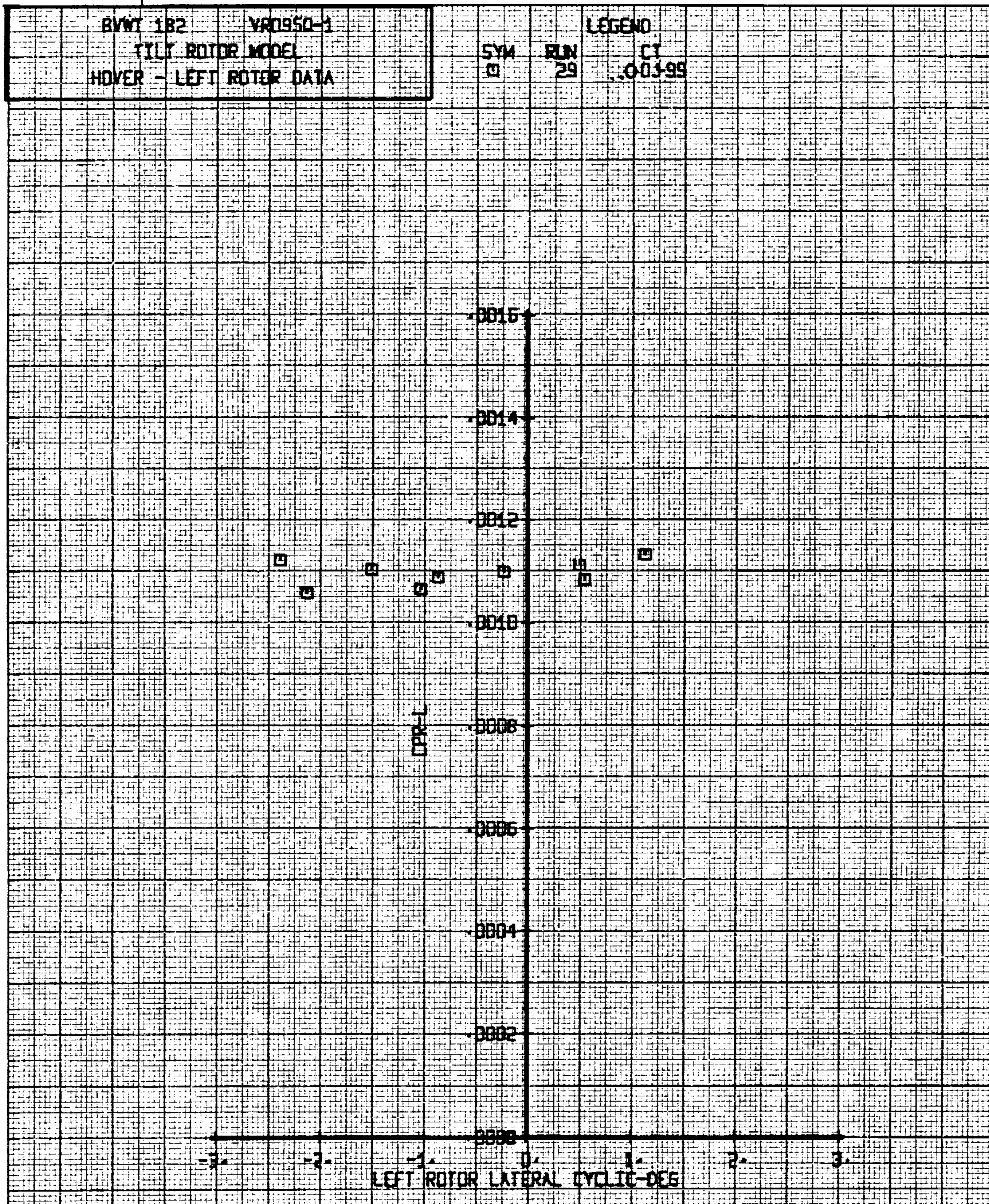

Figure 1-038. Left Rotor Power Coefficient Versus Lateral Cyclic Pitch. I_N = 90° Hover.

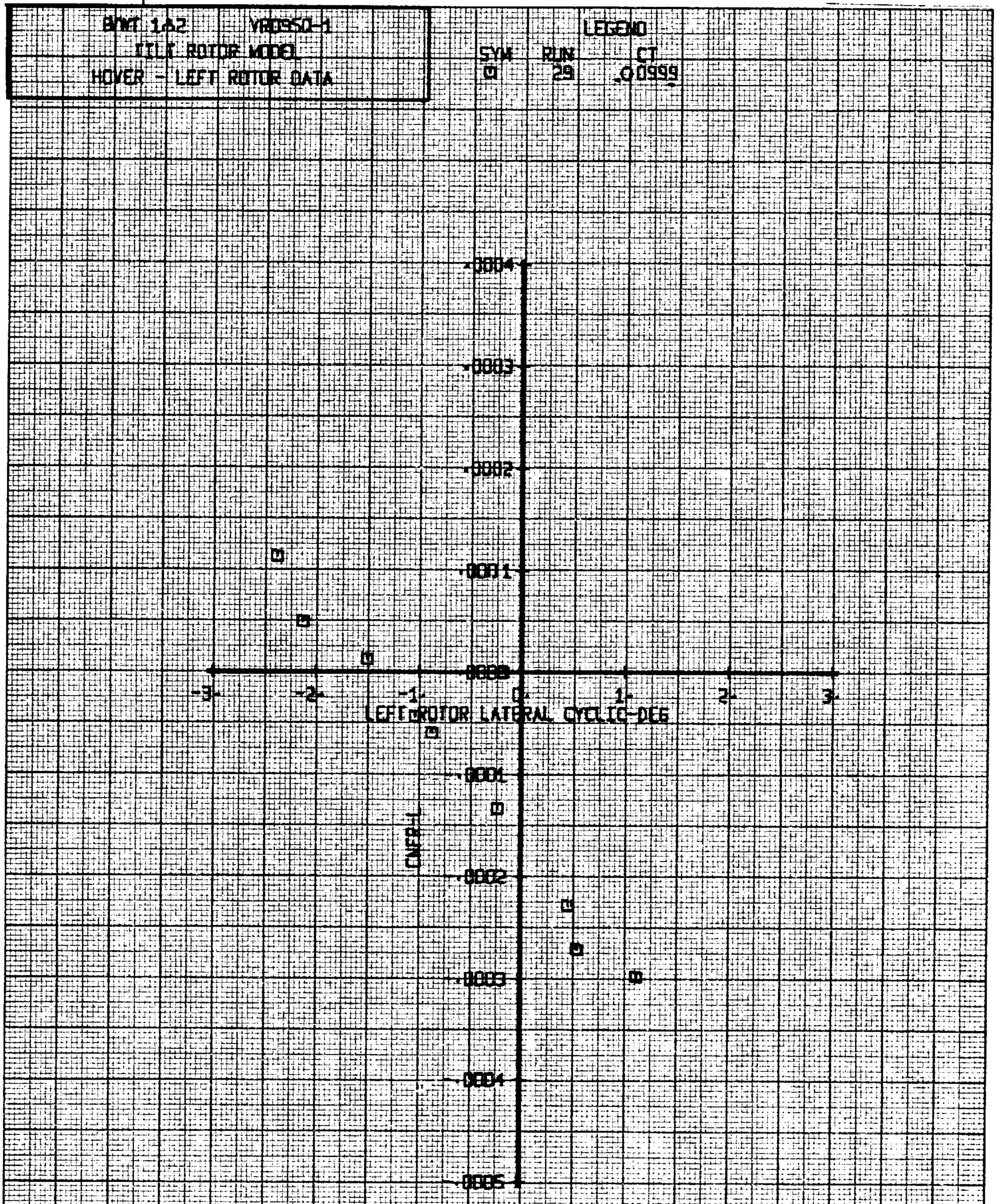

Figure 1-039. Left Rotor Normal Force Coefficient Versus Lateral Cyclic Pitch. I_N = 90° Hover.

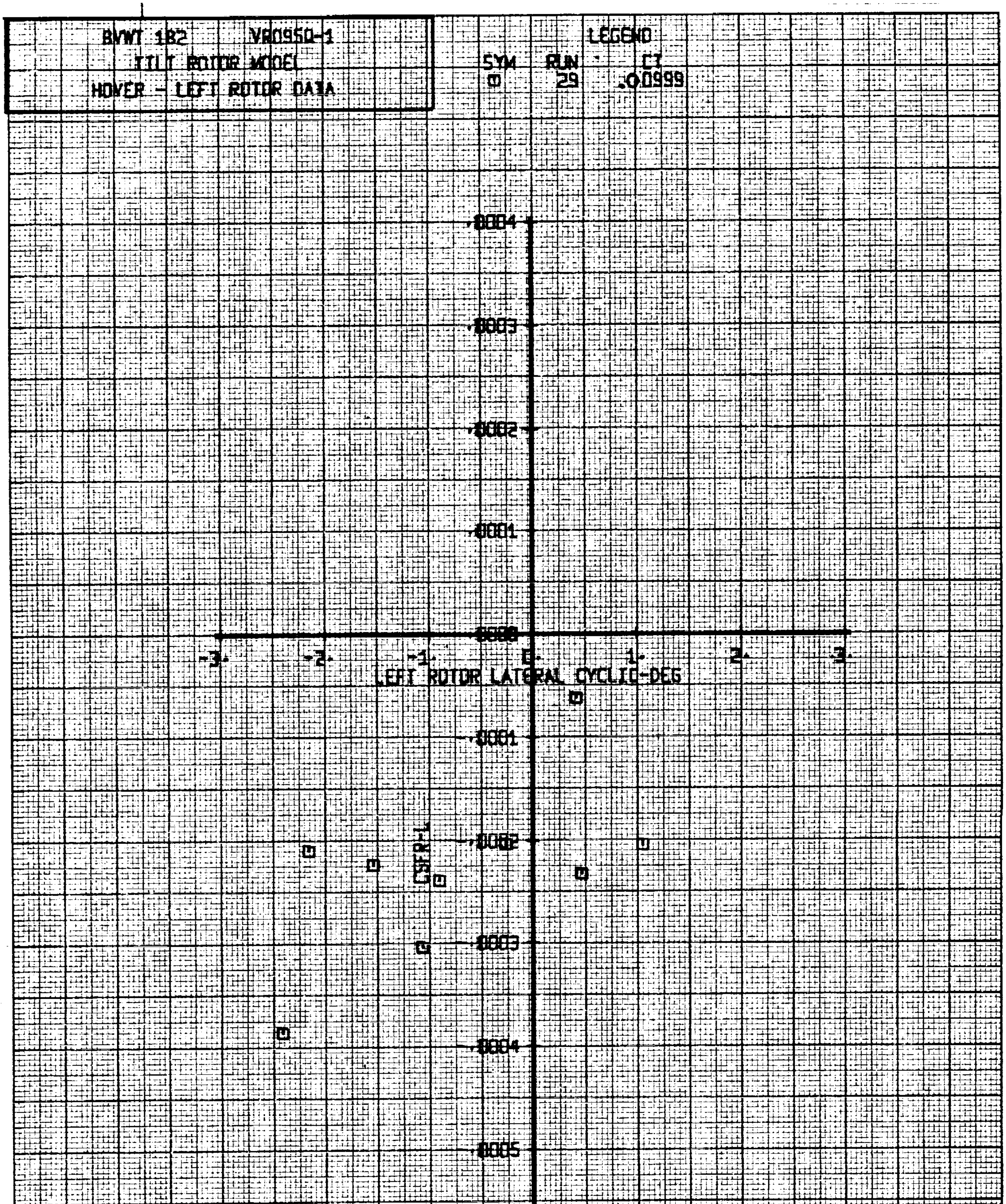

Figure 1-040. Left Rotor Side Force Coefficient Versus Lateral Cyclic Pitch. I_N = 90° Hover.

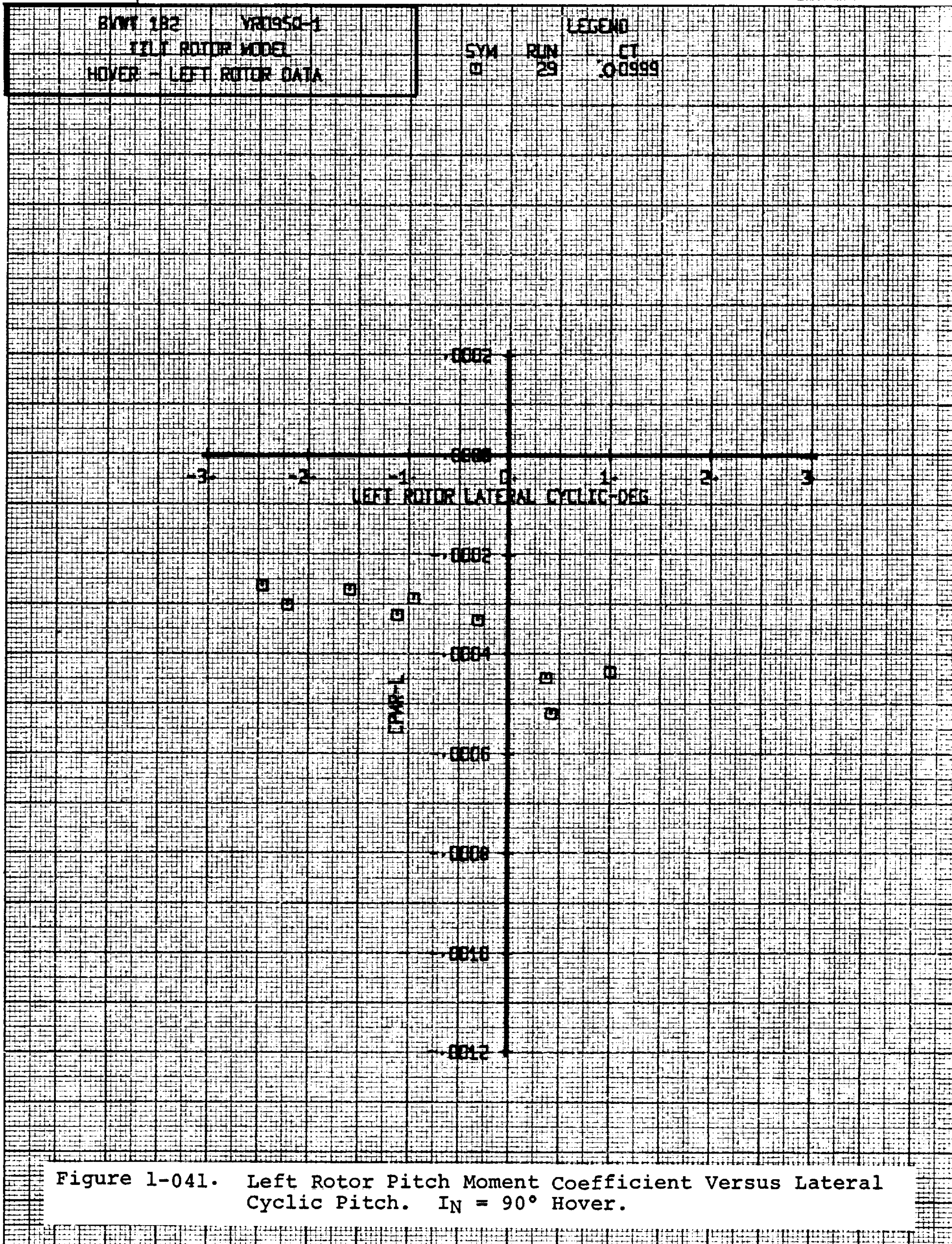

Figure 1-041. Left Rotor Pitch Moment Coefficient Versus Lateral Cyclic Pitch. $I_N = 90°$ Hover.

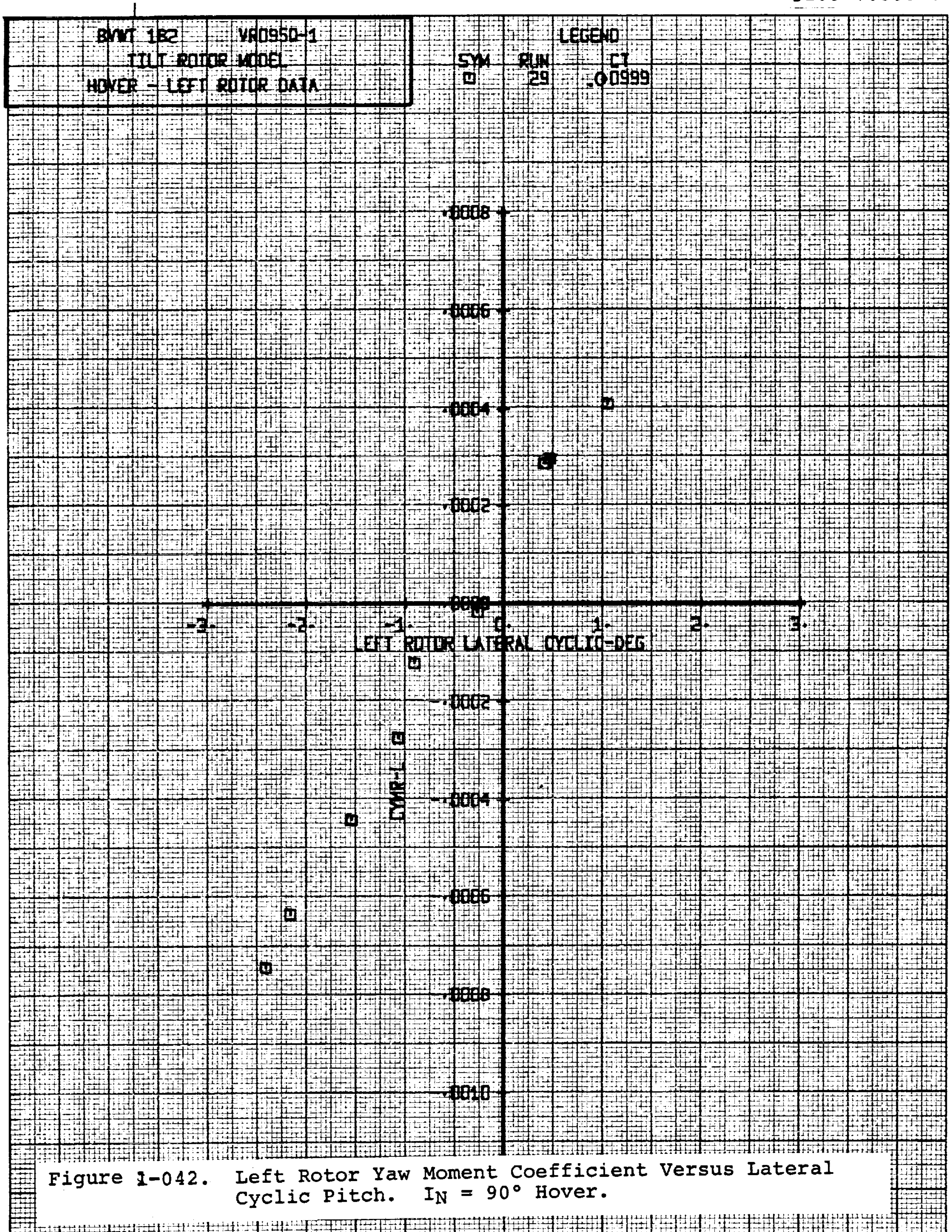

Figure 1-042. Left Rotor Yaw Moment Coefficient Versus Lateral Cyclic Pitch. $I_N = 90°$ Hover.

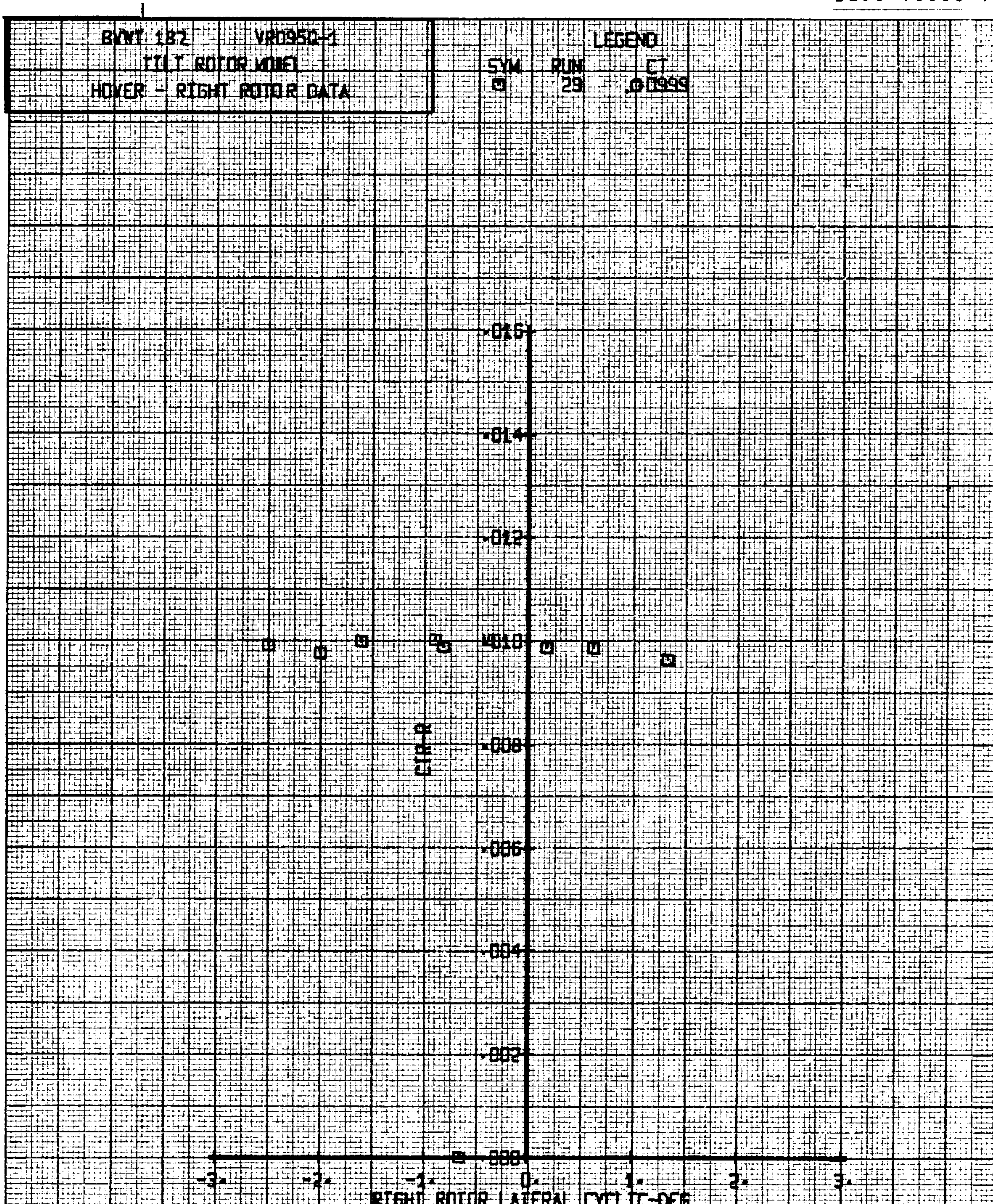

Figure 1-043. Right Rotor Thrust Coefficient Versus Lateral Cyclic Pitch. $I_N = 90°$ Hover.

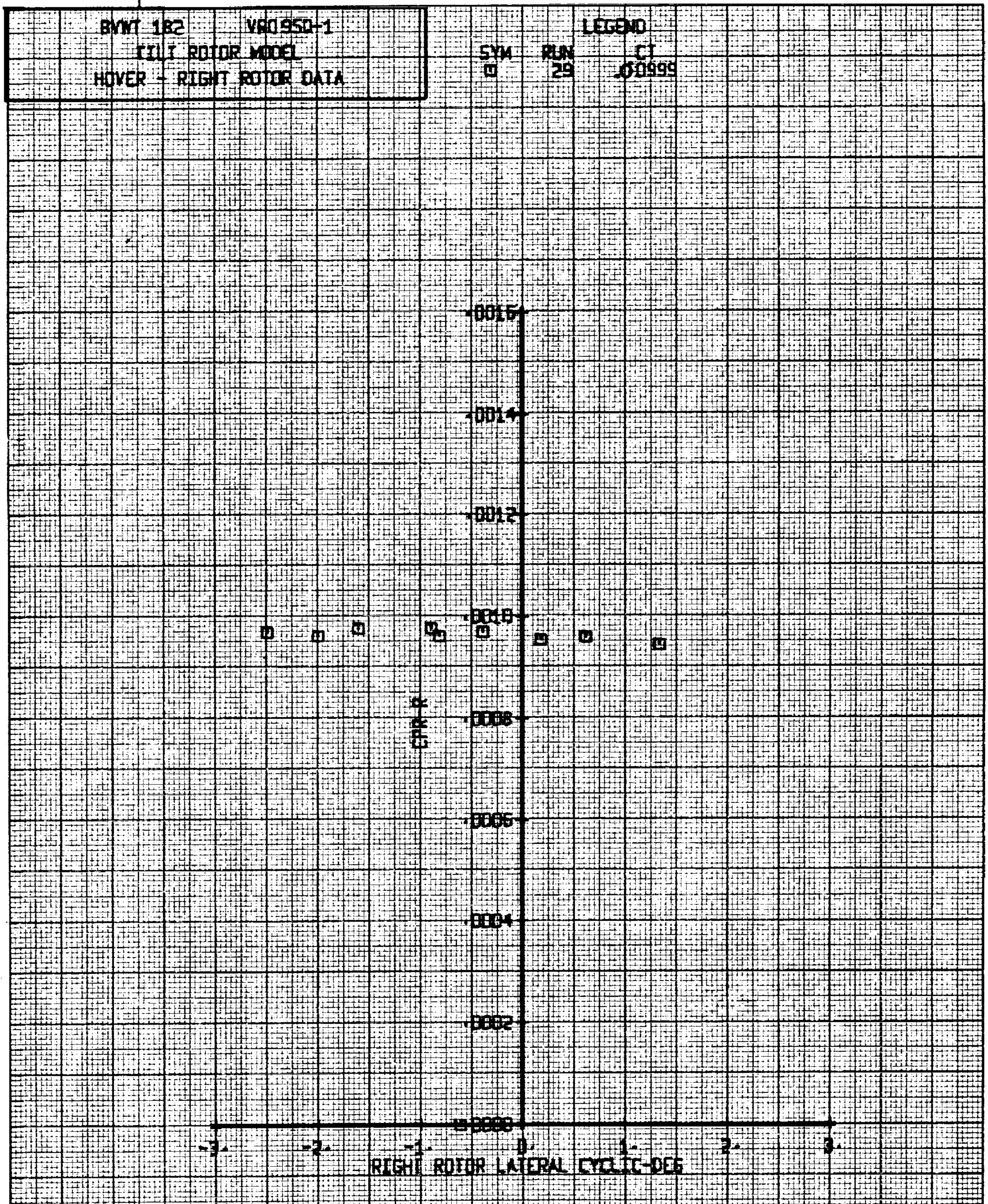

Figure 1-044. Right Rotor Power Coefficient Versus Lateral Cyclic Pitch. I_N = 90° Hover.

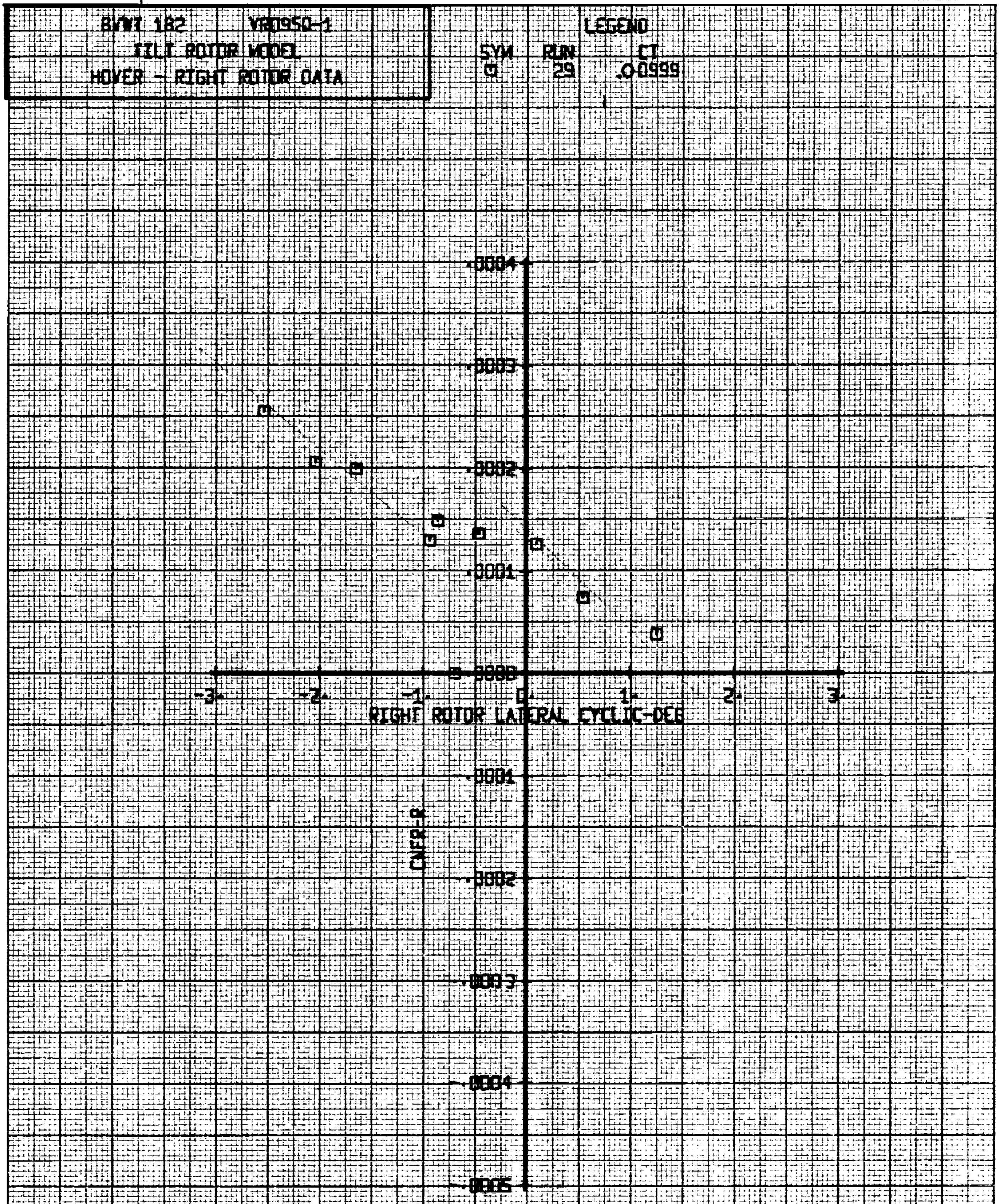

Figure 1-045. Right Rotor Normal Force Coefficient Versus Lateral Cyclic Pitch. I_N = 90° Hover.

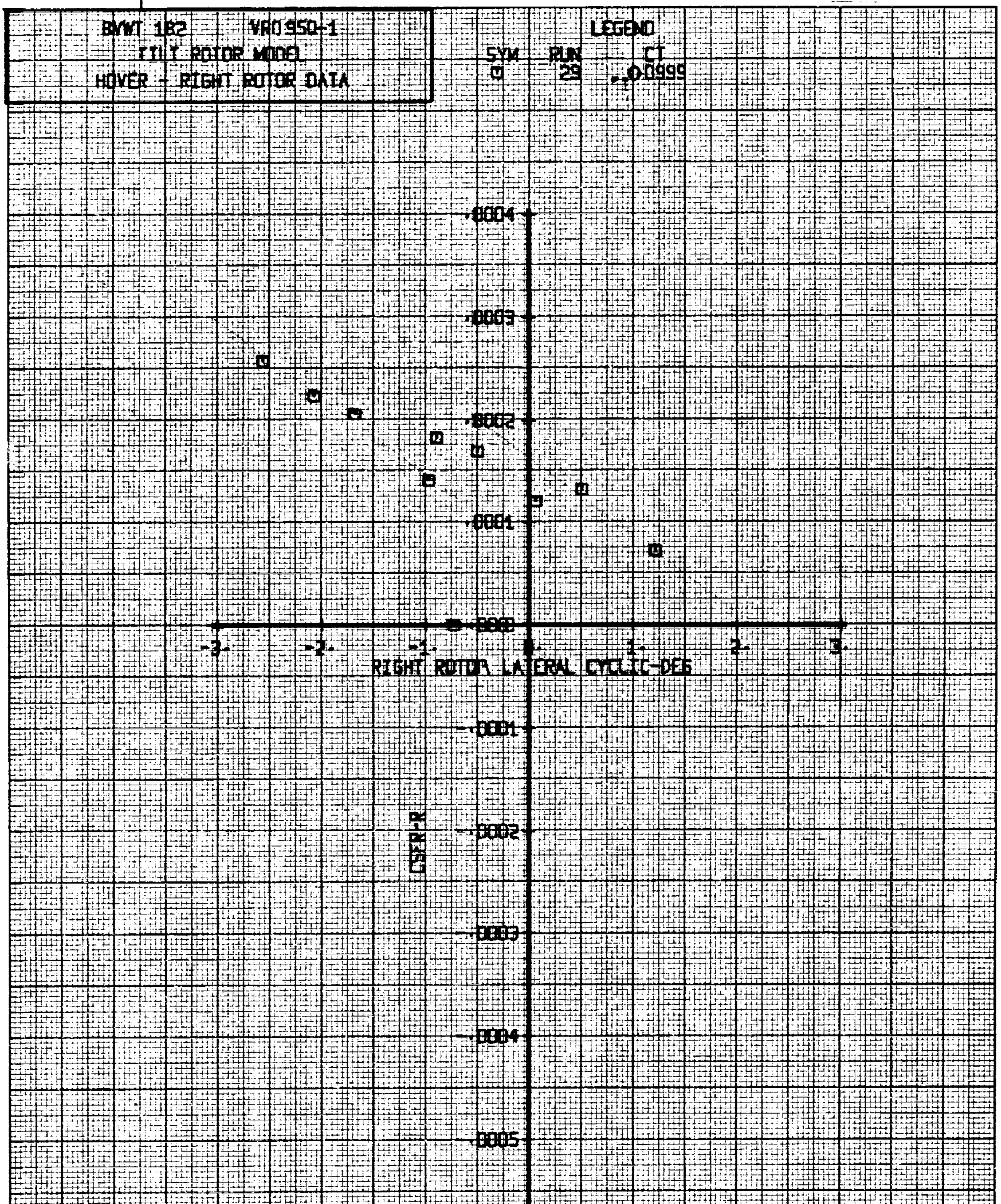

Figure 1-046. Right Rotor Side Force Coefficient Versus Lateral Cyclic Pitch. I_N = 90° Hover.

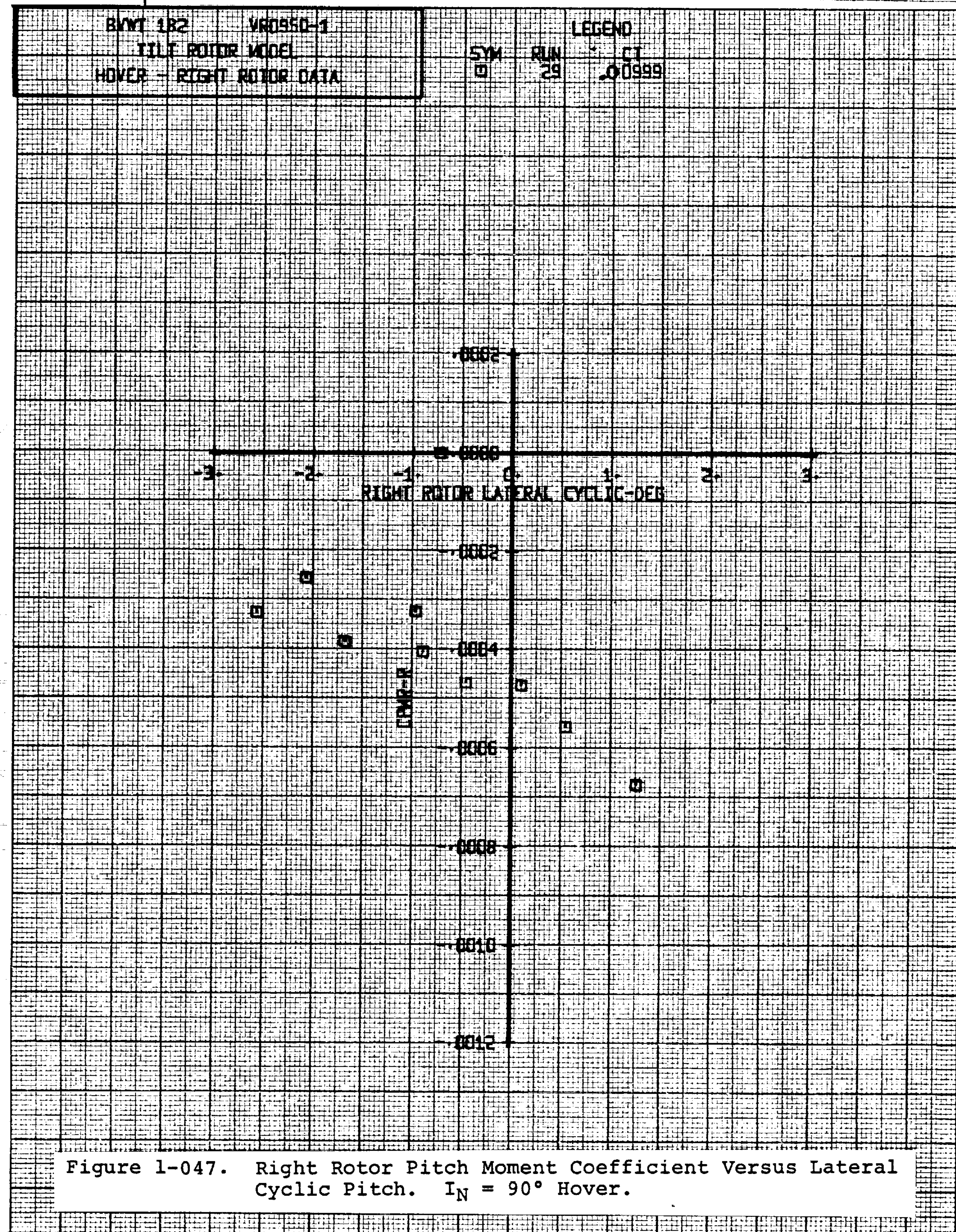

Figure 1-047. Right Rotor Pitch Moment Coefficient Versus Lateral Cyclic Pitch. I_N = 90° Hover.

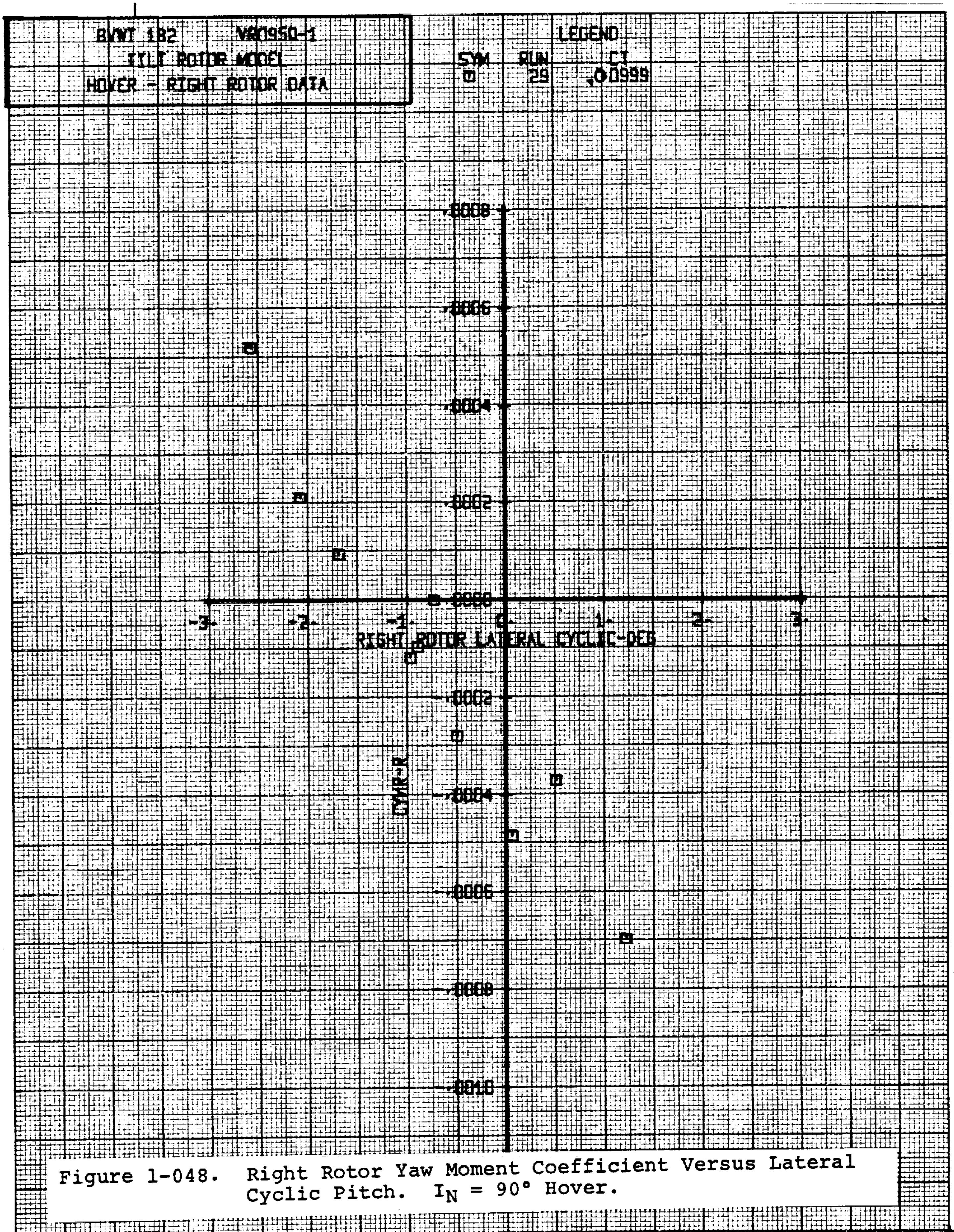

Figure 1-048. Right Rotor Yaw Moment Coefficient Versus Lateral Cyclic Pitch. I_N = 90° Hover.

Figure 1-049. Alternating Left Rotor Blade Chord Bending Moment Versus Lateral Cyclic Pitch. I_N = 90° Hover.

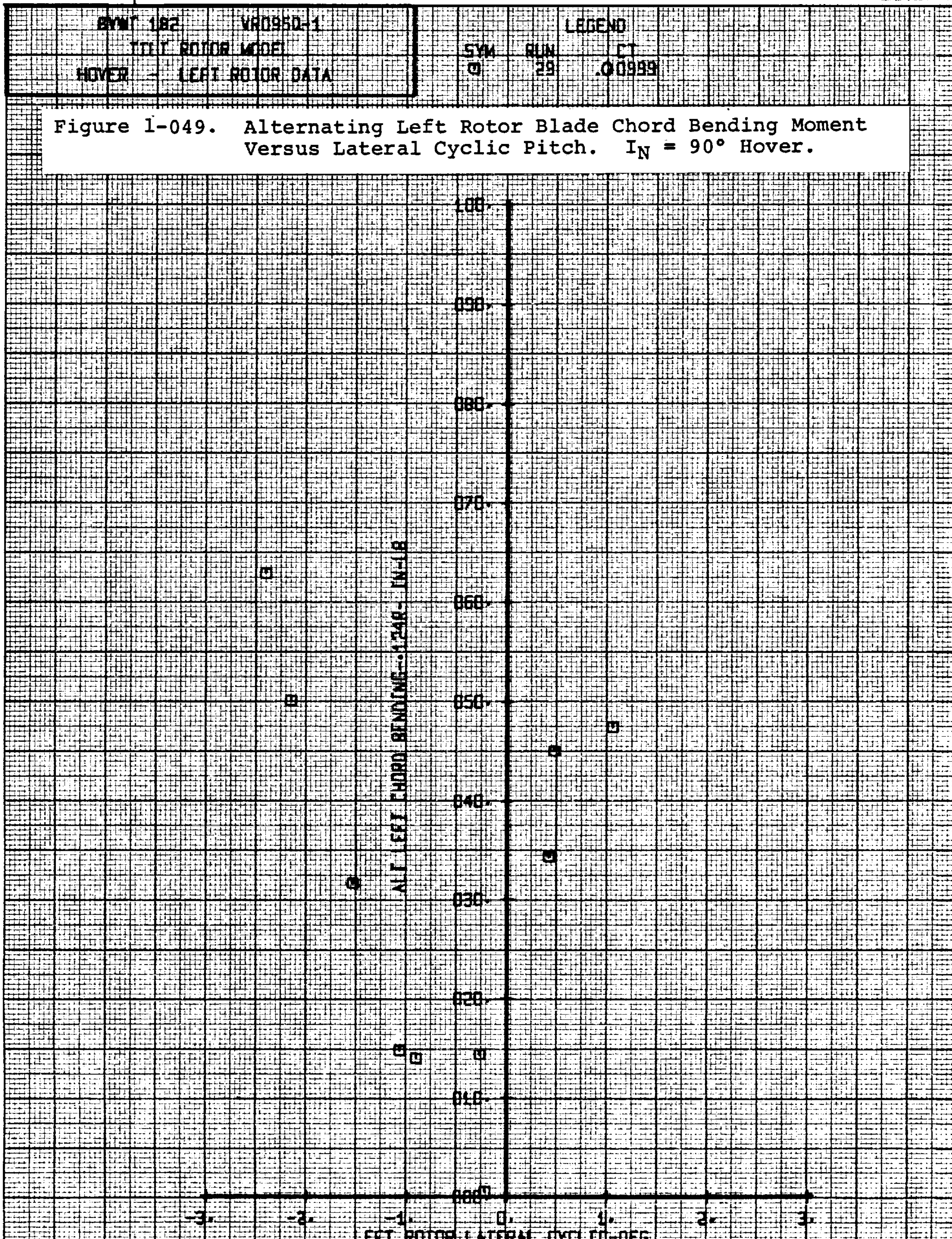

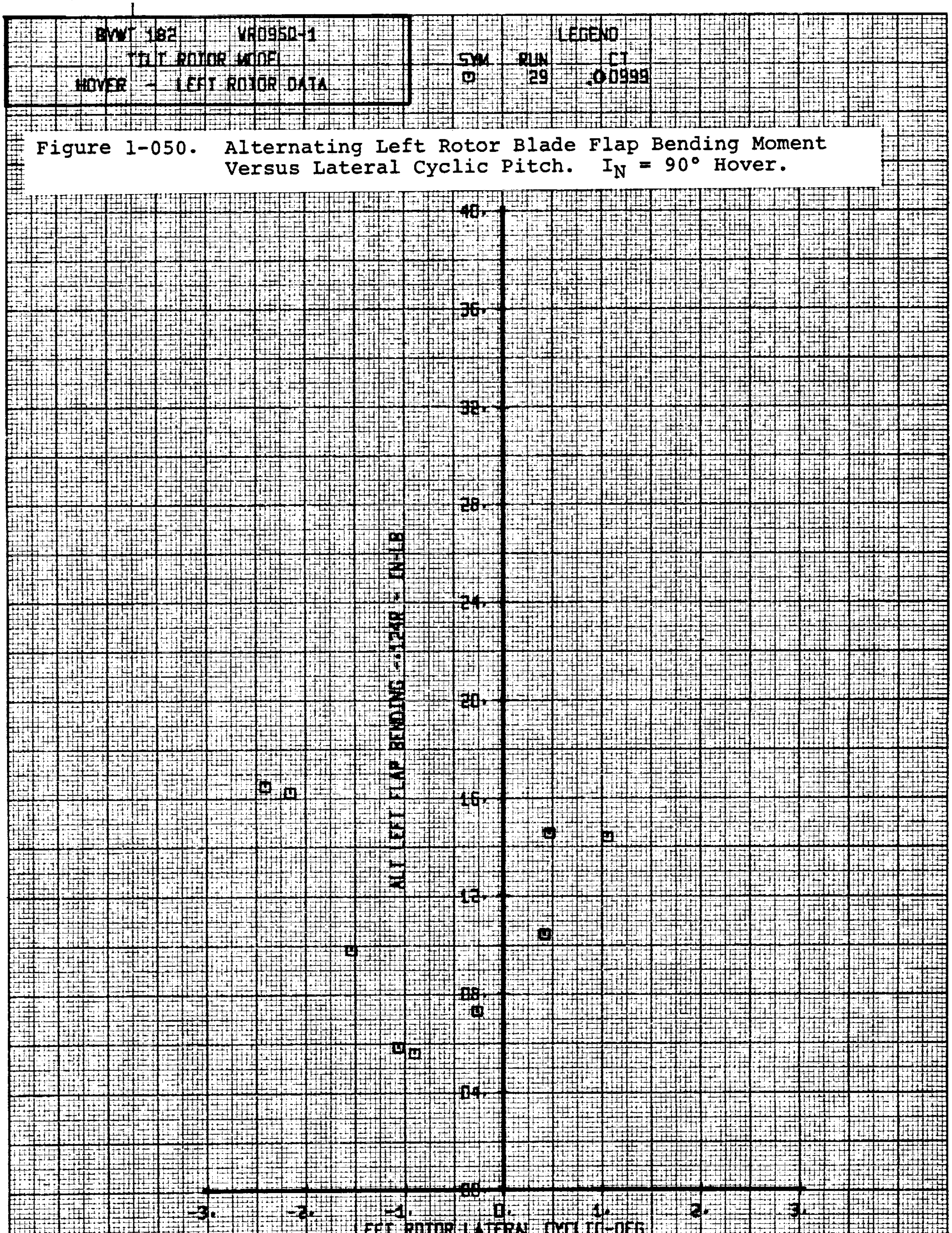

Figure 1-050. Alternating Left Rotor Blade Flap Bending Moment Versus Lateral Cyclic Pitch. I_N = 90° Hover.

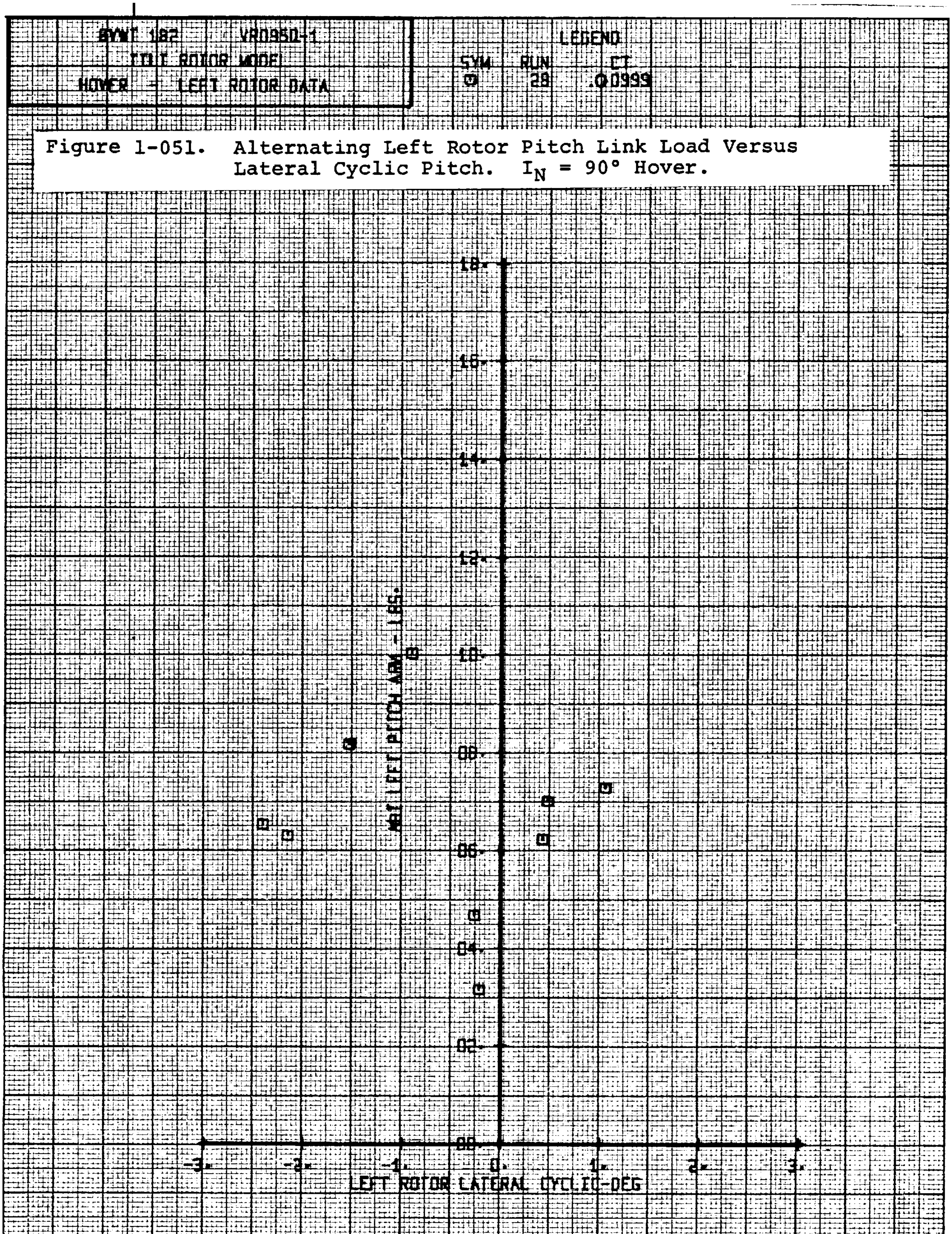

BVWT 182 VR0950-1
TILT ROTOR MODEL
HOVER - LEFT ROTOR DATA
LEGEND
SYM RUN CT
28 .00999
Figure 1-051. Alternating Left Rotor Pitch Link Load Versus Lateral Cyclic Pitch. I_N = 90° Hover.
ALT LEFT PITCH ARM - LBS.
18.
16.
14.
12.
10.
08.
06.
04.
02.
00.
-3.
-2.
-1.
0.
1.
2.
3.
LEFT ROTOR LATERAL CYCLIC-DEG

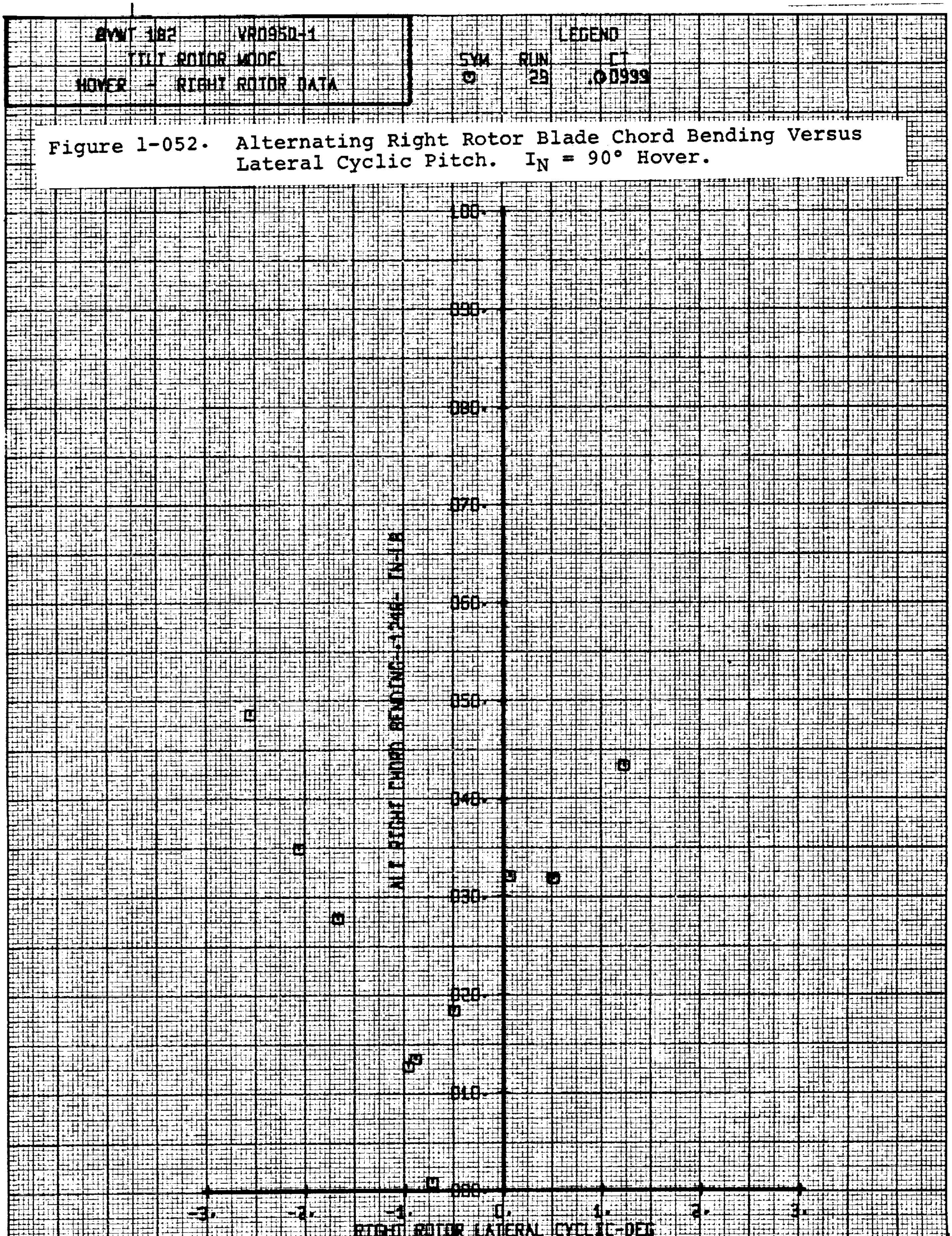

Figure 1-052. Alternating Right Rotor Blade Chord Bending Versus Lateral Cyclic Pitch. I_N = 90° Hover.

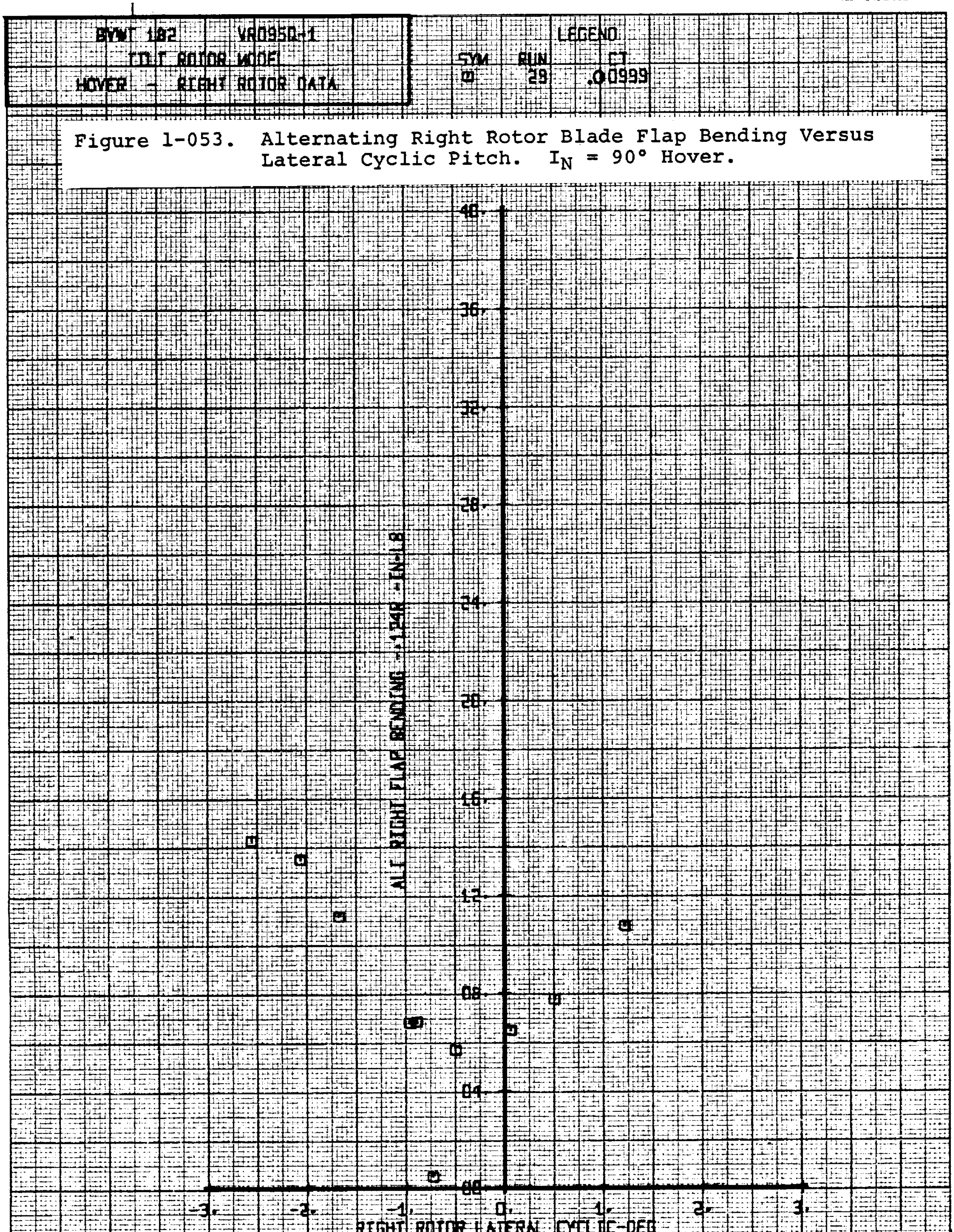

Figure 1-053. Alternating Right Rotor Blade Flap Bending Versus Lateral Cyclic Pitch. I_N = 90° Hover.

Figure 1-054. Alternating Right Rotor Pitch Link Load Versus Lateral Cyclic Pitch. $I_N = 90°$ Hover.

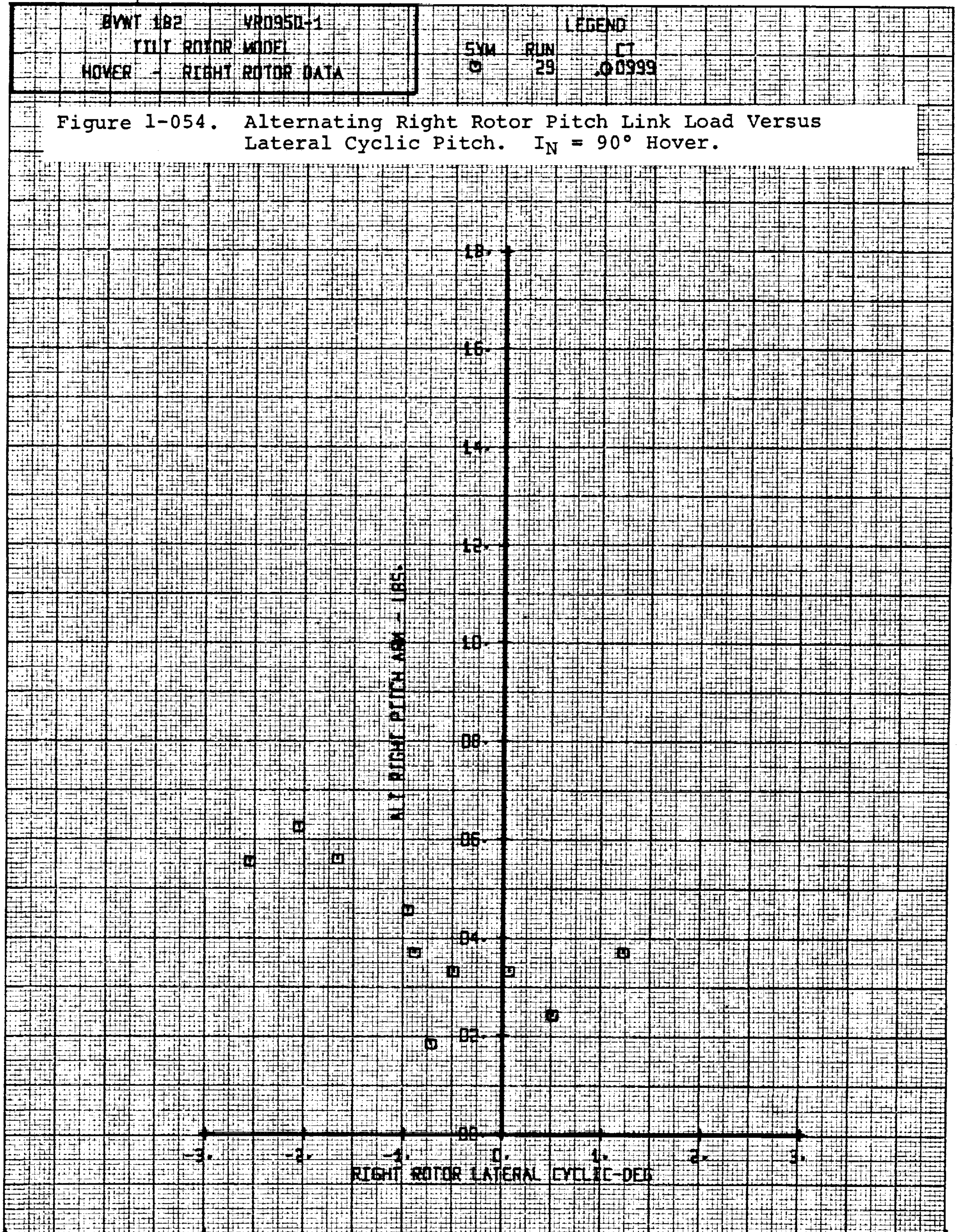

IN = 90^{o} V_{FS} - 45 KTS.

Fig. 2-001. Left Rotor Thrust Coefficient Vs. Angle of Attack.

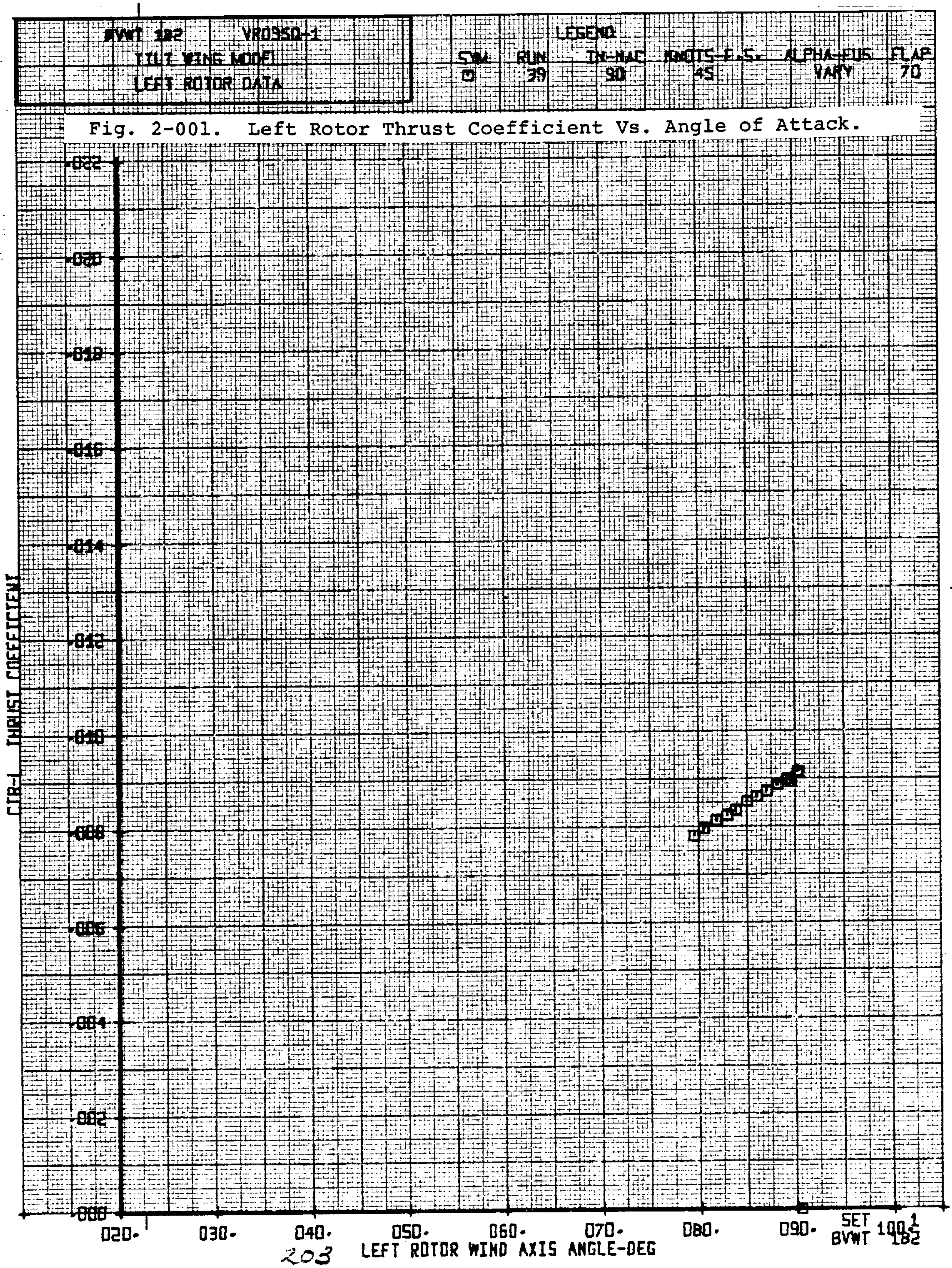

203

Fig. 2-002. Left Rotor Power Coefficient Vs. Angle of Attack.

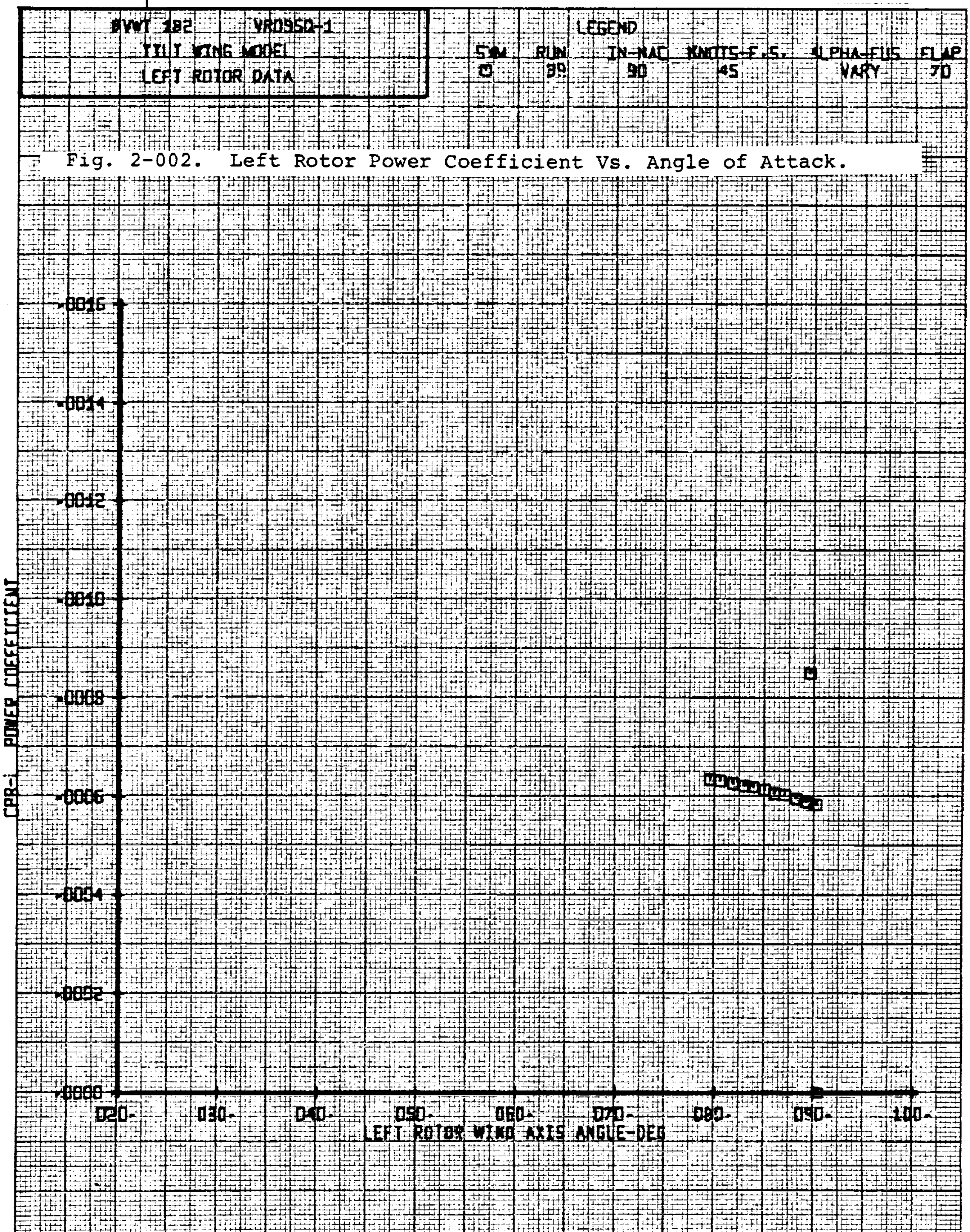

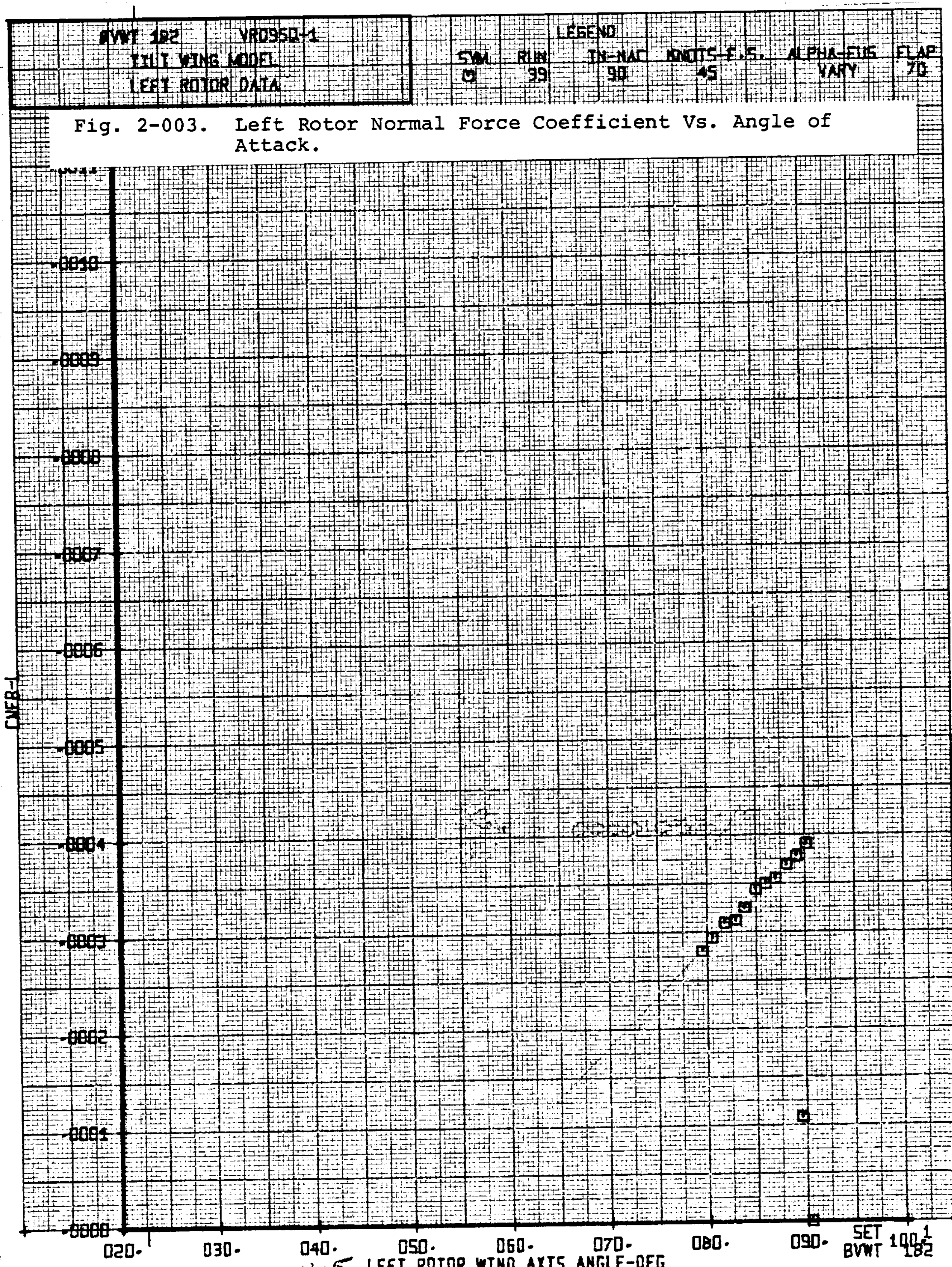

Fig. 2-003. Left Rotor Normal Force Coefficient Vs. Angle of Attack.

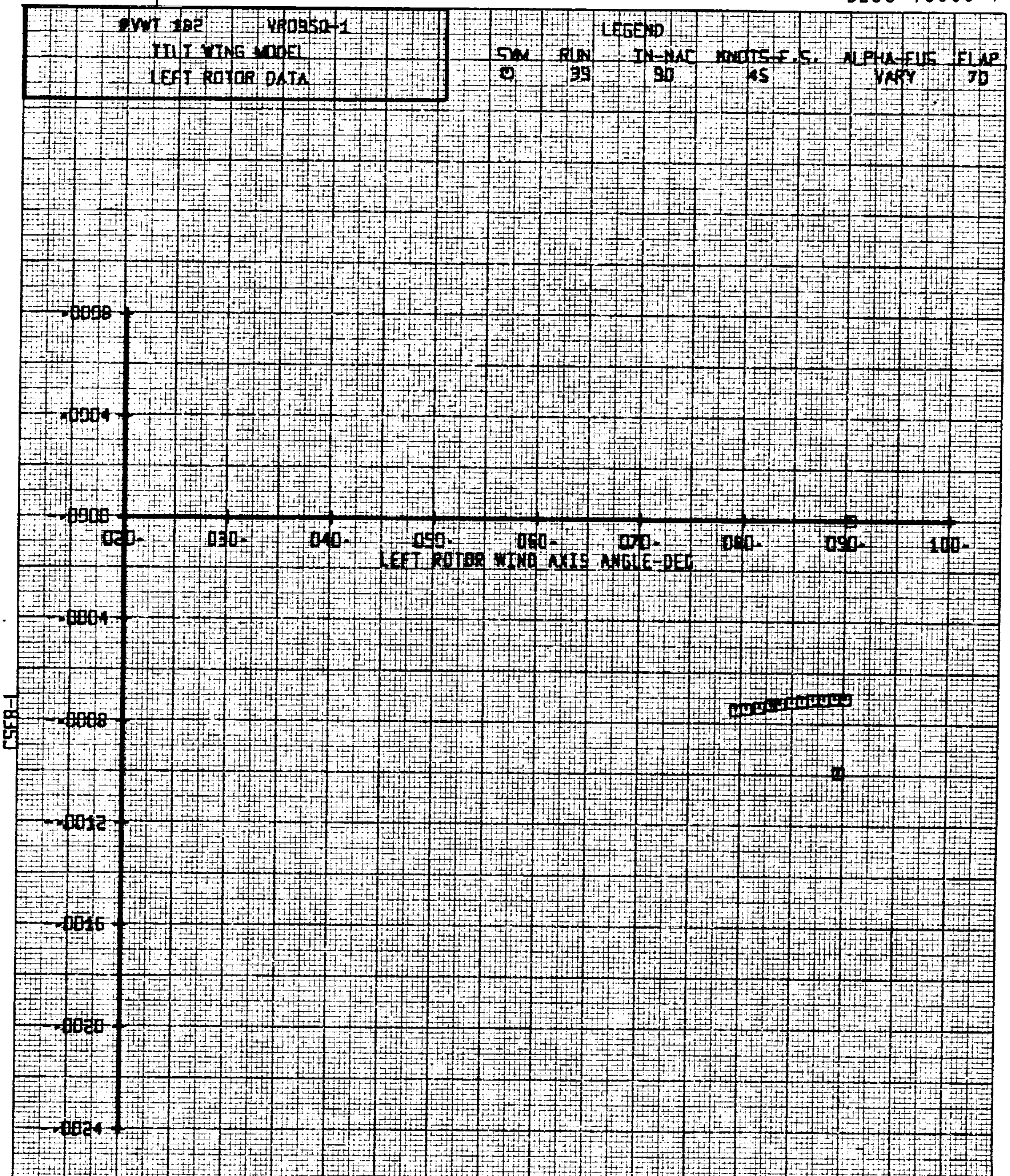

Fig. 2-004. Left Rotor Side Force Coefficient Vs. Angle of Attack.

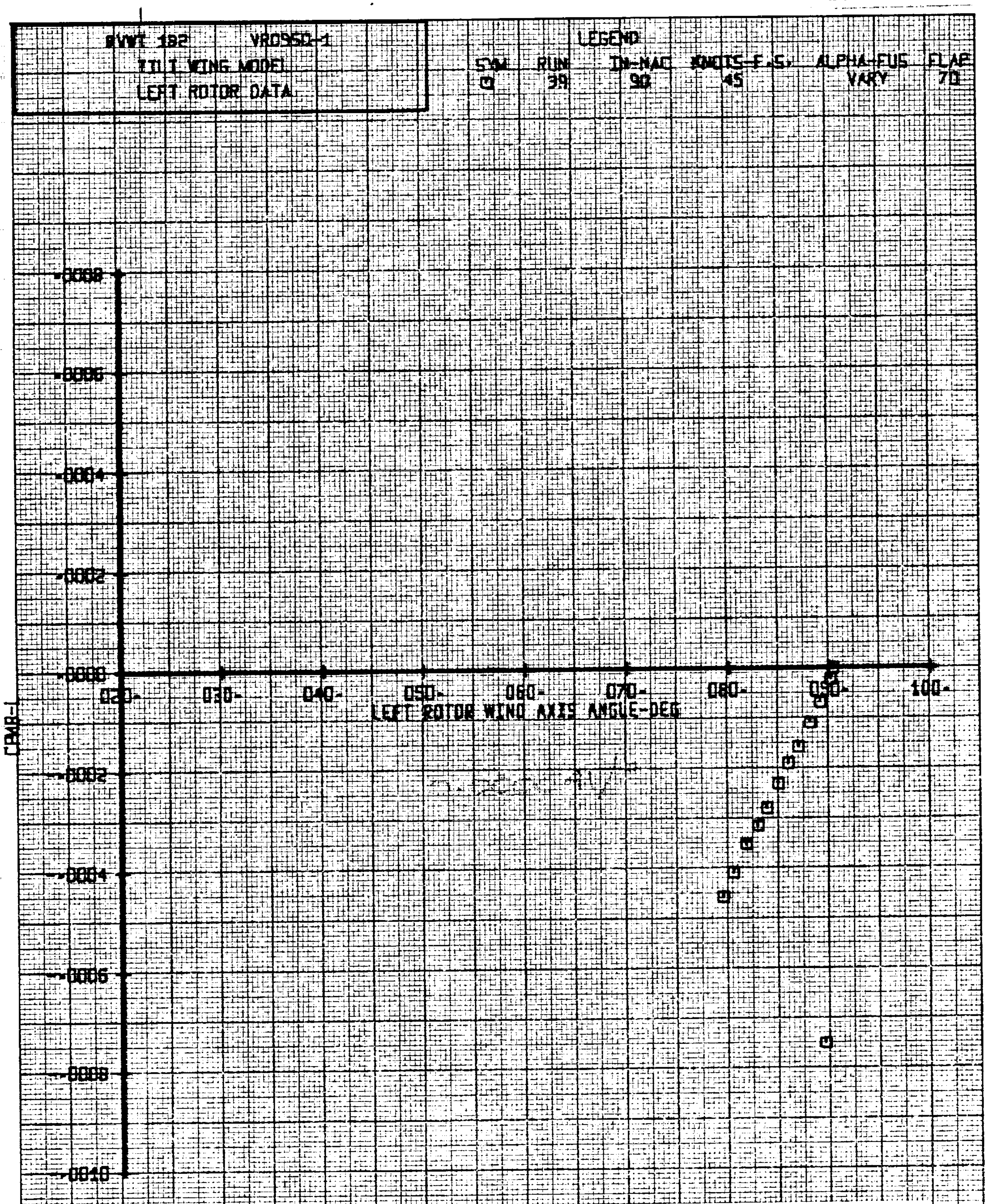

Fig. 2-005. Left Rotor Pitching Moment Vs. Angle of Attack.

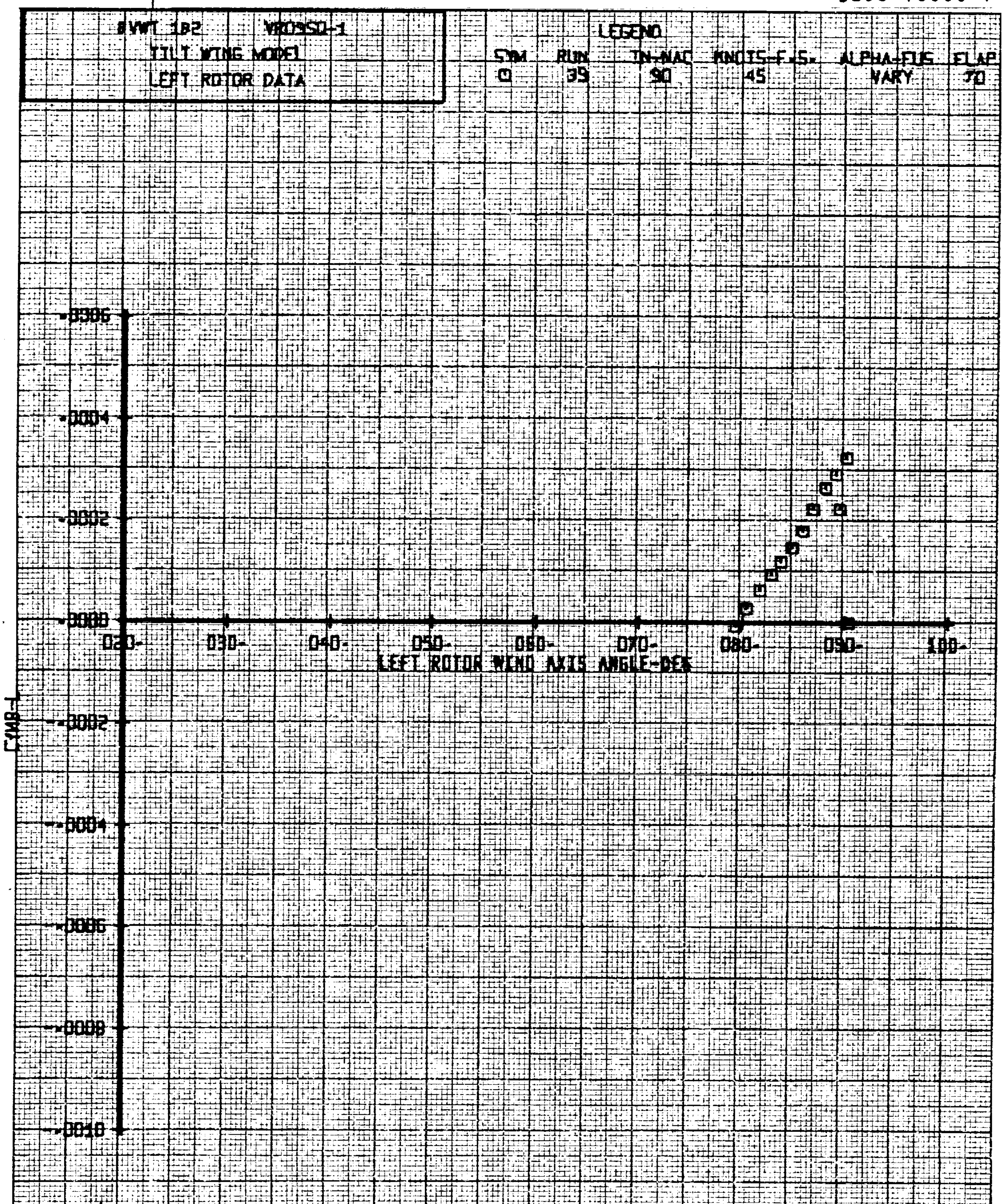

Fig. 2-006. Left Rotor Yawing Moment Vs. Angle of Attack.

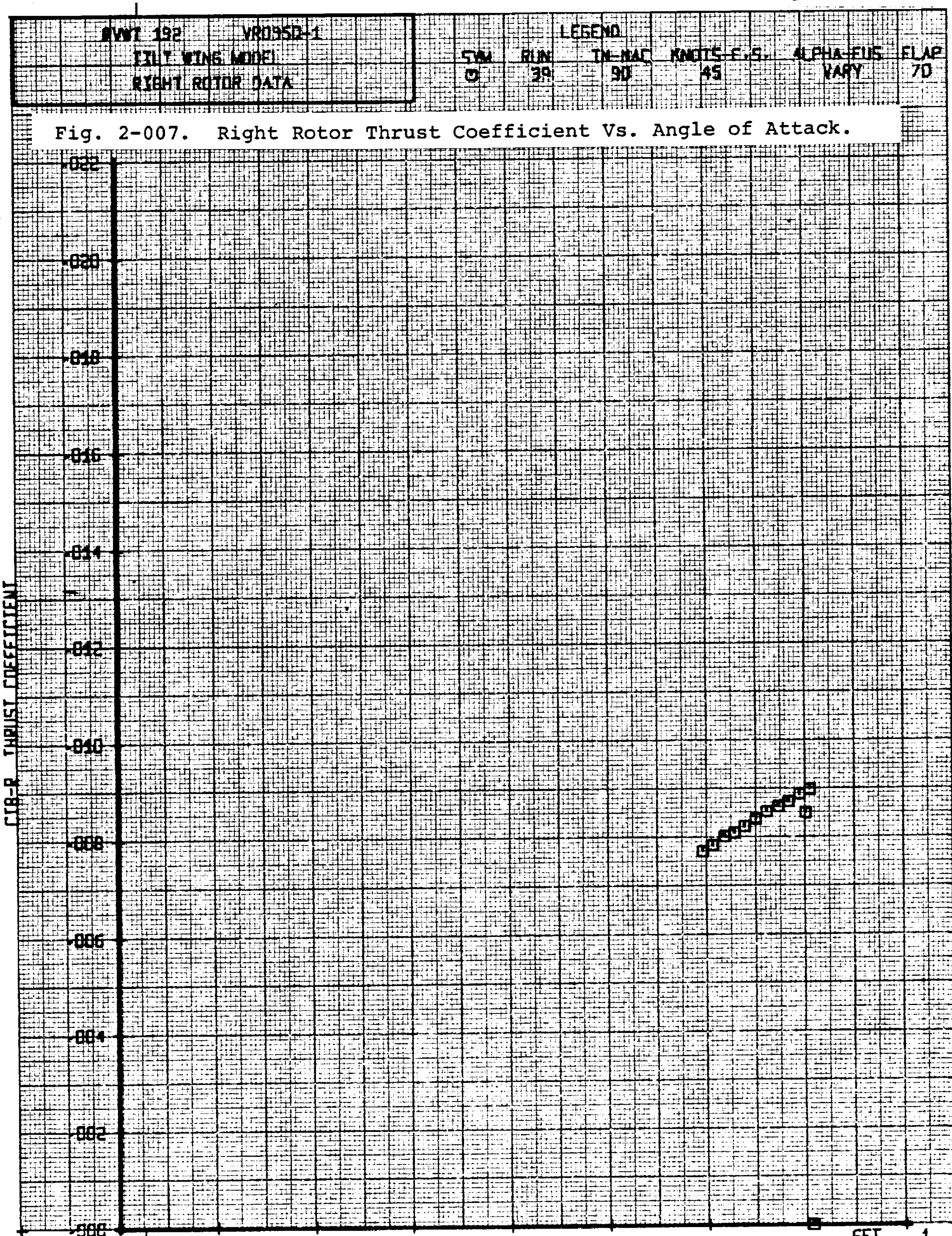

Fig. 2-007. Right Rotor Thrust Coefficient Vs. Angle of Attack.

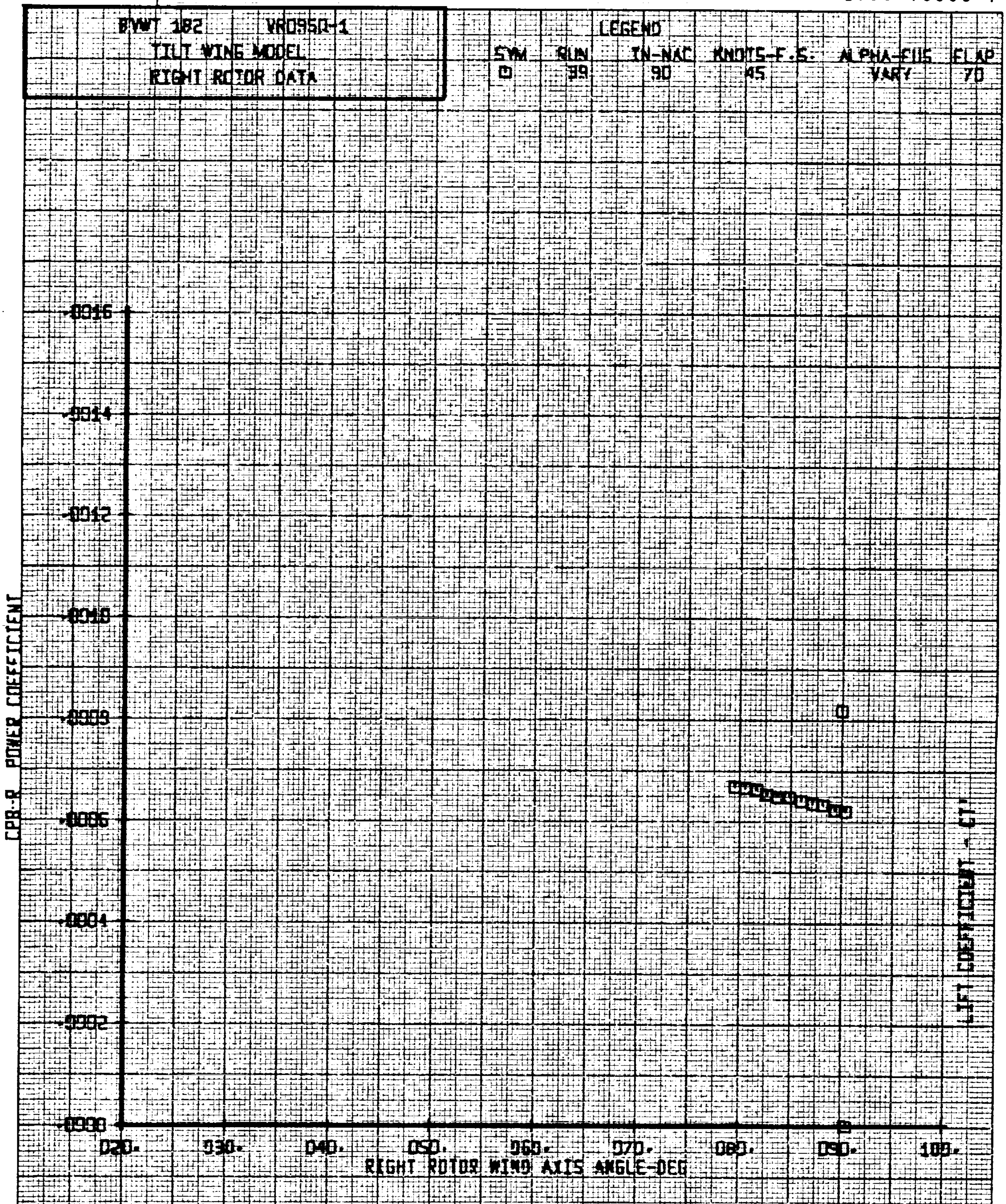

Fig. 2-008. Right Rotor Power Coefficient Vs. Angle of Attack.